

Dissertation zur Erlangung des Doktorgrades
der Fakultät für Chemie und Pharmazie
der Ludwig-Maximilians-Universität München

Lyophilization of Nucleic Acid Nanoparticles

—

Formulation Development, Stabilization Mechanisms,
and Process Monitoring

Julia Christina Kasper
aus Günzburg

2012

Dissertation eingereicht am: 13.03.2012

1. Gutachter: Prof. Dr. Wolfgang Frieß

2. Gutachter: Prof. Dr. Gerhard Winter

Mündliche Prüfung am: 17.04.2012

Erklärung

Diese Dissertation wurde im Sinne von § 7 der Promotionsordnung vom 28. November 2011 von Herrn Prof. Dr. Wolfgang Frieß betreut.

Eidesstattliche Versicherung

Diese Dissertation wurde eigenständig und ohne unerlaubte Hilfe erarbeitet.

München, den 12.03.2012

.....
Julia Kasper

Meinen Eltern

In Liebe und Dankbarkeit

Acknowledgment

This thesis was prepared between March 2009 and February 2012 at the Department of Pharmacy, Pharmaceutical Technology and Biopharmaceutics at the Ludwig-Maximilians-University in Munich under the supervision of Prof. Dr. Wolfgang Frieß.

First and foremost, I would like to express my gratitude to my supervisor, Prof. Dr. Wolfgang Frieß, for giving me the opportunity to join his group and for his professional and dedicated guidance of my work. Moreover, he is kindly acknowledged for all the scientific input and advice during this work. I much appreciate that he had spare time for our extensive scientific discussions and that he also was interested in my point of view. Furthermore, I am thankful for the freedom to develop and pursue my own scientific ideas. I am also grateful for his encouragement and support for submitting and publishing part of this work in numerous peer-reviewed journals and for his support for several grant and scholarship applications. I am especially thankful for the great opportunities to present the work at numerous congresses all over the world and to gain research experience in Prof. Dr. Pikal's lab at the University of Connecticut. I also very much appreciate his personal advice and the pleasant and inspiring working atmosphere in the group that made the preparation of this thesis an instructive and precious time.

I also would like to thank the leader of the chair, Prof. Dr. Gerhard Winter, for providing such excellent working conditions, for his scientific advice, for pushing the discussion in Thursdays' seminars, and for supporting numerous social activities. He is also kindly acknowledged for taking over the co-referee of this thesis.

Moreover, I am highly grateful to Prof. Dr. Ernst Wagner, Dr. Manfred Ogris, Dr. David Schaffert, and Christina Troiber from the chair of Pharmaceutical Biotechnology for their essential advice and support during preparation and publication of the predominant part of this thesis. Prof. Dr. Wagner is kindly

acknowledged for the provision of essential materials and for the access to cell culture experiments. He is gratefully thanked for his scientific and personal advice and for supporting my application for the graduate student scholarship by the German Academic Exchange Service (DAAD). Special thanks is expressed to Dr. David Schaffert and Christina Troiber for polymer and oligomer synthesis and for performance of cell culture experiments. Moreover, Christina Troiber is acknowledged for explaining me the “secrets of synthetic DNA and siRNA delivery” and for valuable scientific discussions.

Furthermore, I would like to express my gratitude to Prof. Dr. Michael Pikal from the School of Pharmacy at the University of Connecticut for hosting me during my research stay, for broadening my freeze-drying and physical chemistry horizon, for his great guidance and scientific advice, and for the welcoming and enthusiastic working atmosphere. Dr. Puneet Sharma and Dr. Meena Thakur are gratefully acknowledged for their support during the practical work in the lab and for valuable and extensive scientific discussions. Prof. Dr. Robin Bogner is thanked for her interest and her scientific input in my work. Prof. Dr. Devendra Kalonia is highly appreciated for the possibility to use the Nanosizer. Moreover, I would like to express my profound appreciation to all my former colleagues at the University of Connecticut for their warm welcome, all the help and support, and also for making my research stay abroad a great time. A special thanks goes to Puneet, Meena, Pooja, Hiroshika, Kelly, and Mary for introducing me to several other cultures and food habits and for joining me for coffee break.

Manfred Resch from INFAP GmbH is kindly thanked for the manufacturing of the optical glass fiber sensors, for the provision with the interrogator unit, and for his input with regard to optical glass fiber sensing. I am also grateful to Dr. Michael Wiggernhorn for his support and input during the process monitoring work.

Thanks are also due to Dr. Sarah K uchler for her support during this work and for the collaborative writing of the book chapter.

I would like to express my gratitude for financial support of this thesis by the “Collagen Modification by Enzymatic Technologies” Cornet grant of the German Federation of Industrial Research Associations, by the excellence cluster “Nanosystems Initiative Munich” (NIM) of the German Research Foundation (DFG), and by the excellence cluster m4 project T12 “synthetic siRNA as new therapeutic platform for personalized medicine” of the Federal Ministry of Education and Research (BMBF).

Dr. Philipp Hadwiger and Dr. Hans-Peter Vornlocher from Axolabs GmbH (formerly Roche Kulmbach GmbH) are kindly acknowledged for providing stabilized siRNAs and their support of this work.

From the Laboratory of Process Analytical Technology at the University of Ghent, Prof. Dr. Thomas de Beer and Siegrid Pieters are kindly thanked for our successful collaboration in the field of on-line process monitoring using spectroscopic tools.

I also would like to express gratitude to Prof. Dr. Friedrich Simmel and Max Scheible from the Department of Physics at the Technical University Munich for their support with atomic force microscopy experiments and to Prof. Dr. Joachim Rädler and Dr. Silvia Milani for their support with fluorescence correlation spectroscopy experiments.

Coriolis Pharma GmbH is kindly acknowledged for the possibility to use the dynamic light scattering plate reader and the nanoparticle tracking analysis equipment. A special thanks goes to Dr. Michael Wiggendorf, Dr. Frank Schaubhut, and Orhan Causevic for their support and help.

From the Department of Chemistry and Pharmacy, I would like to thank Wolfgang Wunschheim for his help with the X-ray powder diffractometer.

I wish to address special thanks to Sarah Claus for scientific input and valuable discussion during preparation of the first and our collaborative writing of the second review article.

Thanks are extended to Prof. Dr. Ernst Wagner, Prof. Dr. Stefan Zahler, Prof. Dr. Franz Paintner, and Prof. Dr. Klaus Wanner for kindly serving as a member for my thesis advisory committee.

The German Academic Exchange Service (DAAD) is kindly acknowledged for supporting my research stay at the University of Connecticut. Moreover, I am grateful to the European Federation for Pharmaceutical Sciences (EUFEPS) for awarding me a travel grant in order to attend the FIP Pharmaceutical Sciences 2010 World Congress and the AAPS Annual Meeting and Exposition in New Orleans, USA. Furthermore, the International Pharmaceutical Excipients Council (IPEC) Foundation is kindly acknowledged for honoring my work with the Graduate Student Scholarship 2011.

Dr. Frank Stieneker und Jürgen Kraske from the International Association for Pharmaceutical Technology (APV) are thanked for their collaboration with regard to the section "What's hot in EJPB" in the APV news and for providing me the possibility to attend several APV seminars.

Dr. Andrea Hawe is also kindly acknowledged. I just realized during the preparation of this thesis how much I have learned from you. Thanks also for the good team play during teaching the Master's course.

Moreover, I would like to thank Imke Leitner for her assistance and for the continuous material supply.

Johannes Mathes, Winfried Schlögl, and Philipp Matthias are kindly acknowledged for IT support.

Thanks are also extended to the student assistants, Julia Reitzel, Simon Body, Felicitas Keller, and Corinna Dürr, for their work.

A special thanks is addressed to the “core lyo team”, Thomas Bosch, Sarah Claus, and Raimund Geidobler, for our joint lyo webinar sessions, for scientific discussions, and for their help in our struggles for starting up and fixing the lyophilizer.

I would like to thank all of my former colleagues for the outstanding working atmosphere and for the good times we spent together.

Particularly, I would like to thank Sarah C., Eva, Kerstin, Winnie, Philipp, Tim, Verena, Madeleine, Imke, and Sarah K. for the establishment of our afternoon`s coffee break and for all the fun that we had together.

I wish to address a special thanks to Sarah C. for the great time we spent together and for her valuable friendship.

A special thanks also goes to Eva who has just not been my “office mate”, but also became a very close friend.

Moreover, I would like to thank Elsa and Kerstin for our many chats and for their friendship.

I would like to address very special thanks to Miriam for our great time together and her precious friendship. I also would like to thank Sarah, Christina, and Martina for our valuable, long-lasting friendships.

Most importantly, I would like to thank my parents. Without you I would not be who I am today. Thanks for all you made possible for me, for always believing in me, for your encouragement and support.

I also would like to express my gratitude to my godmother and to Anton, Sieglinde, and Carolin for all their great support.

Finally, I would like to thank Bernd for his support and patience. Thank you for always being there for me over the past years and for your love.

Table of contents

Acknowledgment	IV
Table of contents	XII
List of abbreviations	XIX

Chapter 1

General introduction	1
Abstract	2
1 Lyophilization in brief	3
1.1 <i>The lyophilization process</i>	<i>3</i>
1.2 <i>The lyophilization equipment</i>	<i>8</i>
2 Recent advances and further challenges in lyophilization	11
2.1 <i>Lyophilization beyond the drying of pharmaceutical proteins</i>	<i>11</i>
2.2 <i>Pharmaceutical applications of lyophilisates in the solid state</i>	<i>12</i>
2.3 <i>Novel formulation aspects</i>	<i>13</i>
2.4 <i>Importance of the freezing step in lyophilization</i>	<i>14</i>
2.5 <i>Lyophilization above Tg`</i>	<i>15</i>
2.6 <i>Stabilization by thermal treatment/ high secondary drying temperatures</i>	<i>16</i>
2.7 <i>Individual factors contributing to protein stability during lyophilization</i>	<i>17</i>
2.8 <i>Enhanced understanding of stabilization mechanisms in the solid state</i>	<i>18</i>
2.9 <i>Quality by design and process analytical technology in lyophilization</i>	<i>19</i>
2.10 <i>Novel container systems</i>	<i>21</i>
2.11 <i>Scale-up equipment issues and the dream of continuous processing</i>	<i>23</i>
2.12 <i>Conclusion and outlook</i>	<i>24</i>
3 Lyophilization of nucleic acid nanoparticles	25
3.1 <i>pDNA and siRNA delivery in gene therapy and the need for long-term stable formulations</i>	<i>25</i>
3.2 <i>The current status on lyophilization of nucleic acid nanoparticles</i>	<i>28</i>
4 References	34

Chapter 2

The freezing step in lyophilization	51
Abstract	52
1 Introduction	53
2 Physico-chemical fundamentals of freezing	55
2.1 Freezing phenomena: supercooling, ice nucleation and ice crystal formation ...	55
2.2 Crystallization and vitrification of solutes	59
2.3 Phase separation and other types of freezing behavior	63
3 Modifications of the freezing step	65
3.1 Shelf-ramped freezing	65
3.2 Pre-cooled shelf method	67
3.3 Annealing	67
3.4 Quench freezing	69
3.5 Directional freezing	69
3.6 Ice fog technique	70
3.7 Electrofreezing	70
3.8 Ultrasound-controlled ice nucleation	72
3.9 Vacuum-induced surface freezing	74
3.10 High pressure shift freezing or depressurization technique	75
3.11 Addition of ice nucleation agents	76
3.12 Non-aqueous co-solvents	77
3.13 Others	79
4 Consequences of the freezing step on general quality attributes of biopharmaceuticals and process performance	80
4.1 Intra-vial and inter-vial uniformity	80
4.2 Sample morphology	83
4.3 Primary and secondary drying performance	84
4.4 Physical state of the sample	89
4.5 Residual moisture content	90
4.6 Reconstitution time	91
5 Consequences of the freezing step on protein stability	93
5.1 General stress factors during freezing	93
5.2 Influence of the freezing step on protein stability	97
6 Conclusion and practical consideration	101
7 References	104

Chapter 3

Objectives of the thesis	113
---------------------------------------	------------

Chapter 4

Establishment of an up-scaled micro-mixer method	115
Abstract	116
1 Introduction	117
2 Materials and methods	119
2.1 Materials	119
2.2 Preparation of plasmid/LPEI polyplexes by pipetting	119
2.3 Up-scaled preparation of plasmid/LPEI polyplexes	119
2.4 Particle size determination	120
2.5 Cell culture	120
3 Results and discussion	122
3.1 Establishment of the up-scaled micro-mixer method for the preparation of plasmid/LPEI polyplexes	122
3.2 Influence of the plasmid concentration on particle size and polydispersity of plasmid/LPEI polyplexes	125
4 Conclusion	127
5 References	128

Chapter 5

Development of a lyophilized plasmid/LPEI polyplex formulation with long-term stability	129
Abstract	130
1 Introduction	132
2 Materials and methods	135
2.1 Materials	135
2.2 Preparation of plasmid/LPEI polyplexes	135
2.3 Freeze-thawing studies	135
2.4 Lyophilization of plasmid/LPEI polyplexes	136
2.5 Long-term stability	136
2.6 Plasmid/LPEI polyplex characterization	136
2.7 Osmometry	137
2.8 Turbidimetry	137
2.9 Light obscuration	137
2.10 Cell culture: cytotoxicity and luciferase reporter gene expression	137
2.11 Karl Fischer titration	138
2.12 Differential scanning calorimetry (DSC)	138
2.13 X-ray powder diffraction (XRD)	139

2.14 Statistical analysis	139
3 Results	140
3.1 Influence of the buffer composition	140
3.2 Freeze-thawing studies	141
3.3 Physico-chemical and biological properties of lyophilized plasmid/LPEI polyplexes	144
3.4 Physico-chemical and biological properties of lyophilized plasmid/LPEI polyplexes after storage	150
4 Discussion	152
5 Conclusion	161
6 References	163

Chapter 6

Investigations on polyplex stability during the freezing step of lyophilization

using controlled ice nucleation	167
Abstract	168
1 Introduction	170
2 Materials and methods	175
2.1 Materials	175
2.2 Sample preparation	175
2.3 Freeze-thaw studies using different freezing protocols	176
2.3.1 Conventional shelf-ramp freezing	176
2.3.2 'Standard' depressurization method	177
2.3.3 Varying ice nucleation temperatures via controlled ice nucleation	177
2.3.4 Varying shelf-ramp rates after controlled ice nucleation	177
2.3.5 Interruption of the freezing process after controlled ice nucleation	178
2.4 Lyophilization	178
2.5 Polyplex characterization	178
2.6 Specific surface area determination	179
2.7 Karl-Fischer titration	179
2.8 Theoretical modeling of the change in sucrose concentration or viscosity during freeze-concentration and correlation to reaction rates	180
2.9 Statistical analysis	183
3 Results	184
3.1 Influence of the 'standard' depressurization method in comparison to conventional shelf-ramp freezing on polyplex stability	184
3.2 Influence of ice nucleation temperature on polyplex stability	188
3.3 Influence of residence time on polyplex stability	190
3.4 Influence of the proceeding of freezing on polyplex stability	192

<i>3.5 Surface area and residual moisture content of selected lyophilized samples</i>	194
<i>3.6 Theoretical modeling of the change in sucrose concentration or viscosity during freeze-concentration and correlation to reaction rates</i>	196
4 Discussion	200
5 Summary and conclusion	212
6 References	214

Chapter 7

Formulation development of lyophilized, long-term stable

siRNA/oligoaminoamide polyplexes	219
Abstract	220
1 Introduction	221
2 Materials and methods	225
<i>2.1 Materials</i>	<i>225</i>
<i>2.2 Preparation of siRNA polyplexes</i>	<i>226</i>
<i>2.3 Freeze-thawing studies</i>	<i>227</i>
<i>2.4 Lyophilization of siRNA polyplexes</i>	<i>227</i>
<i>2.5 Long-term stability testing of lyophilized samples</i>	<i>227</i>
<i>2.6 Reconstitution of lyophilized samples</i>	<i>228</i>
<i>2.7 siRNA polyplex characterization</i>	<i>228</i>
<i>2.8 Cell culture: metabolic activity and gene silencing</i>	<i>228</i>
<i>2.9 Osmometry</i>	<i>229</i>
<i>2.10 Turbidimetry</i>	<i>230</i>
<i>2.11 Light obscuration</i>	<i>230</i>
<i>2.12 Karl Fischer titration</i>	<i>230</i>
<i>2.13 Differential scanning calorimetry (DSC)</i>	<i>231</i>
<i>2.14 X-ray powder diffraction (XRD)</i>	<i>231</i>
<i>2.15 Statistical analysis</i>	<i>231</i>
3 Results	232
<i>3.1 Up-scaled preparation and characterization of siRNA polyplexes</i>	<i>232</i>
<i>3.2 Freeze-thawing studies</i>	<i>233</i>
<i>3.3 Lyophilization of siRNA/oligoaminoamide polyplexes</i>	<i>238</i>
<i>3.4 Long-term stability of lyophilized siRNA/oligoaminoamide polyplexes</i>	<i>241</i>
4 Discussion	247
5 Conclusion	257
6 References	259

Chapter 8

Implementation and evaluation of an optical fiber system as novel process monitoring tool during lyophilization	265
Abstract	266
1 Introduction	267
2 Materials and methods	272
<i>2.1 Materials</i>	<i>272</i>
<i>2.2 The optical fiber system</i>	<i>272</i>
2.2.1 Optical fiber sensor (OFS) structure and characteristics	272
2.2.2 Operation principle	274
2.2.3 System and design variations	275
<i>2.3 Temperature calibration</i>	<i>277</i>
<i>2.4 Measurement of product temperature profiles during lyophilization and freezing experiments</i>	<i>278</i>
<i>2.5 Differential scanning calorimetry</i>	<i>279</i>
3 Results and discussion	280
<i>3.1 Product temperature measurements and end point detection</i>	<i>278</i>
<i>3.2 Sensitivity to physico-chemical events during freezing</i>	<i>281</i>
3.2.1 Supercooling and ice nucleation	281
3.2.2 Crystallization of excipients	283
3.2.3 Glass formation of excipients	285
<i>3.3 Influence of the shielding or unshielding of the OFSs on temperature profiles</i>	<i>288</i>
<i>3.4 Three-dimensional information on temperature profiles in a vial</i>	<i>289</i>
<i>3.5 Non-invasive temperature profiling during lyophilization</i>	<i>293</i>
4 Conclusion	297
5 References	299

Chapter 9

Summary of the thesis	303
Appendix	308
Curriculum vitae	314

List of abbreviations

A	alanine
Agl	silver iodine
API	active pharmaceutical ingredient
A_v	outer area of the vial bottom
C	cysteine
C_{eu}	eutectic concentration
C_{glass}	specific heat of glass
C_{ice}	specific heat of ice
COC	cyclic olefin copolymers
COP	cyclic olefin polymers
C_{water}	specific heat of water
ΔH_f	heat fusion of ice
ΔH_s	heat of sublimation
ΔT	change of temperature
ΔT_f	difference in freezing point depression
ΔX_w	amount of frozen water
DNA	deoxyribonucleic acid
DLR	dry layer resistance
DLS	dynamic light scattering
dm/dt	mass transfer rate
DMRIE-C	1,2-dimyristyloxypropyl-3-dimethylhydroxyethylammonium bromide
DOPE	dioleoylphosphatidylethanolamine
DOTAP	N-[1-(2,3-Dioleoyloxy)propyl]-N,N,N-trimethylammonium methyl-sulfate
DPE	dynamic parameters estimation
dQ/dt	heat transfer rate
DSC	differential scanning calorimetry
DSPE	distearoylphosphatidylethanolamine
DT	drying time
DTG	draw tower grating

EF	electrofreezing
FBG	fibre Bragg grating
FDA	Food and Drug Administration
FDM	freeze-drying microscopy
FR	freezing rate
η	viscosity
HBG	HEPES buffered glucose
HEPES	4-(2-hydroxyethyl)-1-piperazineethane sulfonic acid
HES	hydroxyethyl starch
HP- β -CD	hydroxypropylbetadex, hydroxypropyl- β -cyclodextrin
ICM	ice crystal morphology
INA	ice nucleating agent
INT	ice nucleation temperature
K_c	contact component of vial heat transfer coefficient
K_g	gas conduction component of vial heat transfer coefficient
K_r	radiation component of vial heat transfer coefficient
K_v	heat transfer coefficient of the vial
λ_{FBG}	Bragg wavelength
LDH	lactate dehydrogenase
LPEI	linear polyethylenimine
m_{solute}	mass of solute per vial
mOsm	milli osmol
MTM	manometric temperature measurement
NC	nucleation control
NCE	new chemical entity
NEM	N-ethylmaleimide
NIR	near infrared
ODN	oligodeoxynucleotide
ODT	orally disintegrating tablets
OFS	optical fiber sensor
OleA	oleic acid

P. syringae	Pseudomonas syringae
PAT	process analytical technology
P_c	chamber pressure
PdI, pdi	polydispersity index
PDMAEMA	poly(2-dimethylamino)ethyl methacrylate
pDNA	plasmid deoxyriobnucleic acid
PEG	polyethyleneglycol
PEI	polyethyleniminie
P_{ice}	equilibrium vapor pressure over ice
P_0	equilibrium vapor pressure over ice
PVP	povidone, poly vinyl pyrrolidone
QbD	quality by design
Q_{cool}	heat needed to cool the sampel
Q_{pc}	heat created by phase change
rFVIII	recombinant Factor VIII
RISC	RNA-induced silencing complex
RM	residual moisture
RNA	ribonucleic acid
RNAi	ribonucleic acid interference
R_p	dry layer resistance of the product
R_s	water vapour resistance of the stopper
RTD	resistance temperature detectors
S	succinic
SBECD	sulphobutylehter beta cyclodextrin
SD	standard deviation
siRNA	small interfering ribonucleic acid
SSA	specific surface area
T	(absolute) temperature
TBA	tertiary butyl alcohol, tert-butanol
T_c	collapse temperature

TC	thermocouple
TDLAS	tunable diode laser absorption spectroscopy
T_{eu}	eutectic temperature
T_g	glass transition temperature
T_g'	glass transition temperature of the maximal freeze-concentrate
T_0	"zero mobility" temperature
T_{00}	"zero mobility" temperature of pure water
T_p	product temperature
tp	tetraethylenpentamine
T_s	shelf temperature
WDM	wavelength division multiplexing
XRD	X-ray powder diffraction
X_w	amount of water
Y	tyrosine
Zave	Z-average diameter

Chapter 1

General introduction

Part of the following chapter is intended for publication:

Julia Christina Kasper, Wolfgang Friess

Recent advances and further challenges in lyophilization, *in preparation*.

Abstract

While entering a new century, lyophilization in the pharmaceutical field has been subjected to ongoing development and steady expansion. This chapter aims to highlight recent advances but also to discuss further challenges in lyophilization.

At first, the three major steps of a typical lyophilization process, namely freezing, primary drying, and secondary drying, are described in brief. Additionally, a general description of the essential components and their function in a lyophilizer is given.

With respect to recent advances in lyophilization, the expanded range of pharmaceutical applications based on lyophilization is summarized. Moreover, novel formulation aspects and novel container systems are discussed and the importance of the freezing step is outlined. Furthermore, the dogma of “ never lyophilizing above the glass transition temperature” is argued and recent insights into novel stabilization concepts are provided. Process analytical technology (PAT) and quality by design (QbD) are now leading issues and the design of the lyophilization equipment might have to be reconsidered in the future.

Nowadays, lyophilization has also gained importance for the preservation of nucleic acid based pharmaceuticals. In that context, a brief overview on the basic concepts of pDNA and siRNA delivery in gene therapy is given and the need for lyophilized long-term stable formulations is accentuated. Additionally, currently available literature on the lyophilization of nucleic acid nanoparticles is reviewed in brief.

Keywords

Lyophilization, freeze-drying, gene therapy, pDNA and siRNA delivery, nucleic acid nanoparticles

1 Lyophilization in brief

In general, lyophilization is defined as a stabilizing process in which the sample is frozen followed by a reduction of the solvent content by sublimation and then by desorption to values that will no longer allow biological growth or chemical reactions [1].

The first evidence on freeze-drying of food products is traced back over thousand years when ancient South Americans living in the Andes used a primitive freeze-drying method to preserve potatoes [2]. In 1890, it was reported the first time that biological specimens can be preserved by drying under vacuum conditions and at temperature below 0 °C [3]. The emergence of modern, industrial freeze-drying of pharmaceutical products towards the middle part of the last century is related to the demand for large-scale production of preserved blood plasma [3]. Several years later, the interest in freeze-drying, now often called lyophilization, drastically increased with the growing numbers of antibiotics and other sensitive pharmaceuticals [4]. At the end the of the past century, lyophilization has evolved to a well-established technology for preservation of biopharmaceuticals products [2]. During that time, fundamental concepts with regard to process design and formulation development have been established.

1.1 The lyophilization process

A typical lyophilization process can be divided into three stages: freezing, primary drying, and secondary drying. Figure 1-1 displays a schematic illustration of a typical lyophilization cycle.

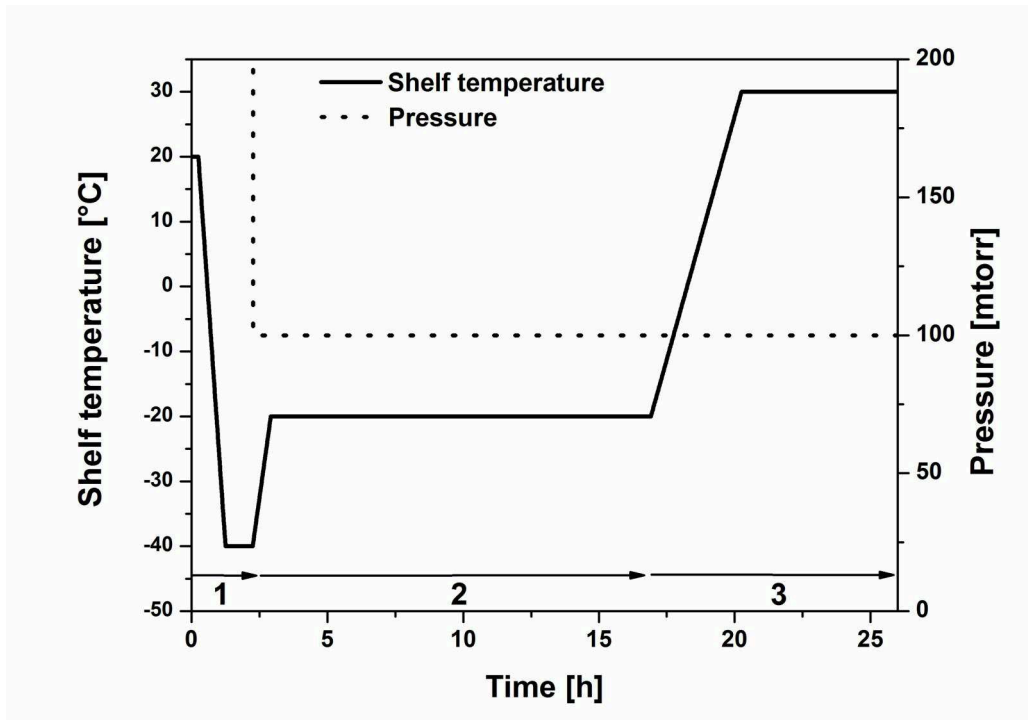


Figure 1-1: Schematic illustration of a typical lyophilization cycle. The solid black line represents the temperature course and the dashed black line represents the pressure course during the different stages of a lyophilization process: 1) freezing, 2) primary drying, and 3) secondary drying.

The freezing step is initiated by cooling the shelves, on which the samples are placed, to the desired freezing temperature and holding the temperature constant for equilibration [5]. In this context, the sample is first cooled until ice nucleation occurs several degrees below the equilibrium freezing point of the sample, referred to as “supercooling” [6]. After ice nucleation, ice crystals start to grow resulting in freeze-concentration of the sample [7]. At this point, two phases are present, i.e. ice and freeze-concentrated solution, and the composition of the sample is determined via the equilibrium freezing curve of water in the presence of the solute [8]. For crystalline excipients, solute crystallization occurs when the product temperature falls below the eutectic temperature (T_{eu}) [9]. However, for amorphous excipients, freeze-concentration continues until the viscosity exceeds a critical value at which glass formation occurs. This temperature, at which maximal freeze-concentration is observed, is

referred to as the glass transition temperature (T_g) [9]. Thus, in order to ensure complete solidification of the sample, the sample has to be frozen below T_g if it is in the amorphous state or below T_{eu} if it is in the crystalline state [10]. As upon completion of freezing the majority of the water has been separated from the solute, the freezing step is the major dehydration step in lyophilization [11]. In general, the freezing step in lyophilization is of paramount importance as it considerably impacts lyophilization performance and product quality [11]. Therefore, physico-chemical fundamentals of freezing, currently available freezing methods, and consequences of the freezing step on process performance and product quality will be discussed in detail in Chapter 2.

After the completion of freezing, an optional annealing step, during which product temperature is held 10 to 20 °C above T_g , can be applied in order to allow for complete crystallization of the excipients and/ or to increase the size of ice crystals [10, 12].

Primary drying, wherein the majority of the water is removed from the product by sublimation, is initiated by introducing vacuum in the product chamber [5]. The chamber pressure has to be reduced below the saturated vapor pressure of ice at the frozen product temperature in order to allow for sublimation. The real driving force for sublimation is provided by the water vapor pressure difference between the product ice interface and the condenser surface [8]. Thus, different chamber pressures below the saturated vapor pressure of ice affect the rate of sublimation but do not affect the driving force in general [8]. The mass transfer of water vapor from the product to the condenser (dm/dt) is largely determined by the dry layer resistance of the product (R_p) but also by the stopper resistance (R_s) and can be described by:

$$\frac{dm}{dt} = \frac{P_{ice} - P_c}{R_p + R_s} \quad (1-1)$$

where P_{ice} is the equilibrium vapor pressure of ice at the sublimation interface temperature and P_c is the chamber pressure [10]. At a given product

temperature (i.e. a given ice vapor pressure), the smallest chamber pressure gives the highest ice sublimation rate [10]. However, too low pressures are also counterproductive for fast sublimation rates by limiting the rate of heat transfer to the product [10]. As the sublimation of water vapor from the frozen sample is an endothermic reaction, with a heat of sublimation ΔH_s of approximately 650 cal/g, the energy for continuing sublimation of ice needs to be supplied from the shelves by heating to increased shelf temperatures [12]. In general, heat transfer to the product is based on three components namely radiation from “warm” surfaces, direct conduction within and between solid phases, and gas conduction (convection) within vapor phases by Brownian diffusion and molecular collision [8]. The heat transfer rate (dQ/dt) to a product in vials can be described by:

$$\frac{dQ}{dt} = A_v \cdot K_v \cdot (T_s - T_p) \quad (1-2)$$

where Q is the energy received by each vial from the shelf, A_v is the outer area of the vial bottom, K_v is the heat transfer coefficient of the vial, T_s is the shelf temperature, and T_p is the product temperature [10, 12]. During steady state of primary drying, the rate of heat input into the product (equation 1-2) is in equilibrium with the rate of heat output by sublimation of ice (equation 1-1) [12]. Thus in order to maximize the sublimation rate, the combination of the highest allowable product temperature, which is in general below T_g' or T_{eu} , and the lowest possible chamber pressure should be used. The complex relationship between chamber pressure, shelf temperature, and product temperature, and its impact on the sublimation rate is illustrated in Figure 1-2.

For instance, at a constant shelf-temperature, the sublimation rate could be decreased (A to B) or increased (A to C) by altering the chamber pressure. However, an increase in chamber pressure results in an increase in product temperature, at the same time [9]. Thus, in order to achieve a safe increase in the sublimation rate at a constant product temperature a reduction of the

chamber pressure with a simultaneous increase in the shelf temperature (A to D) would be required [9].

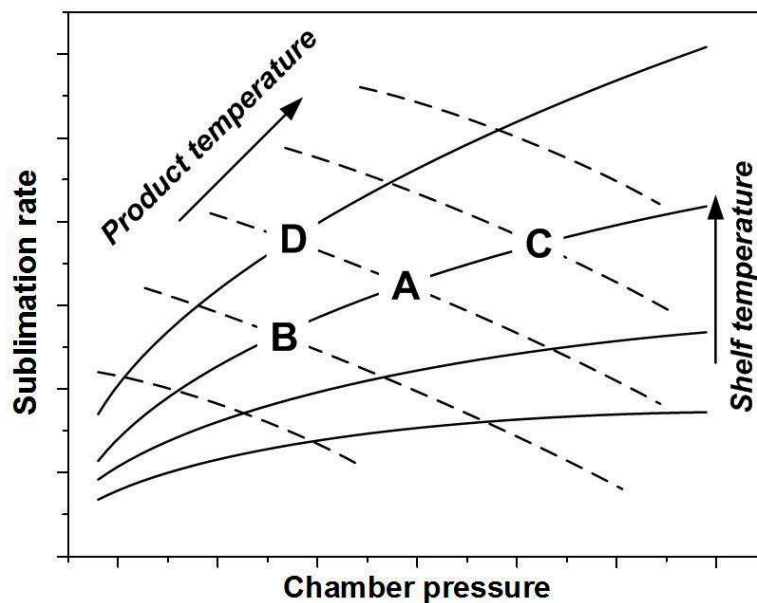


Figure 1-2: The relationship between chamber pressure, shelf temperature, product temperature, and sublimation rate. Redrawn from reference [9].

Primary drying is complete when all frozen bulk water is removed via sublimation [5]. At this point, the product still contains some bound unfrozen water that has to be removed by desorption at higher temperatures during secondary drying [8]. Therefore, shelf temperature is slowly increased, in order to avoid product collapse, to temperatures between 20 °C and 40 °C and maintained at that temperature until the residual moisture content reaches its targeted level of usually less than 1% [10]. The secondary drying rate is mainly determined by the diffusion rate of water from the bulk to the surface and the influence of desorption rates from the surface into the vapor state can in practice almost be neglected [1]. Thus, final moisture levels are only dependent on the shelf temperature and the specific surface area of the cake, but independent of the chamber pressure or the height of the dried product thickness [13].

1.2 The lyophilization equipment

The environmental conditions necessary for the lyophilization process, subambient temperatures and subatmospheric pressures, are achieved by the lyophilization equipment. The following gives a general description of the essential components and their function in a lyophilizer. The general design of a common lyophilizer is displayed in Figure 1-3.

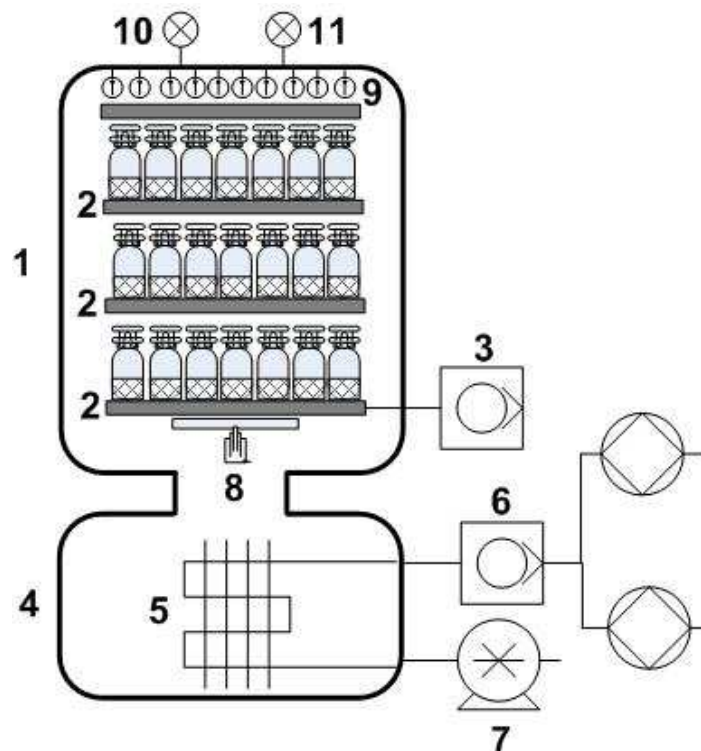


Figure 1-3: General design of a common lyophilizer: 1) product chamber, 2) temperature-controlled shelves, 3) heat transfer system, 4) condenser chamber, 5) ice condenser, 6) refrigeration system, 7) vacuum pump, 8) hydraulic system to move the shelves, 9) connection for temperature probes, 10) capacitance manometer, and 11) pirani gauge.

The freeze-drying chamber or product chamber is a vacuum vessel, generally constructed from stainless steel, that can be accessed by a hinged door [1, 5]. The chamber door is either made from clear acrylic material or stainless steel and is fitted with an elastomer gasket to form a vacuum seal with the product chamber [1, 5].

The product chamber houses one unusable shelf, which serves as a radiation shelf for the top shelf, and the usable shelves, on which the product is placed during lyophilization [1, 5]. The shelves are a hollow construction and contain circulating heat transfer fluid for temperature control. The shelves either remove heat from or supply heat to the product, depending on the step in the lyophilization process (freezing or drying). The shelves can be moved vertically by the aid of a hydraulic system and then serve as stoppering platens to force the slotted stoppers to their final position into the vial [5].

The condenser chamber houses the condenser which operates as a trap to collect solvent vapor by condensing the solvent. The condenser has an enormous pumping capacity in order to efficiently remove a larger vapor volume and to allow the system to achieve lower pressures [5]. In order to be effective, the temperature of the condenser plates has to be at minimum 20 °C lower than the product temperature during primary drying [1]. In contrast to the shelves, which are chilled by heat-transfer fluid, the condenser is generally refrigerated by direct expansion of a refrigerant [1].

The vacuum pumping system in combination with the condenser provides the subambient pressures that are necessary for the primary and secondary drying process [1]. The vacuum pump removes any non-condensable gases that pass through the system, e.g. gases that are introduced into the system through leaks or outgassing, or inert gases, such as nitrogen, that are used for pressure control during drying [1, 5].

Moreover, the lyophilization unit comprises basic instrumentation for process control and monitoring. Shelf temperature is most commonly measured and controlled as the temperature of the circulating heat transfer fluid through the shelf [5]. Chamber pressure is usually measured and controlled with a capacitance manometer. In combination with a conductivity gauge (Pirani gauge), these two pressure measures can be used for manometric endpoint

determination. Here, the endpoint of primary drying is reached when the pressure difference between the Pirani gauge and the capacitance manometer decreases and approaches zero [10]. Finally, product temperature, which depends on the shelf temperature and the chamber pressure, is most commonly monitored by T-type copper-constantan thermocouples (TCs) or 100-ohm platinum resistance temperature detectors (RTDs). Nowadays, with the increasing demand on process analytical technology (PAT), several other tools have been introduced for lyophilization process monitoring and control (see section 2.9). Other recent advances and further challenges in lyophilization will be addressed in the following section.

2 Recent advances and further challenges in lyophilization

Entering a new century, scientists strive for new applications of lyophilization, the technology is subject of ongoing development and even well-accepted dogmas have been challenged. The aim of the following section is to highlight recent advances and to discuss existing and future challenges in lyophilization.

2.1 Lyophilization beyond drying of pharmaceutical proteins

Most current literature in the field of pharmaceutical lyophilization is available on drying of protein drugs for parenteral application. However, research also started to investigate the use of lyophilization for several other pharmaceutical applications. With respect to parenteral, but also non-parenteral, application, substantial effort has been spent to develop lyophilization into a promising approach in order to achieve long-term stable vaccine formulations [14]. Moreover, lyophilization of cells, e.g. red blood cells, is a desirable goal [15], for which however, a complete success has not been reported yet. Additionally, different nanoparticulate systems, employing lyophilization to overcome physical and/or chemical instabilities, have been developed for efficient drug delivery of small molecules, proteins or peptides [16]. With the rapid progress in gene therapy, lyophilization also gained importance for the preservation of nucleic acid based pharmaceuticals (see section 3). Successful gene therapy requires complex nanoparticulate carriers that protect and efficiently deliver their nucleic acid payload. Lyophilization has the capability to both stabilize the nucleic acid against degradation and to preserve the nanoparticle structures [17]. It is important to note that stabilization mechanism and excipients that were established for proteins do not necessarily apply to nanoparticles.

Lyophilized biological reference standards are a new expansion of the traditional field of lyophilization. These biological standards are often derived from a single large-batch of well-characterized biological material and here, lyophilization, often performed in ampoules instead of vials, guarantees long-term stability and ease of distribution [18]. Additionally, as many new chemical entities suffer from poor solubility, the preparation of amorphous solid dispersions by lyophilization, especially from co-solvents systems, is a promising alternative to achieve stable systems with increased bioavailability and a low tendency to recrystallization or particle size increase [19].

2.2 Pharmaceutical applications of lyophilisates in the solid state

The most common use of lyophilization is the manufacturing of parenterals which are reconstituted prior to application. But several other applications of solid lyophilisates have emerged. They take advantage of the unique properties of the highly porous structures. First of all, orally disintegrating tablets (ODTs), which have gained popularity, can be manufactured by lyophilization based technologies such as the Zydis™ (R.P. Scherer, UK), Lyoc™ (Farmalyoc, France) or Quicksolv™ (Janssen Pharmaceutica, USA) technology [20]. ODTs prepared by lyophilization have a unique porosity that guarantees rapid dissolution in the saliva, but may show limited mechanical strength and storage stability. But the gentle preparation method could have high potential for oral vaccine ODTs [21]. Lyophilized three-dimensional scaffolds, for which the porosity can be controlled by varying the freezing conditions, are well-established for wound healing and tissue engineering [22]. Moreover, it is also reported that lyophilized wafers are promising systems for drug delivery via the buccal mucosa [23]. A new interesting approach is “partial lyophilization” with the bulking agent partially suspended at higher concentration in the aqueous liquid which is lyophilized [24-25]. This approach, known as the Lyopan™

technology, consumes less time and energy than previous methods to produce fast-disintegrating tablets, thus making it more economical.

Additionally, lyophilization can also be utilized as the first step to produce dry powder inhalation systems [26-27]. Previously, the lyophilized powder were reduced to respirable powders in a subsequent milling step [26]. Similarly, lyophilized dry powder vaccines for nasal delivery can be prepared [28]. Recently Claus et al. [29] introduced a promising new dry powder inhalation technology based on the direct dispersion of lyophilisates by an air impact. This approach allowed to overcome the disadvantages associated with milling and enabled high fine particle fractions.

2.3 Novel formulation aspects

Good freeze drying practice typically entails minimizing the amount of buffer or salt in order to keep the glass transition temperature (T_g) of the formulation high [30]. However, it was shown that the addition of a plasticizer like glycerol or sorbitol leads to an improved protein stability despite lowering of T_g which was explained by decreased fast glass dynamics (see section 2.8) [31-32].

The expansion of the excipient spectrum by high molecular weight compounds, e.g. dextran, hydroxyethylstarch, polyvinylpyrrolidone, polyethylenglycol might allow for accelerated drying processes and for better storage stability at higher temperatures due to the increased T_g and T_g . But when using these excipients possible phase separation negatively influencing protein stability has to be taken into account [33]. Recently, Padilla and Pikal [34], introduced Raman mapping as a new tool for studying amorphous phase separation in lyophilized protein formulations. Moreover, when using dextran or hydroxyethylstarch in protein formulation, optimal storage stability could only be achieved in combination with disaccharides [35-36]. Thus, the possible benefit of high molecular weight excipients in protein formulation needs to be further evaluated in the future. In contrast, oligosaccharides such as low-molecular weight

dextrans [37] or inulin [38] are clearly beneficial to provide sufficient stabilization of nanoparticles at low osmolalities when a high mass ratio of stabilizer to nanoparticle is required.

NCEs often cannot be lyophilized from aqueous solution due to their poor solubility. One option is the use of non-aqueous co-solvents, mainly tertiary butyl alcohol (TBA), that offers several advantages (e.g. increased drug solubility, acceleration of sublimation rates, decreased reconstitution time, and improved product stability) [39-40]. But limitations, e.g. special equipment requirements, residual solvent levels, toxicity of residual solvents, over-all cost disadvantage, and increased regulatory issues, have to be considered, as well [39-40]. The addition of TBA has recently been shown to constitute a promising approach to incorporate lipophilic drugs in sugar glasses [41] or to improve primary drying rates and product quality of a concentrated formulation with high fill depth [42].

2.4 Importance of the freezing step in lyophilization

Recently, researchers began to stress the importance of the freezing step in lyophilization. A comprehensive review on the freezing step in lyophilization will be given in Chapter 2. In brief, the freezing process is shown to impact intra-vial and inter-vial uniformity [42], primary and secondary drying performance [43-44], the physical state of the sample [45], residual moisture content [46], or reconstitution time [47]. Moreover, there are several studies available that demonstrate the effect of the freezing process on protein stability [46, 48]. However, some of the results on protein stability are contradictory and thus, further investigations are necessary. Recently, it was demonstrated that the ice nucleation temperature during freezing inversely correlated with the recovery of protein activity [49]. Furthermore, the stability of nanoparticulate structures [50-52] is also affected by the freezing step. However, comprehensive studies are still lacking (see Chapter 6).

In order to encounter the up-scaling challenge with regard to the bias in ice nucleation, methods that allow for direct control of ice nucleation are essential [53]. Recently introduced methods, include electro-freezing [54], ultrasound-controlled ice nucleation [55], ice fog technique [56], or depressurization technique [57], among which, ice fog technique and depressurization technique appear to be the most promising with regard to operational handling or applicability in manufacturing scale freeze-drying.

2.5 Lyophilization above T_g'

According to the widespread opinion, collapse, defined as loss of the cake structure caused by viscous flow of the freeze-concentrate during drying [58], is considered detrimental due to the loss of the pharmaceutically elegant cake, high residual moisture levels, prolonged reconstitution times, and the negative impact on protein stability [10]. Hence, good pharmaceutical freeze-drying practice entails keeping the product temperature below the glass transition temperature (T_g') or the slightly higher collapse temperature (T_c) of the product during primary drying, even though drying at higher temperatures would highly accelerate the cost-intensive drying process [10]. Interestingly, there is experimental evidence that collapse itself does not necessarily negatively affect product quality. For instance, it was shown that primary drying above T_g' did not negatively impact the stability of recombinant Factor VIII (rFVIII) or α -amylase [59], lactate dehydrogenase (LDH) [59], and two proteinous toxins [60]. Recently, Schersch et al. [61] showed that protein stability of a monoclonal IgG antibody, a tissue-type plasminogen activator, and LDH in collapsed samples were not negatively affected, but in some cases even slightly improved in comparison to non-collapsed samples. Additionally, no effect on residual moisture levels or reconstitution times was observed. Moreover, the occurrence of collapse had no negative but sometimes even a positive effect on the storage stability of several proteins [58, 62].

In general, if product collapse does not diminish protein stability, still macroscopic collapse has to be prevented to guarantee a pharmaceutically acceptable product. This can be achieved by inclusion of a crystalline bulking agent which provides macroscopic support for the collapsing amorphous phase leading only to macroscopically invisible “small-scale” or micro collapse [10]. In this context, the weight ratio of amorphous excipient to crystalline bulking agent is critical, as an excess of amorphous component can inhibit crystallization of the bulking agent, which actually leads to a lowered T_g' . Promising results were reported for glycine/raffinose or glycine/trehalose mixtures [59], mannitol/sucrose mixtures [61] and lately, for phenylalanine/sucrose or phenylalanine/trehalose mixtures [63].

High-concentration protein formulations represent a special case and might be lyophilized above T_g' without considering the aforementioned limitations due to their pronounced difference between T_g' and T_c as a result of the highly viscous freeze-concentrated phase. Colandene et al. [64] reported for a high-concentration monoclonal antibody formulation lacking a crystalline bulking agent that the difference between T_c and T_g' and also the difference between the onset temperature of collapse and the complete collapse progressively went up as protein concentration increased. Thus, these formulations can be lyophilized above T_g' but below T_c with no detrimental effect on protein stability or cake appearance [64-65]. In this case it is essential to accurately determine T_c , usually by freeze-drying microscopy (FDM) [66]. As an alternative optical coherence tomography based FDM was introduced in order to allow for the measurement of T_c during freeze-drying in a vial [67].

2.6 Stabilization by thermal treatment/ high secondary drying temperatures

Recently, the concept of physical aging of an amorphous sample by thermal treatment to improve API stability was addressed in lyophilization

development [68]. During this temper process a glass will approach the “equilibrium glassy state” asymptotically leading to a change in the physical properties of the glass such as enthalpy, entropy, and volume [69]. Thereby, structural relaxation times are increased and global mobility is decreased. Consequently, as structural relaxation and reactivity are coupled, reaction rates should be minimized upon physical aging [68]. Although it is not assured that the underlying stabilization mechanism in amorphous solids can be fully correlated to structural relaxation dynamics (see section 2.8), there are several studies that support the concept of “stabilization by thermal treatment”. For instance, the chemical stability of maxolactam disodium improved over storage as temper temperatures and times post-lyophilization increased, although a greater initial degradation due to the temper phase was observed [68]. Moreover, post-lyophilization annealing also decelerated bimolecular degradation of sodium ethacrylate [70] and limited aggregation of an IgG1 fusion protein [71] during storage. The optimal treatment temperature can be identified by DSC experiments analyzing the maximum value in enthalpy recovery [70]. Beside these promising results for post-lyophilization tempering, it is also reported that the stability of maxolactam disodium was improved when secondary drying was performed at 60 °C rather than just 40 °C despite identical residual moisture [72]. In conclusion, performing secondary drying at increased temperatures does not only accelerate the final drying phase but might also improve storage stability.

2.7 Individual factors contributing to protein stability during lyophilization

It is well established, that freezing and drying induce different stresses that impact protein stability during lyophilization. Recently, the contribution of individual stress factors was scrutinized. Bhatnagar et al. [73] found that ice formation is the critical factor for LDH stability during freezing by separately

investigating the effect of temperature, ice formation, and freeze-concentration using a temperature-step approach. Moreover, Tang and Pikal [74] proved that proteins can be lyophilized well above T_g without the need for vitrification, as protein unfolding kinetics are highly coupled with system viscosity and thus, protein unfolding is very slow on the time scale of lyophilization, even at temperatures well above T_g . Luthra et al. [75] found that secondary drying is a critical step for LDH stability by differentiating between primary and secondary-drying stresses using a mini freeze-dryer. A more detailed study on the stresses during secondary drying established that both direct excipient interaction and vitrification are required for complete LDH stabilization [76]. In general, although these findings might not fully apply to other proteins, the described procedural methods are useful in order to investigate the factors contributing to the stability of one's protein formulation.

2.8 Enhanced understanding of stabilization mechanisms in the solid state

The stabilization of proteins in a sugar-glass matrix has been attributed to a thermodynamic mechanism according to which sugar molecules stabilized the native protein conformation via "water replacement" [77], or to a kinetic mechanism, which is based on the fact that degradation mechanisms in the vitrified, rigid sugar matrix will be limited [78]. The latter mechanism, the "vitrification hypothesis", coupled the stability of proteins or chemical compounds to the global mobility of the sugar glass matrix, often referred to as structural relaxation or α -relaxation [79]. There is much experimental evidence for the two hypotheses, but neither of both was capable to universally explain and predict stabilization in the glassy solid state [80-82].

Recently, it was shown that local dynamics in sugar glasses, in the term of β -relaxation, correlate strongly with protein or other drug stability [31-32, 68, 81-82]. In an up-to-date publication, Cicerone and

Douglas [83] argued that protein or drug stability is directly linked to high frequency β -relaxation processes of the sugar matrix as these β -relaxations are directly linked to local protein motions and to diffusion of small molecule reactive species in the glass. Moreover, they also showed that the enhanced protein conformational stability in sugar matrixes via “water replacement” does not have a significant impact on the degradation rate of the proteins. In addition, they also reported that protein stability increases continuously with the addition of anti-plasticizing compounds such as glycerol or sorbitol as β -relaxation time is prolonged whereas simultaneously glass transition temperature and α -relaxation time of the sugar matrix are decreased. Thus, the development of formulations or processes that allow for the modification of β -relaxation appears to be a highly interesting approach to improve the stability of drugs in amorphous lyophilisates.

2.9 Quality by design and process analytical technology in lyophilization

With the beginning of the 21st century the FDA started the initiative to shift from traditional rigorous testing of the final product to a “risk based approach” [84-85]. The aim is to design quality into the product (Quality by Design (QbD)) rather than to test quality into the product [86]. Thus, key factors for QbD are identification, understanding, and control of critical process and product parameters [86]. The development of a “design space” and a “control strategy” is required to ensure the production of a product of constant quality, promoting real-time release [86]. The measuring and control of critical process parameters requires the implementation of Process Analytical Technology (PAT) [85]. As these regulatory changes are increasingly adopted in pharmaceutical industry, QbD and PAT form leading issues in lyophilization development. This led to the development of a number of single vial or batch technologies in order to monitor critical product and process parameters.

Traditionally, thermocouples (TCs) or resistance temperature detectors (RTDs) have been utilized to measure product temperature in a few selected vials [88]. Recently, wireless temperatures sensors have been developed in order to allow for automatic loading in manufacturing scale freeze-drying [88]. But there is still need for more sensitive or non-invasive monitoring tools. Moreover, the three-dimensional monitoring of the lyophilization process in a vial would be highly beneficial (see Chapter 8).

A well-established method to determine the endpoint of primary drying is comparative pressure measurements using a capacitance manometer and a Pirani gauge. The technique was just recently shown to be the best choice among several endpoint determination methods [89]. Manometric temperature measurement (MTM), which is based on pressure rise data obtained by a Pirani gauge, was introduced as a non-invasive batch method to predict the average product temperature at the sublimation interface [90-91]. This method has also been used for the analysis of heat and mass transfer parameters [92] and dry layer resistance measurements [92]. Tang et al. [93] used MTM in combination with additional algorithms for the design of the SMART™ freeze-drier which allows for automatic optimization and control of the drying process. Likewise, Barresi and coworkers used a dynamic parameters estimation (DPE) approach in order to estimate several process data [94]. This approach, together with another mathematical model constitutes the basis for the LyoDriver™ technology [95].

Just recently, tunable diode laser absorption spectroscopy (TDLAS), which allows the in-line quantification of the water vapor flux from the chamber to the condenser, was introduced as PAT tool in lyophilization [96]. TDLAS was applied for primary drying endpoint determination [89], non-invasive product temperature measurements [97], vial heat transfer parameter determination [98], process optimization simplification [99], choked flow detection [100],

residual moisture monitoring during secondary drying [101], or for product mass transfer resistance determination, which can be used to estimate the effective pore radius of the dry layer [102]. Overall, TDLAS has great potential to support scale-up of lyophilization processes.

Moreover, near infrared (NIR) or Raman spectroscopy have gained attention as process analytical and process understanding tools in lyophilization despite the fact these two methods represent single-vial approaches with possible sensor placement problems. In combination these two techniques are capable to monitor the solid state of crystallizing excipients through the entire process, the onset of ice nucleation, and the onset and endpoint of ice sublimation [68-70]. In combination with an experimental design approach, these tools were also used for formulation and process optimization of a pharmaceutical product [103]. Just recently, NIR spectroscopy was utilized for in-line monitoring of protein unfolding and protein excipient interactions [104].

Several studies on the application of design space in lyophilization processes have been already published. At first, the design space was obtained by extensive experimental studies [105]. Later on, experimental work was reduced by the use of in-line measurements [106-107]. In a second step, process simulation instead of experimental testing was proposed, as this can significantly shorten the time for design space development [108-111]. Moreover, there are several methods available that consider parameter uncertainty, leading to “shrinkage” of the design space [108-109, 111]. Recently, Fissore et al. [112] described a method that considers changes in the design space with time and Bogner [113] presented a new approach to take vial-to-vial variations into account.

2.10 Novel container systems

As a response to the increasing market of high price biotech products, glass vials have become available that were especially developed for the

requirements of lyophilization. For instance, Schott forma vitrum AG introduced the TopLyo™ tubing vials, which have a customized geometry and carry a hydrophobic inner layer to maximize strength and minimize breakage and to improve heat transfer [114-115]. Furthermore, experiments with the TopLyo™ vials showed less disruption of the lyo cake, less dry material pulling up from the edge, improved cake aesthetics and reduced residual volume, and higher yield of reconstituted product [115]. Additionally, SGD S.A. introduced EasyLyo™, molded vials that are intended to improve heat transfer through the flattened vial bottom and the lighter vial mass [116]. Recently, Hibler et al. [117] compared the TopLyo™ and the EasyLyo™ vials with standard serum tubing and molded vials and found comparable heat transfer coefficients for all vials which is in contrast to traditional theories. However, for a polymer vial (TopPac™) a loss of ~30% in heat transfer was observed.

The development of cyclic olefin polymers (COP) and copolymers (COC) induced the trend to replace glass by break-resistant and surface inert plastic containers [118]. It has been found that lyophilization in the plastic containers led to improved uniformity within the lyophilisate [118]. However, the distinct advantages of break-resistance and low weight of plastic containers might not compensate for their high moisture permeability and new multilayer vials with an additional moisture barrier are approaching the market. Whatever container system different from a glass vial is to be used, such vials from new materials, syringes or cartridges, Lyoguard™ trays or containers, or 96-well plates, they represent new challenges in process development, as a process optimized for standard glass vials has to be reevaluated. The understanding of heat and mass transfer in these container system will help in the development of a robust lyophilization process, as currently reviewed by Patel and Pikal [119].

2.11 Scale-up, equipment issues and the dream of continuous processing

One of the main sources of scale-up difficulties is the difference of ice nucleation in laboratory-scale and manufacturing-scale freeze-drying [53]. This issue is to be addressed by the aforementioned introduction of technologies for controlled ice nucleation. Other critical aspects are differences in shelf-surface temperature distribution, differences in dryer load, differences in heat and mass transfer performance, differences in the contribution of radiative heat, and differences in chamber pressure [119-120]. Recently, the effect of dryer load on critical process parameters was studied on lab scale, pilot scale, and a clinical scale dryer [87]. Here, radiative heat effects, which were decreased for a full dryer load as the fraction of edge vials decreased, were the predominant factor. In general, the effect of radiative heat may be minimized by using trays that have no tray sides and by controlling chamber wall temperatures [121]. Moreover, freeze drying cycle conditions that are developed on a small scale dryer can lead to water vapor flux conditions that the full-scale equipment cannot handle ("choked flow"), resulting in loss of the ability to control chamber pressure [100].

Furthermore, several procedures that use a combination of experimental testing and numerical modeling have been described to facilitate scale-up [122-125]. Modeling of fluid dynamics was also performed to simulate pressure and pressure gradients or the velocity of flow at variable shelf separation distances [124, 126], to illustrate the influence of a sterilization pipe or of the isolation valve in the connection duct on flow velocity [126-127], to quantify the contribution of different heat transfer components at variable pressure and vial separation [128], or to predict 3D unsteady ice accumulation on the condenser [128]. These results might be very useful to reconsider the traditional design of the freeze-drier hardware.

The general problem of batch non-uniformity could be sorted out by switching to a continuous lyophilization process as it has already been established in the food industry, e.g. like the Conrad™ continuous freeze drying plant [129-130]. Here, the frozen product, most often in granular form, is deposited on trays, that enter the cabinet through a specially designed airlock system [130]. The trays are then pushed on heating plates through the various subsequent drying zones. Moreover, the cabinet is equipped with a number of vapor condensers that allow continuous de-icing. In this case, drying times fall in the order of minutes instead of hours or days [129]. Recently, the Meridion Technology GmbH introduced a continuous process line for pharmaceutical applications that combines a spray technology for the production of frozen microspheres with a dynamic bulk lyophilization technology [131]. However, this dream of switching from historical batch-type to continuous processing in pharmaceutical application would also require a fundamental change in mind.

2.12 Conclusion and outlook

In conclusion, the expanding range of pharmaceutical applications and the new approaches to understand and control the combination of formulation and process highlight the high importance of the lyophilization process. Moreover, by extending the formulation spectrum, introducing novel container systems, providing a more comprehensive understanding of stabilization mechanisms, and addressing the demands of QbD and PAT, the development of improved formulations and the design of optimized processes is highly facilitated, resulting in an increased product quality. This also includes that we can leave behind some traditional ways of thinking, like “never lyophilizing above the glass transition temperature” or traditional designs of containers and equipment.

3 Lyophilization of nucleic acid nanoparticles

With the rapid progress in gene therapy, lyophilization has gained importance for the preservation of nucleic acid based pharmaceuticals. In the following section, a brief overview on the basic concepts of pDNA and siRNA delivery in gene therapy will be given and the need for long-term stable formulations will be accentuated. Additionally, currently available scientific literature dealing with lyophilization of nucleic acid nanoparticles will be reviewed in brief.

3.1 pDNA and siRNA delivery in gene therapy and the need for long-term stable formulations

Gene therapy using nucleic acids (i.e. plasmid DNA, oligonucleotides or short interfering RNA) offers significant promise to cure, treat or prevent various incurable diseases [132-133] such as cardiovascular [134], neurological [135-136] and infectious disorders [137], severe combined immunodeficiency [138], cystic fibrosis [139-140], and an alternative method to traditional chemotherapy in tumor treatment [141-142].

In traditional gene therapy, gene substitutes (e.g. pDNA), which are transcriptionally fully competent genes, are introduced into the target cells to replace or substitute a specific gene resulting in the recovered production of a specific protein [133].

Since Fire et al. [143] discovered RNA interference (RNAi) in 1998, this technology has evolved to a promising tool for gene silencing in therapeutic applications [144]. Here, gene inhibitors (e.g. siRNA) are used in order to silence defective genes at the mRNA level [133]. There are two approaches for bringing siRNA to its effect: the stable expression of siRNA precursors or the direct delivery of stabilized synthetic siRNAs [145]. The mechanism of siRNA mediated RNA interference is schematically displayed in Figure 1-4. After entering the cytoplasm of the targeted cell, siRNA duplexes are incorporated

into the RNA-induced silencing complex (RISC). Argonaute 2, a multifunctional protein contained within RISC, unwinds the siRNA and the sense strand of the siRNA is cleaved [145-146]. Then, the activated RISC, which contains the antisense strand of the siRNA, selectively triggers cleavage of mRNA that is complementary to this the antisense strand [145-146].

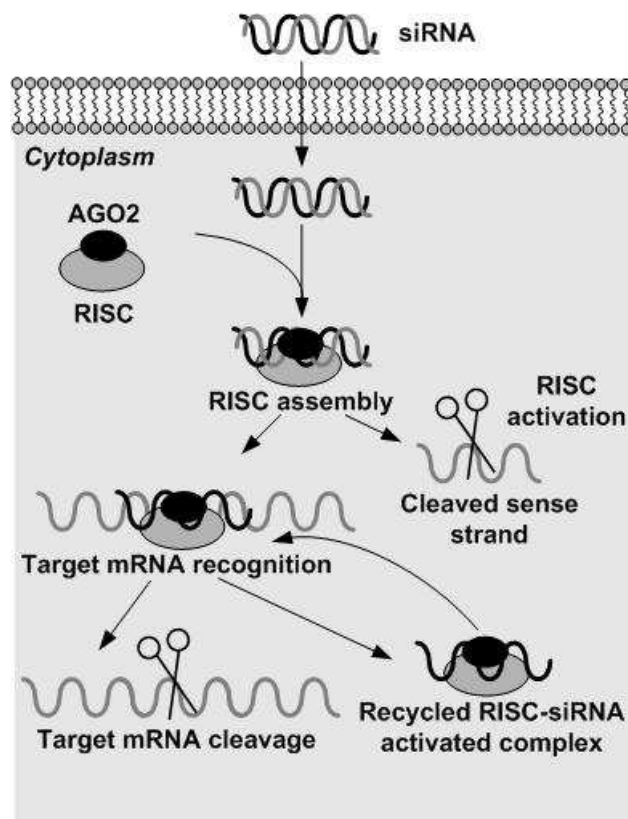


Figure 1-4: The mechanism of siRNA mediated RNA interference: siRNA is incorporated into the RNA-induced silencing complex (RISC) and the sense strand is cleaved by argonaute 2 (AGO2). The activated RISC-siRNA complex binds to and cleaves complementary mRNA and can then be recycled to further destruct identical mRNA targets. Redrawn from reference [145].

However, as unprotected nucleic acids are degraded in plasma within minutes, *in vivo* gene therapy necessitates gene delivery vectors that ideally protect their nucleic acid payload against nucleases and deliver the drug efficiently and selectively to the target site [147].

The most commonly used gene transfer systems applied in clinical trials are viral vectors due to their high gene transfer efficiency [148]. The limitations of

viral vectors in particular concerns about their safety, including immune and toxic reactions, the potential for viral recombination, low transgene loading capabilities, and high costs, render non-viral gene delivery systems a promising alternative [149]. Non-viral vectors are attractive because of their compound stability, easy preparation and purification at low cost, high flexibility, high loading capacity for DNA and as they have been proven safe, non-pathogenic and non-immunogenic in clinical trials [149-150]. Non-viral delivery vectors can be divided into two major classes: cationic lipids or cationic polymers, which interact electrostatically with the negatively charged nucleic acids and form condensed complexes (i.e. lipoplexes or polyplexes) [151-152].

Among the cationic polymers, linear polyethylenimine (LPEI) is the “golden standard” as very efficient gene expression both *in vitro* and *in vivo* has been observed [150, 153-154]. Here, the nano-scaled, positively charged polyplexes, formed between PEI and DNA molecules, enter the cells after cell adhesion by endocytosis and escape from the endo-lysosomal compartment by the so called “proton sponge effect” [155]. However, PEI exhibits polydispersity, significant toxicity, and limited degradability [152], and shows only modest delivery efficiency in the case of siRNA transfer [156-157]. Thus, for efficient and safe clinical siRNA delivery the development of modified polymers, which preferably allow for the establishment of structure activity relationships, is required [158-159]. Currently, a library of more than 300 sequence-defined, precise oligomers has been created by solid-phase assisted synthesis, among which a number of oligomers was highly efficient in siRNA transfer [160].

However, the major drawback of synthetic systems is the low pDNA or siRNA delivery efficiency compared to viral vectors particularly after *in vivo* application and the high instability in aqueous suspensions [161]. To date, the predominant focus has been on the development of more efficient polymers but other crucial

pharmaceutical aspects including quality control, long-term stability, and practicability in clinical trials have been rather ignored [152, 162-163].

A limiting factor for the clinical practicability of synthetic vectors is the requirement for freshly mixing nucleic acid solution with the carrier solution prior to administration because of the high instability of the nanoparticles in liquid environment resulting in particle aggregation, which is known to correlate with a loss of transfection efficiency [17, 52, 164]. The day-to-day preparation poses the risk of batch-to-batch variations, which is afflicted with safety concerns, and the inability to perform extensive quality control prior to the actual administration, due to time constraints [165-167]. Thus, the reproducible production of large standardized and long-term stable batches of pDNA or siRNA nanoparticulate complexes is a desirable goal.

3.2 The current status on lyophilization of nucleic acid nanoparticles

Lyophilization is a highly attractive way to achieve dried pharmaceuticals in general [8, 10] and nucleic acid-based formulations in particular [17]. The advantages of lyophilized formulations are their long-term storage stability at room temperature and their easy handling during shipping and storage [10]. Moreover, lyophilized formulations are ready to use after a simple reconstitution step [17, 161].

One essential prerequisite for the successful development of lyophilized nucleic acid complex formulations is the availability of nanoparticles at a constant and defined quality. The standard preparation of non-viral vectors is performed by mixing the nucleic acid solution with the cationic agent solution (i.e. lipid or polymer) via pipetting, which is restricted to relatively small batches (~ 250 μ L) [161]. This poorly defined and difficult to control preparation method is highly dependent on the operator and can result in the formation of highly heterogeneous complexes with a broad range in size and charge [168-169]. Therefore, the development of an up-scalable, controllable, and reproducible

method for the preparation of large, standardized batches of well-defined polyplexes is a necessary prerequisite for lyophilization development (see Chapter 4).

The lyophilization process involves two stresses, freezing and drying, that are known to be damaging to macromolecules and nanoparticles, unless appropriate stabilizers are used [161]. Table 1-1 provides an overview on excipients that are described in literature for the stabilization of nucleic acid nanoparticles.

Table 1-1: Overview on excipients that are described in literature for the stabilization of nucleic acid nanoparticles upon lyophilization.

Cationic agent	Nucleic acid	Excipient	Reference
DOTAP/DOPE	pDNA	0.5 M sucrose or trehalose	[170]
DAC-30™	pDNA	250 mM sucrose or 220 mM mannitol with 29 mM sucrose	[165]
DMRIE-C	pDNA	1% to 5% PEG, HES, mannitol, sucrose, trehalose, lactose, glucose	[171]
DOTAP/DOPE/DSPE-PEG	pDNA	12.6% sucrose, trehalose, inulin, dextran	[38]
Transferrin-PEI	pDNA	10% sucrose	[172]
PDMAEMA	pDNA	> 2.5% or 10% sucrose	[164, 173]
Branched-PEI	pDNA	1% Dextran 3000	[37]
PEI	ODN or pDNA	10 to 50 µg/mL trehalose, mannitol, or sucrose	[174]
Chitosan or <i>TransIT</i> -TKO	siRNA	10% sucrose	[175]
DOTAP/DOPE	siRNA	278 mM sucrose, trehalose, glucose, lactose	[176]
PEI F25	siRNA	5% glucose	[177]

Several mechanisms how cryoprotectants and lyoprotectants may stabilize nucleic acid nanoparticles during freezing and drying have been described but are still not fully understood [17, 178]. For cryoprotection during freezing “preferential exclusion”, “vitrification”, and “particle isolation” have been

discussed [17]. According to the “preferential exclusion hypothesis”, established for protein stabilization, solutes are preferentially excluded from the surface resulting in the formation of a stabilizing solvent layer [17, 178-179]. However, it is questionable if this hypothesis can be adapted to nucleic acid nanoparticles, as the relatively high amounts of cryoprotectants required point to a nonspecific bulk stabilization [17, 178-179]. Based on the “glass formation or vitrification hypothesis”, nucleic acid nanoparticles are entrapped in the amorphous gassy matrix when the sample is cooled below the glass transition temperature (T_g) limiting particle mobility and thus, preventing particle aggregation [17, 178]. As some sugars were able to preserve particle size at temperatures well above T_g vitrification cannot be the only stabilization mechanism [180]. The “particle isolation hypothesis” states that particles have to be sufficiently separated in the freeze-concentrate in order to inhibit particle aggregation, which is observed above a critical excipient to complex ratio [180]. However, these three mechanisms are not suitable to solely explain the stabilization of nucleic acid nanoparticles during freezing. Thus, the influence of freezing on nucleic acid nanoparticles and underlying stabilization mechanisms during freezing will be addressed in detail in Chapter 6.

Among synthetic delivery systems most literature is available on lyophilization of lipid DNA complexes or complexes based on polymers like poly(2-dimethylamino)ethyl methacrylate (PDMAEMA). In a very first study, Anchordoquy et al. [170] showed that pDNA-DOTAP/DOEP lipoplexes had to be lyophilized in the presence of quite high amounts of sucrose or trehalose (0.5 M) in order to maintain transfection activity and particle size. Similarly, Clement et al. [165] were able to successfully lyophilize pDNA lipoplexes in the presence of sucrose or mannitol sucrose mixtures (250 mM). Moreover, Cherng et al. [164] reported that a sucrose concentration $\geq 2.5\%$ was required to

maintain transfection efficiency and particle size of PDMAEMA polyplexes upon freeze-thawing and lyophilization. In a follow on study, they proved the long-term stability of these formulations at 4 °C and 20 °C for 10 months, but when stored at 40 °C for 2 months or longer PDMAEMA polyplexes aggregated and lost their transfection efficiency [173]. Besides the use of disaccharides, Hinrichs et al. [39] introduced oligosaccharides such as inulin or dextran as stabilizers for the lyophilization of pDNA-DOTAP/DOPE or -DOTAP/DOPE/DSPE-PEG lipoplexes. In this case, dextran was not suitable for sufficient protection of PEGylated lipoplexes. Allison et al. [171] used a variety of different stabilizers (PEG, HES, mannitol, sucrose, trehalose, lactose, glucose) in order to investigate their protective mechanism during lyophilization of cationic lipid-DNA complexes. They found that large polymeric sugars, such as HES, did completely fail to protect lipoplexes upon lyophilization and that excipients that crystallize during lyophilization, such as mannitol, are also less effective compared to disaccharides.

However, only little is reported in literature on the lyophilization of PEI-based polyplexes. Talsma et al. showed that 10% sucrose was required in order to reasonably maintain gene delivery efficient (~ 5fold decrease), whereas in the absence of sucrose the transfection efficiency dropped by a factor of 100-1000 [172]. Moreover, Anchordoquy et al. [37], introduced low molecular weight dextrans for the stabilization of pDNA-bPEI polyplexes at low osmolalities during lyophilization, which then could be concentrated tenfold upon rehydration in reduced volumes. However, in this context, particle integrity was only evaluated based on turbidity values. The only study on lyophilization of PEI based polyplexes that also investigated particle size, in addition to transfection efficiency or turbidity, was published by Brus et al. [174]. They observed only marginal changes in size and transfection efficiency for complexes of short oligodeoxynucleotides (ODN) and PEI after lyophilization in

the presence of low amounts of stabilizers (50 µg/mL). In contrast, pDNA-PEI complexes were found to drastically aggregate and biological activity decreased.

With regard to lyophilization of siRNA nanoparticles, only limited information is available, as well. Wu et al. [181] reported that siRNA-loaded lipid particles could be prepared by hydration of a stable freeze-dried matrix, containing siRNA and lipids. But here, only this preparation method was compared to an established direct preparation procedure and the influence of the lyophilization process itself on particle size and biological activity was not studied. Kundu et al. [183] evaluated the storage stability of lyophilized lipid-based siRNA nanosome formulations, but also did not investigate the influence of the lyophilization process. Moreover, Andersen et al. [175] described lyophilized chitosan or lipid siRNA formulations that are coated on cell culture plates as high-throughput screening tool and reported that 10% sucrose was required to sufficiently preserve particle size and gene silencing activity. Additionally, Yadava et al. [176] reported that siRNA lipoplexes could only be lyophilized with maintenance of transfection efficacy and with only a slight increase in particle size in the presence of stabilizers, such as glucose or sucrose. Similar results were published by Werth et al. [177], who showed that 5% glucose was required to preserve the transfection efficacy of low molecular weight polyethylenimine based siRNA polyplexes, but atomic force microscopy demonstrated a broadening of the polyplex particle size.

In conclusion, this brief overview on the current status of lyophilization of nucleic acid nanoparticles illustrates that until now neither plasmid DNA/ LPEI polyplexes (see Chapter 5) nor siRNA polyplexes (see Chapter 7) could be perfectly stabilized by lyophilization. Moreover, besides the preservation of transfection efficiency, crucial quality control parameters, such as retention of particle size, number of subvisible particles in a formulation, or relevant

characteristics of the lyophilisates, such as physical state, glass transition temperature or residual moisture content, have been rather ignored in the past. However, the possibility to produce long-term stable, transfection efficient pDNA or siRNA polyplexes with a defined pharmaceutical quality would be an important step closer from promising technology to application.

4 References

- [1] T. Jennings, *Lyophilization, Introduction and Basic Principles*, Interpharm Press, Englewood, USA, 1999.
- [2] H.R. Constantino, M.J. Pikal, Preface, in: H.R. Constantino, M.J. Pikal (Eds.) *Lyophilization of Biopharmaceuticals*, AAPS Press, Arlington, VA, USA, 2004.
- [3] B. Couriel, Freeze Drying: Past, Present, and Future, *PDA J. Pharm. Sci. Technol.*, 34 (1980) 352-357.
- [4] L. Rey, J.C. May, *Freeze Drying/ Lyophilization of Pharmaceutical and Biological Products*, in, Informa Healthcare, London, 2010.
- [5] E. Trappler, *Lyophilization Equipment*, in: H.R. Constantino, M.J. Pikal (Eds.) *Lyophilization of Biopharmaceuticals*, AAPS Press, Arlington, VA, USA, 2004.
- [6] S.L. Nail, S. Jiang, S. Chongprasert, S.A. Knopp, *Fundamentals of Freeze-Drying*, in: S.L. Nail, M.J. Akers (Eds.) *Development and Manufacture of Protein Pharmaceuticals*, Kluwer Academic/ Plenum Publisher, New York, 2002.
- [7] J.A. Searles, *Freezing and Annealing Phenomena in Lyophilization*, in: L. Rey, J.C. May (Eds.) *Freeze-Drying/Lyophilization of Pharmaceutical and Biological Products*, Marcel Dekker, Inc. USA, New York, 2004.
- [8] F. Franks, *Freeze-drying of bioproducts: putting principles into practice*, *Eur. J. Pharm. Biopharm.*, 45 (1998) 221-229.
- [9] F. Franks, T. Auffret, *Freeze-Drying of Pharmaceuticals and Biopharmaceuticals*, RSCPublishing, Cambridge, UK, 2007.
- [10] X. Tang, M. Pikal, *Design of Freeze-Drying Processes for Pharmaceuticals: Practical Advice*, *Pharm. Res.*, 21 (2004) 191-200.
- [11] M.J. Pikal, S. Rambhatla, R. Ramot, *The Impact of the Freezing Stage in Lyophilization: Effects of the Ice Nucleation Temperature on Process Design and Product Quality*, *Am. Pharm. Review*, 5 (2002) 48-53.
- [12] B.S. Chang, S.Y. Patro, *Freeze-drying process development for protein pharmaceuticals*, in: H.R. Constantino, M.J. Pikal (Eds.) *Lyophilization of Biopharmaceuticals*, AAPS Press, Arlington, VA, USA, 2004.

- [13] M.J. Pikal, S. Shah, M.L. Roy, R. Putman, The secondary drying stage of freeze drying: drying kinetics as a function of temperature and chamber pressure, *Int. J. Pharm.*, 60 (1990) 203-207.
- [14] J. Chesko, C. Fox, T. Dutil, T. Vedvick, S. Reed, Lyophilization and Stabilization of Vaccines, in: *Development of Vaccines*, John Wiley & Sons, Inc., 2011, pp. 385-397.
- [15] K.L. Scott, J. Lecak, J.P. Acker, Biopreservation of Red Blood Cells: Past, Present, and Future, *Trans. Med. Reviews*, 19 (2005) 127-142.
- [16] W. Abdelwahed, G. Degobert, S. Stainmesse, H. Fessi, Freeze-drying of nanoparticles: Formulation, process and storage considerations, *Adv. Drug Delivery Rev.*, 58 (2006) 1688-1713.
- [17] S.D. Allison, T.J. Anchordoquy, Lyophilization of Nonviral Gene Delivery Systems, in: M.A. Findeis (Ed.) *Nonviral Vectors for Gene Therapy: Methods and Protocols*, Humana Press Inc., New York, 2001, pp. 225-252.
- [18] P. Matejtschuk, M. Stanley, P. Jefferson, Freeze-drying of biological standards, in: L. Rey, J.C. May (Eds.) *Freeze Drying/ Lyophilization of Pharmaceutical and Biological Products*, Informa Healthcare, London, 2010, pp. 317-353.
- [19] T. Vasconcelos, B. Sarmiento, P. Costa, Solid dispersions as strategy to improve oral bioavailability of poor water soluble drugs, *Drug Discov. Today*, 12 (2007) 1068-1075.
- [20] S.V. Sastry, J.R. Nyshadham, J.A. Fix, Recent technological advances in oral drug delivery – a review, *Pharm. Sci. Technol. Today*, 3 (2000) 138-145.
- [21] C. Dexiang, Fast-dissolving tablet vaccines for enteric and other mucosal pathogens made by lyophilization - A case study in vaccine stabilization, in: *PepTalk 2012*, January 9 -13, San Diego, USA, 2012.
- [22] M. Geiger, W. Friess, Collagen sponge implants - applications, characteristics and evaluation, *PharmTech Europe*, February 1, (2002).
- [23] I. Ayensu, J.C. Mitchell, J.S. Boateng, Development and physico-mechanical characterisation of lyophilised chitosan wafers as potential protein drug delivery systems via the buccal mucosa, *Colloids Surf., B.*, 91 (2012) 258-265.
- [24] K.H. Bauer, A partially freeze-dried lyophilization technology for producing fast-melting tablets, *PharmTech Europe*, September 1, (2007).

- [25] K.H. Bauer, Manufacturing of a rapidly desintegrating presentation starting from a solid powder and a step of freeze drying, assignee: Pantec AG, (2005), EP20050803087.
- [26] J. Keith A, Preparation of peptide and protein powders for inhalation, *Adv. Drug Delivery Rev.*, 26 (1997) 3-15.
- [27] S.A. Shoyele, S. Cawthorne, Particle engineering techniques for inhaled biopharmaceuticals, *Adv. Drug Delivery Rev.*, 58 (2006) 1009-1029.
- [28] J.P. Amorij, A. Huckriede, J. Wilschut, H. Frijlink, W. Hinrichs, Development of Stable Influenza Vaccine Powder Formulations: Challenges and Possibilities, *Pharm. Res.*, 25 (2008) 1256-1273.
- [29] S. Claus, T. Schoenbrodt, C. Weiler, W. Friess, Novel dry powder inhalation system based on dispersion of lyophilisates, *Eur. J. Pharm. Sci.*, 43 (2011) 32-40.
- [30] E.Y. Shalaev, T.D. Johnson-Elton, L. Chang, M.J. Pikal, Thermophysical Properties of Pharmaceutically Compatible Buffers at Sub-Zero Temperatures: Implications for Freeze-Drying, *Pharm. Res.*, 19 (2002) 195-201.
- [31] M.T. Cicerone, C.L. Soles, Fast Dynamics and Stabilization of Proteins: Binary Glasses of Trehalose and Glycerol, *Biophys. J.*, 86 (2004) 3836-3845.
- [32] L. Chang, D. Shepherd, J. Sun, X. Tang, M.J. Pikal, Effect of sorbitol and residual moisture on the stability of lyophilized antibodies: Implications for the mechanism of protein stabilization in the solid state, *J. Pharm. Sci.*, 94 (2005) 1445-1455.
- [33] T.W. Randolph, Phase separation of excipients during lyophilization: Effects on protein stability, *J. Pharm. Sci.*, 86 (1997) 1198-1203.
- [34] A.M. Padilla, M.J. Pikal, The study of phase separation in amorphous freeze-dried systems, part 2: Investigation of raman mapping as a tool for studying amorphous phase separation in freeze-dried protein formulations, *J. Pharm. Sci.*, 100 (2011) 1467-1474.
- [35] S.D. Allison, M.C. Manning, T.W. Randolph, K. Middleton, A. Davis, J.F. Carpenter, Optimization of storage stability of lyophilized actin using combinations of disaccharides and dextran, *J. Pharm. Sci.*, 89 (2000) 199-214.
- [36] W. Garzon-Rodriguez, R.L. Koval, S. Chongprasert, S. Krishnan, T.W. Randolph, N.W. Warne, J.F. Carpenter, Optimizing storage stability of lyophilized recombinant human interleukin-11 with disaccharide/hydroxyethyl starch mixtures, *J. Pharm. Sci.*, 93 (2004) 684-696.

- [37] T.J. Anchordoquy, T.K. Armstrong, M.d.C. Molina, Low molecular weight dextrans stabilize nonviral vectors during lyophilization at low osmolalities: concentrating suspensions by rehydration to reduced volumes, *Journal of Pharmaceutical Sciences*, 94 (2005) 1226-1236.
- [38] W.L.J. Hinrichs, N.N. Sanders, S.C. De Smedt, J. Demeester, H.W. Frijlink, Inulin is a promising cryo- and lyoprotectant for PEGylated lipoplexes, *J. Controlled Release*, 103 (2005) 465-479.
- [39] D.L. Teagarden, D.S. Baker, Practical aspects of lyophilization using non-aqueous co-solvent systems, *Eur. J. Pharm. Sci.*, 15 (2002) 115-133.
- [40] S. Vessot, J. Andrieu, A Review on Freeze Drying of Drugs with tert-Butanol (TBA) Water Systems: Characteristics, Advantages, Drawbacks, *Drying Technol.*, 30 (2012) 377-385.
- [41] D.J. Van Drooge, W.L.J. Hinrichs, H.W. Frijlink, Incorporation of lipophilic drugs in sugar glasses by lyophilization using a mixture of water and tertiary butyl alcohol as solvent, *J. Pharm. Sci.*, 93 (2004) 713-725.
- [42] J. Liu, T. Viverette, M. Virgin, M. Anderson, P. Dalal, A Study of the Impact of Freezing on the Lyophilization of a Concentrated Formulation with a High Fill Depth, *PDA J. Pharm. Sci. Technol.*, 10 (2005) 261-272.
- [43] M.J. Pikal, S. Rambhatla, R. Ramot, The impact of the freezing stage in lyophilization: effects of the ice nucleation temperature on process design and product quality, *Am. Pharm. Rev.*, 5 (2002) 48-53.
- [44] J.A. Searles, J.F. Carpenter, T.W. Randolph, The ice nucleation temperature determines the primary drying rate of lyophilization for samples frozen on a temperature-controlled shelf, *J. Pharm. Sci.*, 90 (2001) 860-871.
- [45] X. Liao, R. Krishnamurthy, R. Suryanarayanan, Influence of Processing Conditions on the Physical State of Mannitol—Implications in Freeze-Drying, *Pharm. Res.*, 24 (2007) 370-376.
- [46] S. Passot, I.C. Trelea, M. Marin, M. Galan, G.J. Morris, F. Fonseca, Effect of Controlled Ice Nucleation on Primary Drying Stage and Protein Recovery in Vials Cooled in a Modified Freeze-Dryer, *J. Biomech. Eng.*, 131 (2009) 074511-074515.
- [47] J.A. Searles, Freezing and annealing phenomena in lyophilization, in: L. Rey, J.C. May (Eds.) *Freeze Drying/ Lyophilization of Pharmaceutical and Biological Products*, Informa Healthcare, London, 2010, pp. 52-81.

- [48] J.-M. Sarciaux, S. Mansour, M.J. Hageman, S.L. Nail, Effects of buffer composition and processing conditions on aggregation of bovine IgG during freeze-drying, *J. Pharm. Sci.*, 88 (1999) 1354-1361.
- [49] T. Cochran, S.L. Nail, Ice nucleation temperature influences recovery of activity of a model protein after freeze drying, *J. Pharm. Sci.*, 98 (2009) 3495-3498.
- [50] M.K. Lee, M.Y. Kim, S. Kim, J. Lee, Cryoprotectants for freeze drying of drug nano-suspensions: Effect of freezing rate, *J. Pharm. Sci.*, 98 (2009) 4808-4817.
- [51] F. De Jaeghere, E. Allémann, J. Feijen, T. Kissel, E. Doelker, R. Gurny, Freeze-Drying and Lyopreservation of Diblock and Triblock Poly(Lactic Acid)- Poly(Ethylene Oxide) (PLA-PEO) Copolymer Nanoparticles, *PDA J. Pharm. Sci. Technol.*, 5 (2000) 473-483.
- [52] T.J. Anchordoquy, L.G. Girouard, J.F. Carpenter, D.J. Kroll, Stability of lipid/DNA complexes during agitation and freeze- thawing, *J. Pharm. Sci.*, 87 (1998) 1046-1051.
- [53] S. Rambhatla, R. Ramot, C. Bhugra, M. Pikal, Heat and mass transfer scale-up issues during freeze drying: II. Control and characterization of the degree of supercooling, *AAPS PharmSciTech*, 5 (2004) 54-62.
- [54] A. Petersen, H. Schneider, G. Rau, B. Glasmacher, A new approach for freezing of aqueous solutions under active control of the nucleation temperature, *Cryobiology*, 53 (2006) 248-257.
- [55] K. Nakagawa, A. Hottot, S. Vessot, J. Andrieu, Influence of controlled nucleation by ultrasounds on ice morphology of frozen formulations for pharmaceutical proteins freeze-drying, *Chem. Eng. Res. Des.*, 45 (2006) 783-791.
- [56] S. Patel, C. Bhugra, M. Pikal, Reduced Pressure Ice Fog Technique for Controlled Ice Nucleation during Freeze-Drying, *AAPS PharmSciTech*, 10 (2009) 1406-1411.
- [57] B.M. Rampersad, R.R. Sever, B. Hunek, T.H. Gasteyer, Freeze-dryer and method of controlling the same, Patent Application Publication, United States, 2010.
- [58] D.Q. Wang, J.M. Hey, S.L. Nail, Effect of collapse on the stability of freeze-dried recombinant factor VIII and α -amylase, *J. Pharm. Sci.*, 93 (2004) 1253-1263.
- [59] K. Chatterjee, E.Y. Shalaev, R. Suryanarayanan, Partially crystalline systems in lyophilization: II. Withstanding collapse at high primary drying temperatures and impact on protein activity recovery, *J. Pharm. Sci.*, 94 (2005) 809-820.

- [60] S. Passot, F. Fonseca, N. Barbouche, M. Marin, M. Alarcon-Lorca, D. Rolland, M. Rapaud, Effect of Product Temperature During Primary Drying on the Long-Term Stability of Lyophilized Proteins, *PDA J. Pharm. Sci. Technol.*, 12 (2007) 543-553.
- [61] K. Schersch, O. Betz, P. Garidel, S. Muehlau, S. Bassarab, G. Winter, Systematic investigation of the effect of lyophilizate collapse on pharmaceutically relevant proteins I: Stability after freeze-drying, *J. Pharm. Sci.*, 99 (2010) 2256-2278.
- [62] K. Schersch, O. Betz, P. Garidel, S. Muehlau, S. Bassarab, G. Winter, Systematic investigation of the effect of lyophilizate collapse on pharmaceutically relevant proteins II: Stability during storage at elevated temperatures, *J. Pharm. Sci.*, in press (2012).
- [63] T. Bosch, N. Erlewein, W. Gerhard, Influence of formulation composition on physical characteristics of collapse-dried lyophilizates, in: *Freeze-drying of pharmaceuticals and biologicals*, September 28 - October 01, Garmisch-Partenkirchen, Germany, 2010.
- [64] J.D. Colandene, L.M. Maldonado, A.T. Creagh, J.S. Vrettos, K.G. Goad, T.M. Spitznagel, Lyophilization cycle development for a high-concentration monoclonal antibody formulation lacking a crystalline bulking agent, *J. Pharm. Sci.*, 96 (2007) 1598-1608.
- [65] S.M. Patel, S. Pansare, Effect of drying a high concentration lyophilized MAb at, above, and below T_g , in: *PepTalk 2012*, January 9-13, 2012, San Diego, USA, 2012.
- [66] E. Meister, H. Gieseler, Freeze-dry microscopy of protein/sugar mixtures: Drying behavior, interpretation of collapse temperatures and a comparison to corresponding glass transition Data, *J. Pharm. Sci.*, 98 (2009) 3072-3087.
- [67] K. Greco, Accurate prediction of collapse temperature using optical coherence tomography (OCT) based freeze drying microscopy, in: *PepTalk 2012*, January 9-13, 2012, San Diego, USA, 2012.
- [68] A.M. Abdul-Fattah, K.M. Dellerman, R.H. Bogner, M.J. Pikal, The effect of annealing on the stability of amorphous solids: Chemical stability of freeze-dried moxalactam, *J. Pharm. Sci.*, 96 (2007) 1237-1250.
- [69] I.M. Hodge, Physical aging in polymer glasses, *Science*, 267 (1995) 1945- 1947.
- [70] B. Wang, M.J. Pikal, The impact of thermal treatment on the stability of freeze dried amorphous pharmaceuticals: I. dimer formation in sodium ethacrylate, *J. Pharm. Sci.*, 99 (2010) 663-682.

- [71] B. Wang, M.T. Cicerone, Y. Aso, M.J. Pikal, The impact of thermal treatment on the stability of freeze-dried amorphous pharmaceuticals: II. aggregation in an IgG1 fusion protein, *J. Pharm. Sci.*, 99 (2010) 683-700.
- [72] M.J. Pikal, Thermometric seminars on calorimetry in materials sciences, Stockholm, Sweden, 1996.
- [73] B.S. Bhatnagar, M.J. Pikal, R.H. Bogner, Study of the individual contributions of ice formation and freeze-concentration on isothermal stability of lactate dehydrogenase during freezing, *J. Pharm. Sci.*, 97 (2008) 798-814.
- [74] X. Tang, M.J. Pikal, Measurement of the Kinetics of Protein Unfolding in Viscous Systems and Implications for Protein Stability in Freeze-Drying, *Pharm. Res.*, 22 (2005) 1176-1185.
- [75] S. Luthra, J.-P. Obert, D.S. Kalonia, M.J. Pikal, Investigation of drying stresses on proteins during lyophilization: Differentiation between primary and secondary-drying stresses on lactate dehydrogenase using a humidity controlled mini freeze-dryer, *J. Pharm. Sci.*, 96 (2007) 61-70.
- [76] S. Luthra, J.-P. Obert, D.S. Kalonia, M.J. Pikal, Impact of critical process and formulation parameters affecting in-process stability of lactate dehydrogenase during the secondary drying stage of lyophilization: A mini freeze dryer study, *J. Pharm. Sci.*, 96 (2007) 2242-2250.
- [77] S.J. Prestrelski, N. Tedeschi, T. Arakawa, J.F. Carpenter, Dehydration-induced conformational transitions in proteins and their inhibition by stabilizers, *Biophys. J.*, 65 (1993) 661-671.
- [78] F. Franks, R. Hatley, S. Mathias, Materials science and the production of shelf-stable biologicals, *Biopharm.*, 4 (1991) 40– 42 , 55.
- [79] S. Yoshioka, Y. Aso, Correlations between molecular mobility and chemical stability during storage of amorphous pharmaceuticals, *J. Pharm. Sci.*, 96 (2007) 960-981.
- [80] L. Chang, D. Shepherd, J. Sun, D. Ouellette, K.L. Grant, X. Tang, M.J. Pikal, Mechanism of protein stabilization by sugars during freeze-drying and storage: Native structure preservation, specific interaction, and/or immobilization in a glassy matrix?, *J. Pharm. Sci.*, 94 (2005) 1427-1444.

- [81] B. Wang, S. Tchessalov, M.T. Cicerone, N.W. Warne, M.J. Pikal, Impact of sucrose level on storage stability of proteins in freeze-dried solids: II. Correlation of aggregation rate with protein structure and molecular mobility, *J. Pharm. Sci.*, 98 (2009) 3145-3166.
- [82] M.J. Pikal, D. Rigsbee, M.L. Roy, D. Galreath, K.J. Kovach, B. Wang, J.F. Carpenter, M.T. Cicerone, Solid state chemistry of proteins: II. The correlation of storage stability of freeze-dried human growth hormone (hGH) with structure and dynamics in the glassy solid, *J. Pharm. Sci.*, 97 (2008) 5106-5121.
- [83] M.T. Cicerone, J.F. Douglas, [small beta]-Relaxation governs protein stability in sugar-glass matrices, *Soft Matter*, 8 (2012) 2983-2991.
- [84] Pharmaceutical cGMPs for the 21st century - A risk based approach, Food and Drug Administration (FDA), 2002.
- [85] Guidance for Industry, PAT - A Framework for Innovative Pharmaceutical Development, Manufacturing and Quality Assurance, Food and Drug Administration (FDA), 2004.
- [86] Q8 (R2) - Pharmaceutical Development, International Conference in Harmonization (ICH), 2009.
- [87] S.M. Patel, F. Jameel, M.J. Pikal, The effect of dryer load on freeze drying process design, *J. Pharm. Sci.*, 99 (2010) 4363-4379.
- [88] S. Schneid, H. Gieseler, Evaluation of a New Wireless Temperature Remote Interrogation System (TEMPRIS) to Measure Product Temperature During Freeze Drying, *AAPS PharmSciTech*, 9 (2008) 729-739.
- [89] S. Patel, T. Doen, M. Pikal, Determination of End Point of Primary Drying in Freeze-Drying Process Control, *AAPS PharmSciTech*, 11 (2010) 73-84.
- [90] N. Milton, M.J. Pikal, M.L. Roy, S.L. Nail, Evaluation of Manometric Temperature Measurement as a Method of Monitoring Product Temperature During Lyophilization, *PDA J. Pharm. Sci. Technol.*, 51 (1997) 7-16.
- [91] X. Tang, S. Nail, M. Pikal, Evaluation of manometric temperature measurement, a process analytical technology tool for freeze-drying: Part I, product temperature measurement, *AAPS PharmSciTech*, 7 (2006) E95-E103.

- [92] X. Tang, S. Nail, M. Pikal, Evaluation of manometric temperature measurement (MTM), a process analytical technology tool in freeze drying, part III: Heat and mass transfer measurement, *AAPS PharmSciTech*, 7 (2006) E105-E111.
- [93] X. Tang, S.L. Nail, M.J. Pikal, Freeze-Drying Process Design by Manometric Temperature Measurement: Design of a Smart Freeze-Dryer, *Pharm. Res.*, 22 (2005) 685-700.
- [94] S.A. Velardi, V. Rasetto, A.A. Barresi, Dynamic Parameters Estimation Method: Advanced Manometric Temperature Measurement Approach for Freeze-Drying Monitoring of Pharmaceutical Solutions, *Ind. Eng. Chem. Res.*, 47 (2008) 8445-8457.
- [95] R. Pisano, D. Fissore, S.A. Velardi, A.A. Barresi, In-line optimization and control of an industrial freeze-drying process for pharmaceuticals, *J. Pharm. Sci.*, 99 (2010) 4691-4709.
- [96] S.M. Patel, M. Pikal, Process Analytical Technologies (PAT) in freeze-drying of parenteral products, *PDA J. Pharm. Sci. Technol.*, 14 (2009) 567-587.
- [97] S.C. Schneid, H. Gieseler, W.J. Kessler, M.J. Pikal, Non-invasive product temperature determination during primary drying using tunable diode laser absorption spectroscopy, *J. Pharm. Sci.*, 98 (2009) 3406-3418.
- [98] W.Y. Kuu, S.L. Nail, G. Sacha, Rapid determination of vial heat transfer parameters using tunable diode laser absorption spectroscopy (TDLAS) in response to step-changes in pressure set-point during freeze-drying, *J. Pharm. Sci.*, 98 (2009) 1136-1154.
- [99] W.Y. Kuu, S.L. Nail, Rapid freeze-drying cycle optimization using computer programs developed based on heat and mass transfer models and facilitated by tunable diode laser absorption spectroscopy (TDLAS), *J. Pharm. Sci.*, 98 (2009) 3469-3482.
- [100] S.M. Patel, S. Chaudhuri, M.J. Pikal, Choked flow and importance of Mach I in freeze-drying process design, *Chem. Eng. Sci.*, 65 (2010) 5716-5727.
- [101] S. Schneid, H. Gieseler, W. Kessler, M.J.A.A. Pikal, S.D. Meeting, CA, USA, 2007., Tunable Diode Laser Absorption Spectroscopy (TDLAS) as a residual moisture monitor for the secondary drying stage of freeze drying., in: *AAPS Annual Meeting, San Diego, USA, 2007.*
- [102] W.Y. Kuu, K.R. O' Bryan, L.M. Hardwick, T.W. Paul, Product mass transfer resistance directly determined during freeze-drying cycle runs using tunable diode laser absorption spectroscopy (TDLAS) and pore diffusion model, *PDA J. Pharm. Sci. Technol.*, 16 (2011) 343-357.

- [103] T.R.M. De Beer, M. Wiggernhorn, A. Hawe, J.C. Kasper, A. Almeida, T. Quinten, W. Friess, G. Winter, C. Vervaet, J.P. Remon, Optimization of a pharmaceutical freeze-dried product and its process using an experimental design approach and innovative process analyzers, *Talanta*, 83 (2011) 1623-1633.
- [104] S. Pieters, T. De Beer, J.C. Kasper, D. Boulpaep, O. Waszkiewicz, M. Goodarzi, C. Tistaert, W. Friess, J.-P. Remon, C. Vervaet, Y. Vander Heyden, Near-Infrared Spectroscopy for In-Line Monitoring of Protein Unfolding and Its Interactions with Lyoprotectants during Freeze-Drying, *Anal. Chem.*, 84 (2011) 947-955.
- [105] B.S. Chang, N.L. Fischer, Development of an Efficient Single-Step Freeze-Drying Cycle for Protein Formulations, *Pharm. Res.*, 12 (1995) 831-837.
- [106] L.M. Hardwick, C. Paunicka, M.J. Akers, Critical factors in the design and optimization of lyophilisation processes, *Innovations Pharm. Technol.*, (2008) 70– 74.
- [107] S.L. Nail, J.A. Searles, Elements of quality by design in development and scale-up of freeze-dried parenterals, *Biopharm. Int.*, 21 (2008) 44-52.
- [108] R.H. Bogner, K. Quian, M.J. Pikal, Freeze dry process optimization from a statistical analysis of the impact of variation in critical drying parameters: Accepting risk at a known cost., in: *Freeze-drying of pharmaceuticals and biologicals*, August 7-9, Breckenridge, USA, 2008.
- [109] R.H. Bogner, M.J. Pikal, The incredible shrinking design space: Using risk tolerance to define design space for primary drying, in: *Freeze-drying of pharmaceuticals and biologicals*, September 28 - October 01, Garmisch-Partenkirchen, Germany, 2010.
- [110] S.L. Nail, Experience with tunable diode laser absorption spectroscopy at laboratory and production scales, in: *Freeze-drying of pharmaceuticals and biologicals*, September 28 - October 01, Garmisch-Partenkirchen, Germany, 2010.
- [111] A. Giordano, A.A. Barresi, D. Fissore, On the use of mathematical models to build the design space for the primary drying phase of a pharmaceutical lyophilization process, *J. Pharm. Sci.*, 100 (2011) 311-324.
- [112] D. Fissore, R. Pisano, A.A. Barresi, Advanced approach to build the design space for the primary drying of a pharmaceutical freeze-drying process, *J. Pharm. Sci.*, 100 (2011) 4922-4933.

- [113] R.H. Bogner, Vial-to-vial variation for freeze-dried products during primary drying: a new way to approach design space, in: *PepTalk 2012*, January 9 -13, San Diego, USA, 2012.
- [114] SCHOTT begins mass production of TopLyo(TM) pharma packaging for freeze-dried drugs, <http://www.schott.com/english/news/press.html?NID=2690>, accessed: 2012-02-27, SCHOTT forma vitrum AG, 2009.
- [115] C. Dietrich, F. Maurer, H. Roehl, W. Friess, Pharmaceutical packaging for lyophilization applications, in: L. Rey, J.C. May (Eds.) *Freeze Drying/ Lyophilization of Pharmaceutical and Biological Products*, Informa Healthcare, London, 2010.
- [116] Introducing EasyLyo(TM) simply stronger vials, http://www.sgd-pharma.com/spip.php?article258&var_recherche=easylyo, accessed: 2012-02-27, SGD S.A., 2010.
- [117] S. Hibler, C. Wagner, H. Gieseler, Vial freeze-drying, part 1: New insights into heat transfer characteristics of tubing and molded vials, *J. Pharm. Sci.*, 101 (2012) 1189-1201.
- [118] F.L. DeGrazio, Closure and Container Considerations in Lyophilization, in: L. Rey, J.C. May (Eds.) *Freeze Drying/ Lyophilization of Pharmaceutical and Biological Products*, Informa Healthcare, London, 2010, pp. 396-412.
- [119] S. Patel, M. Pikal, Emerging Freeze-Drying Process Development and Scale-up Issues, *AAPS PharmSciTech*, 12 (2011) 372-378.
- [120] A.A. Barresi, Overcoming common lyophilization scale-up issues, *PharmTech Europe*, July 15, (2011).
- [121] K.H. Gan, R. Bruttini, O.K. Crosser, A.I. Liapis, Freeze-drying of pharmaceuticals in vials on trays: effects of drying chamber wall temperature and tray side on lyophilization performance, *Int. J. Heat Mass Transfer*, 48 (2005) 1675-1687.
- [122] S.C. Tsinontides, P. Rajniak, D. Pham, W.A. Hunke, J. Placek, S.D. Reynolds, Freeze drying—principles and practice for successful scale-up to manufacturing, *Int. J. Pharm.*, 280 (2004) 1-16.
- [123] T. Kramer, D.M. Kremer, M.J. Pikal, W.J. Petre, E.Y. Shalaev, L.A. Gatlin, A procedure to optimize scale-up for the primary drying phase of lyophilization, *J. Pharm. Sci.*, 98 (2009) 307-318.
- [124] V. Rasetto, D.L. Marchisio, D. Fissore, A.A. Barresi, On the use of a dual-scale model to improve understanding of a pharmaceutical freeze-drying process, *J. Pharm. Sci.*, 99 (2010) 4337-4350.

- [125] D. Fissore, A.A. Barresi, Scale-up and Process Transfer of Freeze-Drying Recipes, *Drying Technol.*, 29 (2011) 1673-1684.
- [126] A. Ganguly, A.A. Alexeenko, S.L. Nail, Simulations of vapor flow in freeze-drying: does convection matter in scale-up, in: *PepTalk 2012*, January 9 -13, San Diego, USA, 2012.
- [127] A.A. Alexeenko, A. Ganguly, S.L. Nail, Computational analysis of fluid dynamics in pharmaceutical freeze-drying, *J. Pharm. Sci.*, 98 (2009) 3483-3494.
- [128] A.A. Alexeenko, A. Ganguly, S.L. Nail, Modelling and simulation of vapor/ice dynamics in pharmaceutical freeze-drying, in: *Freeze-drying of pharmaceuticals and biologicals*, September 28 - October 01, Garmisch-Partenkirchen, Germany, 2010.
- [129] L. Rey, Glimpses into the realm of freeze-drying: classical issues and new ventures, in: L. Rey, J.C. May (Eds.) *Freeze Drying/ Lyophilization of Pharmaceutical and Biological Products*, Informa Healthcare, London, 2010.
- [130] Conrad(TM) the continuous freeze drying plant, <http://www.niro.com/niro/cmsdoc.nsf/WebDoc/ndkk5hvgk3continuousplantconrad>, accessed: 2012-03-06, GEA niro.
- [131] Meridion process Line, Meridion SprayCon, and Meridion LyoMotion, <http://www.meridion-technologies.com/>, accessed: 2012-03-06, Meridion Technologies GmbH.
- [132] J.K. Raty, J.T. Pikkarainen, T. Wirth, S. Yla-Herttuala, Gene therapy: the first approved gene-based medicines, molecular mechanisms and clinical indications, *Curr. Mol. Pharmacol.*, 1 (2008) 13-23.
- [133] A. Pathak, S. Patnaik, K.C. Gupta, Recent trends in non-viral vector-mediated gene delivery, *Biotechnol. J.*, 4 (2009) 1559-1572.
- [134] V.J. Dzau, K. Beatt, G. Pompilio, K. Smith, Current perceptions of cardiovascular gene therapy, *Am. J. Cardiol.*, 92 (2003) 18-23.
- [135] E.A. Burton, J.C. Glorioso, D.J. Fink, Gene therapy progress and prospects: Parkinson's disease, *Gene Ther.*, 10 (2003) 1721-1727.
- [136] J.M. Alisky, B.L. Davidson, Gene Therapy for Amyotrophic Lateral Sclerosis and Other Motor Neuron Diseases, *Hum. Gene Ther.*, 11 (2000) 2315-2329.
- [137] B.A. Bunnell, R.A. Morgan, Gene therapy for infectious diseases, *Clin. Microbiol. Rev.*, 11 (1998) 42-56.

- [138] W. Qasim, H.B. Gaspar, A.J. Thrasher, Progress and prospects: gene therapy for inherited immunodeficiencies, *Gene Ther.*, 16 (2009) 1285-1291.
- [139] U. Griesenbach, E.W. Alton, Cystic fibrosis gene therapy: successes, failures and hopes for the future, *Expert Rev. Resp. Med.*, 3 (2009) 363-371.
- [140] M. Conese, S.D. Gioia, S. Castellani, Gene therapy for cystic fibrosis, *Expert Opin. Ther. Pat.*, 18 (2008) 929-943.
- [141] A. El-Aneed, Current strategies in cancer gene therapy, *Eur. J. Pharmacol.*, 498 (2004) 1-8.
- [142] M. Gottesman, Cancer gene therapy, *The Lancet Oncology*, 6 (2005) 75-75.
- [143] A. Fire, S. Xu, M.K. Montgomery, S.A. Kostas, S.E. Driver, C.C. Mello, Potent and specific genetic interference by double-stranded RNA in *Caenorhabditis elegans*, *Nature*, 391 (1998) 806-811.
- [144] K. Gao, L. Huang, Nonviral Methods for siRNA Delivery, *Mol. Pharmaceut.*, 6 (2008) 651-658.
- [145] K.A. Whitehead, R. Langer, D.G. Anderson, Knocking down barriers: advances in siRNA delivery, *Nat. Rev. Drug Discov.*, 8 (2009) 129-138.
- [146] T.A. Rand, S. Petersen, F. Du, X. Wang, Argonaute2 Cleaves the Anti-Guide Strand of siRNA during RISC Activation, *Cell*, 123 (2005) 621-629.
- [147] H.G. Abdelhady, S. Allen, M.C. Davies, C.J. Roberts, S.J.B. Tendler, P.M. Williams, Direct real-time molecular scale visualisation of the degradation of condensed DNA complexes exposed to DNase I, *Nucl. Acids Res.*, 31 (2003) 4001-4005.
- [148] M.L. Edelstein, M.R. Abedi, J. Wixon, Gene therapy clinical trials worldwide to 2007 - an update, *J. Gene Med.*, 9 (2007) 833-842.
- [149] M.A. Mintzer, E.E. Simanek, Nonviral Vectors for Gene Delivery, *Chem. Rev.*, 109 (2008) 259-302.
- [150] M.E. Bonnet, P. Erbacher, A.L. Bolcato-Bellemin, Systemic delivery of DNA or siRNA mediated by linear polyethylenimine (L-PEI) does not induce an inflammatory response, *Pharm. Res.*, 25 (2008) 2972-2982.
- [151] D.W. Pack, A.S. Hoffman, S. Pun, P.S. Stayton, Design and development of polymers for gene delivery, *Nat. Rev. Drug Discov.*, 4 (2005) 581-593.

- [152] D. Schaffert, E. Wagner, Gene therapy progress and prospects: synthetic polymer-based systems, *Gene Ther.*, 15 (2008) 1131-1138.
- [153] L. Wightman, R. Kircheis, V. Rossler, S. Carotta, R. Ruzicka, M. Kursa, E. Wagner, Different behavior of branched and linear polyethylenimine for gene delivery in vitro and in vivo, *J. Gene Med.*, 3 (2001) 362-372.
- [154] M. Breunig, U. Lungwitz, R. Liebl, J. Klar, B. Obermayer, T. Blunk, A. Goepferich, Mechanistic insights into linear polyethylenimine-mediated gene transfer, *Biochim. Biophys. Acta*, 1770 (2007) 196-205.
- [155] N.D. Sonawane, F.C.J. Szoka, A.S. Verkman, Chloride Accumulation and Swelling in Endosomes Enhances DNA Transfer by Polyamine-DNA Polyplexes, *J. Biol. Chem.* 278 (2003) 44826-44831.
- [156] M. Meyer, E. Wagner, Recent Developments in the Application of Plasmid DNA-Based Vectors and Small Interfering RNA Therapeutics for Cancer, *Hum. Gene Ther.*, 17 (2006) 1062-1076.
- [157] A. Kwok, S.L. Hart, Comparative structural and functional studies of nanoparticle formulations for DNA and siRNA delivery, *Nanomed. Nanotechnol. Biol. Med.*, 7 (2011) 210-219.
- [158] E. Wagner, Polymers for siRNA Delivery: Inspired by Viruses to be Targeted, Dynamic, and Precise, *Acc. Chem. Res.*, doi: 10.1021/ar2002232 (2012).
- [159] C. Troiber, E. Wagner, Nucleic Acid Carriers Based on Precise Polymer Conjugates, *Bioconjugate Chem.*, 22 (2011) 1737-1752.
- [160] D. Schaffert, C. Troiber, E.E. Salcher, T. Fröhlich, I. Martin, N. Badgujar, C. Dohmen, D. Edinger, R. Kläger, G. Maiwald, K. Farkasova, S. Seeber, K. Jahn-Hofmann, P. Hadwiger, E. Wagner, Solid-Phase Synthesis of Sequence-Defined T-, i-, and U-Shape Polymers for pDNA and siRNA Delivery, *Angew. Chem. Int. Ed.*, 50 (2011) 8986-8989.
- [161] T.J. Anchordoquy, G.S. Koe, Physical stability of nonviral plasmid-based therapeutics, *J. Pharm. Sci.*, 89 (2000) 289-296.
- [162] S.C. De Smedt, J. Demeester, W.E. Hennink, Cationic Polymer Based Gene Delivery Systems, *Pharm. Res.*, 17 (2000) 113-126.

- [163] T.J. Anchordoquy, S.D. Allison, M.d.C. Molina, L.G. Girouard, T.K. Carson, Physical stabilization of DNA-based therapeutics, *Drug Discov. Today*, 6 (2001) 463-470.
- [164] J.-Y. Cherng, P. van de Wetering, H. Talsma, D.J.A. Crommelin, W.E. Hennink, Freeze-Drying of Poly((2-dimethylamino)ethyl Methacrylate)-Based Gene Delivery Systems, *Pharm. Res.*, 14 (1997) 1838-1841.
- [165] J. Clement, K. Kiefer, A. Kimpfler, P. Garidel, R. Peschka-Süss, Large-scale production of lipoplexes with long shelf-life, *Eur. J. Pharm. Biopharm.*, 59 (2005) 35-43.
- [166] C. Brus, E. Kleemann, A. Aigner, F. Czubayko, T. Kissel, Stabilization of oligonucleotide-polyethylenimine complexes by freeze-drying: physicochemical and biological characterization, *J. Controlled Release*, 95 (2004) 119-131.
- [167] T.J. Anchordoquy, T.K. Armstrong, M.D.C. Molina, S.D. Allison, Y. Zhang, M.M. Patel, Y.K. Lentz, G.S. Koe, Formulation considerations for DNA-based therapeutics, in: D.R. Lu, S. Oeie (Eds.) *Cellular Drug Delivery*, Humana Press Inc. , Totowa, 2004, pp. 237-263.
- [168] Y. Maitani, Y. Aso, A. Yamada, S. Yoshioka, Effect of sugars on storage stability of lyophilized liposome/DNA complexes with high transfection efficiency, *Int. J. Pharm.*, 356 (2008) 69-75.
- [169] O. Zelphati, C. Nguyen, M. Ferrari, J. Felgner, Y. Tsai, P.L. Felgner, Stable and monodisperse lipoplex formulations for gene delivery, *Gene Ther.*, 5 (1998) 1272-1282.
- [170] T.J. Anchordoquy, J.F. Carpenter, D.J. Kroll, Maintenance of Transfection Rates and Physical Characterization of Lipid/DNA Complexes after Freeze-Drying and Rehydration, *Arch. Biochem. Biophys.*, 348 (1997) 199-206.
- [171] S.D. Allison, T.J. Anchordoquy, Mechanisms of protection of cationic lipid-DNA complexes during lyophilization, *J. Pharm. Sci.*, 89 (2000) 682-691.
- [172] H. Talsma, J.-Y. Cherng, H. Lehrmann, M. Kursa, M. Ogris, W.E. Hennink, M. Cotten, E. Wagner, Stabilization of gene delivery systems by freeze-drying, *Int. J. Pharm.*, 157 (1997) 233-238.
- [173] J.-Y. Cherng, H. Talsma, D. Crommelin, W. Hennink, Long Term Stability of Poly((2-dimethylamino)ethyl Methacrylate)-Based Gene Delivery Systems, *Pharm. Res.*, 16 (1999) 1417-1423.

- [174] C. Brus, E. Kleemann, A. Aigner, F. Czubayko, T. Kissel, Stabilization of oligonucleotide–polyethylenimine complexes by freeze-drying: physicochemical and biological characterization, *J. Controlled Release*, 95 (2004) 119-131.
- [175] M.Ø. Andersen, K.A. Howard, S.R. Paludan, F. Besenbacher, J. Kjems, Delivery of siRNA from lyophilized polymeric surfaces, *Biomaterials*, 29 (2008) 506-512.
- [176] P. Yadava, M. Gibbs, C. Castro, J. Hughes, Effect of Lyophilization and Freeze-thawing on the Stability of siRNA-liposome Complexes, *AAPS PharmSciTech*, 9 (2008) 335-341.
- [177] S. Werth, B. Urban-Klein, L. Dai, S. Höbel, M. Grzelinski, U. Bakowsky, F. Czubayko, A. Aigner, A low molecular weight fraction of polyethylenimine (PEI) displays increased transfection efficiency of DNA and siRNA in fresh or lyophilized complexes, *J. Controlled Release*, 112 (2006) 257-270.
- [178] T.J. Anchordoquy, T.K. Armstrong, M.d.C. Molina, S.D. Allison, Y. Zhang, M.M. Patel, Y.K. Lentz, G.S. Koe, Physical Stabilization of Plasmid DNA-based Therapeutics During Freezing and Drying, in: H.R. Costantino, P. M.J. (Eds.) *Lyophilization of Biopharmaceuticals*, AAPS Press, Arlington, VA, 2004, pp. 605-641.
- [179] J.F. Carpenter, J.H. Crowe, The mechanism of cryoprotection of proteins by solutes, *Cryobiology*, 25 (1988) 244-255.
- [180] S.D. Allison, M.d.C. Molina, T.J. Anchordoquy, Stabilization of lipid/DNA complexes during the freezing step of the lyophilization process: the particle isolation hypothesis, *Biochim. Biophys. Acta - Biomembranes*, 1468 (2000) 127-138.
- [181] S. Wu, L. Putral, M. Liang, H.-I. Chang, N. Davies, N. McMillan, Development of a Novel Method for Formulating Stable siRNA-Loaded Lipid Particles for in-vivo use, *Pharm. Res.*, 26 (2009) 512-522.
- [182] A.K. Kundu, P.K. Chandra, S. Hazari, G. Ledet, Y.V. Pramar, S. Dash, T.K. Mandal, Stability of lyophilized siRNA nanosome formulations, *Int. J. Pharm.* 423 (2011) 525-534.

Chapter 2

The freezing step in lyophilization

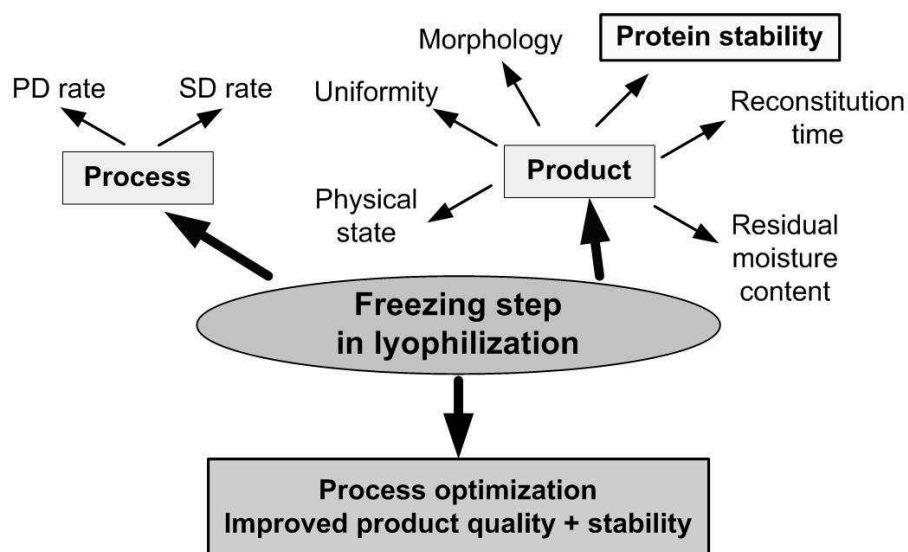
The following chapter has been published as review article in the European Journal of Pharmaceutics and Biopharmaceutics and appears in this thesis with the journal`s permission:

Julia Christina Kasper and Wolfgang Friess

The freezing step in lyophilization: Physico-chemical fundamentals, freezing methods and consequences on process performance and quality attributes of biopharmaceuticals

Eur. J. Pharm. Biopharm. 78 (2011) 248-263

Graphical Abstract



Abstract

Lyophilization is a common, but cost-intensive, drying process to achieve protein formulations with long-term stability. In the past, typical process optimization has focused on the drying steps and the freezing step was rather ignored. However, the freezing step is an equally important step in lyophilization, as it impacts both process performance and product quality.

While simple in concept, the freezing step is presumably the most complex step in lyophilization. Therefore, in order to get a more comprehensive understanding of the processes that occur during freezing, the physico-chemical fundamentals of freezing are first summarized. The available techniques that can be used to manipulate or directly control the freezing process in lyophilization are also reviewed. In addition, the consequences of the freezing step on quality attributes, such as sample morphology, physical state of the product, residual moisture content, reconstitution time, and performance of the primary and secondary drying phase, are discussed. A special focus is given to the impact of the freezing process on protein stability.

This review aims to provide the reader with an awareness of not only the importance but also the complexity of the freezing step in lyophilization and its impact on quality attributes of biopharmaceuticals and process performance. With a deeper understanding of freezing and the possibility to directly control or at least manipulate the freezing behavior, more efficient lyophilization cycles can be developed, and the quality and stability of lyophilized biopharmaceuticals can be improved.

Keywords

Lyophilization, freeze-drying, modifications of the freezing step, influence on process performance, influence on product quality, influence on protein stability

1 Introduction

Lyophilization also known as freeze-drying is an important and well-established process to improve the long-term stability of labile drugs, especially therapeutic proteins [1]. About 50% of the currently marketed biopharmaceuticals are lyophilized, representing the most common formulation strategy [2]. In the freeze-dried solid state, chemical or physical degradation reactions are inhibited or sufficiently decelerated, resulting in an improved long-term stability [3]. Besides the advantage of better stability, lyophilized formulations also provide easy handling during shipping and storage [1].

A traditional lyophilization cycle consists of three steps; freezing, primary drying, and secondary drying [1]. During the freezing step, the liquid formulation is cooled until ice starts to nucleate, which is followed by ice growth. This results in the separation of most of the water into ice crystals from a matrix of glassy and/or crystalline solutes [4,5]. During primary drying, the crystalline ice formed during freezing is removed by sublimation. Therefore, the chamber pressure is reduced well below the vapor pressure of ice, and the shelf temperature is raised to supply the heat removed by ice sublimation [6]. At the completion of primary drying, the product can still contain approximately 15–20% of unfrozen water, which is then desorbed during the secondary drying stage, usually at elevated temperature and low pressure, to finally allow the desired low moisture content to be achieved [7].

In general, lyophilization is a very time- and energy-intensive drying process [8]. Freezing is typically over within a few hours, while drying often requires days. Within the drying phase, however, secondary drying is relatively short (~hours) compared to primary drying (~days) [1,4]. For that reason, lyophilization cycle development has typically focused on optimizing the primary drying step, i.e. shortening the primary drying time by adjusting the shelf temperature and/or chamber pressure without influencing product quality [5,9]. Although freezing is

one of the most critical stages during lyophilization, the importance of the freezing process has rather been neglected in the past [10].

The freezing step is of paramount importance. Freezing itself is the major dehydration step in lyophilization [6]. Solvent water is removed from the liquid formulation in the form of a pure solid ice phase, leading to a dramatic concentration of the solutes [11,12]. Moreover, the kinetics of ice nucleation and crystal growth determine the physical state and morphology of the frozen cake and consequently the final properties of the freeze-dried product [11-13]. Ice morphology is directly correlated with the rate of sublimation in primary and secondary drying [14]. In addition, freezing is a critical step with regards to the biological activity and stability of the active pharmaceutical ingredients (API), especially pharmaceutical proteins [1].

While simple in concept, the freezing process is presumably the most complex but also the most important step in the lyophilization process [10]. To meet this challenge, a thorough understanding of the physico-chemical processes that occur during freezing is required. Moreover, in order to optimize the freeze-drying process and product quality, it is vital to control the freezing step. But the random nature of ice nucleation makes this challenging. However, several approaches have been developed to trigger ice nucleation during freezing.

The purpose of this review is to provide the reader with an awareness of the importance and complexity of the physico-chemical processes that occur during freezing. Furthermore, currently available freezing techniques are summarized, and an attempt is made to address the consequences of the freezing procedure on process performance and product quality. A special focus is given to the critical factors that influence protein stability. Understanding and controlling the freezing step in lyophilization will lead to optimized, more efficient lyophilization cycles as well as products with an improved stability.

2 Physico-chemical fundamentals of freezing

In general, freezing is defined as the process of ice crystallization from supercooled water [15]. The freezing process first involves the cooling of the solution until ice nucleation occurs. Ice crystals begin to grow at a certain rate, resulting in freeze-concentration of the solution, a process that can result in both crystalline and amorphous solids, or in mixtures [11]. The following sections (2.1–2.3) summarize the physico-chemical fundamentals of freezing.

First, the distinction between cooling rate and freezing rate should be emphasized. The cooling rate is defined as the rate at which a solution is cooled. The freezing rate is the rate of post-nucleation ice crystal growth, which is largely determined by the amount of supercooling prior to nucleation [16,17]. Therefore, the freezing rate of a formulation is not necessarily related to its cooling rate [18].

2.1 Freezing phenomena: supercooling, ice nucleation and ice crystal formation

In order to review the physico-chemical processes that occur during freezing of pure water, the relationship between time and temperature during freezing is displayed in Figure 2-1. When pure water is cooled at atmospheric pressure, it does not freeze spontaneously at its equilibrium freezing point (0 °C) [19]. The retention of the liquid state below the equilibrium freezing point of the solution is termed as “supercooling” [19]. Supercooling (represented by line A) always occurs during freezing, often in the range of 10–15 °C or more [12,18]. The degree of supercooling depends on the solution properties and process conditions and is defined as the difference between the equilibrium ice formation temperature and the actual temperature at which ice crystals first form [1,6,11,20]. As discussed later, it is necessary to distinguish between “global supercooling”, in which the entire liquid volume exhibits a similar level of

supercooling, and “local supercooling”, in which only a small volume of the liquid is supercooled [14]. Supercooling is a non-equilibrium, meta-stable state, which is similar to an activation energy necessary for the nucleation process [21]. Due to density fluctuations from Brownian motion in the supercooled liquid water, water molecules form clusters with relatively long-living hydrogen bonds [22] with similar molecular arrangements as in ice crystals [11,15]. Because this process is energetically unfavorable, these clusters break up rapidly [15]. The probability for these nuclei to grow in both number and size is more pronounced at lowered temperatures [15]. Once the critical mass of nuclei is reached, ice crystallization occurs rapidly in the entire system (point B) [15,21,22].

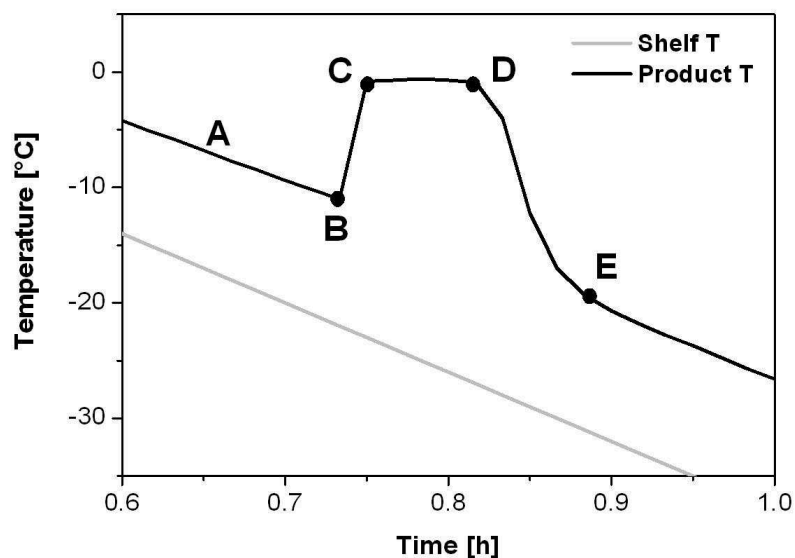


Figure 2-1: Temperature profile measured with a thermocouple for a pure water sample during shelf-ramped freezing at $-1\text{ }^{\circ}\text{C}/\text{min}$. The figure was created from own data by the authors.

The limiting nucleation temperature of water, referred to as the “homogeneous nucleation temperature”, appears to be at about $-40\text{ }^{\circ}\text{C}$. At this temperature, the pure water sample will contain at least one spontaneously formed active water nucleus, capable of initiating ice crystal growth [11]. However, in all pharmaceutical solutions and even in sterile-filtered water for injection, the nucleation observed is “heterogeneous nucleation”. Meaning that ice-like

clusters are formed via adsorption of layers of water on “foreign impurities” [6,11]. Such “foreign impurities” may be the surface of the container, particulate contaminants present in the water, or even sites on large molecules such as proteins [23–25].

Once stable ice crystals are formed, their growth proceeds by the addition of molecules to the interface [22]. However, only a fraction of the freezable water freezes immediately, as the supercooled water can absorb only 15 cal/g of the 79 cal/g of heat given off by the exothermic ice formation [12,22]. Therefore, once crystallization begins, the product temperature rises rapidly to near the equilibrium freezing point [12,26]. After the initial ice network has formed (point C), additional heat is removed from the solution by further cooling, and the remaining water freezes when the previously formed ice crystals grow [12]. Ice crystal growth is controlled by the latent heat release and the cooling rate which the sample is exposed to [22]. The freezing time is the time taken from the completed ice nucleation to the time of removal of latent heat (from point C to point D). The temperature drops when the freezing of the sample is completed (point E) [21].

The number of ice nuclei formed, the rate of ice growth, and the ice crystals' size depend on the degree of supercooling [14,20]. The higher the degree of supercooling, the higher the rate of nucleation and the faster the effective rate of freezing. This results in a high number of small ice crystals. In contrast, at a lower degree of supercooling, one observes a lower number of large ice crystals [14,19]. The rate of ice crystal growth can be expressed as a function of the degree of supercooling [23]. For example, for water for injection showing a degree of supercooling of 10 ± 3 °C, an ice crystal growth rate of about 5.2 cm/s results [23]. In general, a slower cooling rate leads to a faster freezing rate and vice versa. Thus, in case of cooling rate versus freezing rate, it has to be kept in mind “slow is fast and fast is slow”.

Nevertheless, one has to distinguish between the two basic freezing mechanisms; global supercooling and directional solidification. When global supercooling occurs, which is typically the case for shelf-ramped freezing, the entire liquid volume achieves a similar level of supercooling and solidification progresses through the already nucleated volume [12,14]. In contrast, directional solidification occurs when a small volume is supercooled, which is the case for high cooling rates, e.g., with nitrogen immersion. Here, the nucleation and solidification front are in close proximity in space and time and move further into non-nucleated solution. In this case, a faster cooling rate will lead to a faster freezing rate [12,14].

However, ice nucleation in general is a stochastically event [6,18]. Ice nucleation and, in consequence, ice crystal size distribution will differ from vial-to-vial, resulting in a large sample heterogeneity within one batch [6,14,27]. During freezing, the growth of ice crystals within one vial can also be heterogeneous, influencing intra-vial uniformity [5].

So far 10 polymorphic forms of ice have been described. However, at temperatures and pressures typical for lyophilization, the stable crystal structure of ice is limited to the hexagonal type, in which each oxygen atom is tetrahedrally surrounded by four other oxygen atoms [23]. The fact that the ice crystal morphology is a unique function of the nucleation temperature was first reported by Tammann in 1925 [28]. In general, three different types of growth of ice crystals around nuclei can be observed in solution [15]. (i) If the water molecules are given sufficient time, they arrange themselves regularly into hexagonal crystals, called dendrites; (ii) if the water molecules are incorporated randomly into the crystal at a fast rate, “irregular dendrites” or axial columns that originate from the center of crystallization are formed; (iii) at higher cooling rates, many ice spears can originate from the center of crystallization without side branches, referred to as spherulites. However, the ice morphology

depends not only on the degree of supercooling but also on the freezing mechanism. It is reported that “global solidification” creates spherulitic ice crystals, whereas “directional solidification” results in directional lamellar morphologies with connected pores [12,14]. While some solutes will have almost no effect on ice structure, other solutes can affect not only the ice structure but also its physical properties [19]. Based on Raoult’s Law, the presence of solutes at high concentrations will result in a depression of the freezing point of the solution and in a faster ice nucleation because of the promotion of heterogeneous nucleation. This leads to an enormously lowered degree of supercooling [21].

2.2 Crystallization and vitrification of solutes

The hexagonal structure of ice is of great importance in the lyophilization of pharmaceutical formulations, while most solutes cannot fit in the dense structure of the hexagonal ice as it forms [23]. Consequently, the concentration of the solute constituents of the formulation is increased in the interstitial region between the growing ice crystals. This is referred to as “cryoconcentration” [11,12]. If this separation does not occur, a solid solution is formed with a greatly reduced vapor pressure and the formulation cannot be lyophilized [23]. The total solute concentration increases rapidly and is only a function of the temperature and independent of the initial concentration [4]. For example, for an isotonic saline solution a 20-fold concentration increase is reported when cooled to $-10\text{ }^{\circ}\text{C}$, and all other components in a mixture show similar concentration increases [4]. Upon further cooling, the solution will increase to a critical concentration, above which the concentrated solution will either undergo eutectic freezing or vitrification [7].

An eutectic mixture is formed by the simple crystallization of solutes from cryoconcentrated solution [19]. For example, mannitol, glycine, sodium chloride, and phosphate buffers are known to crystallize upon freezing, if present as the

major component [12]. When such a solution is cooled, pure ice crystals will form first. Two phases are present, ice and freeze-concentrated solution. The composition is determined via the equilibrium freezing curve of water in the presence of the solute (Figure 2-2).

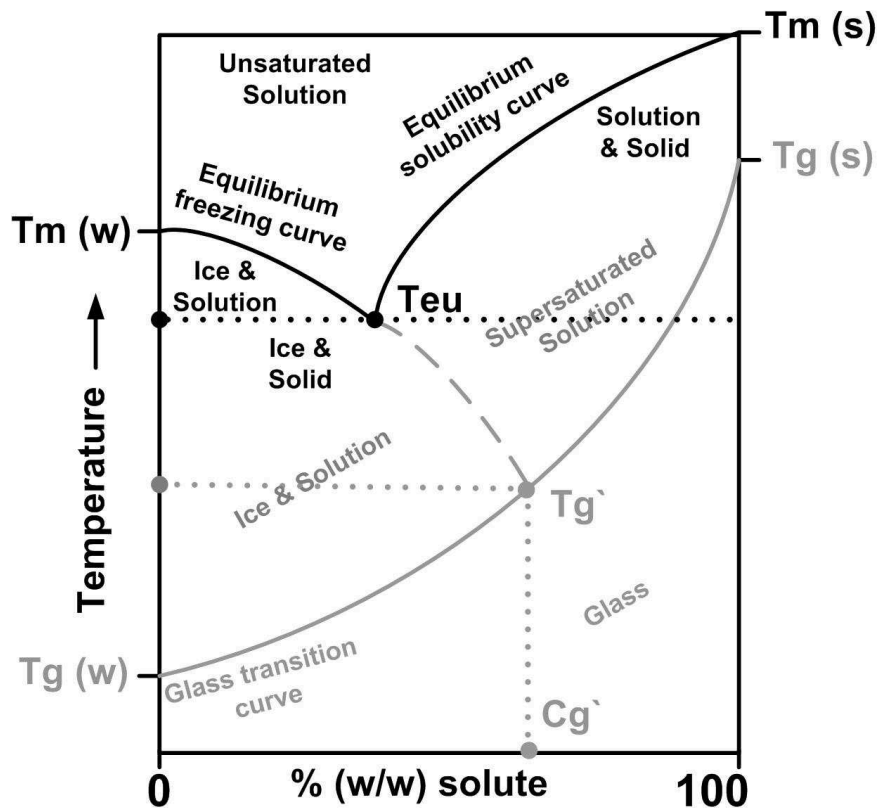


Figure 2-2: State diagram for a water (w)/solute (s) system. $T_m(w)$ and $T_m(s)$: melting temperatures of water and solute, T_{eu} : eutectic temperature, $T_g(w)$ and $T_g(s)$: glass transition temperature of water and solute and T_g' : glass transition temperature of the maximally freeze-concentrated solution. Crystallization (black drawings) of a solute occurs below T_{eu} . In the case of vitrification (gray drawings), the solute does not crystallize at T_{eu} , freeze-concentration proceeds and transits into a glass state at T_g' . The figure was modified from Ref. [18]

The system will then follow the specific equilibrium freezing curve, as the solute content increases as more pure water is removed via ice formation. The lowest temperature at which the solute remains a liquid is the eutectic melting temperature (T_{eu}). As the solution reaches T_{eu} and a certain solute concentration (C_{eu}), the freezing curve will meet the solubility curve. Here, the freeze-concentrate is saturated and eutectic freezing, which means solute

crystallization, will occur [7,19]. Only below T_{eu} , the system can be completely solidified [19]. The T_{eu} and C_{eu} are independent of the initial concentration of the solution [7]. In general, the lower the solubility of a given solute in water, the higher the T_{eu} [19]. A general rule for multi-component systems is that the crystallization of any component is influenced, i.e. hindered, by other components [11]. In practice, similar to the supercooling of water, only a few solutes will spontaneously crystallize at T_{eu} [11]. Such delayed crystallization of solutes from a freezing solution is termed supersaturation and can lead to an even more extreme freeze-concentration [11]. Moreover, supersaturation can inhibit complete crystallization, leading to a meta-stable glass formation (e.g., mannitol) [12,23]. It is also possible that crystalline states exist in a mixture of different polymorphs or as hydrates [11]. For example, mannitol can exist in the form of several polymorphs (α , β and δ), and under certain processing conditions, it can crystallize as a monohydrate [11].

The phase behavior is extremely different for polyhydroxy compounds, like sucrose, which do not crystallize at all from a freezing solution in real time [11]. The fact that sucrose does not crystallize during freeze-concentration is an indication of its extremely complex crystal structure [11]. The interactions between sugar -OH groups and those between sugar -OH groups and water molecules are closely similar in energy and configuration, resulting in very low nucleation probabilities [11]. In this case, water continues to freeze beyond the eutectic melting temperature, and the solution becomes increasingly supersaturated and viscous [11]. The increasing viscosity slows down ice crystallization until at some characteristic temperature no further freezing occurs [11]. This is called glassification or vitrification [18]. The temperature at which the maximal freeze-concentration (C_g) occurs is referred to as the glass transition temperature (T_g) [11,29]. This is the intersection of the freezing point depression curve and the glass transition or isoviscosity curve, shown in the

“supplemented phase diagram” [30] or “state diagram” (Figure 2-2) [11]. T_g' is the point on the glass transition curve, representing a reversible change between a viscous, rubber-like liquid and a rigid glass system [19]. In the region of the glass transition, the viscosity of the freeze-concentrate changes about four orders of magnitude over a temperature range of a few degrees [19]. T_g' depends on the composition of the solution, but is independent of the initial concentration [4,11,27]. For example, the maximal freeze-concentration of sucrose is a concentration of 72–73% [31]. In addition to T_g' , the collapse temperature (T_c) of a product is used to define more precisely the temperature at which a structural loss of the product will occur. In general, T_c is several degrees higher than T_g' as the high viscosity of the sample close to T_g' will prevent viscous flow [10]. The glassy state is a solid solution of concentrated solutes and unfrozen, amorphous water. It is thermodynamically unstable with respect to the crystal form, but the viscosity is high enough, in the order of 10^{14} Pa s, so that any motion is in the order of mm/year [4,11,29].

The important difference between eutectic crystallization and vitrification is that the interstitial between the ice crystal matrices in crystalline material consists of an intimate mixture of small crystals of ice and solute, whereas the interstitial region in amorphous solutes consists of solid solution and unfrozen, amorphous water [19,23]. Therefore, in crystalline material, nearly all water is frozen and can easily be removed during primary drying without requiring secondary drying [19]. However, in amorphous solutes, about 20% of unfrozen water is associated with the solid solution, which must be removed by a diffusion process during secondary drying [19]. Moreover, the T_{eu} for crystalline material and the T_g' , respectively T_c , for amorphous material define the maximum allowable product temperature during primary drying [19]. Eutectic melting temperatures are relatively high compared to glass transition temperatures, allowing a higher product temperature during primary drying and resulting in

more efficient drying processes [19]. If the product temperature exceeds this critical temperature, crystalline melting or amorphous collapse will occur. This loss of structure in the freeze-dried products is termed “cake collapse” [11,19].

2.3 Phase separation and other types of freezing behavior

A property characteristic of multi-component aqueous solutions (particularly those containing at least one polymer component) is the liquid–liquid phase separation during freezing into two liquid equilibrium phases, which are enriched in one component [11,19]. This phase separation behavior has been reported for aqueous solutions of polymers such as PEG/dextran or PVP/dextran but is also reported for proteins and excipients [32,33]. When a critical concentration of the solutes is reached, the enthalpically unfavorable interactions between the solutes exceed the favorable entropy of a solution with complete miscibility [34]. Another proposed explanation is that solutes have different effects on the structure of water, leading to phase separation [35].

Besides the separation into two amorphous phases, two other types of phase separation are stated in literature; crystallization of amorphous solids and amorphization from crystalline solids [18]. Crystallization of amorphous solids often occurs when meta-stable glasses are formed during freezing. Upon extremely fast cooling, a compound that normally would crystallize during slower freezing is entrapped as an amorphous, meta-stable glass in the freeze-concentrate [12,23]. However, with subsequent heating above T_g , it will undergo crystallization, which is the basis for annealing during freeze-drying (see Section 3.3) [19]. Without annealing, the meta-stable glass can crystallize spontaneously out of the amorphous phase during drying or storage [18]. Amorphization from crystalline solids, that can be buffer components or stabilizers, predominantly occurs during the drying step and not during the freezing step [18,36].

Additionally, lyotropic liquid crystals, which have the degree of order between amorphous and crystalline, are reported to form as a result of freeze-concentration. However, their influence on critical quality attributes of the lyophilized product is not clarified [19]. Clathrates, also termed gas hydrates, are also known to form, especially in the presence of non-aqueous co-solvents, when the solute alters the structure of the water [23].

3 Modifications of the freezing step

As aforementioned, the ice nucleation temperature defines the size, number, and morphology of the ice crystals formed during freezing. Therefore, the statistical nature of ice nucleation poses a major challenge for process control during lyophilization. This highlights the importance of a controlled, reproducible and homogeneous freezing process. Several methods have already been developed in order to control and optimize the freezing step. Some only tend to influence ice nucleation by modifying the cooling rate, and some just statistically increase the mean nucleation temperature. Few others allow a true control of the nucleation at the desired nucleation temperature.

3.1 Shelf-ramped freezing

Shelf-ramped freezing is a conventional freezing condition that is most often employed in lyophilization [37]. Here, the filled vials are placed on the shelves of the lyophilizer, and the shelf temperature is then decreased linearly (0.1 °C/min up to 5 °C/min, depending on the capacity of the lyophilizer) with time [37,38]. Both water and ice have low thermal conductivities and large heat capacities. The thermal conductivity between vials and shelf is limited; thus, the shelf-ramped cooling rate is inherently slow [11]. In order to ensure the complete solidification of the samples, they must be cooled below T_g for amorphous material and, respectively, below T_m for crystalline material. Traditionally, many lyophilization cycles use a final shelf temperature of -50 °C or lower as this was the maximal cooling temperature of the freeze-drier [7]. It is now suggested to use a final shelf temperature of -40 °C if the T_g or T_m is higher than -38 °C, or to use a temperature 2 °C less than the T_g and T_m [1]. Complete solidification also requires a significant amount of time [11]. The time for complete solidification generally depends on the fill volume. The larger the fill volume, the more time is required for complete solidification [11]. Tang et al. [1] suggest that the final shelf temperature should be held for 1 h for samples

with a fill depth of less than or equal to 1 cm or 2 h for samples with a fill depth of greater than 1 cm. Fill depths greater than 2 cm should be avoided. However, the holding time should be increased proportionately when such high depths are required.

To obtain a more homogeneous freezing, the vials are often equilibrated for about 15-30 min at a lowered shelf temperature (5-10 °C) before the shelf temperature is linearly decreased [1]. The vials are either directly loaded on the cooled shelves or loaded at ambient temperatures, and the shelf temperature is then decreased to the hold temperature [1,5,9].

Two-step freezing is another modification of the shelf-ramped freezing process, where a “supercooling holding” is applied. Here, the shelf temperature is decreased from either room temperature or the preset lowered shelf temperature, to about -5 to -10 °C and held for 30-60 min. This leads to a more homogenous supercooling state across the total fill volume [1,5]. When the shelf temperature is then further decreased, relatively homogeneous ice formation is observed [5].

Although shelf-ramped frozen samples show a high degree of supercooling, ice crystal growth proceeds extremely fast when the nucleation temperature is reached and results in many small ice crystals [9,39]. The ice nucleation cannot be directly controlled when shelf-ramped freezing is applied and is therefore quite random [4]. It is not practical to manipulate the ice nucleation temperature as the cooling rates are limited inside the lyophilizer and the degree of supercooling might not change within such a small range [1,14]. A drawback of shelf-ramped freezing is the fact that different vials may become subject to different degrees of supercooling, typically about ± 3 °C from the mean [4]. This results in a great variability in product quality and process performance [4].

3.2 Pre-cooled shelf method

When applying the pre-cooled shelf method, the vials are placed on the lyophilizer shelf that has already cooled to the desired final shelf temperature, e.g. $-40\text{ }^{\circ}\text{C}$ or $-45\text{ }^{\circ}\text{C}$ [1,13,14]. It is reported that the placement of samples on a pre-cooled shelf results in higher nucleation temperatures ($-9.5\text{ }^{\circ}\text{C}$) compared to the conventional shelf-ramped freezing ($-13.4\text{ }^{\circ}\text{C}$) [14]. Moreover, the freezing rate after ice nucleation is actually slower compared to shelf-ramped freezing due to the lowered degree of supercooling and more limited time for thermal equilibration throughout the fill volume [40]. A large heterogeneity in supercooling between vials is also observed with this method [14]. A distinct influence of the loading shelf temperature on the nucleation temperature is described in literature [13,14]. Searles et al. [14] found that the nucleation temperatures for samples placed on a shelf at $-44\text{ }^{\circ}\text{C}$ were several degrees higher than for samples placed on a $-40\text{ }^{\circ}\text{C}$ shelf. Thus, the shelf temperature should be chosen with care when using this method.

3.3 Annealing

Annealing is a hold step at a temperature above the glass transition temperature [12]. Annealing is generally performed to allow for complete crystallization of crystalline compounds and to improve inter-vial heterogeneity and drying rates [1,19]. Tang et al. [1] proposed the following annealing protocol: When the final shelf temperature is reached after the freezing step, the product temperature is increased to $10\text{-}20\text{ }^{\circ}\text{C}$ above T_g' but well below T_{eu} and held for several hours. The shelf temperature is then decreased and held at the final shelf temperature. Annealing has a rigorous effect on the ice crystal size distribution [17,41] and can eliminate the interdependence between the ice nucleation temperature and ice crystal size and morphology. If the sample temperature exceeds T_g' , the system follows the equilibrium freezing curve and some of the ice melts [12,41]. The raised water content and the increased

temperature enhance the mobility of the amorphous phase and all species in that phase [12]. Increased mobility of the amorphous phase enables the relaxation into physical states of lower free energy [12]. According to the Kelvin equation, ice crystals with smaller radii of curvature will melt preferentially due to their higher free energy compared to larger ice crystals [12,37,41]. Ostwald ripening (recrystallization) results in the growth of dispersed crystals larger than a critical size at the expense of smaller ones and is a consequence of these chemical potential driving forces [12,41]. Small ice crystals do not reform upon refreezing of the annealed samples, as the present large ice crystals serve as nucleation sites for additional crystallization [41]. The mean ice crystal radius rises with time^{1/3} during annealing [37,41]. As a consequence of that time dependency, the inter-vial heterogeneity in ice crystal size distribution is reduced with increasing annealing time. Meaning, vials comprised of smaller ice crystals “catch up” with the vials that contained larger ice crystals at the start of annealing [12,17,37,41]. Searles et al. [41] found that when annealing multiple sheets of lamellar ice crystals with a high surface area merged to form pseudo-cylindrical shapes with a lower interfacial area. In addition to the increased ice crystal size, it was also observed that annealing opened up holes on the surface of the lyophilized cake. The hole formation is explained by the diffusion of water from melted ice crystals through the frozen matrix at the increased annealing temperature. And in the case of meta-stable glass formation of crystalline compounds, annealing facilitates complete crystallization [42]. Above T_g , the meta-stable glass is re-liquefied and crystallization occurs when enough time is provided. Furthermore, annealing can also promote the completion of freeze-concentration (devitrification), as it allows amorphous water to crystallize [41]. This is of importance when samples are frozen too fast, and water capable of crystallization was entrapped as amorphous water in the glassy matrix. The phenomenon of annealing also becomes relevant when samples are optimally

frozen, but then kept at suboptimal conditions in the lyophilizer or in a freezer before lyophilization is performed [11]

3.4 Quench freezing

Quench freezing, also referred to as vial immersion, is the process of immersing vials into either liquid nitrogen or liquid propane (ca. $-200\text{ }^{\circ}\text{C}$) or a dry ice/acetone or dry ice/ethanol bath (ca. $-80\text{ }^{\circ}\text{C}$), long enough for complete solidification. The vials are then placed on a pre-cooled shelf [9,16]. In this case, ice crystal formation begins on both the vial wall and bottom, where the heat transfer media has contact [10]. This freezing method results in a lowered degree of supercooling, as well as a high freezing rate. Because the sample temperature is decreased quickly, small ice crystals are formed. Liquid nitrogen immersion has been said to induce less supercooling than slower methods [9,37,39]. However, this faster cooling method actually induces supercooling only in a small sample volume before nucleation starts and freezes by directional solidification [12,14]. While it is reported that external quench freezing might be advantageous for some applications [39], this uncontrolled freezing method promotes heterogeneous ice crystal formation and is not applicable in large-scale manufacturing [7].

3.5 Directional freezing

Directional or vertical freezing can be performed in order to generate straight, vertical ice crystallization. Ice nucleation is induced at the bottom of the vial by contact with dry ice and followed by slow freezing on a pre-cooled shelf [9]. In this case, the ice propagation is vertical, and lamellar ice crystals are formed [9].

Unidirectional solidification is a similar approach described by Schoof et al. [43] as the solidification through a gradient freezing stage which is based on the Power Down principle. Homogenous ice crystal morphology here occurs with a

temperature gradient between the upper and the lower cooling stage of 50 K/cm.

3.6 Ice fog technique

In 1990, Rowe [44] described an ice fog technique for the controlled ice nucleation during freezing. After the vials are cooled to the desired nucleation temperature, on the lyophilizer shelf, a flow of cold nitrogen is released into the chamber. The high humidity of the chamber generates an ice fog, a vapor suspension of small ice particles. The ice fog penetrates into the vials, where it initiates ice nucleation at the solution surface [45]. Rambhatla et al. [20] successfully implemented this technique for temperature controlled nucleation, in the range of $-1\text{ }^{\circ}\text{C}$ to $-11\text{ }^{\circ}\text{C}$, in laboratory scale lyophilizers. The challenge in this study was the induction of ice nucleation in all vials at the same time. Because the small particle of the ice fog does not reach all the vials simultaneously, intervial heterogeneity occurs [20]. Therefore, Patel et al. introduced a variation in the ice fog method, in which a reduced pressure in the chamber was applied to enable a faster and more uniform freezing [45]. With this modification, a rapid ice nucleation within one minute and a uniform ice crystal structure in all vials were observed. Although it is a promising technique to control ice nucleation inside the lyophilizers, it is not yet implemented in largescale, commercial lyophilization [20].

3.7 Electrofreezing

Electrofreezing (EF) is another method to control ice nucleation. In this method, a high voltage pulse is applied to generate an ice nucleus on a platinum electrode, which initiates ice crystallization [46,47]. The capability of high voltage to induce ice nucleation in supercooled water was first reported by Rau [48] in 1951. There are still, however, discussions about the basic mechanisms of EF, including the influence on molecular dynamics [46], bubble

formation and breakdown [48], and electrolytic formation of hydrated metal-ion complexes [49]. For this external freezing method, samples are first cooled to the desired temperature. Ice nucleation is then induced by EF, and samples are further cooled. For direct EF, a simple and disposable electrode setup composed of a gold wire can be used to allow the ice nucleation of many samples at the same time (Figure 2-3a) [47]. However, the presence of high amounts of excipients, especially salts, inhibits ice nucleation [46,47]. Special electrode caps (Figure 2-3b), called indirect EF, were developed as a result, to achieve ice nuclei generation independent from the sample composition [47]. In these caps, the ice nucleus is formed on the platinum electrode in a separate small volume of water. It then grows through a narrow cannula and PTFE-tube into the sample [47].

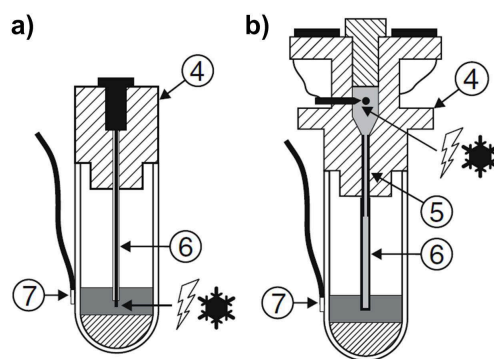


Figure 2-3: Schematic drawing of the electrodes used for (a) direct and (b) indirect electrofreezing, adapted from Ref. [47].

This method only allows the parallel freezing of eight samples under identical conditions [46]. The ice nucleation temperature can be induced at the desired temperature by electrofreezing (-1.5 to -8.5 °C for indirect EF and -4.5 to -8.5 °C for direct EF) [47]. Small spherical ice crystals grow when the ice nucleation temperature is low and large plate-like ice crystals form at higher ice nucleation temperatures [47]. However, this freezing method has only been applied in

modified cryotubes, and the need for individual electrodes for each sample diminishes the applicability in manufacturing.

3.8 Ultrasound-controlled ice nucleation

Nucleation can be induced by ultrasonic vibration. This was first applied in the food science field, e.g. for manufacturing of ice cream [15]. Inada et al. [50] reported that the phase change from supercooled water to ice, by ultrasonic vibration, can be actively controlled at the desired freezing temperature. The mechanisms of sono-nucleation are still being discussed [51–53]. Acoustic cavitation, which results in the formation of air bubbles in the liquid, is a key factor. In addition, during the final stage of collapse of a cavitating bubble, the equilibrium freezing temperature of water increases due to very high pressures. This results in an increased supercooling level, which is the driving force for ice nucleation.

Nakagawa et al. [54] introduced ultrasound-controlled nucleation for lyophilization of pharmaceutical proteins. An ultrasound transducer, which is connected to an ultrasound generator, is attached to an aluminum plate, which is combined with a cooling stage to cool the vials (Figure 2-4). Ice nucleation is triggered with an ultrasound wave once the vials have reached a desired temperature. Samples are then continually cooled down to the final temperature to allow for complete solidification.

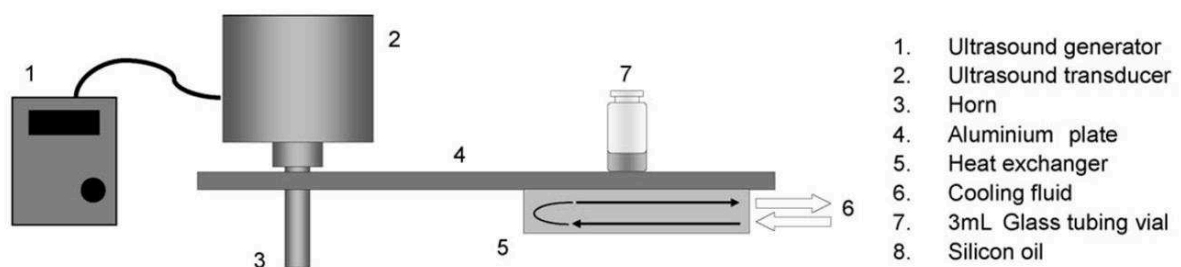


Figure 2-4: Cooling stage with ultrasound system proposed by Nakagawa et al. [54].

Larger and directional ice crystals of the dendrite type were found when the sample was nucleated at higher temperatures, while smaller and heterogeneous ice crystals were formed at lower nucleation temperatures. It was also observed that ice crystal initiated by ultrasound started at the bottom of the vial and progressed to the top, resulting in the possible formation of a cryoconcentrated solution layer at the top of the sample. In comparison with the samples nucleated at the same nucleation temperature without ultrasound, no significant differences in ice morphology were observed. This indicates that the ice morphology depends only on the nucleation temperature, and not on the mode of nucleation. In a follow-up study, Hottot et al. [55] investigated the effect of ultrasound-controlled nucleation on structural and morphological properties of freeze-dried mannitol solutions. They found that a compromise between nucleation temperature level and ultrasound pulse power is necessary to get the most stable mannitol polymorph with a highly permeable cake structure [55]. Saclier et al. [53,56] found in a theoretical model and also experimentally that the size and circularity of the ice crystals depends on both supercooling and the acoustic power used. In the aforementioned studies, the controlled ice nucleation during freezing was always performed externally. Passot et al. [57] used a prototype freeze-dryer, in which one of the shelves is equipped with the ultrasound technology. In accordance, they found that the controlled nucleation by ultrasound was possible at a nucleation temperature close to the equilibrium freezing point and that the homogeneity of the whole batch (100 vials) could be improved.

A significant intra-vial heterogeneity of ice crystal distribution with smaller ice crystals at the vial bottom compared to larger ice crystals at the top was observed by applying ultrasound-induced ice nucleation [54]. Thus, Nakagawa et al. [54] applied an additional annealing step to reduce the intra-vial heterogeneity. A good mechanical and thermal contact between the more or

less curved vial bottoms and the plate surface is another challenge for successful implementation [54]. However, an advantage of ultrasound-controlled nucleation is the ability to be applied without the need for direct contact with the product and is thus chemically non-invasive [15].

3.9 Vacuum-induced surface freezing

At low pressure, evaporation of water is favored. Known as self-cooling, the associated enthalpy of evaporation reduces the local temperature in the water surface, such that the water surface freezes, and a thin film of ice is formed [58,59]. Based on this concept, Kramer et al. [59] introduced a “vacuum-induced surface freezing” technique. The vials were placed onto the pre-cooled shelves (+10 °C) of the freeze-drier, and the pressure was reduced to 1 mbar (equal to 750 mTorr). After 5 min under these conditions, a 1-3 mm thick layer of ice was formed on the surface of the sample. In order to prevent further water loss by boiling and inhibit melting of the ice film on the surface, the chamber pressure was released to atmospheric pressure as fast as possible, and the shelf temperature was simultaneously decreased to 3-4 °C below the eutectic melting temperature of the formulation. This temperature was held for 1 h, and the shelf temperature was subsequently decreased to -40 °C. The release of the vacuum and reduction in the shelf temperature lead to the growth of dendritic ice crystals, resulting in the formation of long, chimney-like, extremely large ice crystals.

It is still unclear whether this technique can be scaled up for commercial applications. Moreover, this method has high risks of uncontrolled boiling, which can result in a “puff off” [5] when the unfrozen portion in the vial boils and blows up the frozen surface. This can influence the concentration of the sample [10] and could also influence the API. Therefore, Liu et al. [5] modified this method as follows: The temperature was held at -10 °C for equilibration before pulling a vacuum to 600 mTorr to induce freezing. In parallel, the shelf temperature was

rapidly (>1 °C/min) decreased to -45 °C. They showed that the lowered initial shelf temperature is necessary because when performed at higher temperatures ice is only formed at the top of the vial. The heat uptake by evaporation is not enough to lower the temperature of the whole fill volume and therefore results in a two-layer solidification (the first from vacuum-induced freezing, the second from shelf cooling).

3.10 High-pressure shift freezing or depressurization technique

“High-pressure assisted freezing” was the first freezing method in which increased pressures were applied to promote freezing [15,60]. Under high pressure, the freezing point of water is lowered and a large number of small ice crystals are formed [61]. This method also generates smaller ice crystals compared to other conventional rapid freezing methods, such as liquid nitrogen immersion [62]. So far, this method was only applied in food science.

Later, researchers from the same group investigated a “high-pressure shift freezing” method [63,64] where the pressure is released slowly or quickly. The phase transition from liquid to solid occurs as a result of the pressure change, and instantaneous ice formation is promoted. In 2007, Gasteyer et al. [65] introduced an analogous method, referred to as “depressurization method”, for the controlled ice nucleation in samples intended for lyophilization. The samples are initially cooled to the equilibrium freezing temperature in a pressurized gas atmosphere, which is subsequently de-pressurized to induce ice nucleation.

This freezing method involves several steps. The freeze-dryer is loaded, and air within the chamber is purged with a pressurization gas, e.g. argon or nitrogen. The chamber is pressurized up to less than 50 psig (approximately 2600 Torr or 3.5 bar), and the samples are cooled to and equilibrated at the desired nucleation temperature. The samples are then nucleated by depressurizing the freeze-drying chamber. After the nucleation, the samples are further cooled to the final shelf temperature. The detailed construction of a freeze-dryer, that is

applicable for that purpose, is described in more detail in a follow-up patent by Rampersad et al. [66]. The system consists of a freeze-drying chamber, a gas circuit to pressurize the freeze-drying chamber, and a separate circuit for depressurization.

Bursac et al. [67] demonstrated that this freezing method could be applied in both laboratory and small commercial-scale freeze-dryers for a wide range of formulations and containers. They showed that the nucleation of aqueous samples could be well controlled within 1 °C of the equilibrium freezing point. One main advantage of this technique is that the samples are only contacted by inert gas, which is removed from the vials during lyophilization [67]. The technique can be implemented with minor additions to equipment on freeze-dryers that are designed to withstand pressures, i.e. during steam sterilization [66,67]. However, in the presence of a capacitance manometer, or if the product chamber is not intended and approved for such high pressures, the adaptation of this technique will be very cost-intensive. This required equipment has now been integrated in commercially available freeze-dryers with the “ControlLyTM nucleation on demand technology” [68].

3.11 Addition of ice nucleating agents

In general, all insoluble impurities have the potential to serve as ice nucleating agent (INA) [15]. INAs promote a heterogeneous ice nucleation process that occurs at higher temperatures compared to samples that do not contain INAs [15]. The most studied nonbiogenic INA is silver iodine (AgI), which is also used for cloudseeding and snow-making [15,69]. AgI enhances ice nucleation not only because of crystal structure's similarity to ice [70] but also because of an electric field mechanism [71]. Among the biogenic INAs, six different species of ice nucleation bacteria have been studied in food science, of which *Pseudomonas syringae* is most widely used [15,69]. These biogenic INAs favor

ice nucleation, because their structure is similar to that of the ice crystal lattice, lacks surface charge and is of high hydrophobicity [15,72,73].

Searles et al. [14] used *P. syringae* (0.001% w/v) and AgI (1 mg/ml) to alter the ice nucleation temperature during freezing of a 10% HES solution. The addition of *P. syringae* reduced supercooling (nucleation at -1.8 °C compared to -13.4 °C for control samples) and directional solidification with complete lamellar ice crystal structure [14]. Samples seeded with AgI nucleated in a temperature range between -5 °C and -7.5 °C in the center of the meniscus, where most of the AgI was concentrated and a mixture between spheroidal and lamellar ice crystal structures was formed [14]. Liu et al. [5] found in the case of high fill depth, AgI (0.1 mg per vial) limited supercooling (about -2 °C). However, this study also showed that ice grew from the bottom to the top of the vial and dendritic ice crystals were observed. Nucleation efficiency for *P. syringae* depends on the INA concentration [69]. This also seems to be the case for AgI. Searles et al. [14] also showed that vials with high particulate contamination from drying the open vials after washing in an uncontrolled laboratory environment also slightly decreased the degree of supercooling to -11.4 °C compared to -13.4 °C in conventional shelf-ramped freezing. Overall, the presence of INAs increases the average nucleation temperature but does not allow controlled nucleation, and individual vials may show a great heterogeneity. Moreover, the addition of ice nucleating agents is not of practical use for FDA-regulated and approved pharmaceutical products.

3.12 Non-aqueous co-solvents

Teagarden and Baker [74] published a comprehensive review on the potential of non-aqueous co-solvents in lyophilization. The use of non-aqueous co-solvents has both advantages and disadvantages [74]. The advantages include increased sublimation rate leading to a decreased drying time, potentially increased wettability, improved reconstitution characteristics, increased

solubility and stability of some drugs in solution, and enhanced sterility assurance [74]. Operator safety concerns due to high degree of flammability or explosion potential is one disadvantage. Toxicity and regulatory issues because of residual solvent levels can also arise [74]. The most extensively used co-solvent in lyophilization is tertiary butyl alcohol, tert-butanol (TBA). This is due to the fact that it is 100% miscible in water shows a high freezing point (24 °C) and a high vapor pressure (26.8 mm Hg at 20 °C) [74]. Other co-solvents that do not freeze completely in commercial freeze-driers are very difficult to use and often result in unacceptable freeze-dried cakes [74]. In general, the specific effect of TBA is related to the modification of the ice crystal habit which leads to the growth of needle-shaped crystals [11]. However, the water–TBA mixture shows an extremely complex series of eutectic, peritectic, and hydration phenomena [11]. Kasraian et al. [75] suggested a phase diagram for TBA-water systems, which can be described as side-by-side placement of two simple eutectic phase diagrams: one for water-TBA hydrate with Teu at 20% TBA and one for TBA hydrate-TBA with Teu at 90% TBA. Depending on the concentration of TBA used, ice, solid TBA hydrate, or solid TBA will separate upon cooling. At concentrations lower than 20%, pure ice will form and leads to increasingly concentrated TBA solutions. TBA crystallizes as TBA hydrate when the concentration is increased to 20% TBA.

The size and morphology of the ice crystals depends on the amount of TBA present. In the presence of 1% TBA, the ice crystal morphology does not differ from pure water [75]. At a concentration of 3% larger, dendritic ice crystals form. Above this concentration, but still below the eutectic concentration of 20%, needle-shaped ice crystals form [75]. In accordance, Liu et al. [5] found that with the presence of 5% TBA, large needle-like ice crystals were formed and grew faster than the ice crystals in the control. It is also reported that the freezing rate also influences the size of the ice crystals with the presence of TBA. Smaller ice

crystals for fast freezing and bigger ice crystals for slower freezing [76]. Moreover, the collapse temperature of e.g. sucrose, is not influenced by TBA addition (3-10% w/v) [77].

The level of residual solvent in the final product can be critical when TBA is added to the samples. It is influenced by the initial TBA concentration, the freezing rate, and the physical state of the solute [76]. In general, crystalline samples contain very low levels of residual TBA. With the presence of an amorphous solid, the removal of TBA is hindered when used at low initial concentrations (<2%), as TBA does not crystallize but is dispersed in the amorphous phase. Complete crystallization is inhibited during fast freezing, resulting in high residual TBA levels. Annealing, which promotes TBA crystallization, lowers residual TBA levels [78]. An additional critical point is the time between filling the highly volatile solvent and freezing of the solution. During this time, some dissolved substances can be carried along the evaporating stream and recondense near the top of the vial. This time span should be kept as short as possible in order to avoid dry powder spots near the neck of the vial after drying. This will also avoid reduced cake heights [74].

3.13 Others

Vial pretreatment by scoring, scratching, or roughening can also be applied to lower the degree of supercooling during freezing. Searles et al. [14] used scored vials, scratched at the bottom interior surface with a metal scribe. The produced surface defects or scraped glass particles were supposed to catalyze ice nucleation. However, only a marginal increase in ice nucleation temperature to $-13.1\text{ }^{\circ}\text{C}$, compared to $-13.4\text{ }^{\circ}\text{C}$ for shelf-ramped frozen samples, was observed. With regard to particle contamination, this method is undesirable for pharmaceuticals. Randolph et al. [37] suggested the incorporation of ice nucleation chemistry into the vial interior. However, no successful implementation has been demonstrated yet.

4 Consequences of the freezing step on general quality attributes of biopharmaceuticals and process performance

As aforementioned, the freezing process directly influences number, size, and shape of ice crystal formation. The ice crystal properties are set early in the freezing process by the ice nucleation temperature. The properties are also influenced by the freezing rate and the time required for complete solidification and directly impact several quality attributes of the biopharmaceutical such as morphology, product uniformity, physical state, residual moisture content, or reconstitution time and also primary and secondary drying performance, as summarized in Table 2-1. However, the quality attributes of the biopharmaceutical and process performances are not influenced only by the process conditions. It should also be emphasized that the quality attributes are also influenced by factors such as formulation composition, fill volume and fill depth or properties of the glass vials.

4.1 Intra-vial and inter-vial uniformity

The growth of ice crystals during freezing as well as the distribution of solutes across the vial can be heterogeneous. Both are reflected by intra-vial uniformity [5]. Intra-vial heterogeneity results in unpredictable changes in sublimation rate during drying and, in the most extreme case unacceptable quality of the biopharmaceutical [5]. The lower the temperature equilibration in the sample, the more heterogeneous ice crystals form across the vial. For example, ice crystal distribution is more homogeneous in the two-step shelf-ramped frozen samples when compared to those in shelf-ramped freezing without a holding step [5]. More time is available with a slower freezing rate for the solute to concentrate ahead of the advancing freezing front.

Table 2-1: Summary of the various freezing methods, which allow or do not allow nucleation control (NC), and their impact on ice nucleation temperature (INT), freezing rate (FR), freezing type (global supercooling versus directional solidification), ice crystal morphology (ICM), specific surface area (SSA), dry layer resistance (DLR), and drying time (DT). Percentages are referred to the values obtained for shelf-ramped freezing. All trends are estimated to best knowledge. ↑↑↑ or ↓↓↓: extremely high or low, ↑↑ or ↓↓: very high or low, ↑ or ↓: high or low.

Freezing Method	Description	NC	INT	FR	FT	ICM	SSA	DLR	DT	Examples
Shelf-ramped freezing	Shelf temperature is decreased	No	↓↓	↑↑	global	very small,	↑↑	↑↑	↑↑	[14] 10% HES: INT -13.4°C
Two-/three-step freezing	Like shelf-ramped freezing but	No	↓	↑	global	small,	↑	↑	↑	[5]: 15% SBECD: DT -3%
Precooled shelf method	Vials are placed on a pre-cooled	No	↑	↓	global/	mixed	↓	↓	↓	[14] 10% HES: INT -9.5°C, DT -
Annealing	Holding step above Tg`	No	—	↓↓↓ a	global*	very large,	↓↓	↓↓	↓↓	[41] 10% HES: DT up to -350%
Quench freezing	Immersion of the vials in liquid	No	↑	↑↑↑	direction	very small,	↑↑↑	↑↑↑	↑↑↑	[108] buffer with NaCl: SSA
Vertical freezing	Nucleation at vial bottom with	No	↑	↓↓	direction	large,	↓↓	↓↓	↓↓	[9] DT -28%
Ice-fog technique	Ice fog generates small ice	Yes	↑↑	↓↓	direction	large	↓↓	↓↓	↓↓	[20] HES 5%: INT -1.5°C, DT -
Electrical	High voltage generates ice	Yes	↑↑	↓↓	direction	large,	↓↓	↓↓	↓↓	[47] 10% HES: INT -2°C, DT -
Ultrasound	Ultrasound triggered nucleation	Yes	↑↑	↓↓	global	large,	↓↓	↓↓	↓↓	[54] 10% mannitol: INT -1°C,
Vacuum induced freezing	Self-cooling of the sample on the	Yes	↑↑	↓↓	direction	large,	↓↓	↓	↓	[5] 15% SBECD: -9% DT
Depressurization	Ice nucleation as a result of	Yes	↑↑	↓↓	direction	large	↓↓	↓↓	↓↓	[9] 5% sucrose: SSA -50%, DT
Agl	Ice nucleating agent acts as "ice	No	↑	↓	global/	lamellar/	↓	↓	↓	[5] 15% SBECD: DT -6%
P. syringae	Ice nucleating agent acts as "ice	No	↑	↓	global	large,	↓	↓	↓	[14] 10% HES: INT -1.8°C, DT -
Non-aqueous cosolvent:	Ice crystal habit is altered	No	—	—	global	large,	↓↓	↓↓	↓↓	[5] 15% SBECD: DT -24%
Scored vial	Surface defects catalyze ice nucleation	No	↓	↓	global	small, spherulitic	↑	↑	↑	[77] 10% HES: INT -13.1°C, DT -8%

a For annealing not the freezing rate but the long time provided for ice crystal growth is indicated.

For shelf-ramped freezing, high heterogeneity in solute distribution across the vial is reported, especially at high fill volumes [5]. Patapoff et al. [9] concluded when the sample was frozen by shelf-ramping with a first fast and later slower increase in dry layer resistance that the structure of the dried cake varied in the vertical direction. Liu et al. [5] determined the vertical heterogeneity by three-section weight analysis. In shelf-ramped freezing, a highly concentrated core was found in the middle. In this study, the best intra-vial uniformity resulted from shelf-ramped two-step freezing or by addition of TBA. If the controlling parameters are not sufficiently adjusted, vacuum-induced freezing often results in two-layer solidification: one from vacuum-induced freezing and one from shelf cooling [5]. Annealing is suggested to improve intra-vial and also inter-vial heterogeneity [20,41,54]. During annealing, larger ice crystals grow at the expense of smaller ones, leading to a large and more uniform ice crystal size that is no longer dependent on ice nucleation temperature.

Inter-vial or batch uniformity is a consequence of the stochastic phenomenon of nucleation. Thus, all the vials in a batch do not have the same nucleation temperature and will not behave equally during drying [56]. Passot et al. [57] found that the ultrasound and pre-cooled shelf method allowed a significant increase in inter-vial uniformity when compared to shelf-ramped freezing. The optimal batch uniformity was obtained by the addition of a nucleating agent. Annealing also has an inter-vial homogenization effect [41]. Webb et al. [79] demonstrated that the variations in primary drying endpoints were three to four times larger for non-annealed versus annealed samples. Bursac et al. [67] showed that the depressurization technique improved batch homogeneity with a 60% decrease in standard variations between vials. Although ice nucleating agents can also improve inter-vial uniformity, the best way to produce a homogeneous batch is to directly control the ice nucleation temperature in all vials of a batch during freezing.

4.2 Sample morphology

Sublimation of the ice crystals leaves pores in the solute matrix. The texture and porosity of the final, dried biopharmaceutical product are directly fixed by the details of ice growth in the freezing process. It is proposed that the cake texture changes from a homogeneous, sponge-like structure for samples with a high degree of supercooling to a lamellar structure with a degree of orientation for samples with a low degree of supercooling. In addition to the degree of supercooling, freezing rate and time required for complete solidification also determine ice crystal morphology. In general, freezing methods where supercooling exceeds 5 °C freeze by global supercooling and result in a dispersed spherulitic morphology. The size of the spheroidal pores correlates directly with the degree of supercooling. Directional solidification is often observed at very high cooling rates, or when ice nucleation is induced close to the equilibrium freezing point. This directional solidification shows lamellar plate morphology, and the interface velocity is a major determinant [12,14].

High freezing rate after slow cooling via shelf-ramped freezing results in very small spherulitic pores, approximately 100 µm in diameter, and a sponge-like matrix [14]. In the two-step freezing process, the samples are first equilibrated in a super-cooled state across the whole sample volume [5]. Thus, when shelf temperature is further increased, rapid and homogeneous freezing occurs and results in small, uniform, spherulitic pores. In the pre-cooled shelf method, a lower and less consistent degree of supercooling is observed [14]. As the time for temperature equilibration is limited, an enormous temperature gradient can be observed inside the sample. This leads to smaller pores at the bottom and large pores near the top. Liquid nitrogen immersion freezes by directional solidification in combination with a high freezing rate, resulting in small lamellar-oriented pores [80]. In comparison with the pre-cooled shelf method, the temperature gradient during vertical freezing is more pronounced. This forms

chimney-like large lamellar structures [9]. The addition of an annealing step promotes the formation of large spherulitic pores due to Ostwald ripening [41]. Freezing by directional solidification is assumed in all methods that allow controlled nucleation at a temperature close to the equilibrium temperature and could result in large chimney-like pores. Vacuum-induced freezing leads to long parallel chimney-like pores with a diameter of approximately 200 μm [59]. The controlled nucleation via depressurization of a 5% sucrose solution resulted in an increased pore diameter of 120 μm compared to 50 μm in shelf-ramped freezing [67]. Large chimney-like pores at the top and smaller lamellar pores at the bottom were observed in samples frozen by ultrasound-induced nucleation [54]. Large lamellar, highly oriented pores were detected when electrofreezing at high nucleation temperatures [47]. In the presence of AgI, a mixed morphology of the cake is produced. A trend of dominating lamellar structures appears at the top where ice nucleation starts, while spheroidal structures appear at the bottom [14]. Supercooling is almost eliminated with the addition of *P. syringae* and thus enables a directional solidification with total lamellar morphology [14]. TBA influences the ice crystal habit and promotes the formation of large, needle-shaped pores stretching from the top to the bottom [5].

4.3 Primary and secondary drying performance

The primary drying rate or the sublimation during primary drying can be expressed by the following equation [6]:

$$\frac{dm}{dt} = \frac{P_o - P_c}{R_p + R_s} \quad (2-1)$$

The mass transfer rate for the water vapor is represented by dm/dt . P_o is the equilibrium vapor pressure over ice at the product temperature, while P_c is the chamber pressure. R_p is the dry product layer resistance to vapor transfer, and R_s is the resistance of the stopper. R_p is much larger than R_s , especially for

samples of high concentration and high fill depth [81]. According to this equation, the sublimation rate is directly correlated to the dry layer resistance of the product, which is determined by the freezing step related pore size of the product. The smaller the pores in the solute matrix previously occupied by ice crystals, the greater the resistance to water vapor flow from the product and the slower the sublimation rate [6].

In secondary drying, the remaining unfrozen water, which can be about 20% for amorphous samples, requires diffusion through the solid matrix and a desorption step from the surface of the matrix [6]. Therefore, the sublimation rate in secondary drying strongly correlates with thickness and surface area of the interstitial matrix [57].

Low supercooling close to the equilibrium freezing point results in the formation of large ice crystals and low surface area, and thus accelerated primary drying but slower secondary drying [57]. In contrast, a high degree of supercooling during freezing results in many small crystals and larger surface area and thus slower sublimation but faster desorption [57]. Primary drying dominates for most formulations with a low solid content [6]. Searles et al. [14] showed that a 1% increase in ice nucleation temperature resulted in a 3% increase in drying times. Freezing processes that result in pronounced supercooling, like shelf-ramped freezing or two-step freezing, require a substantially extended primary drying time compared to the other available methods [5,41].

The pre-cooled shelf method can be used to reduce the drying time in cases when freezing has to be performed on the shelf of the freeze-drier without the possibility for controlled ice nucleation. Searles et al. [14] found that this method leads to an increase in drying rate by about 14% compared to shelf-ramped freezing. Similar results were obtained by Passot et al. [57], who described an approximately 18% shorter sublimation time.

However, annealing appears to be the most effective possibility to decrease drying rates in this case. Searles et al. [41] reported that annealing for only 30 min increased the primary drying rate by a factor of 3.5 because larger ice crystals were formed due to Ostwald ripening. It was also found that the formation of large holes on the cake surface of the annealed surface could additionally have facilitated sublimation. In general, higher annealing temperatures and longer annealing times correlate with a faster drying rate [12]. All drying rates are limited to maximum values that were reached when the sublimation rate is no longer controlled by mass transfer but by energy transfer [12]. However, annealing was not always found to increase the drying rate, as the physical state of the sample can also have an impact. For example, it was observed that in systems that contain a crystalline phase, such as mannitol/ trehalose/ sodium chloride, primary drying time was increased due to changes in the pore structure via changes in crystallinity [42].

Meanwhile, freezing by immersion in liquid nitrogen has been shown to result in very small ice crystals and large surface area, and thus decreased primary drying rates compared to shelf-ramped freezing were observed [14]. The non-vertical ice formation obtained by ice growth starting from the wall of the vial additionally contributes to the restricted ice sublimation for samples frozen by liquid nitrogen immersion [9].

The controlled nucleation via depressurization of a 5% sucrose solution resulted in a increased pore size and led to a shortened drying time by 27% according to Bursac et al. [67]. In comparison, Kramer et al. [59] showed that the vacuum-induced surface freezing method led to the formation of large, chimney-like pores, resulting in decreased primary drying times of 25% for a 2% mannitol formulation and of 15% for a 2% sucrose formulation. Conversely, Nakagawa et al. [54] reported that the controlled ice nucleation by ultrasound close to the equilibrium freezing temperature (-2 °C) increased the primary

drying rate by 60% when compared to samples that nucleated at lower temperatures (-8 °C). Passot et al. [57] observed only an 18% decrease in sublimation time for samples nucleated using ultrasound. When the biogenic ice nucleation agent *P. syringae* was added to the samples, a 30% [57] and 60% [14] increase in drying rate was experienced. In this case, the faster drying rate was not only a result of the lowered degree of supercooling but also attributed to an increase in lamellar ice crystal content [14].

The addition of TBA was also found to increase the ice sublimation rate [82]. Kasraian et al. [77] found that the addition of 5% TBA to a 5% sucrose solution resulted in an approximate 10-fold decrease in product resistance and drying time. A reason for this is that TBA has the ability to modify the crystal habit of ice so that large needle-shaped ice crystals are formed and resulted in a decreased mass transfer resistance [76]. The fact that TBA itself has a high vapor pressure also plays a role in the increase of sublimation rates [74,82,83]. Daoussi et al. [83] reported a 10-30 times higher sublimation rate of a 90% TBA sample when compared to traditional aqueous formulations.

The drying performance can be influenced by the direction of ice crystal formation and by the direct correlation between drying rate and pore size. The connection between pores and the formation of a skin on the top of the cake may also have an influence on the drying performance. For example, it was found that in vertically oriented ice obtained by vertical freezing, the sublimation rate was 40% faster and drying time was 50% shorter compared to standard-frozen solutions [9]. Moreover, ice-structures formed by top-down freezing could be an additional factor for the increased drying rates with the presence of TBA [5]. With high solid content in combination with small ice crystals, the ice crystals can be completely coated by an amorphous matrix. In this case, sublimation is extremely slowed while the water vapor has to diffuse across the amorphous layer, due to the lack of connections between pores [9,11].

Moreover, during slow freezing, the solute can concentrate ahead of the advancing freezing front and in extreme cases produce an almost impermeable glassy product skin at the top of the vial [11]. Patapoff et al. [9] reported that the dry layer resistance is high as the sublimation front moves through the skin. The resistance then increased more slowly once the sublimation front passed the skin.

To generally optimize the process time of lyophilization, the product temperature should be as high as possible, while still low enough to avoid product melting or collapse. A controlled product temperature needs to be in equilibrium with the heat transfer rate to the product and removal of heat by sublimation, which is directly correlated to the mass transfer rate of water vapor [6]. Searles et al. [41] found that the product temperature of an annealed sample was 5 °C cooler than the corresponding non-annealed sample due to an increased heat removal by the sublimation.

The mass transfer is directly correlated to product resistance. At low product resistance, the process is no longer controlled by mass transfer. It is instead controlled by heat transfer. In this case, the product temperature moves toward a temperature at which the vapor pressure of ice equals the chamber pressure. It is then insensitive to additional energy input [12]. This allows further optimizing of the drying time by increasing the shelf temperature well above T_g [11]. The same effect was observed when using TBA as non-aqueous co-solvent [77]. In contrast to pure sucrose samples, sucrose samples with TBA addition showed a fast sublimation rate and did not show collapse. This can be explained by the maintenance of a low product temperature due to the rapid sublimation and by the faster decrease in water content and increase in viscosity that prevented viscous flow of the sample.

4.4 Physical state of the sample

The physical state of excipients is of significant importance for lyophilized biopharmaceuticals. It can influence reconstitution time, storage stability, and protein stability and governs the risk of vial breakage. Various studies demonstrate that the freezing rate can affect the physical state of the solutes. This was comprehensively studied for mannitol samples [84–90]. For example, after fast freezing ($-20\text{ }^{\circ}\text{C}/\text{min}$), mannitol was found to be amorphous. This amorphous form transformed to a meta-stable crystalline state in the frozen matrix [84]. In contrast, when the sample was cooled at $-2\text{ }^{\circ}\text{C}/\text{min}$, mannitol was crystalline [85].

The freezing process impacts also the preferred formation of different polymorphs. Izutsu et al. [86] detected a mixture of α - and β -polymorphs after slow freezing of 10% mannitol samples, and the formation of mainly the δ -polymorph after fast freezing. Cannon and Trappler [87] observed for a 70 mM mannitol sample that shelf-ramped freezing resulted mostly in the δ -polymorph with a minor presence of the α -polymorph. Freezing on a pre-cooled shelf produced mostly the α -polymorph with a minor β -content. A hold step at $-20\text{ }^{\circ}\text{C}$ during shelf-ramped freezing led to δ -polymorph formation, and after annealing at $-20\text{ }^{\circ}\text{C}$ for 1 h only the β -polymorph was detected.

Kim et al. [88] reported that the physical state is affected by the freezing rate and the mannitol concentration. Fast freezing of a 10% mannitol sample produced the δ -polymorph, whereas fast freezing of 5% mannitol resulted primarily in the β -form. In addition, Nakagawa et al. [89] found that the freezing step influences the vertical distribution of mannitol polymorphs in the sample along the direction of heat flux during freezing. The polymorphic form was also influenced by the absence or presence of protein [90]. The formation of mannitol hemi-hydrate was completely inhibited with the presence of protein [90].

In order not to form a meta-stable state and not to decrease the T_g of the formulation, annealing is essential for the crystallization of bulking agents such as glycine or mannitol [18,19]. For example, Hawe et al. [91] found that the application of an annealing step during lyophilization could increase the mannitol crystallinity in mannitol–sucrose–NaCl formulations. However, the annealing step favored the formation of mannitol hydrate, which is known to convert into the anhydrous polymorph upon storage.

4.5 Residual moisture content

All freezing methods that increase crystal size, thus decreasing the SSA, result in a limited desorption rate during secondary drying. Consequently, there is an increased residual moisture content in the final biopharmaceutical product if secondary drying time is not adequately adjusted [5]. When compared to shelf-ramped frozen samples, Liu et al. [82] observed a slight increase in the residual moisture content for 15% sulfobutylether-7-beta-cyclodextrin (SBECD) samples after annealing, two-step freezing and vacuum-induced freezing.

A twofold increase in residual moisture content of samples frozen with the ice nucleating agent AgI is correlated with a large increase in ice crystal size. Interestingly, the addition of TBA did influence the ice crystal morphology but the residual moisture content was not changed. In contrast to the pronounced increase in residual moisture content for samples containing AgI, Passot et al. [57] did not detect an increase in residual moisture content for samples with added *P. syringae*. The application of ultrasound did, however, induce nucleation, resulting in a 50% increase in the residual moisture content of 5% sucrose samples [57]. The increase in the freezing rate during shelf-ramped freezing from 0.2 to 1.0 °C/min also slightly increased the residual moisture content, which is comparable to the moisture content after freezing on pre-cooled shelves [57,59].

In accordance with Liu et al. [5], Webb et al. [79] found a slightly increased residual moisture content in annealed versus non-annealed sucrose/HES/interferon- γ samples. Kramer et al. [59] reported that for mannitol samples the residual moisture content was higher after vacuum-induced freezing in comparison with shelf-ramped freezing. However, this was not the case for sucrose and glycine samples.

4.6 Reconstitution time

There are several factors that can influence the reconstitution properties of a lyophilized sample. These include the morphology of the cake, the surface area of the cake, the presence of cake collapse or meltback, the presence of hydrophobic coatings, the homogeneity of the dry matrix, and the formation of channels between pores and the physical solid state [74]. Therefore, it is difficult to propose a general relation between freezing process and reconstitution time.

It is proposed that the changes that allow more efficient water vapor transport during drying may also improve wettability of the porous cake [12]. However, limited literature is available with regard to the correlation between freezing step and reconstitution time.

Annealing can affect reconstitution time, but the absolute influence is controversially discussed [12]. For example, Searles et al. [41] found that annealed HES samples were completely dissolved slightly faster than unannealed samples. In contrast, Webb et al. [79] reported slower dissolution for annealed HES and sucrose/ HES formulations. The shorter reconstitution time observed by Searles et al. [41] upon annealing was explained by the formation of holes in the dried layers of the cake, facilitating liquid penetration. It is generally assumed that increased pore size produced by annealing increases the thickness of the matrix layers and reduces the surface area. Therefore, this process will prolong reconstitution times [41]. Based on this observation, it can

be assumed that freezing methods resulting in a low surface will slow down reconstitution. However, further studies are needed to proof this assumptions.

In addition to sample morphology, the physical state of the samples could also influence reconstitution time. The amorphous form has a higher solubility compared to the crystalline form. Different polymorphic forms also have different dissolution rates [92]. Kim et al. [88] demonstrated that slow freezing of 10% mannitol resulted in a mixture of α - and β -polymorphs with a reconstitution time of 78 s while nitrogen immersion produced the δ -polymorph with a reconstitution time of 36 s. This cannot be solely attributed to different dissolution rates of mannitol polymorphs, as the SSA was additionally affected by the freezing method. Modifying the reconstitution time by altering freezing process is also of high interest with regard to the high reconstitution times observed for lyophilized high-concentration protein samples [93].

5 Consequences of the freezing step on protein stability

In addition to the consequences of the freezing step on general quality attributes of biopharmaceuticals and drying performance, the freezing step will also affect protein stability. There are several factors that contribute to the detrimental effects on proteins during freezing. Most of the effects can be directly correlated to the freezing protocol used.

5.1 General stress factors during freezing

The three main stress factors that occur during freezing that could impact protein stability are cold denaturation, ice formation, and freeze-concentration [16].

The protein's free energy of unfolding typically shows a parabolic function of temperature and becomes negative not only at high but also at low temperatures. This is referred to as cold denaturation [94–96]. Cold denaturation is related only to decreased temperatures and occurs in the absence of freezing. Therefore, it must be completely differentiated from freezing denaturation [97]. Cold denaturation is reported for a high number of proteins [16]. However, the impact of cold denaturation on protein stability in lyophilization is regarded as marginal. This is because the estimated cold denaturation temperatures are often well below lyophilization temperatures and are even further reduced in the presence of saccharides and polyols. Additionally, the rate of unfolding can be sufficiently slow on the time scale of the lyophilization process. Drying can be finished before significant unfolding occurs [1,12,16,98].

The more significant changes in protein stability occur when ice crystallizes in the solution, promoting freeze-concentration and leading to a large ice–water interface. The solutes concentrate upon freeze-concentration and buffer components can crystallize, leading to a drastic pH shift. And depending on the formulation composition, liquid–liquid phase separation can occur.

Freeze-concentration of the solutes during freezing can also raise the solute concentration to a destabilizing level [32]. The rate of bimolecular degradation reactions is increased at high concentrations. However, the decrease in temperature and the increase in viscosity exhibit a counteracting effect and limit the extent of the rise in reaction rates [16]. When electrolytes are present in the protein formulation, the increase in concentration also increases the ionic strength. This will potentially destabilize proteins [16]. Here, the thermodynamic stability of the native conformation is reduced via charge-shielding effects or preferential binding of ions to the protein surface [95]. The role of freeze-concentration on protein stability has been mostly speculated based on experience with enzymes, which might noticeably differ when stabilizers are present [16]. For instance, Bhatnagar et al. [97] found no lactate dehydrogenase (LDH) degradation in ice-free sucrose solutions, whereas significant degradation was observed in the freeze-concentrate of the same composition.

All pKa and pKb values are directly affected by temperature, depending on the buffer-type, and causes the pH to change during cooling [11]. However, the selective crystallization of buffer salts during freeze-concentration results in more drastic pH shifts during freezing and is thus more detrimental with regard to protein stability. For instance, the decrease in pH can be 3 pH units or more for sodium phosphate buffers. The basic disodium salt is less soluble and has a higher eutectic point than the monosodium salt, leading to its precipitation [16]. Gomez et al. [99] observed that the extent of salt precipitation and pH decrease during non-equilibrium freezing, observed in lyophilization, are smaller than those predicted by the equilibrium freezing behavior. At extreme pH values, increased electrostatic repulsion between equal charges in proteins will induce protein unfolding or denaturation [94]. Freezing of a LDH solution in sodium phosphate buffer resulted in a pH drop from 7.5 to 4.5 and caused protein

denaturation [100]. Generally, the pH shift during freezing can be minimized by the optimal choice of buffer salts, keeping the buffer concentration at a minimum, maintaining all buffer species in the amorphous state via the addition further solutes, or by adjusting the freezing method [1,16,19].

In addition to the crystallization of buffer salts during freeze-concentration, crystallization of additional solutes such as mannitol or glycine revokes their stabilizing effect on proteins [16,101]. In general, the crystallization of the solutes strongly depends on cooling rate and annealing conditions. It also depends on the presence of other co-solutes [32]. For example, inhibition of mannitol or glycine crystallization by adding sufficient co-solutes resulted in an increased LDH stabilization [85].

Liquid-liquid phase separation of amorphous solutes can also be observed as a result of freeze-concentration. Phase separation is most common when polymers like PEG, PVP, dextran, or ficoll are used as cryoprotectants [32]. Phase separation will lead to the loss of the stabilizing effect of the excipient and thus negatively influence protein stability. Izutsu and Kojima [72] reported that freeze-concentration separated combinations of proteins (lysozyme, ovalbumin, BSA) and non-ionic polymers (ficoll, PVP) into different amorphous phases. Heller et al. [33] showed that the effects of liquid-liquid phase separation in PEG/dextran systems can be detrimental on the stability of recombinant human hemoglobin during freezing and drying. The phase separation promoted the protein partitioning into a PEG-rich and a dextran-rich phase and that the two phases differed in their lyoprotective properties [34].

The formation of large ice-water interfaces due to ice crystallization occurs during freezing. This can promote surface-induced denaturation of surface-sensitive proteins. The mechanism of protein denaturation at the ice surface is still being discussed. One hypothesis states the generation of an interfacial electrical field, via the preferential partitioning of one ionic species into the ice

lattice, influences protein stability [102]. Another hypothesis states that ice formation leads to an ordering of the water molecules in the direct vicinity of the protein. When the protein adsorbs on the ice, the ordered water is unblocked and entropy increases. This provides a thermodynamic driving force for protein unfolding [16,103].

Protein denaturation at the ice surface can be reduced or prevented by addition of nonionic surfactants, which compete with proteins for adsorption at the ice-water interface [16]. Chang et al. [104] observed a strong correlation between the tendency of a protein for freeze denaturation and its tendency for surface denaturation. As the ice crystal surface area during freezing is predetermined by the freezing protocol, the stability of a surface sensitive protein is additionally strongly influenced by the sole freezing step.

It must be kept in mind that in addition to the freezing process, the formulation strongly affects freezing-induced protein stabilization. Cryoprotectants stabilize proteins during freezing by “preferential exclusion” [105]. These solutes tend to be excluded from the surface of the protein and therefore lead to a “preferential hydration” of the protein and increases the thermodynamic stability of the native state [105]. Other factors can also control the stabilizing effects of cryoprotectants. These factors include the role of the stabilizer in minimizing protein adsorption on the ice surface, stress occurring late in freezing and the increased viscosity of the freeze-concentrate [12]. Stabilizers may also operate, at least in part, through their ability to prevent crystallization of buffer components, thereby reducing a potential pH shift [12]. Moreover, the vitrification hypothesis is discussed, according to which protein mobility and kinetics of unfolding are reduced in the glassy state [106].

5.2 Influence of the freezing step on protein stability

The freezing procedure in lyophilization can influence the crystallization of buffer components and other solutes, liquid–liquid phase separation and also the extent of the ice–water surface.

With respect to protein denaturation at the ice–water interface, there exists a strong correlation between freezing rate and protein stability. At high freezing rates, smaller ice crystals and larger ice–water interfaces are formed, leading to a greater extent of surface-induced denaturation of surface-sensitive proteins [94]. It is therefore recommended to use freezing conditions that reduce ice crystal interfaces in order to minimize surface-induced protein destabilization. Strambini and Gabellieri [107] showed that the increase in ice crystal surface area induced changes in protein structure and protein aggregation. There are several studies demonstrating that faster freezing resulting in larger ice-water interfaces, when compared to slow freezing, caused increased protein instabilities. Sarciaux et al. [108] found a lower level of insoluble aggregates of bovine IgG in phosphate buffer with shelf-ramped freezing in comparison with liquid nitrogen immersion after lyophilization. Eckhardt et al. [109] observed the same trend for human growth hormone during freeze-thawing. Chang et al. [104] showed that slow freezing resulted in less turbidity of various proteins upon freeze-thawing as opposed to freezing in liquid nitrogen. Jiang and Nail [40] investigated the effect of different freezing methods on catalase, β -galactosidase, and LDH activity in phosphate buffers. The highest level of protein activity was observed when pre-cooled shelf (-40 °C) freezing was applied. Intermediate recovery was obtained by shelf-ramped freezing (-0.5 °C/min) and lowest recovery by liquid nitrogen immersion. In this case, no direct correlation between cooling rate and protein stability could be proposed.

This emphasizes again the importance of distinguishing between cooling rate and actual freezing rate. Although the cooling rate is slower for shelf-ramped freezing than for the pre-cooled shelf method, the freezing rate is higher due to the higher degree of supercooling and improved thermal equilibrium throughout the sample volume. The cooling rate and the freezing rate are fast in the case of freezing by liquid nitrogen immersion, as the freezing behavior is shifted to directional solidification. Cochran et al. [38] used various methods to influence nucleation temperature during freezing and found an inverse relationship between the extent of supercooling and recovery of LDH activity after lyophilization and reconstitution.

Annealing is directly correlated with a decrease in the specific surface area and is thus known to impact protein stability. Sarciaux et al. [108] found that annealing reduced the percentage of bovine IgG aggregates from 33% to 12%, attributing to the reduction in aggregation due to the lower surface area of the annealed samples. Ironically, during annealing, the protein has at first to endure the surface denaturation stresses during “normal” freezing. The ice surface is reduced only after annealing. It seems that the unfolding due to surface denaturation is reversible in the liquid state and is only fixed after drying. This is also consistent with the finding of Sarciaux et al. [108] that there was no damage of IgG after freeze-thawing but after lyophilization when freezing occurred rapidly. Webb et al. [68] hypothesized that aggregation of recombinant human interferon during freeze-drying and spray-freeze-drying is a result of a retained internal stress in the glass that forms on freezing and not as a result of adsorption at the ice surface. However, there are some contradictions found in literature to the aforementioned relation between freezing rate, ice surface area, and protein stability. For example, Nema and Avis [110] found that fast freezing results in a reduced loss of LDH activity compared to slow freezing. They explained their finding by the fact that fast freezing minimizes the time that a

protein spends in the freeze-concentrated environment where degradation reactions can take place. Additionally, Heller et al. [39] observed that damage to hemoglobin in PEG/dextran formulations can be avoided by rapidly freezing the samples in liquid nitrogen. In this case, however, protein damage was a result of phase separation, which is more pronounced during slow freezing.

On the other hand, annealing not only decreases the ice surface area but also promotes crystallization of some solutes which can be associated with a pronounced loss in protein activity. For example, Izutsu et al. [111] showed that the activity of beta-galactosidase in the presence of mannitol or inositol decreased after annealing. The same trend was observed for LDH and L-asparaginase when mannitol crystallization was promoted due to the annealing step [86]. It was also found that inhibition of crystallization of mannitol with the presence of additional solutes can improve protein stability [85]. However, even under fairly aggressive annealing conditions the protein itself can inhibit mannitol crystallization [112].

The freezing rate will also influence the selective precipitation of buffer salts, thus influencing the extent of changes in the pH during freezing. Each buffer salt has its own critical cooling rate, above which crystallization is inhibited and will not result in a pH shift [113]. Annealing will further accentuate pH shifts and the protein will be exposed to unfavorable pH values for a increased period of time [41].

There is only limited information available on the influence of protein stability with freezing procedures other than shelf-ramped freezing and liquid nitrogen immersion. Passot et al. [57] found that the freezing method only influenced the recovery of catalase when the poor stabilizer maltodextrin was used. Under these conditions, a higher activity was observed after lyophilization and storage when the ultrasound technology or the pre-cooled shelf method was used. Bursac et al. [67] found for samples of 1 mg/ml LDH in 5% mannitol, a 22%

decrease in protein activity frozen with the depressurization technique. Whereas stochastic shelf-ramped freeze-thawing results in a 39% loss of activity.

Even the storage stability of a protein can be impacted by the freezing procedure. Hsu et al. [114] observed that fast freezing during lyophilization of a recombinant tissue plasminogen activator resulted in weaker storage stability of the protein. The authors proposed that the protein diffuses during freezing into the large ice–water interface and is then less protected by the excipient during storage. This is in accordance with the finding of Patapoff et al. [9] that the aggregation rate of a therapeutic protein is decreased upon storage when an annealing step was performed during lyophilization. The pH drop during freezing can also potentially affect the storage stability of lyophilized proteins as lyophilized proteins exhibit a “pH memory” [115–117]. For example, lyophilized interleukin aggregated more rapidly when formulated in a phosphate buffer at pH 6.5 in comparison with a citrate buffer at the same pH during storage [115]. Furthermore, the crystallization of meta-stable amorphous excipients or conversion hydrates to the anhydrous polymorphs can affect storage stability of proteins. For example, mannitol crystallization might be inhibited during fast freezing, but in situ crystallization of the meta-stable mannitol could be facilitated under storage conditions. The protein-stabilizing effect will be lost as a result. In addition, meta-stable mannitol hydrate transfers with liberation of water under storage conditions that can be critical with regard to protein stability [91].

In summary, the stability of proteins during freezing is affected differently by varying freezing rates and depending on the present protein denaturation mechanism. These mechanisms include surface-induced denaturation, pH-induced denaturation, denaturation due to the crystallization of the stabilizing excipient or phase-separation-induced denaturation.

6 Conclusion and practical considerations

During freezing, the samples first experience supercooling until heterogeneous ice nucleation occurs. The ice nuclei then grow, leading to cryoconcentration of the sample. Eutectic crystallization or vitrification of the solutes is observed when a critical concentration is exceeded. In regard to global supercooling versus directional

solidification, the ice crystal number and size is directly controlled by the degree of supercooling or by the freezing rate.

The random nature of ice nucleation is a big challenge for process control and results in vial-to-vial and batch-to-batch heterogeneity. Especially, the difference in the degree of supercooling when operating in a typical sterile manufacturing environment, containing much less foreign particles that can act as heterogeneous ice nucleation sites, is one of the biggest challenges in up-scaling [20]. In this case, samples show a more pronounced degree of supercooling and result in smaller ice crystals and increased product layer resistance. Longer drying rates are also required, and there is an increased risk for product lost [1]. Freezing methods that directly control ice nucleation are therefore essential in order to counter this challenge.

Various freezing methods have been developed in order to manipulate the freezing behavior. However, only a few are capable to directly control ice nucleation and have the potential to be applied in manufacturing scale.

The freezing step is of significant importance during lyophilization because it is the main desiccation step. Moreover, the freezing procedure directly impacts ice crystal formation and thus product morphology. Freezing methods that result in a high degree of supercooling freeze by global supercooling and result in the formation of small, spherulitic ice crystals. The size of these crystals is directly correlated to the degree of supercooling. Procedures that induce ice nucleation

at a low degree of supercooling freeze by global solidification. In this case, the interface velocity determines the size of the ice crystals.

Primary drying rates correlate with dried product resistance. Resistance is determined by pore size and the orientation of the pores. The formation of a skin at the top of the product can also determine resistance. Thus, freezing methods that result in the formation of large, vertically oriented ice crystals can drastically decrease primary drying time and show a decrease in product temperatures. This is due to the shift from mass transfer to heat transfer controlled product resistance, which results in more space for process optimization. However, reduction in primary drying time frequently involves the extension of the secondary drying step. Although primary drying times dominate, a compromise between primary and secondary drying rate must be found in order to minimize the total cycle length and reach the desired final moisture content.

The freezing step also affects the physical state of the excipients. Depending on the freezing rate, various polymorphs can be formed and the formation of metastable amorphous states or hydrate formation can be promoted. This can severely influence storage stability or lead to vial cracking during drying.

The freezing step also impacts the selective crystallization of excipients, especially in buffer components. This potentially leads to significant pH shifts, induces liquid–liquid phase separation and determines the extent of ice-water interfaces. Protein stability is therefore directly dependent on the freezing procedure. In the case of a surface-sensitive protein, slow freezing rates and the application of an annealing step could improve protein stability. For these slow freezing conditions, however, buffer crystallization and phase separation can be more pronounced. This can negatively impact protein stability. Fast freezing rates should be used and annealing should be avoided if a shift in pH, crystallization or phase separation of the stabilizing excipients is observed.

Thus, process optimization and formulation development should be accomplished hand in hand. Freezing methods that allow controlled ice nucleation at temperatures close to the equilibrium freezing point are suggested. These methods result in the formation of large oriented ice crystal, increase the drying rates, improve batch uniformity, reduce meta-stable glass formation, facilitate process scale-up and minimize protein damage at the reduced ice-water interfaces. Annealing provides a promising alternative if no controlled ice nucleation method is available. The presence of additives like ice nucleating agents or TBA could also have a positive effect. However, ice nucleating agents have to face regulatory concerns.

The awareness of the complexity of the freezing process and its consequences on product quality and process performance is essential for successful lyophilization. The knowledge of how to control, or at least manipulate, the freezing step will help to develop more efficient lyophilization cycles and biopharmaceutical products with an improved stability.

7 References

- [1] X. Tang, M. Pikal, Design of freeze-drying processes for pharmaceuticals: practical advice, *Pharm. Res.* 21 (2004) 191-200.
- [2] H.R. Constantino, Excipients of use in lyophilized pharmaceutical peptide, protein, and other bioproducts, in: H.R. Constantino (Ed.), *Lyophilization of Biopharmaceuticals*, AAPS Press, Arlington, VA, USA, 2004.
- [3] J.F. Carpenter, M.J. Pikal, B.S. Chang, T.W. Randolph, Rational design of stable lyophilized protein formulations: some practical advice, *Pharm. Res.* 14 (1997) 969-975.
- [4] F. Franks, Freeze-drying of bioproducts: putting principles into practice, *Eur. J. Pharm. Biopharm.* 45 (1998) 221-229.
- [5] J. Liu, T. Viverette, M. Virgin, M. Anderson, P. Dalal, A study of the impact of freezing on the lyophilization of a concentrated formulation with a high fill depth, *Pharm. Dev. Technol.* 10 (2005) 261-272.
- [6] M.J. Pikal, S. Rambhatla, R. Ramot, The impact of the freezing stage in lyophilization: effects of the ice nucleation temperature on process design and product quality, *Am. Pharm. Rev.* 5 (2002) 48-53.
- [7] P. Cameron, *Good Pharmaceutical Freeze-Drying Practice*, Interpharm Press, Inc., Buffalo Grove, USA, 1997.
- [8] G.-W. Oetjen, P. Haseley, *Freeze-Drying*, Wiley-VHC Verlag, Weinheim, 2004.
- [9] T.W. Patapoff, D.E. Overcashier, The importance of freezing on lyophilization cycle development, *Biopharm* 15 (2002) 16-21.
- [10] T. Jennings, The Freezing Process, in: *Lyophilization, Introduction and Basic Principles*, Interpharm Press, Englewood, USA, 1999.
- [11] F. Franks, T. Auffret, *Freeze-Drying of Pharmaceuticals and Biopharmaceuticals*, RSC Publishing, Cambridge, UK, 2007.
- [12] J.A. Searles, Freezing and annealing phenomena in lyophilization, in: L. Rey, J.C. May (Eds.), *Freeze-Drying/Lyophilization of Pharmaceutical and Biological Products*, Marcel Dekker, Inc., USA, New York, 2004.
- [13] A. Hottot, S. Vessot, J. Andrieu, Freeze drying of pharmaceuticals in vials: influence of freezing protocol and sample configuration on ice morphology and freeze-dried cake texture, *Chem. Eng. Process.* 46 (2007) 666-674.
- [14] J.A. Searles, J.F. Carpenter, T.W. Randolph, The ice nucleation temperature determines the primary drying rate of lyophilization for samples frozen on a temperature-controlled shelf, *J. Pharm. Sci.* 90 (2001) 860-871.

- [15] G. Petzold, J. Aguilera, Ice morphology: fundamentals and technological applications in foods, *Food Biophys.* 4 (2009) 378-396.
- [16] B.S. Bhatnagar, R.H. Bogner, M.J. Pikal, Protein stability during freezing: separation of stresses and mechanisms of protein stabilization, *Pharm. Dev. Technol.* 12 (2007) 505-523.
- [17] J.J. Schwegman, F.C. John, L.N. Steven, Evidence of partial unfolding of proteins at the ice/freeze-concentrate interface by infrared microscopy, *J. Pharm. Sci.* 98 (2009) 3239-3246.
- [18] J. Liu, Physical characterization of pharmaceutical formulations in frozen and freeze-dried solid states: techniques and applications in freeze-drying development, *Pharm. Dev. Technol.* 11 (2006) 3-28.
- [19] S.L. Nail, S. Jiang, S. Chongprasert, S.A. Knopp, Fundamentals of freeze-drying, in: S.L. Nail, M.J. Akers (Eds.), *Development and Manufacture of Protein Pharmaceuticals*, Kluwer Academic/Plenum Publisher, New York, 2002.
- [20] S. Rambhatla, R. Ramot, C. Bhugra, M. Pikal, Heat and mass transfer scale-up issues during freeze drying: II. Control and characterization of the degree of supercooling, *AAPS PharmSciTech* 5 (2004) 54-62.
- [21] M. Akyurt, G. Zaki, B. Habeebullah, Freezing phenomena in ice- water systems, *Energy Convers. Manage.* 43 (2002) 1773-1789.
- [22] M. Matsumoto, S. Saito, I. Ohmine, Molecular dynamics simulation of the ice nucleation and growth process leading to water freezing, *Nature* 416 (2002) 409- 413.
- [23] T. Jennings, The importance of process water, in: *Lyophilization, Introduction and Basic Principles*, Interpharm Press, Englewood, USA, 1999.
- [24] P.W. Wilson, A.F. Heneghan, A.D.J. Haymet, Ice nucleation in nature: supercooling point (SCP) measurements and the role of heterogeneous nucleation, *Cryobiology* 46 (2003) 88-98.
- [25] G. Blond, Velocity of linear crystallization of ice in macromolecular systems, *Cryobiology* 25 (1988) 61-66.
- [26] M.J. Pikal, S. Shah, D. Senior, J.E. Lang, Physical chemistry of freeze-drying: measurement of sublimation rates for frozen aqueous solutions by a microbalance technique, *J. Pharm. Sci.* 72 (1983) 635-650.
- [27] R.H.M. Hatley, A. Mant, Determination of the unfrozen water content of maximally freeze-concentrated carbohydrate solutions, *Int. J. Biol. Macromol.* 15 (1993) 227-232.
- [28] G.H.J.A. Tammann, *The States of Aggregation: The Changes in the State of Matter in their Dependence upon Pressure and Temperature*, Van Nostrand Company, Inc., New York, 1925.

- [29] V. Kett, D. McMahon, K. Ward, Thermoanalytical techniques for the investigation of the freeze drying process and freeze-dried products, *Curr. Pharm. Biotechnol.* 6 (2005) 239-250.
- [30] A.P. MacKenzie, Non-equilibrium freezing behaviour of aqueous systems, *Philos. Trans. Roy. Soc. London, Ser. B* 278 (1977) 167-189.
- [31] Y. Roos, M. Karel, Phase transitions of amorphous sucrose and frozen sucrose solutions, *J. Food Sci.* 56 (1991) 266-267.
- [32] T.W. Randolph, Phase separation of excipients during lyophilization: effects on protein stability, *J. Pharm. Sci.* 86 (1997) 1198-1203.
- [33] M.C. Heller, J.F. Carpenter, T.W. Randolph, Effects of phase separating systems on lyophilized hemoglobin, *J. Pharm. Sci.* 85 (1996) 1358-1362.
- [34] M.C. Heller, J.F. Carpenter, T.W. Randolph, Manipulation of lyophilization-induced phase separation: implications for pharmaceutical proteins, *Biotechnol. Prog.* 13 (1997) 590-596.
- [35] B.Y. Zaslavsky, T.O. Bagirov, A.A. Borovskaya, N.D. Gulaeva, L.H. Miheeva, A.U. Mahmudov, M.N. Rodnikova, Structure of water as a key factor of phase separation in aqueous mixtures of two nonionic polymers, *Polymer* 30 (1989) 2104-2111.
- [36] A. Pyne, K. Chatterjee, R. Suryanarayanan, Crystalline to amorphous transition of disodium hydrogen phosphate during primary drying, *Pharm. Res.* 20 (2003) 802-803.
- [37] T.W. Randolph, J.A. Searles, Freezing and annealing phenomena in lyophilization: effects upon primary drying rate, morphology, and heterogeneity, *Am. Pharm. Rev.* 5 (2002) 40-47.
- [38] T. Cochran, S.L. Nail, Ice nucleation temperature influences recovery of activity of a model protein after freeze drying, *J. Pharm. Sci.* 98 (2009) 3495-3498.
- [39] M.C. Heller, J.F. Carpenter, T.W. Randolph, Protein formulation and lyophilization cycle design: prevention of damage due to freeze-concentration induced phase separation, *Biotechnol. Bioeng.* 63 (1999) 166-174.
- [40] S. Jiang, S.L. Nail, Effect of process conditions on recovery of protein activity after freezing and freeze-drying, *Eur. J. Pharm. Biopharm.* 45 (1998) 249-257.
- [41] J.A. Searles, J.F. Carpenter, T.W. Randolph, Annealing to optimize the primary drying rate, reduce freezing-induced drying rate heterogeneity, and determine T_g in pharmaceutical lyophilization, *J. Pharm. Sci.* 90 (2001) 872-887.
- [42] X. Lu, M.J. Pikal, Freeze-drying of mannitol-trehalose-sodium chloride-based formulations: the impact of annealing on dry layer resistance to mass transfer and cake structure, *Pharm. Dev. Technol.* 9 (2004) 85-95.
- [43] H. Schoof, J. Apel, I. Heschel, G. Rau, Control of pore structure and size in freeze-dried collagen sponges, *J. Biomed. Mater. Res.* 58 (2001) 352-357.

- [44] T.D. Rowe, A technique for the nucleation of ice, in: International Symposium on Biological Product Freeze-Drying and Formulation, 1990.
- [45] S. Patel, C. Bhugra, M. Pikal, Reduced pressure ice fog technique for controlled ice nucleation during freeze-drying, *AAPS PharmSciTech* 10 (2009) 1406-1411.
- [46] A. Petersen, H. Schneider, G. Rau, B. Glasmacher, A new approach for freezing of aqueous solutions under active control of the nucleation temperature, *Cryobiology* 53 (2006) 248-257.
- [47] A. Petersen, G. Rau, B. Glasmacher, Reduction of primary freeze-drying time by electric field induced ice nucleus formation, *Heat Mass Transfer* 42 (2006) 929-938.
- [48] W. Rau, Eiskeimbildung durch Dielektrische Polarisierung, *Z. Naturforsch.* 6 (1951) 649-657.
- [49] T. Hozumi, A. Saito, S. Okawa, K. Watanabe, Effects of electrode materials on freezing of supercooled water in electric freeze control, *Int. J. Refrig.* 26 (2003) 537-542.
- [50] T. Inada, X. Zhang, A. Yabe, Y. Kozawa, Active control of phase change from supercooled water to ice by ultrasonic vibration 1. Control of freezing temperature, *Int. J. Heat Mass Transfer* 44 (2001) 4523-4531.
- [51] X. Zhang, T. Inada, A. Yabe, S. Lu, Y. Kozawa, Active control of phase change from supercooled water to ice by ultrasonic vibration 2. Generation of ice slurries and effect of bubble nuclei, *Int. J. Heat Mass Transfer* 44 (2001) 4533-4539.
- [52] X. Zhang, T. Inada, A. Tezuka, Ultrasonic-induced nucleation of ice in water containing air bubbles, *Ultrason. Sonochem.* 10 (2003) 71-76.
- [53] M. Saclier, R. Peczalski, J. Andrieu, A theoretical model for ice primary nucleation induced by acoustic cavitation, *Ultrason. Sonochem.* 17 (2010) 98-105.
- [54] K. Nakagawa, A. Hottot, S. Vessot, J. Andrieu, Influence of controlled nucleation by ultrasounds on ice morphology of frozen formulations for pharmaceutical proteins freeze-drying, *Chem. Eng. Process.* 45 (2006) 783-791.
- [55] A. Hottot, K. Nakagawa, J. Andrieu, Effect of ultrasound-controlled nucleation on structural and morphological properties of freeze-dried mannitol solutions, *Chem. Eng. Res. Des.* 86 (2008) 193-200.
- [56] M. Saclier, R. Peczalski, J. Andrieu, Effect of ultrasonically induced nucleation on ice crystals' size and shape during freezing in vials, *Chem. Eng. Sci.* 65 (2010) 3064-3071.
- [57] S. Passot, I.C. Trelea, M. Marin, M. Galan, G.J. Morris, F. Fonseca, Effect of controlled ice nucleation on primary drying stage and protein recovery in vials cooled in a modified freeze-dryer, *J. Biomech. Eng.* 131 (2009) 074511-074515.
- [58] K. McDonald, D.-W. Sun, Vacuum cooling technology for the food processing industry: a review, *J. Food Eng.* 45 (2000) 55-65.

- [59] M. Kramer, B. Sennhenn, G. Lee, Freeze-drying using vacuum-induced surface freezing, *J. Pharm. Sci.* 91 (2002) 433-443.
- [60] P.D. Sanz, L. Otero, C. de Elvira, J.A. Carrasco, Freezing processes in highpressure domains, *Int. J. Refrig.* 20 (1997) 301-307.
- [61] B. Li, D.-W. Sun, Novel methods for rapid freezing and thawing of foods – a review, *J. Food Eng.* 54 (2002) 175-182.
- [62] M.N. Martino, L. Otero, P.D. Sanz, N.E. Zaritzky, Size and location of ice crystals in pork frozen by high-pressure-assisted freezing as compared to classical methods, *Meat Sci.* 50 (1998) 303-313.
- [63] L. Otero, P.D. Sanz, High-pressure shift freezing. Part 1. Amount of ice instantaneously formed in the process, *Biotechnol. Prog.* 16 (2000) 1030-1036.
- [64] P.P. Fernández, L. Otero, B. Guignon, P.D. Sanz, High-pressure shift freezing versus high-pressure assisted freezing: effects on the microstructure of a food model, *Food Hydrocolloids* 20 (2006) 510-522.
- [65] T.H. Gasteyer, R.R. Sever, B. Hunek, N. Grinter, M.L. Verdone, Lyophilization system and method, in: Patent Application Publication, United States, 2007.
- [66] B.M. Rampersad, R.R. Sever, B. Hunek, T.H. Gasteyer, Freeze-dryer and method of controlling the same, in: Patent Application Publication, United States, 2010.
- [67] R. Bursac, R. Sever, B. Hunek, A practical method for resolving the nucleation problem in lyophilization, *Bioprocess Int.* (2009) 66-72.
- [68] <<http://www.spscientific.com/ControlLyoTechnology>> (accessed 12.02.10).
- [69] N. Cochet, P. Widehem, Ice crystallization by *Pseudomonas syringae*, *Appl. Microbiol. Biotechnol.* 54 (2000) 153-161.
- [70] B. Vonnegut, The nucleation of ice formation by silver iodide, *J. Appl. Chem.* 18 (1947) 593-595.
- [71] M. Gavish, J. Wang, M. Eisenstein, M. Lahav, L. Leiserowitz, The role of crystal polarity in alpha-amino acid crystals for induced nucleation of ice, *Science* 256 (1992) 815-818.
- [72] K.-i. Izutsu, S. Kojima, Freeze-concentration separates proteins and polymer excipients into different amorphous phases, *Pharm. Res.* 17 (2000) 1316-1322.
- [73] L.R. Maki, E.L. Galyan, M.-M. Chang-Chien, D.R. Caldwell, Ice nucleation induced by *Pseudomonas syringae*, *Appl. Environ. Microbiol.* 28 (1974) 456-459.
- [74] D.L. Teagarden, D.S. Baker, Practical aspects of lyophilization using nonaqueous co-solvent systems, *Eur. J. Pharm. Sci.* 15 (2002) 115-133.
- [75] K. Kasraian, P.P. DeLuca, Thermal analysis of the tertiary butyl alcohol/water system and its implications on freeze-drying, *Pharm. Res.* 12 (1995) 484-490.

- [76] S. Wittaya-Areekul, S.L. Nail, Freeze-drying of tert-butyl alcohol/water cosolvent systems: effects of formulation and process variables on residual solvents, *J. Pharm. Sci.* 87 (1998) 491-495.
- [77] K. Kasraian, P.P. DeLuca, The effect of tertiary butyl alcohol on the resistance of the dry product layer during primary drying, *Pharm. Res.* 12 (1995) 491-495.
- [78] S. Wittaya-Areekul, G.F. Needham, N. Milton, M.L. Roy, S.L. Nail, Freeze-drying of tert-butanol/water cosolvent systems: a case report on formation of a friable freeze-dried powder of tobramycin sulfate, *J. Pharm. Sci.* 91 (2002) 1147-1155.
- [79] S.D. Webb, J.L. Cleland, J.F. Carpenter, T.W. Randolph, Effects of annealing lyophilized and spray-lyophilized formulations of recombinant human interferon- γ , *J. Pharm. Sci.* 92 (2003) 715-729.
- [80] S.D. Webb, J.L. Cleland, J.F. Carpenter, T.W. Randolph, Effects of annealing lyophilized and spray-lyophilized formulations of recombinant human interferon- γ , *J. Pharm. Sci.* 92 (2003) 715-729.
- [81] M.J. Pikal, M.L. Roy, S. Shah, Mass and heat transfer in vial freeze-drying of pharmaceuticals: role of the vial, *J. Pharm. Sci.* 73 (1984) 1224-1237.
- [82] J. Oesterle, F. Franks, T. Auffret, The influence of tertiary butyl alcohol and volatile salts on the sublimation of ice from frozen sucrose solutions: implications for freeze-drying, *Pharm. Dev. Technol.* 3 (1998) 175-183.
- [83] R. Daoussi, S. Vessot, J. Andrieu, O. Monnier, Sublimation kinetics and sublimation end-point times during freeze-drying of pharmaceutical active principle with organic co-solvent formulations, *Chem. Eng. Res. Des.* 87 (2009) 899-907.
- [84] R.K. Cavatur, N.M. Vemuri, A. Pyne, Z. Chrzan, D. Toledo-Velasquez, R. Suryanarayanan, Crystallization behavior of mannitol in frozen aqueous solutions, *Pharm. Res.* 19 (2002) 894-900.
- [85] A. Pyne, K. Chatterjee, R. Suryanarayanan, Solute crystallization in mannitol-glycine systems - implications on protein stabilization in freeze-dried formulations, *J. Pharm. Sci.* 92 (2003) 2272-2283.
- [86] K. Izutsu, S. Yoshioka, T. Terao, Effect of mannitol crystallinity on the stabilization of enzymes during freeze-drying, *Chem. Pharm. Bull.* 42 (1994) 5-8.
- [87] A.J. Cannon, E.H. Trappler, The influence of lyophilization on the polymorphic behavior of mannitol, *PDA J. Pharm. Sci. Technol.* 54 (2000) 13-22.
- [88] A.I. Kim, M.J. Akers, S.L. Nail, The physical state of mannitol after freeze-drying: effects of mannitol concentration, freezing rate, and a noncrystallizing cosolute, *J. Pharm. Sci.* 87 (1998) 931-935.
- [89] K. Nakagawa, W. Murakami, J. Andrieu, S. Vessot, Freezing step controls the mannitol phase composition heterogeneity, *Chem. Eng. Res. Des.* 87 (2009) 1017-1027.

- [90] X. Liao, R. Krishnamurthy, R. Suryanarayanan, Influence of processing conditions on the physical state of mannitol - implications in freeze-drying, *Pharm. Res.* 24 (2007) 370-376.
- [91] A. Hawe, W. Frieß, Impact of freezing procedure and annealing on the physico-chemical properties and the formation of mannitol hydrate in mannitol-sucrose-NaCl formulations, *Eur. J. Pharm. Biopharm.* 64 (2006) 316-325.
- [92] P. Hiwale, A. Amin, L. Kumar, A.K. Bansal, Variables affecting reconstitution time of dry powder for injection, *Pharm. Technol.* 2 (July) (2008).
- [93] S.J. Shire, Z. Shahrokh, J. Liu, Challenges in the development of high protein concentration formulations, *J. Pharm. Sci.* 93 (2004) 1390-1402.
- [94] W. Wang, Lyophilization and development of solid protein pharmaceuticals, *Int. J. Pharm.* 203 (2000) 1-60.
- [95] E.Y. Chi, S. Krishnan, T.W. Randolph, J.F. Carpenter, Physical stability of proteins in aqueous solution: mechanism and driving forces in nonnative protein aggregation, *Pharm. Res.* 20 (2003) 1325-1336.
- [96] K. Dill, Dominant forces in protein folding, *Biochemistry* 29 (1990) 7133-7155.
- [97] B.S. Bhatnagar, M.J. Pikal, R.H. Bogner, Study of the individual contributions of ice formation and freeze-concentration on isothermal stability of lactate dehydrogenase during freezing, *J. Pharm. Sci.* 97 (2008) 798-814.
- [98] X.C. Tang, M.J. Pikal, The effect of stabilizers and denaturants on the cold denaturation temperatures of proteins and implications for freeze-drying, *Pharm. Res.* 22 (2005) 1167-1175.
- [99] G. Gomez, M.J. Pikal, N. Rodriguez-Hornedo, Effect of initial buffer composition on pH changes during far-from-equilibrium freezing of sodium phosphate buffer solutions, *Pharm. Res.* 18 (2001) 90-97.
- [100] T.J. Anchordoquy, J.F. Carpenter, Polymers protect lactate dehydrogenase during freeze-drying by inhibiting dissociation in the frozen state, *Arch. Biochem. Biophys.* 332 (1996) 231-238.
- [101] D. Piedmonte, C. Summers, A. McAuley, L. Karamujic, G. Ratnaswamy, Sorbitol crystallization can lead to protein aggregation in frozen protein formulations, *Pharm. Res.* 24 (2007) 136-146.
- [102] E.J. Workman, S.E. Reynolds, Electrical phenomena occurring during the freezing of dilute aqueous solutions and their possible relationship to thunderstorm electricity, *Phys. Rev.* 78 (1950) 254.
- [103] W. Norde, Adsorption of proteins from solution at the solid-liquid interface, *Adv. Colloid Interface Sci.* 25 (1986) 267-340.

- [104] B.S. Chang, B.S. Kendrick, J.F. Carpenter, Surface-induced denaturation of proteins during freezing and its inhibition by surfactants, *J. Pharm. Sci.* 85 (1996) 1325-1330.
- [105] J.F. Carpenter, T. Arakawa, J.H. Crowe, Interactions of stabilizing additives with proteins during freeze-thawing and freeze-drying, *Dev. Biol.* 74 (1992) 225-238 (discussion 238-229).
- [106] M.J. Pikal, Mechanisms of protein stabilization during freeze-drying and storage: the relative importance of thermodynamic stabilization and glassy state relaxation dynamics, in: L. Rey, J.C. May (Eds.), *In Freeze-Drying/ Lyophilization of Pharmaceutical and Biological Products*, Marcel Dekker, Inc., New York, 2004, pp. 63-107.
- [107] G.B. Strambini, E. Gabellieri, Proteins in frozen solutions: evidence of ice-induced partial unfolding, *Biophys. J.* 70 (1996) 971-976.
- [108] J.-M. Sarciaux, S. Mansour, M.J. Hageman, S.L. Nail, Effects of buffer composition and processing conditions on aggregation of bovine IgG during freeze-drying, *J. Pharm. Sci.* 88 (1999) 1354-1361.
- [109] B.M. Eckhardt, J.Q. Oeswein, T.A. Bewley, Effect of freezing on aggregation of human growth hormone, *Pharm. Res.* 8 (1991) 1360-1364.
- [110] S. Nema, K.E. Avis, Freeze-thaw studies of a model protein, lactate dehydrogenase, in the presence of cryoprotectants, *J. Parenter. Sci. Technol.* 47 (1993) 76-83.
- [111] K. Izutsu, S. Yoshioka, T. Terao, Decreased protein-stabilizing effects of cryoprotectants due to crystallization, *Pharm. Res.* 10 (1993) 1232-1237.
- [112] D. Dixon, S. Tchessalov, A. Barry, N. Warne, The impact of protein concentration on mannitol and sodium chloride crystallinity and polymorphism upon lyophilization, *J. Pharm. Sci.* 98 (2009) 3419-3429.
- [113] B.S. Chang, C.S. Randall, Use of subambient thermal analysis to optimize protein lyophilization, *Cryobiology* 29 (1992) 632-656.
- [114] C.C. Hsu, H.M. Nguyen, D.A. Yeung, D.A. Brooks, G.S. Koe, T.A. Bewley, R. Pearlman, Surface denaturation at solid-void interface - a possible pathway by which opalescent participates form during the storage of lyophilized tissue-type plasminogen activator at high temperatures, *Pharm. Res.* 12 (1995) 69-77.
- [115] B.S. Chang, G. Reeder, J.F. Carpenter, Development of a stable freeze-dried formulation of recombinant human interleukin-1 receptor antagonist, *Pharm. Res.* 13 (1996) 243-249.
- [116] X.M. Lam, H.R. Costantino, D.E. Overcashier, T.H. Nguyen, C.C. Hsu, Replacing succinate with glycolate buffer improves the stability of lyophilized interferon- γ , *Int. J. Pharm.* 142 (1996) 85-95.
- [117] H.R. Costantino, K. Griebenow, R. Langer, A.M. Klibanov, On the pH memory of lyophilized compounds containing protein functional groups, *Biotechnol. Bioeng.* 53 (1997) 345-348.

Chapter 3

Objectives of the thesis

The objective of the thesis was the lyophilization of cationic polymer-based pDNA or siRNA nanoparticles (i.e. pDNA or siRNA polyplexes) with a special focus on the development of long-term stable formulations, the investigation of stabilization mechanisms especially during freezing, and the advanced monitoring of the lyophilization process.

One essential prerequisite for the successful development of lyophilized nucleic acid complex formulations is the availability of the initial nanoparticles at a constant and defined quality. Thus, the first aim of this thesis was to establish and up-scale a micro-mixer method for the standardized and reproducible preparation of plasmid/LPEI polyplexes in order to overcome the drawbacks that are related to the classical preparation by mixing via pipetting (Chapter 4). In a second step, this approach had to be transferred to up-scale the preparation of siRNA/oligoaminoamide polyplexes (Chapter 7).

In order to avoid the risks associated with the need for always fresh preparation of the polyplexes by the mixing nucleic acid component with the carrier solution in clinical application, the production of large standardized batches of well-defined, transfection efficient polyplexes with long-term stability by lyophilization is a desirable goal. Thus, one primary objective of this thesis was the development of lyophilized, long-term stable formulations for plasmid/LPEI

polyplexes (Chapter 5). In this context, a variety of excipients was tested and an extended set of analytical methods were to be employed to assure the pharmaceutical product quality.

It was found that the undesirable aggregation of plasmid/LPEI polyplexes occurs predominantly during the freezing and not during the drying step of the lyophilization process. Hence, an additional focus of this thesis was on the effect of different freezing parameters, such as ice nucleation temperature or freezing rate, on the stability of plasmid/LPEI polyplexes, in order to better understand the underlying stabilization mechanisms (Chapter 6). The theoretical background on the freezing process, physico-chemical fundamentals of freezing, available freezing methods, and consequences of freezing on product quality was reviewed beforehand (Chapter 2).

On the basis of the successful development of lyophilized plasmid/LPEI polyplexes, a further objective of this thesis was the formulation development of lyophilized, long-term stable siRNA/oligoaminoamide polyplexes (Chapter 7). In this context, the correlation between the chemical structure of the used oligomers and the freeze-thaw stability of the corresponding siRNA polyplexes had to be studied and the possibility to achieve high concentration siRNA polyplex formulations by reconstitution to reduced volumes needed to be evaluated.

Finally, an optical fiber system, that is based on fiber Bragg gratings, was to be established as a novel process monitoring tool during lyophilization (Chapter 8). Here, the potential of the optical fiber sensors for non-invasive or three-dimensional temperature monitoring and the sensitivity of the sensors to detect physico-chemical events during freezing was of high interest.

Chapter 4

Establishment of an up-scaled micro-mixer method

The following chapter has been published in the European Journal of Pharmaceutics and Biopharmaceutics and appears in this thesis with the journal's permission:

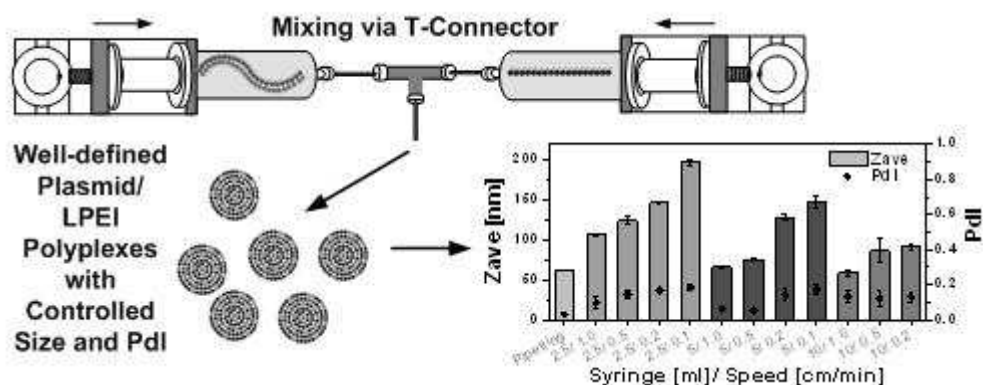
Julia Christina Kasper, David Schaffert*, Manfred Ogris, Ernst Wagner, Wolfgang Friess

The establishment of an up-scaled micro-mixer method allows the standardized and reproducible preparation of well-defined plasmid/LPEI polyplexes

Eur. J. Pharm. Biopharm. 77 (2011) 182-185

*LPEI synthesis and cell culture experiments were performed by D. Schaffert.

Graphical Abstract



Abstract

Polyplexes based on linear polyethylenimine (LPEI) and plasmid DNA are known as efficient non-viral gene delivery systems. However, the requirement for freshly prepared complexes prior to administration due to their instability in aqueous suspension poses the risk of batch-to-batch variations. Therefore, the aim of the study was the establishment of a reproducible and up-scalable method for the preparation of well-defined polyplexes.

Polyplexes consisting of pCMVLuc plasmid and 22 kDa linear polyethylenimine (LPEI) were prepared by classical pipetting or with a micro-mixer method using different mixing speeds and plasmid DNA concentrations (20–400 µg/mL). The z-average diameter of the polyplexes was measured by dynamic light scattering. Metabolic activity and transfection efficiency was evaluated on murine neuroblastoma cells after transfection with polyplexes.

When varying mixing speeds of the micro-mixer, polyplex size (59–197 nm) and polydispersity index (0.05–0.19) could be directly controlled. The z-average diameter (65–170 nm) and polydispersity index (0.05–0.22) of the polyplexes increased with increasing plasmid DNA concentration (20–400 µg/mL).

The established up-scaled micro-mixer method allows the standardized and reproducible preparation of well-defined, transfection-competent plasmid/LPEI polyplexes with high reproducibility.

Keywords

Non-viral gene delivery, well-defined polyplexes, up-scaled preparation, influence of mixing speed, influence of concentration

1 Introduction

Non-viral, plasmid-based therapeutics represent a new class of pharmaceuticals that offer the potential to cure several diseases currently considered untreatable [1]. Non-viral vectors, based on DNA complexes with cationic lipids (lipoplexes) or polycationic polymers (polyplexes), are attractive because of their low cost and high flexibility and have been proven safe and non-immunogenic in clinical trials [1,2]. On the other hand, depending on the polymer used, polyplexes suffer from drawbacks such as toxicity and non-specific interactions with the cells [3]. Another limiting factor for their clinical practicability is the requirement for freshly prepared formulations prior to administration because of the tendency towards particle aggregation in liquid formulations [2,4]. However, the day-to-day preparation poses the risk of batch-to-batch variability, including significant variations in product quality, safety and transfection rates, and the inability to perform extensive quality control prior to the actual administration due to time constraints [2,4]. Currently, the classical preparation of non-viral vectors, mixing a solution of DNA with a solution of cationic agents (i.e. lipid or polymer) via pipetting, is restricted to relatively small volumes [1]. This poorly defined and difficult to control preparation method can result in the formation of highly heterogeneous complexes with a broad range of sizes and charge ratios [5]. Thus, the controlled reproducible production of standardized batches of well-defined non-viral complexes is a major challenge [4,5]. Zelphati et al. [5] developed an automated and controllable production process for the preparation of lipoplexes utilizing a specially designed continuous flow pumping system, in which the DNA and liposome solution are mixed at 90° angles at the junction of a T-connector. In accordance to that first effort, Clement et al. [4] introduced a continuous mixing technique for the large-scale preparation of lipoplexes.

However, such automated up-scaled mixing has not yet been established for the preparation of polyplexes.

Hence, we aimed at establishing an up-scaled method for the reproducible preparation of well-defined polyplexes based on plasmid DNA and 22 kDa LPEI. The influence of the preparation procedure (classical pipetting versus up-scaled preparation), the mixing speed and the plasmid/LPEI concentration on particle size, polydispersity and in vitro performance (transfection efficiency and toxicity) of the polyplexes was investigated.

2 Materials and methods

2.1 Materials

The plasmid (pCMVLuc) was produced by PlasmidFactory (Bielefeld, Germany). As described, 22 kDa LPEI was synthesized by acid-catalyzed hydrolyses from commercial poly(2-ethyl-2-oxazoline) (Sigma Aldrich, Steinheim, Germany) [6]. Plasmid and LPEI stock solutions were diluted in 10 mM L-histidine (Merck, Darmstadt, Germany) buffer pH 6.0, so that mixing equal volumes of the two dilutions always resulted in a N/P ratio (molar ratio of LPEI nitrogen (N) to DNA phosphate (P)) of 6/1. Indicated polyplex concentrations always refer to the plasmid DNA concentration of the samples.

2.2 Preparation of plasmid/LPEI polyplexes by pipetting

For the traditional preparation of the polyplexes ($n=3$), 250 μL of plasmid solution were pipetted into the same volume of LPEI solution in a 1.5-mL reaction tube, mixed by rapid pipetting and incubated for 30 min at room temperature. For direct comparison with the up-scaled method, polyplexes were also prepared ($n=3$) at increased volumes, mixing 2.5 mL of plasmid solution with 2.5 mL of LPEI solution with a 5-mL pipette in a 15-mL reaction tube.

2.3 Up-scaled preparation of plasmid/LPEI polyplexes

Equal volumes (2.5 mL) of plasmid solution and LPEI solution were loaded into two separate syringes with luer lock tip (Terumo, Leuven, Belgium), connected via polyetheretherketone tubings (0.5 mm inner diameter, 5.0 cm length) to a T-connector (Micro Tee P-890) (Upchurch Scientific, Oak Harbor, USA) and fixed into two common syringe drivers. The mixing occurred when the carriages on the syringe driver pushed the plunger of the syringes simultaneously at the same speed. The flow rate could be controlled either by using different-sized syringes (2.5, 5.0 or 10.0 mL) and/or by adjusting the plunger speed (0.1, 0.2,

0.5 or 1.0 cm/min) on the syringe driver. After mixing (n=3), the polyplexes were incubated for 30 min at room temperature.

2.4 Particle size determination

The z-average particle diameter was measured by dynamic light scattering (DLS) using the DLS plate reader DynaPro Titan (Wyatt Technology, Dernbach, Germany) at a laser wavelength of 830 nm and a scattering angle of 150°. One hundred microliters per sample (n=3) was pipetted into 96 UV-well plates (Costar™, Corning, USA) and analyzed at room temperature using five acquisitions, with 5 s each. Polyplexes were assumed as linear polymers with a refractive index increment value dn/dc of 0.185, and for the dispersant, the refractive index of water (1.33) was used. The functionality of the DLS plate reader was checked by polystyrene nanosphere-sized standards (Thermo Fisher Scientific, Fremont CA, USA). DLS autocorrelation data were analyzed with the Dynamics V6 software based on cumulant analysis with respect to particle size and polydispersity.

2.5 Cell culture

In vitro transfection experiments were performed using murine neuroblastoma (Neuro-2A) cells. Two parallel transfection series were carried out in separate 96-well plates. Cells were seeded 24 h prior to transfection with a density of 10^4 cells in 200 μ L/well of culture medium containing 10% serum, 100 U/mL penicillin and 100 μ g/mL streptomycin. Immediately before transfection, medium was removed and 100 μ L of polyplexes diluted in culture medium (200 ng DNA) was added to the cells for 24 h until cytotoxicity and luciferase activity were analyzed. Cytotoxicity was evaluated 24 h after treatment by methylthiazoletetrazolium (MTT)/thiazolyl blue assay [7]. Metabolic activity (%) was expressed relative to the metabolic activity of untreated control cells (HBG buffer pH 7.4 only (5% glucose, 20 mM 4-(2-hydroxyethyl)-1-piperazineethane-

sulfonic acid) (both, Merck, Darmstadt, Germany)), defined as 100%. To determine the luciferase reporter gene expression, the medium was removed and cells were lysed in 50 μ l 0.5X Promega cell lysis solution 24 h after initial transfection. Luciferase light units were recorded with a Lumat LB9507 instrument (Berthold, Bad Wildbad, Germany) from a 22 μ L aliquot of the cell lysate with 10-s integration time after automatic injection of freshly prepared luciferase assay reagent using the Luciferase assay system (Promega, Mannheim, Germany). Luciferase activity (%) of the samples was expressed relative to the luciferase activity of plasmid/LPEI control polyplexes (formulated in HBG buffer via pipetting), defined as 100%.

3 Results and discussion

3.1 Establishment of the up-scaled micro-mixer method for the preparation of plasmid/LPEI polyplexes

Particle size and aggregation behaviour of the complexes are strongly affected by the preparation conditions like the way of adding the polymer solution to the nucleic acid solution or vice versa, diluting the complexes after their preparation or the used complexation time [8]. Up to date, the classical preparation of plasmid/LPEI polyplexes is to mix plasmid and LPEI solutions via pipetting that is traditionally performed at small volumes and often results in more or less heterogeneous batches [1,5]. Therefore, we established an up-scaled method for the preparation of polyplexes in accordance to the method described by Zelphati et al. [5]. Using two common syringe drivers, the plasmid and LPEI solutions were mixed at the junction of a T-connector and the mixing speed was controlled by syringe size and/or plunger speed (Figure 4-1).

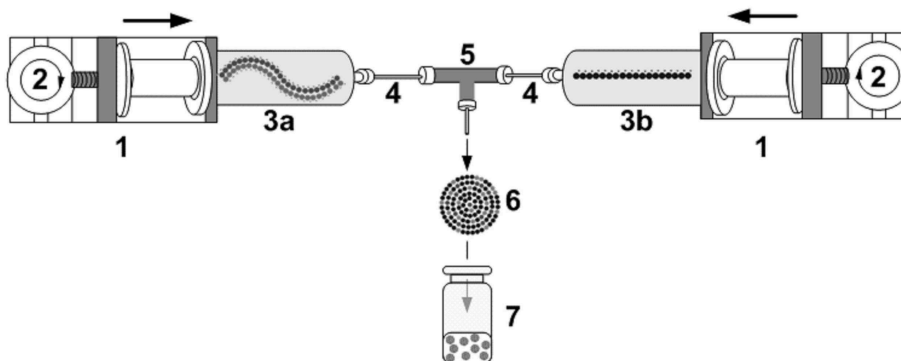


Figure 4-1: Schematic representation of the up-scaled micro-mixer method for the preparation of plasmid/LPEI polyplexes: (1) syringe driver, (2) plunger speed control, (3a) syringe with luer lock tip loaded with poly-nucleic acid solution, (3b) syringe with luer lock tip loaded with polycation solution, (4) polyetheretherketone tubings, (5) T-connector site of mixing, (6) formed polyplex, (7) glass vial.

Plasmid/LPEI polyplexes prepared by the up-scaled micro-mixer method at varied mixing speeds were compared to those prepared by classical pipetting. In general, with increasing mixing speeds, achieved by using increased plunger speeds and/or bigger syringe sizes, the z-average diameter as well as the polydispersity index (Pdl) of the plasmid/LPEI polyplexes decreased from approximately 200 to 50 nm and 0.2 to 0.05, respectively (Figure 4-2). Only when using a 10-mL syringe, the polydispersity index of about 0.15 remained constant with increasing flow rate as the handling of the small filling volume compared to the high volume of the syringe was hindered. In addition, polyplexes were prepared by pipetting at large volume (5 mL). This preparation method resulted in larger and more heterogeneous polyplexes compared to pipetting at low volumes (0.5 mL).

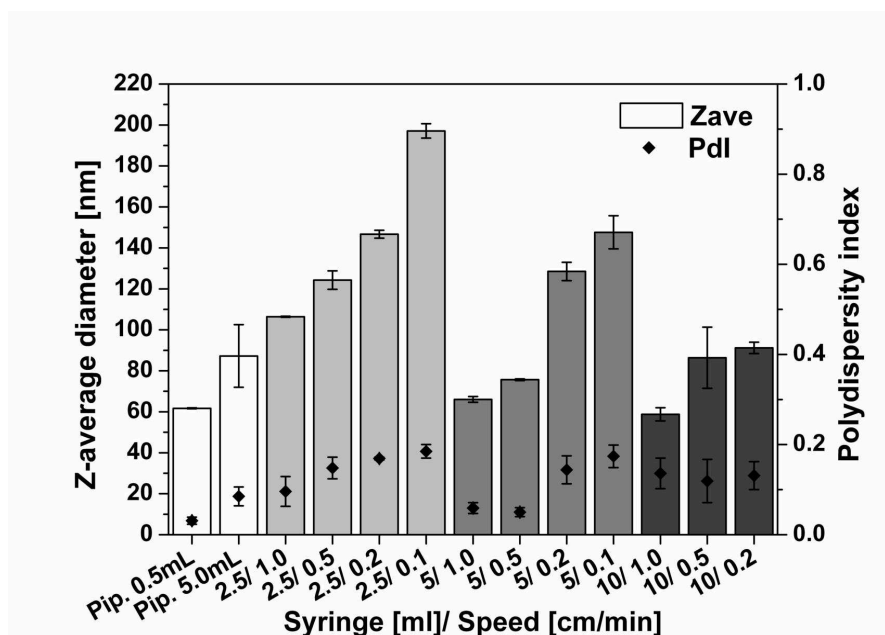


Figure 4-2: z-average diameter (nm) and Pdl of plasmid/LPEI polyplexes (20 $\mu\text{g/ml}$) prepared by classical pipetting (Pip.) at low volumes (0.5 mL) or at large volumes (5 mL) or by the up-scaled preparation method using different syringe sizes (2.5, 5 and 10 ml) and different plunger speeds (1.0, 0.5, 0.2 and 0.1 cm/min). Values represent the mean \pm 1 SD (n=3).

As traditionally pipetting and using the up-scaled micro-mixer method with a mixing speed of about 10.6 mL/min (1.0 cm/min in combination with a 5-mL syringe, 13 mm inner syringe diameter) led to comparable results (polyplex size

65 nm, Pdl 0.05), polyplexes prepared with these two settings were tested in cell culture experiments (Figure 4-3). No differences in metabolic activity or reporter gene expression for up-scaled and classically prepared polyplexes were observed. Hence, we conclude that in vitro results were not significantly influenced by the preparation method.

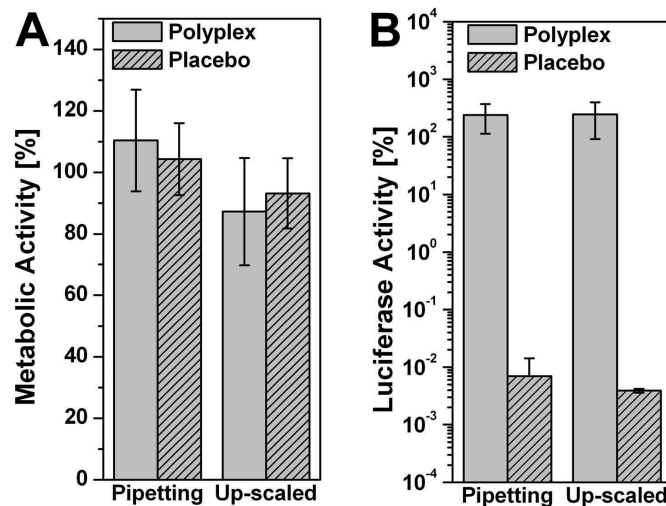


Figure 4-3: Influence of the preparation method, pipetting (0.5 mL) versus up-scaled preparation, of freshly prepared plasmid/LPEI polyplexes and corresponding placebo formulations (only buffer) on (A) the metabolic activity (%) relative to HBG-treated murine neuroblastoma (Neuro-2A) cells determined via MTT assay and (B) in vitro transfection activity in murine neuroblastoma (Neuro-2A) cells determined as luciferase activity, normalized to the activity of the LPEI/CMVLuc control. Experiments were performed in quintuplicates using N/P 6.

Large batches of polyplexes should not be simply prepared by mixing increased volumes of plasmid and polymer solution via pipetting. This approach can lead to heterogeneous batches of larger polyplexes, as the mixing process at larger volume becomes less controllable. The establishment of a controllable and up-scalable micro-mixer method for the highly reproducible preparation of homogenous, standardized and well-defined polyplexes can minimize handling inconsistencies among different operators. Concerns regarding the order of addition, adding the DNA solution to the polymer solution or vice versa, are avoided by mixing the two solution feeds at a constant N/P ratio during the entire procedure leading to homogenous and standardized batches. Moreover,

by using this method, the size and polydispersity of the plasmid/LPEI polyplexes can be directly controlled via the mixing speed. Up to now, an automated up-scaled mixing method was only established for the preparation of lipoplexes [4,5]. Zelphati et al. [5] introduced an analogous method for the preparation of cationic lipoplexes with well-defined sizes and also demonstrated that the particle size is influenced by the mixing rate. Using this method, the preparation volume is limited by the syringe size but can be easily scaled up. For example, Clement et al. [4] showed that mixing the two solutions via pumping is a viable alternative to the use of syringes, allowing the preparation of almost unlimited batch volumes.

3.2 Influence of the plasmid concentration on particle size and polydispersity of plasmid/LPEI polyplexes

In a next step, the influence of the preparation concentration on particle size and polydispersity of plasmid/LPEI polyplexes was evaluated. Plasmid/LPEI polyplexes were prepared at various plasmid DNA concentrations by the up-scaled micro-mixer method and compared to polyplexes prepared by classical pipetting (Figure 4-4).

The z-average diameter and the Pdl decreased with decreasing plasmid DNA concentration and ranged from 170 nm respectively Pdl 0.22 at a plasmid DNA concentration of 400 $\mu\text{g}/\text{mL}$ to 65 nm respectively Pdl 0.05 at 20 $\mu\text{g}/\text{mL}$. At low concentrations, the z-average diameter and the Pdl for polyplexes prepared by the up-scaled micro-mixer method were identical compared to those prepared by classical pipetting. However, with increasing concentration, the polydispersity of samples prepared by classical pipetting increased drastically compared to the micro-mixer method. The sample at 400 $\mu\text{g}/\text{mL}$ prepared by classical pipetting had to be diluted for the dynamic light-scattering measurements due to high scattering by extremely large particles.

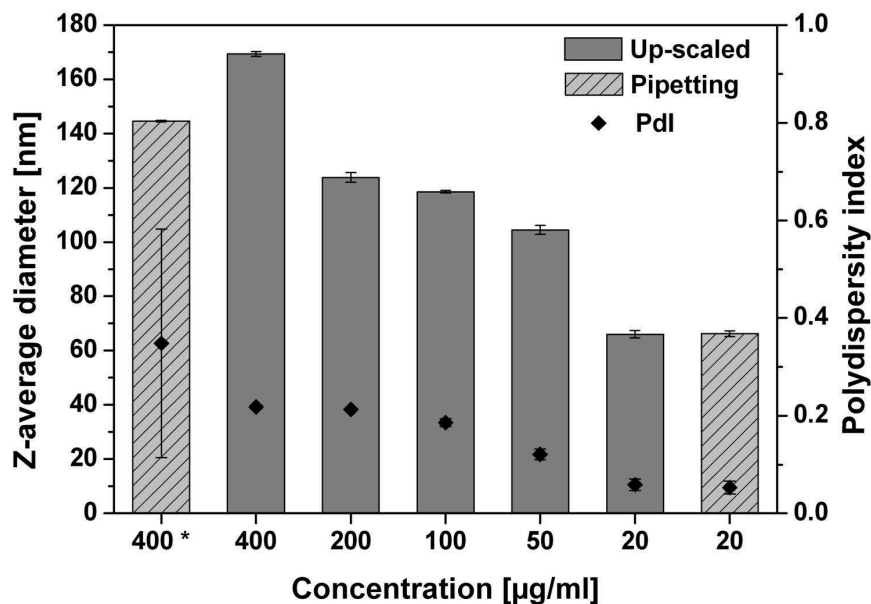


Figure 4-4: z-Average diameter (nm) and PDI of plasmid/LPEI polyplexes prepared at different concentrations (20, 50, 100, 200 and 400 $\mu\text{g/ml}$) in L-histidine buffer pH 6.0 by classical pipetting (0.5 mL) and by the up-scaled preparation method using a 5-ml syringe and a mixing speed of 1.0 cm/min ($n = 3$). *Sample had to be diluted (1:10) prior to DLS measurement).

The results indicate that at higher concentrations, polyplexes become more unstable, leading to a stronger aggregation. This fact has been already observed and discussed in literature [9,10]. For example, Duguid et al. [10] showed that the hydrodynamic diameter of polyplexes composed of poly-(L-lysine) and synthetic polypeptides varied from 30-60 nm at a DNA concentration of 20 $\mu\text{g/mL}$ to 80-160 nm at 400 $\mu\text{g/mL}$ along with a large increase in polydispersity. Commonly, polyplexes are prepared at 50 $\mu\text{g/mL}$ for in vitro experiments, whereas higher concentrations of 1-5 mg/mL can be only achieved if polyplexes are chemically modified to inhibit aggregation [11]. Especially at high concentrations, a more distinct heterogeneity of the polyplexes was observed when prepared via the classical preparation method. An explanation for this might be that higher polymer and DNA masses are mixed in a less controlled fashion at one time.

4 Conclusion

It is very difficult to achieve the same quality attributes of polyplexes when these carrier systems are prepared at large volumes by simple pipetting compared to the standard laboratory pipette mixing at low volume. The established micro-mixer method allows the highly reproducible preparation of large, standardized batches of homogenous, well-defined and transfection-competent polyplexes, banishes the risk of batch-to-batch variations and prevents handling inconsistencies among different operators, resulting in an increased polyplex quality. Moreover, by using this preparation method, the size and polydispersity of plasmid/LPEI polyplexes can be directly controlled via the mixing speed. The z-average diameter and the Pdl of the polyplexes increased with increasing plasmid DNA concentration. The benefit of the up-scaled micro-mixer method is accentuated especially at high concentration as far less heterogeneity was observed in the up-scaled micro-mixer method compared to the classically produced particle preparations. Using this method, the batch volume can be easily further increased, which might be of high importance with regard to the production of large standardized batches of stable polyplex formulations. Thus, the possibility to reproducibly manufacture large standardized batches of well-defined, transfection-competent polyplexes is an important step closer from promising technology to clinical application.

5 References

- [1] T.J. Anchordoquy, G.S. Koe, Physical stability of nonviral plasmid-based therapeutics, *J. Pharm. Sci.* 89 (2000) 289-296.
- [2] H. Talsma, J.-Y. Cherng, H. Lehrmann, M. Kursa, M. Ogris, W.E. Hennink, M. Cotten, E. Wagner, Stabilization of gene delivery systems by freeze-drying, *Int. J. Pharm.* 157 (1997) 233-238.
- [3] E. Wagner, Strategies to improve DNA polyplexes for in vivo gene transfer: will 'artificial viruses' be the answer?, *Pharm Res.* 21 (2004) 8-14.
- [4] J. Clement, K. Kiefer, A. Kimpfler, P. Garidel, R. Peschka-Süss, Large-scale production of lipoplexes with long shelf-life, *Eur. J. Pharm. Biopharm.* 59 (2005) 35-43.
- [5] O. Zelphati, C. Nguyen, M. Ferrari, J. Felgner, Y. Tsai, P.L. Felgner, Stable and monodisperse lipoplex formulations for gene delivery, *Gene Ther.* 5 (1998) 1272-1282.
- [6] D. Schaffert, M. Kiss, W. Rödl, A. Shir, A. Levitzki, M. Ogris, E. Wagner, Poly(I:C)-mediated tumor growth suppression in EGF-receptor overexpressing tumors using EGF-polyethylene glycol-linear polyethylenimine as carrier, *Pharm. Res.* (2010) 1-11.
- [7] T. Mosmann, Rapid colorimetric assay for cellular growth and survival: application to proliferation and cytotoxicity assays, *J. Immunol. Methods* 65 (1983) 55-63.
- [8] M.T. Kennedy, E.V. Pozharski, V.A. Rakhmanova, R.C. MacDonald, Factors governing the assembly of cationic phospholipid– DNA complexes, *Biophys. J.* 78 (2000) 1620--1633.
- [9] J.Y. Cherng, H. Talsma, R. Verrijck, D.J.A. Crommelin, W.E. Hennink, The effect of formulation parameters on the size of poly((2-dimethylamino)ethyl methacrylate) – plasmid complexes, *Eur. J. Pharm. Biopharm.* 47 (1999) 215-224.
- [10] J.G. Duguid, C. Li, M. Shi, M.J. Logan, H. Alila, A. Rolland, E. Tomlinson, J.T. Sparrow, L.C. Smith, A physicochemical approach for predicting the effectiveness of peptide-based gene delivery systems for use in plasmid-based gene therapy, *Biophys. J.* 74 (1998) 2802-2814.
- [11] C.A. Fernandez, K.G. Rice, Engineered nanoscaled polyplex gene delivery systems, *Mol. Pharm.* 6 (2009) 1277-1289.

Chapter 5

Development of a lyophilized plasmid/LPEI polyplex formulation with long-term stability

The following chapter has been published in the Journal of Controlled Release and appears in this thesis with the journal's permission:

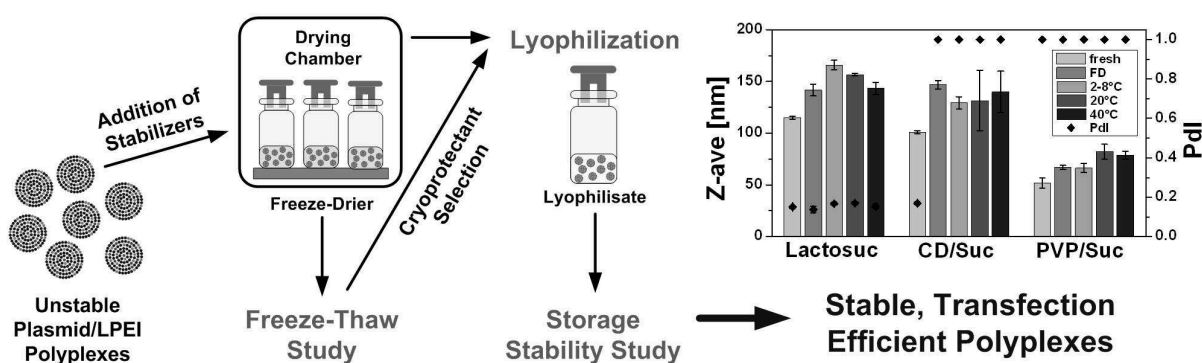
Julia Christina Kasper, David Schaffert*, Manfred Ogris, Ernst Wagner, Wolfgang Friess

Development of a lyophilized plasmid/LPEI polyplex formulation with long-term stability - A step closer from promising technology to application

J. Controlled Release 151 (2011) 246-255

*LPEI synthesis and cell culture experiments were performed by D. Schaffert.

Graphical Abstract



Abstract

Cationic polymer/DNA complexes are limited by their instability in aqueous suspensions and usually have to be freshly prepared prior to administration. Thus, the development of isotonic lyophilized polyplex formulations with long-term stability is a desirable goal.

Polyplexes based on 22 kDa linear polyethylenimine were prepared using a micro-mixer method. Freeze-thawing and lyophilization were performed on a pilot scale freeze-drier. Several excipients (trehalose, sucrose, lactosucrose, dextran, hydroxypropylbetadex or povidone and combinations thereof) at varying concentrations were evaluated for their stabilizing potential against freezing and dehydration induced stresses. For stability testing the lyophilized samples were stored for 6 weeks at 2–8 °C, 20 °C and 40 °C, respectively. Polyplex samples were characterized for particle size, zeta potential, their in vitro transfection efficiency and metabolic activity in Neuro-2A cells. In addition, liquid samples were investigated for turbidity and number of subvisible particles and solid samples were analyzed for residual moisture content, glass transition temperature and sample morphology.

L-histidine buffer pH 6.0 was selected as effective buffer. In isotonic formulations with 14% lactosucrose, 10% hydroxypropylbetadex/ 6.5% sucrose or 10% povidone/ 6.3% sucrose, particle size was <170 nm for all formulations and did not change after storage for 6 weeks at 40 °C. Polyplexes formulated with lactosucrose or hydroxypropylbetadex/sucrose showed high transfection efficiencies and cellular metabolic activities. Absence of large aggregates was indicated by turbidity and subvisible particle number measurements. The current standard limits for particulate contamination for small volume parenterals were met for all formulations. All samples were amorphous with low residual moisture levels (<1.3%) and high glass transition temperatures (>90 °C).

Keywords

Non-viral gene delivery, freeze-thawing, lyophilization, long-term stability, preserved transfection efficiency

1 Introduction

Non-viral gene delivery systems offer a significant promise to cure, treat or prevent various, up to now, incurable diseases [1]. Most nonviral gene delivery vectors are based on cationic lipids (lipoplexes) or cationic polymers (polyplexes) which interact electrostatically with the negatively charged nucleic acids and form condensed complexes [1]. Among the cationic polymers, linear polyethylenimine (LPEI) is the most potent polycationic transfection agents, known as a “golden standard” for polymeric gene delivery [1].

The major drawbacks of these non-viral vectors are the limited efficacy in delivering DNA compared to viral vectors particularly after in vivo application, and the high instability in aqueous suspensions [2]. To date, the predominant focus in non-viral gene therapy has been on the development of more efficient vectors but other crucial pharmaceutical aspects including quality control, long-term stability and practicability in clinical trials have been rather ignored [3,4]. A limiting factor for the clinical practicability is the requirement for freshly prepared formulations prior to administration because of the tendency towards particle aggregation in liquid formulations, which is known to correlate with a loss of transfection efficiency [5-7]. However, the day-to-day preparation poses the risk of batch to batch variations, including significant variations in product quality, safety and transfection rates, and the inability to perform extensive quality control prior to the actual administration, due to time constraints [5,7]. Thus, to achieve stable, transfection competent non-viral complexes is a desirable goal [5] and an important step from a promising technology to application [7].

Lyophilization is a very gentle and therefore highly attractive way to achieve dried pharmaceuticals in general [8,9] and DNA-based formulations in particular [6,7,10]. Freeze-dried formulations possess the advantage of long-term storage stability. However, the lyophilization process involves two stresses, freezing and drying, that are known to be damaging to

macromolecules and nanoparticulate structures, unless appropriate stabilizers are used [2,11]. During freezing, particle stability can be influenced by cryoconcentration of the complexes or other solutes leading to a complex-rich phase or increased ionic strength [8,9,11], by exposure to ice-liquid interfaces [12], by pH shifts due to selective crystallization of buffer species [13], and by mechanical damage due to growing crystals of ice or excipient [9,12]. During drying the removal of the ice and unfrozen water, which act as stabilizing hydration shell, can affect the stability of the complexes [11] and additional damage after lyophilization may result from the effects of dehydration–rehydration on complexes [6].

Freeze-thawing and lyophilization in the absence of excipients cause complexes to aggregate and reduced transfection rates [14,15]. However, several studies have shown that the addition of excipients can protect the product from freezing and drying stresses and can increase storage stability of proteins or liposomes [16,17] and nonviral vectors [6]. Different excipients have been used as stabilizers: monosaccharides (glucose), disaccharides (trehalose and sucrose), oligosaccharides (inulin and isomaltotriose) or polysaccharides/polymers (hydroxyethyl starch, high molecular weight dextrans, and polyvinylpyrrolidone) [11,18-20]. The choice of stabilizer is critical but also the mass ratio stabilizer/nanoparticle is important [11,15].

Moreover, the reconstituted preparations should not greatly exceed isotonicity [2]. Among non-viral delivery systems most literature is available on freeze-thawing and freeze-drying studies of lipid–DNA complexes [15,21-26] or complexes based on polymers like poly (2-dimethylamino)ethyl methacrylate (PDMAEMA) [14,27,28]. However, only little is known on freeze-thawing [29–31] and freeze-drying [7,10,29] of PEI-based polyplexes. Here, the main focus was generally to preserve transfection efficiency. Brus et al. [10] also investigated particle size, in addition to transfection efficiency. They observed only marginal

changes in size and transfection efficiency for complexes of short oligodeoxynucleotides and PEI after lyophilization. In contrast, plasmid/PEI complexes were found to aggregate and biological activity decreased.

The aim of the study was to develop a lyophilized formulation for plasmid/LPEI polyplexes with long-term stability. Therefore, freeze-thawing studies were performed prior to lyophilization to select the best cryoprotectant for effective particle stabilization at isotonic concentrations. Here, a variety of excipients were tested: trehalose, sucrose, lactosucrose, hydroxypropylbetadex (HP- β -CD), and dextran or povidone (PVP). A selection of formulations was lyophilized and long-term storage stability over 6 weeks was investigated. Plasmid/LPEI polyplexes were characterized with respect to their hydrodynamic radius and polydispersity using dynamic light scattering as well as their transfection efficiency and their influence on the metabolic activity of murine neuroblastoma cells. In addition, freshly prepared or reconstituted, liquid formulations were analyzed for their osmotic pressure, turbidity and amount of subvisible particles. Dried formulations were examined by Karl Fischer titration, differential scanning calorimetry (DSC) and X-ray powder diffraction (XRD). The ability to prepare lyophilized polyplexes with high transfection efficiency and long-term stability would be an important step towards clinic-friendly drugs.

2 Materials and methods

2.1 Materials

The plasmid (pCMVLuc) was produced by PlasmidFactory (Bielefeld, D). 22 kDa LPEI was synthesized as described in [32]. Dilutions of plasmid and LPEI were prepared in HBG buffer pH 7.4 (5% glucose, 20mM HEPES) or a 10mM L-histidine buffer pH 6.0 (all, Merck, Darmstadt, D), so that mixing equal volumes of the two dilutions resulted in a N/P ratio of 6/1. The stabilizer sucrose (Südzucker, Mannheim, D), trehalose 100 and lactosucrose (purity 92.8%) (Nyuka-Oliga™ LS-90P) (Hayashibara, Okayama, Jp), hydroxypropylbetadex (HP-β-CD) (CavasoI™ W7 HP) (Wacker, Munich, D), povidone (PVP) (Kollidon™ 17 PF, BASF, Ludwigshafen,D), dextran 8 (Serva,Heidelberg, D) and polysorbate 20 (Tween 20™, Merck, Darmstadt, D) were used without further purification. Stabilizer solutions [% w/v] were prepared in 10mM L-histidine buffer pH 6.0 and mixed 1:1 with the formed polyplexes. 2R glass vials (Fiolax™ clear, Schott, Müllheim, D) with rubber stoppers (West, Eschweiler, D) were used.

2.2 Preparation of plasmid/LPEI polyplexes

Plasmid/LPEI polyplexes were prepared by an established micromixer method [33] (see Chapter 4).

2.3 Freeze-thawing studies

For the freeze-thawing studies, 100 µg/mL plasmid/LPEI polyplexes were prepared (5.0 mL syringe, mixing speed of 1.0 cm/min) in the 10 mM L-histidine buffer pH 6.0. 125 µL polyplex solution was mixed with 125 µL stabilizer solution in 2R vials resulting in a plasmid concentration of 50 µg/mL. Freeze-thawing was performed once or five times on a pilot scale freeze-drier (Lyostar II, SP Scientific, Stone Ridge USA). Samples were frozen at -1 °C/min to -50 °C. After

30 min at $-50\text{ }^{\circ}\text{C}$, the samples were thawed at $1\text{ }^{\circ}\text{C}/\text{min}$ to $10\text{ }^{\circ}\text{C}$ with a 30 min hold.

2.4 Lyophilization of plasmid/LPEI polyplexes

Three isotonic formulations (14% lactosucrose, 10% HP- β -CD with 6.5% sucrose or 10% PVP with 6.3% sucrose) at $50\text{ }\mu\text{g}/\text{mL}$ plasmid were lyophilized on the pilot scale freeze-drier. For cell culture experiments, the samples were prepared under aseptic conditions. $500\text{ }\mu\text{L}$ sample per 2R vial was frozen at $-1\text{ }^{\circ}\text{C}/\text{min}$ to $-50\text{ }^{\circ}\text{C}$ and held for 120 min. Primary drying was performed at 34 mTorr and $-20\text{ }^{\circ}\text{C}$. During the first two-thirds of the primary drying step, the product temperature, monitored with thermocouples, was kept below the glass transition temperature of the maximally frozen concentrate (T_g') which was determined by DSC and the endpoint of primary drying was defined by manometric endpoint determination. Secondary drying was performed at $20\text{ }^{\circ}\text{C}$ and 8 mTorr. Samples were stoppered at 600 Torr nitrogen. Lyophilized samples were reconstituted with $500\text{ }\mu\text{L}$ purified water.

2.5 Long-term stability

For stability testing the sealed, lyophilized samples were stored at $2\text{-}8\text{ }^{\circ}\text{C}$, $20\text{ }^{\circ}\text{C}$ and $40\text{ }^{\circ}\text{C}$ for 6 weeks.

2.6 Plasmid/LPEI polyplex characterization

Using the dynamic light scattering (DLS) platereader DynaPro Titan (Wyatt Technology, Dernbach, D) the particle size of the polyplexes was measured. $100\text{ }\mu\text{L}$ sample ($n=3$) per well of a 96 UV-well plate (CostarTM, Corning, USA) was analyzed at RT using 5 acquisitions, with 5 s each. For all samples the corresponding preset refractive index parameters were used. For the polyplexes the refractive index increment value dn/dc for linear polymers of 0.185 was assumed. The viscosity of the samples was determined using a

microviscosimeter (AMVn, Anton Paar, Ostfildern, D). DLS autocorrelation data was analyzed with the Dynamics V6 software.

The zeta-potential was determined using the Zetasizer Nano ZS (Malvern Instruments, Herrenberg, D) in a DTS 1060c cell with 10 up to 100 subruns of 10 s at 20 °C (n=3) and was calculated by the Smoluchowski equation.

2.7 Osmometry

The osmotic pressure of 150 µL of each lyophilized polyplex formulation (n=3) was determined after reconstitution with an automatic semi-micro osmometer (Knauer, Berlin, D).

2.8 Turbidimetry

Turbidity of 1.5 mL of freshly prepared or reconstituted samples in formazine nephelometric units (FNU) was determined (n=3) by using a NEPHLA turbidimeter (Dr. Lange, Düsseldorf, D).

2.9 Light obscuration

Subvisible particle analysis was carried out according to Ph.Eur. 2.9.19 [34] using a particle counter SVSS-C (PAMAS, Rutesheim, D). Three measurements of 0.3 mL of a 1.5 mL sample were performed with a pre-run volume of 0.3 mL at a fixed fill rate, emptying rate and rinse rate of 5 mL/min (n=3).

2.10 Cell culture: cytotoxicity and luciferase reporter gene expression

In vitro transfection experiments were performed on murine neuroblastoma (Neuro-2A) cells. Cells were seeded 24 h prior to transfection with a density of 10^4 cells in a 200 µL culture medium, containing 10% serum, 100 U/mL penicillin and 100 µg/mL streptomycin, per well. Immediately before transfection, the medium was removed and 100 µL of a dilution of polyplexes (200 ng DNA) in culture medium was added to the cells. Cytotoxic potency was

evaluated 24 h after treatment by methylthiazoletetrazolium (MTT)/thiazolyl blue assay [35]. Metabolic activity was calculated relative to untreated control cells (HBG buffer only). To determine gene expression, the medium was removed and cells were lysed in a 50 μ L 0.5X Promega cell lysis solution 24 h after transfection. Luciferase light units were recorded with a Lumat LB9507 (Berthold, Bad Wildbad, D) from a 20 μ L aliquot with 10 s integration time after injection of Luciferase assay reagent (Promega, Mannheim, D). Luciferase activity [%] was expressed relative to the Luciferase activity of plasmid/LPEI reference polyplexes (formulated in HBG buffer via pipetting).

2.11 Karl Fischer titration

Lyophilized samples (n=3) were dissolved in dried Methanol (Hydranal™ Methanol, Fluka, Sigma-Aldrich, D), and the methanol samples were injected into the titration solution (Hydranal™ Coulomat AG, Riedel-de Haen, Seelze, D) and titrated using a Metrohm 756 KF Coulometer (Metrohm, Herisau, CH). Empty vials were treated identically as blanks.

2.12 Differential scanning calorimetry (DSC)

DSC measurements were carried out in 40 μ L aluminium crucibles using a Mettler Toledo DSC821 (Mettler Toledo GmbH, Giessen, D). For determination of glass transition temperature of the maximally frozen concentrate (Tg') 30 μ L of the samples were analyzed (n=3). Samples were cooled from 20 °C to -50 °C with -1 °C/min, held at -50 °C for 10 min and reheated to 20 °C with 5 °C/min. Approximately 10 mg of the lyophilized product (n=3) were weighed into 40 μ L aluminium crucibles in a glove box, purged with dry air. Samples were cooled from 20 °C to 0 °C with -5 °C/min, held at 0 °C for 1 min and reheated to 150 °C with 10 °C/min.

2.13 X-ray powder diffraction (XRD)

XRD was performed with a XRD 3000 TT (Seifert, Ahrenburg, D). Sample was filled in a copper sample holder with 1 mm fill depth and exposed to CuK α radiation (40 kV, 30 mA, wavelength 154.17 pm). Samples were analyzed with steps of 0.05° 2- θ and a duration of 2 s per step from 5 to 45° 2- θ .

2.14 Statistical analysis

Statistically significant differences were determined using a two-tailed student *t* test with a GraphPad Software, QuickCalcs (La Jolla, CA, USA). Mean values having *p* values >0.05 were judged to be not significantly different.

3 Results

3.1 Influence of the buffer composition

Typically, low molality buffers such as 10 or 20 mM HEPES at a pH of 7.4 are used for the preparation of polyplexes and tonicity is adjusted using sugars like glucose [28]. As HEPES is not listed as an approved inactive ingredient by the US Food and Drug Administration [36] the initial buffer composition (HBG buffer pH 7.4 which contained 5% glucose and 20 mM HEPES) was changed to L-histidine buffer pH 6.0 to move a step closer towards application. To evaluate the influence of the buffer composition on the z-average diameter, polydispersity index, zeta-potential and transfection efficiency of plasmid/LPEI polyplexes, complexes were prepared in HBG buffer pH 7.4 or L-histidine buffer pH 6.0.

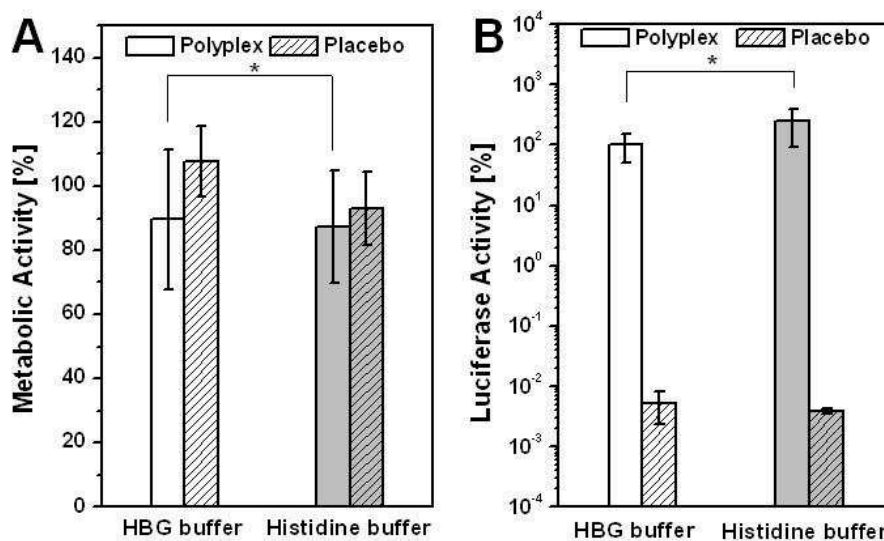


Figure 5-1: Influence of the formulation buffer on (A) the metabolic activity of Neuro-2A cells and (B) transfection activity in Neuro-2A cells (n=5); (*p>0.05: mean values are not significantly different).

Polyplexes formulated in HBG buffer pH 7.4 were found to have a z-average diameter of about 176 nm with a polydispersity index of 0.18 and a zeta-potential of 29.6 mV. When using 10 mM L-histidine buffer pH 6.0 the size and the polydispersity index decreased to 118 nm and 0.13 respectively and the

zeta-potential was raised to 36.3 mV. In vitro performance (metabolic activity/gene expression) was not significantly influenced by the buffer system (Figure 5-1).

3.2 Freeze-thawing studies

In order to select the most effective cryoprotectant and its stabilizing concentration freeze-thawing studies were performed, prior to freeze-drying. Therefore, plasmid/LPEI polyplexes were prepared in 10 mM L-histidine buffer pH 6.0 at a plasmid DNA concentration of 50 µg/mL using a micro-mixer method [33]. These polyplexes exhibited a z-average diameter of 104 nm and a zeta potential of 39.9 mV. The polyplexes were freeze-thawed once or five times without stabilizers or in the presence of trehalose, sucrose, lactosucrose or HP-β-CD at various concentrations (8, 12, 16 and 20%). The high molecular weight excipients dextran and povidone were only tested at a concentration level of 20% to stay closer to isotonicity. Subsequently samples were analyzed for their z-average diameter by DLS (Figure 5-2), as particle size is an important quality criterion.

Without the addition of stabilizers the z-average diameter drastically increased already after one freeze-thawing cycle. The formation of these large polyplex aggregates might explain the observed tenfold decrease of reporter gene expression in cell culture (Fig. 5B). With increasing concentrations of the commonly used disaccharides trehalose or sucrose the z-average diameter of the polyplexes was increasingly preserved upon freeze-thawing. To inhibit an increase in particle size after one freeze-thawing cycle in the case of sucrose or trehalose as stabilizer a concentration of 20% was required, greatly exceeding isotonicity and indicating the prerequisite of a certain stabilizer/polyplex mass ratio. Lactosucrose, a trisaccharide, HP-β-CD, a cyclic heptasaccharide, dextran, a polysaccharide, and povidone, a vinyl polymer, represent alternative

cryoprotectants as these excipients showed lowered osmotic pressure at equal stabilizer/polyplex mass ratios.

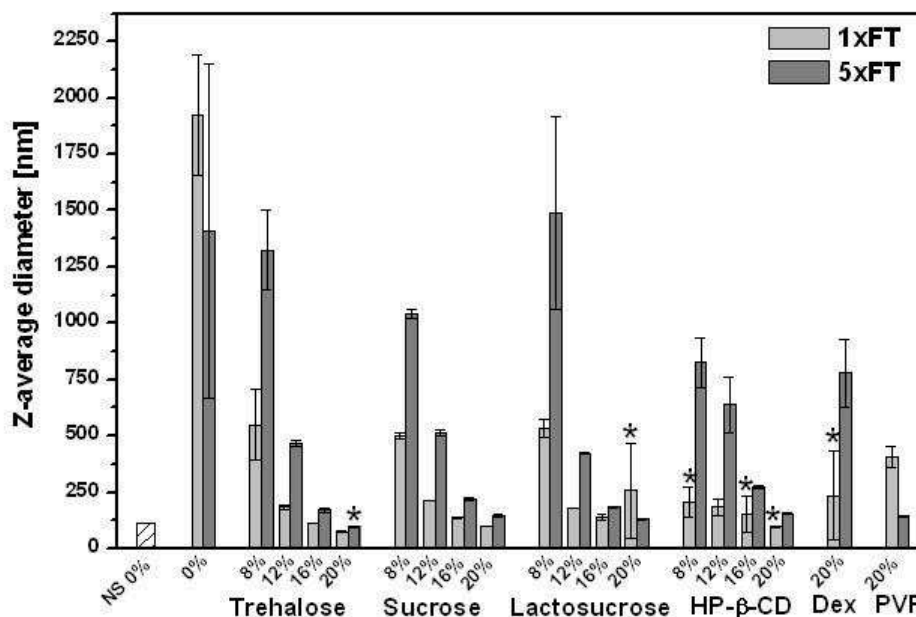


Figure 5-2: Z-average diameter [nm] of freshly prepared, non-stressed (NS) or once (1×FT) or five times (5×FT) freeze-thaw stressed plasmid/LPEI polyplexes (50 µg/mL) formulated in L-histidine buffer pH 6.0 without (0%) or with the addition of stabilizers (trehalose, sucrose, lactosucrose, HP-β-CD, dextran (Dex) or PVP) at varying concentrations (8, 12, 16 or 20%) (n=3); (*p>0.05: samples are not significantly different compared to the non-stressed sample).

At corresponding concentrations the stabilizing effects of lactosucrose and HP-β-CD were comparable to trehalose or sucrose. Dextran at high concentrations was a poor cryoprotectant for reproducible polyplex stabilization. Povidone showed promising stabilization effects after five freeze-thaw cycles. Based on these results, isotonic polyplex formulations were prepared and particle size was analyzed after freeze-thawing (Figure 5-3).

After one freeze-thawing cycle using trehalose or sucrose at isotonic concentrations the increase in z-average diameter and polydispersity was more pronounced compared to the other selected recipients. Addition of 0.02% of the surfactant polysorbate 20 did not significantly improve the preservation of particle size. Using lactosucrose, HP-β-CD/sucrose or PVP/sucrose, satisfactory polyplex stabilization with an increase in size of less than 40% was

observed. HP- β -CD and povidone were combined with sucrose as sucrose is a commonly used stabilizer in lyophilization. However, the observed polydispersity index of 1 for PVP/sucrose samples indicates a multimodal size distribution due to the fact that not only the polyplexes but also the polymer povidone contributes to the intensity versus size distribution determined by DLS, as seen from the analysis of placebo samples (data not shown), and leads to a decreased z-average diameter.

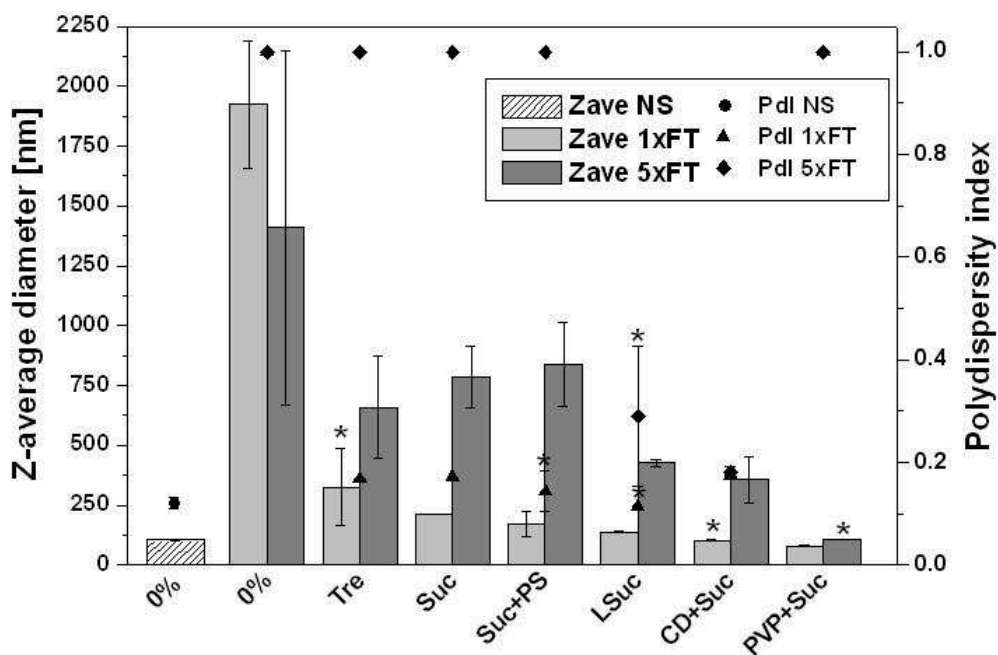


Figure 5-3: Z-average diameter [nm] and polydispersity index of freshly prepared, nonstressed (NS) or once (1xFT) or five times (5xFT) freeze-thaw stressed plasmid/LPEI polyplexes (50 μ g/mL) formulated in L-histidine buffer pH 6.0 without (0%) or with the addition of stabilizers at isotonic concentrations of 9% trehalose (Tre), 9% sucrose (Suc), 9% sucrose with 0.02% PS 20 (Suc+PS), 14% lactosucrose (LSuc), 10% HP- β -CD/6.5% sucrose (CD+Suc) or 10% PVP/6.3% sucrose (PVP+Suc) (n=3); (*p>0.05: samples are not significantly different compared to the non-stressed sample).

As the latter three isotonic formulations, showed the best protection against freeze-thawing induced aggregation of polyplexes, these formulations were selected for freeze-drying and long-term stability studies.

3.3 Physico-chemical and biological properties of lyophilized plasmid/LPEI polyplexes

The isotonic polyplex formulations with lactosucrose, HP- β -CD/sucrose and PVP/sucrose as stabilizers were lyophilized using a conservative freeze-drying cycle. To insure the complete solidification and glass formation, the samples were frozen to $-50\text{ }^{\circ}\text{C}$ well below the T_g' of the samples (Table 5-1). Moreover, by monitoring the product temperature during lyophilization we insured that the temperature was maintained below T_g' at least in the first two-thirds of the primary drying step. All lyophilized samples, except the sample without stabilizers, showed good cake appearance and instantly ($<5\text{ s}$) dissolved in water.

Tabelle 5-1: T_g' prior to freeze drying (prior to FD) and T_g and residual moisture (RM) of solid freeze dried formulations directly after freeze-drying (after FD) and after 6 weeks of storage at $2\text{-}8\text{ }^{\circ}\text{C}$, $20\text{ }^{\circ}\text{C}$ and $40\text{ }^{\circ}\text{C}$ (n=3).

		prior to FD	after FD	2-8 °C	20 °C	40 °C
14% lacto-sucrose	T_g'/T_g [°C]	-25.11 ± 0.06	113.6 ± 0.3	112.4 ± 0.3	111.4 ± 0.4	108.9 ± 0.75
	RM [%w/w]		0.36 ± 0.04	0.41 ± 0.11	0.51 ± 0.07	0.85 ± 0.18
10% HPβCD+ 6.5% sucrose	T_g'/T_g [°C]	-22.77 ± 0.08	115.7 ± 2.2	109.2 ± 2.9	104.7 ± 0.6	91.8 ± 0.4
	RM [%w/w]		0.10 ± 0.01	0.10 ± 0.02	0.27 ± 0.06	0.71 ± 0.04
10% PVP+ 6.3% sucrose	T_g'/T_g [°C]	-26.08 ± 0.06	108.7 ± 0.6	106.6 ± 2.2	104.4 ± 1.0	102.5 ± 0.1
	RM [%w/w]		0.17 ± 0.01	0.18 ± 0.01	0.40 ± 0.02	1.26 ± 0.04

After reconstitution few large, visible undissolved particles were observed for the lyophilized samples without stabilizers, and for all other lyophilized samples no particles or turbidity was visible by the naked eye. The z-diameter and polydispersity index increased drastically after lyophilization for the samples without stabilizers (Figure 5-4). This increase appears to be less pronounced compared to the samples without stabilizers after one freeze-thaw cycle.

However, for the samples lyophilized without stabilizers extremely large, visible particles were observed and only the soluble fraction of the polyplexes was analyzed.

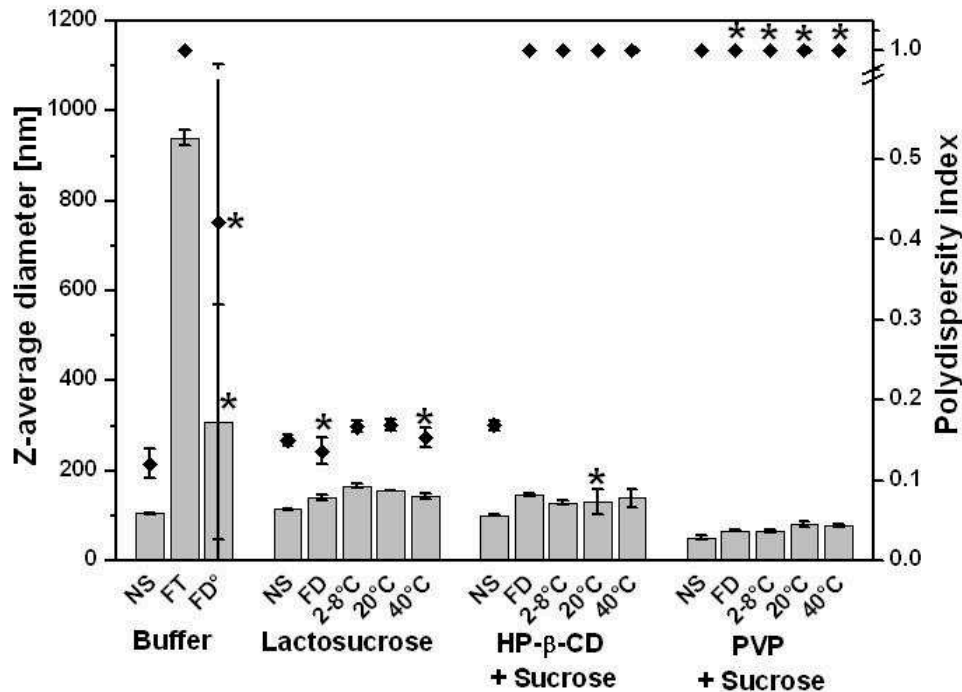


Figure 5-4: Z-average diameter (nm) and polydispersity index of plasmid/LPEI polyplexes (50 µg/mL) formulated in histidine buffer without (buffer) or with the addition of stabilizers (14% lactosucrose, 10% HP-β-CD/6.5% sucrose or 10% PVP/6.3% sucrose). Samples were freshly prepared and non-stressed (NS), freeze-thawed (FT), freeze-dried (FD) or freeze-dried and stored at 2-8 °C, 20 °C or 40 °C for 6 weeks (n=3). Polyplexes precipitated; (*p>0.05: samples are not significantly different compared to the corresponding non-stressed sample).

Metabolic activity was not reduced for the lyophilized polyplex sample without stabilizers (Figure 5-5A). However, freeze-drying of polyplexes in the absence of stabilizers had a detrimental effect on reporter gene expression resulting in a hundredfold reduced luciferase activity while freeze-thaw stressing of the formulation only resulted in a tenfold decrease of activity (Figure 5-5B). All stabilizer containing samples showed a marginal (<45%) but, due to the small standard deviations among the triplicates, partially significant rise in the z-average diameters (Figure 5-4). However, for the HP-β-CD/sucrose formulation an increased Pdl of 1.0 was measured. Taking the DLS size distribution by

intensity into account, an additional peak in the low nanometer range was observed (data not shown). This peak was also detected for lyophilized placebo HP- β -CD/sucrose formulations in the absence of polyplexes, indicating that small particles are formed by the excipient itself during freeze-drying.

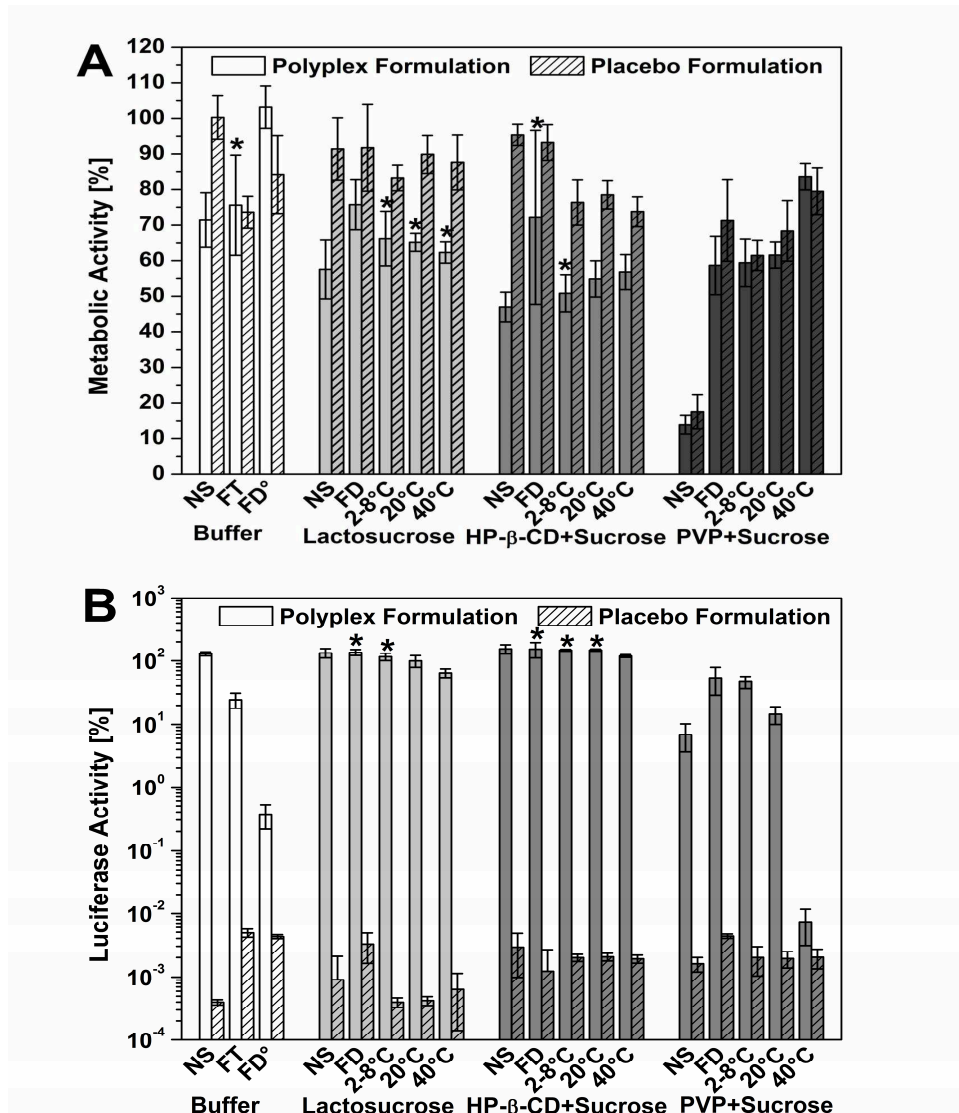


Figure 5-5: Influence of the formulation of plasmid/LPEI polyplexes and corresponding placebo samples on (A) the metabolic activity of Neuro-2A cells and (B) relative in vitro transfection activity in Neuro-2A cells (n=5). Samples were formulated in histidine buffer pH 6.0 without (buffer) or with the addition of stabilizers (14% lactosucrose, 10% HP- β -CD/6.5% sucrose or 10% PVP/6.3% sucrose). Samples were freshly prepared and non-stressed (NS), freeze-thawed (FT) or freeze-dried (FD) and stored at 2-8 °C, 20 °C or 40 °C for 6 weeks. Polyplexes precipitated; (* $p > 0.05$: samples are not significantly different compared to the corresponding freshly prepared and non-stressed sample).

After freeze-drying, turbidity (Figure 5-6) raised only marginally but significantly for HP- β -CD/sucrose and povidone/sucrose formulations. For the lactosucrose formulation a more pronounced increase in turbidity was observed. However, here, the placebo lactosucrose formulation containing no polyplexes showed a higher turbidity compared to the corresponding polyplex formulation.

In a next step, the number and size of individual sub-visible particles in a size range between 1 μ m and 200 μ m were determined (Figure 5-7).

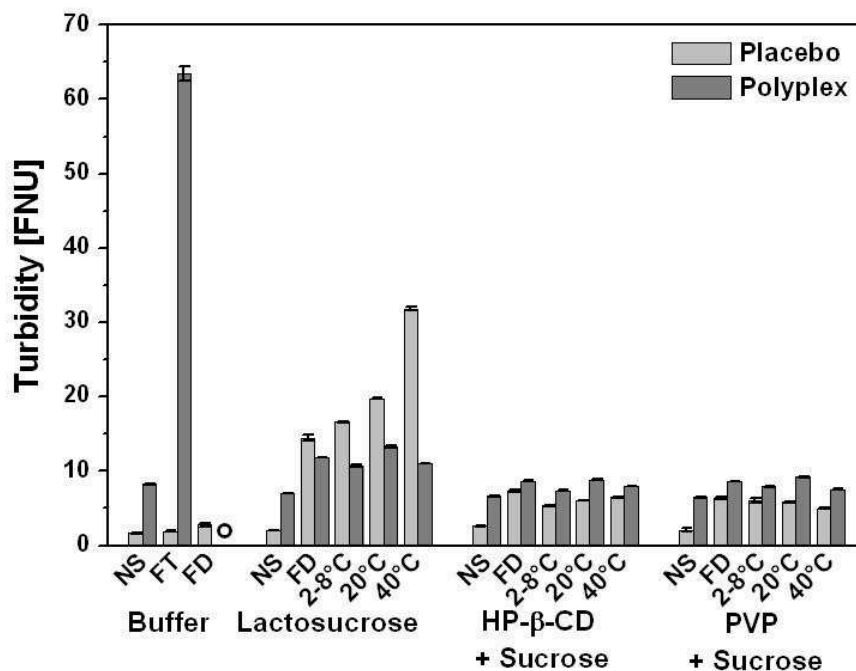


Figure 5-6: Turbidity in formazine nephelometric units (FNU) of plasmid/LPEI polyplex (50 μ g/mL) and corresponding placebo samples formulated in histidine buffer pH 6.0 without (buffer) or with the addition of stabilizers at isotonic concentrations (14% lactosucrose, 10% HP- β -CD/6.5% sucrose or 10% povidone/6.3% sucrose). Samples were freshly prepared and non-stressed (NS), freeze-thawed (FT), freeze-dried (FD) or freeze-dried and stored at 2-8 $^{\circ}$ C, 20 $^{\circ}$ C or 40 $^{\circ}$ C for 6 weeks (n=3). Polyplexes precipitated. All lyophilized and stored samples were significantly different ($p \leq 0.05$) compared to the corresponding freshly prepared and non-stressed polyplex sample.

In contrast to the one time freeze-thawed sample without stabilizers, which showed drastically increased particle numbers in all size ranges, the freeze-dried sample without stabilizers exhibited only slightly raised particle numbers,

because most of the polyplexes had precipitated and could not be analyzed, as aforementioned.

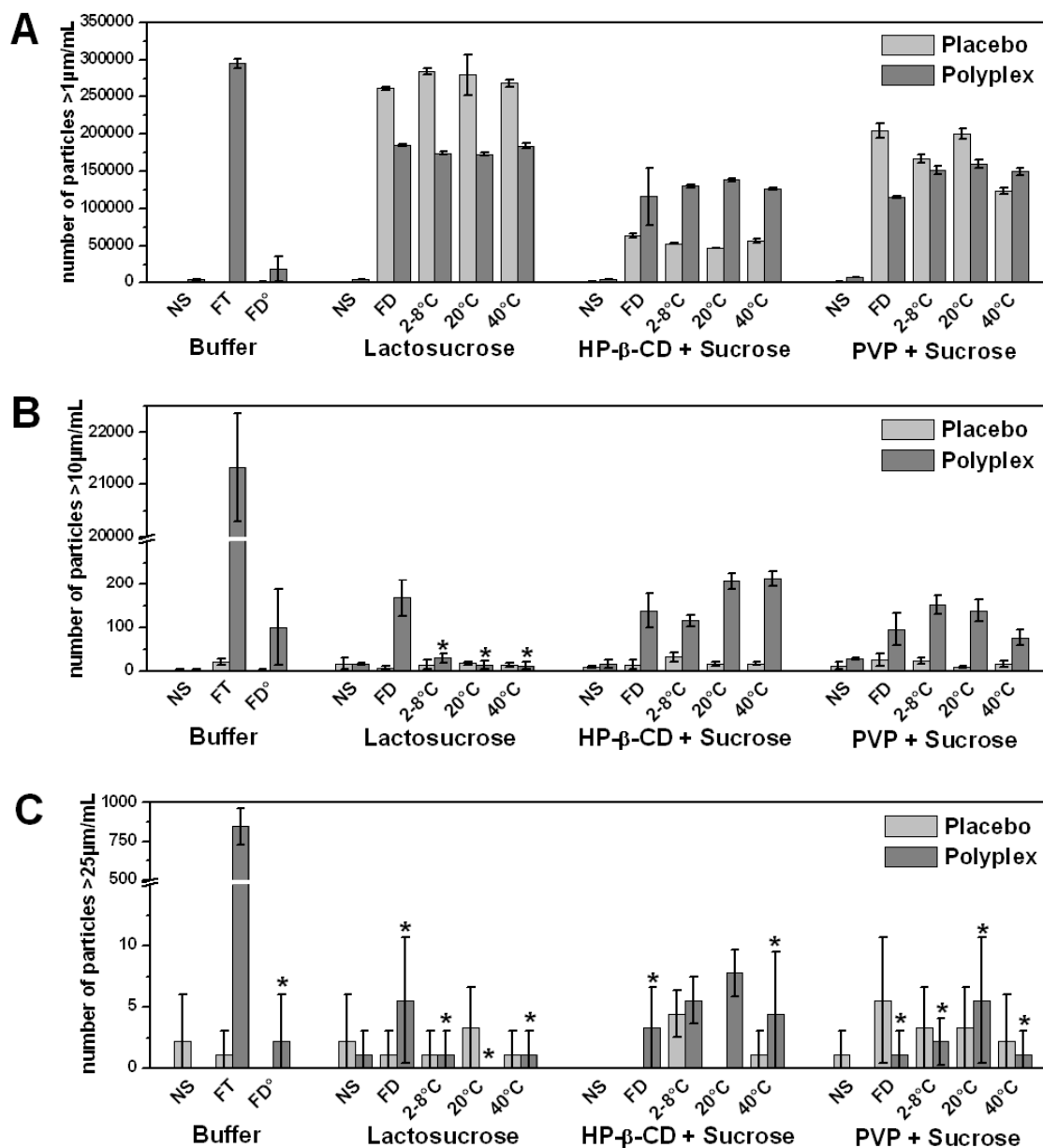


Figure 5-7: Number of sub-visible particles/mL with a particle diameter bigger than 1 μm (A), bigger than 10 μm (B) or bigger than 25 μm (C) of plasmid/LPEI polyplex (50 μg/ mL) samples and corresponding placebo samples formulated in histidine buffer pH 6.0 without (buffer) or with the addition of stabilizers (14% lactosucrose, 10% HP-β-CD/ 6.5% sucrose or 10% PVP/6.3% sucrose). Samples were freshly prepared and nonstressed (NS), freeze-thawed (FT), freeze-dried (FD) or freeze-dried and stored at 2-8 °C, 20 °C or 40 °C for 6 weeks (n=3). Polyplexes precipitated; (*p>0.05: samples are not significantly different compared to the corresponding freshly prepared and non-stressed polyplex sample).

All freeze-dried formulations showed drastically increased numbers of subvisible particles in the size range $\geq 1 \mu\text{m}$. However, the increase in particle numbers $\geq 1 \mu\text{m}$ for the freeze-dried formulations was less distinct compared to the freeze-thawed sample without stabilizers. Moreover, the corresponding placebo formulations, containing no polyplexes, showed almost the same or even slightly higher numbers of subvisible particles $\geq 1 \mu\text{m}$. In the size ranges $\geq 10 \mu\text{m}$ and $\geq 25 \mu\text{m}$ the amount of subvisible particles was only slightly increased in the formulations after freeze-drying compared to the freeze-thawed sample without stabilizers. These results confirm the ability of the selected stabilizers to inhibit the formation of large polyplex aggregates. The osmolality of the lyophilized and reconstituted samples was determined to be close to isotonicity for all samples and varied between 276 and 290 mOsm/kg.

Additionally, the influence of the lyophilized formulations on metabolic activity (Figure 5-5A) and the in vitro transfection efficiency of the lyophilized polyplexes (Figure 5-5B) were tested and compared to freshly prepared samples. Freshly prepared and lyophilized lactosucrose or HP- β -CD /sucrose samples had no significant effect on in vitro performance. Freshly prepared polyplex solutions containing PVP/sucrose as well as the corresponding placebo formulation severely interfered with the metabolic activity of the Neuro-2A cells resulting in a drop of metabolic activity to 20% and a hundredfold decrease in reporter gene expression after polyplex application. Freeze-drying diminished this effect leading to a significantly increased metabolic activity, however not completely. For all freeze-dried samples the residual moisture levels were low ($<0.4\%$) (Table 5-1). The glass transition temperature determined by DSC ranged from 108.7 to 115.8 °C (Table 1). All samples were totally amorphous as no peaks of crystallinity were observed in the XRD spectra (data not shown).

3.4 Physico-chemical and biological properties of lyophilized plasmid/LPEI polyplexes after storage

In order to evaluate long-term stability the sealed lyophilized formulations were stored at 2-8 °C, 20 °C and 40 °C for 6 weeks. After reconstitution, samples were analyzed for polyplex particle size, turbidity, amount of subvisible particles, transfection efficiency and influence on metabolic activity in murine neuroblastoma cells. Solid samples were characterized by Karl-Fischer titration, DSC and XRD.

After storage the z-average diameter of the polyplexes was less than 170 nm for all formulations, stress conditions and time points (Figure 5-4). Storage temperature did not influence particle size when polyplexes were formulated with lactosucrose or HP- β -CD/sucrose. For the PVP/sucrose formulations polyplex size was found to slightly increase with elevated storage temperature. A polydispersity index of 1.0 was determined for the HP- β -CD/sucrose and PVP/sucrose formulations due to the additional peaks in the low nanometer range observed in the intensity versus size distribution determined by DLS for the polyplex but also for the placebo formulations (data not shown). However, no additional peaks in the intensity versus size distribution at bigger particle diameters were detected. Turbidity of the samples after storage was comparable to the turbidity determined directly after lyophilization (Figure 5-6). Only the lactosucrose placebo formulations showed an increase in turbidity with elevated storage temperature. Furthermore, the number of subvisible particles $\geq 1 \mu\text{m}$ did not significantly change during storage for the lactosucrose and HP- β -CD/sucrose formulations and increased about 25% for the PVP/sucrose formulations independent of storage temperature (Figure 5-7). The lactosucrose formulations showed a substantial decrease in the number of subvisible particles $\geq 10 \mu\text{m}$ after storage at all temperatures. The number of subvisible particles $\geq 10 \mu\text{m}$ increased for the HP- β -CD/sucrose formulation when stored

at 20 °C or 40 °C and for the PVP/ sucrose formulation when stored at 2-8 °C or 20 °C. No formation of particles $\geq 25 \mu\text{m}$ was observed.

In cell culture (Figure 5-5), metabolic activity was not significantly changed by lactosucrose and HP- β -CD/sucrose formulations independent of storage temperature and only a marginal decrease in reporter gene expression was observed when cells were treated with polyplex formulations which had been stored at elevated temperatures. For the PVP/sucrose formulations metabolic activity was not changed when stored at 2-8 °C and 20 °C respectively. Storage at elevated temperature further affected transfection efficiency with a slight decrease when stored at 20 °C and a complete collapse of delivery efficiency although metabolic activity was still high when stored at 40 °C.

For all formulations residual moisture content was only slightly increased when stored at 2-8 °C for 6 weeks. However, when samples were stored at 20 °C and 40 °C residual moisture increased with increasing storage temperature but was still less than 1.4% for all samples. An opposed trend was observed for the glass transition temperature. Here, T_g decreased with increasing storage temperature. All samples remained in the amorphous state as no peak of crystallinity was detected with XRD after storage (data not shown).

4 Discussion

In general, the size and charge of polyplexes are influenced by the ionic strength of the buffer and the degree of protonation of the polycation depending on the surrounding pH [37]. As an increased salt concentration reduces the hydrate layer around the particles and promotes their aggregation ionic strength of the buffer should be low [37]. To keep ionic strength low, but to provide sufficient buffer capacity L-histidine buffer pH 6.0 was selected because it provides high buffer capacity at low concentrations (10 mM) as its pKa of 6.1 is close to the buffers' pH. As PEI has a very high density of amines, the degree of protonation changes with pH. At physiological pH only 10-15% of the amines are protonated whereas at a pH of 6.0 30-35% of the amines are protonated [38]. Thus, the more acidic pH of the L-histidine buffer leads to a higher degree of protonation resulting in the formation of smaller polyplexes in combination with an increased zeta-potential. This increased positive surface charge can prevent polyplex aggregation by repulsion of positive charges [37]. Therefore, a higher stability of the plasmid/LPEI polyplexes prepared in L-histidine buffer is expected compared to those prepared in HBG buffer.

As aforementioned, the stability of polyplexes can be drastically affected during freezing. Several studies reported that complex size increased drastically without the presence of stabilizers after freeze-thawing [14,18,26,28]. As alterations in particle size are known to influence toxicity and biodistribution in vivo, particle size is a critical issue in product development and is therefore routinely monitored in quality control [29]. The dramatic increase in particle size of polyplexes in the absence of stabilizers indicates the necessity of using cryoprotectants to inhibit freezing-induced aggregation. We found dextran to be a poor cryoprotectant for the stabilization of polyplexes. Accordingly, it is reported that dextran also failed to protect frozen PEGylated lipopolyplexes [39]. Overall, the stabilizer/polyplex weight ratio seems to be the more critical

parameter as large particle aggregates were formed at low excipient/polyplex ratios. Recent studies have also shown that a certain concentration of stabilizers is required for the preservation of particle size depending on the particle concentration [23,26]. In our study, 20% sucrose was necessary to stabilize plasmid/LPEI polyplexes, corresponding to a sucrose/DNA weight ratio of 4000. In comparison, Talsma et al. [7] showed that a sucrose/DNA ratio of 10000 was required to protect transferrin-PEI complexes. In another study, full conservation of the size of PEI-based polyplexes was observed at a sucrose/DNA ratio of 7500 [21]. For the protection of DMAEMA polyplexes a sucrose/DNA ratio of 1250 was sufficient [28]. In contrast to these results for polyplexes, lipoplexes could be successfully protected in general at lower sucrose/DNA ratios [15,21–23]. These high amounts of excipients, necessary for polyplex stabilization during freezing, do not only result in a hypertonic formulation but also in prolonged lyophilization cycles.

The mechanism how cryoprotectants stabilize non-viral vectors during freezing is still not fully understood [6]. Here, preferential exclusion [6,16], vitrification [6] and particle isolation [23] are discussed. According to the preferential exclusion hypothesis, established for protein stabilization, the solutes are unable to access the surface of the protein and are therefore preferentially excluded from contact with the protein's surface resulting in the formation of a stabilizing solvent layer [6,16]. However, it is not clear whether the preferential exclusion hypothesis can be adapted to the stabilization of non-viral vectors. The relatively high amounts of cryoprotectants that are necessary to preserve particle size during freezing suggest that the stabilization is related to nonspecific bulk characteristics of the formulation [20]. Based on the vitrification hypothesis the non-viral vectors are entrapped in the amorphous glassy matrix, which forms when the sample is cooled below the glass transition temperature of the maximally freeze-concentrated system (T_g) [6,20]. The high viscosity of

these glasses immobilizes the non-viral vectors [29], inhibits their diffusion on a relevant time scale [20] and prevents their bimolecular collision [6]. However, vitrification cannot be the only stabilization mechanism because some sugars are able to maintain particle size at temperatures well above T_g' [23]. The particle isolation hypothesis is based on the fact that crowding of particles facilitates aggregation and that there is a critical excipient/complex ratio at which protection is observed, as particles are more distinctly diluted in the freeze-concentrate with increasing excipient concentration [23]. Moreover, during cooling, the viscosity of the solute freeze-concentrate increases with decreasing temperatures and leads to a retarded and limited vector diffusion. Therefore, viscosity of the freeze-concentrated matrix only needs to be high enough independent of the type of excipient used, and matrix vitrification may not be required, in order to prevent aggregation [6].

In absence of stabilizer polyplexes were also found to dramatically aggregate during lyophilization leading to the precipitation of large visible particles. As for the freeze-thawed sample without stabilizers only an increase in particle size and turbidity but no precipitation was observed, and it can be concluded that the dehydration of the samples during drying adds further stress in addition to the freezing step. For all formulations, containing lactosucrose, HP- β -CD /sucrose and PVP/ sucrose only a slightly increased particle size (<45%) was observed. This is the first time, to our knowledge, that only such a marginal increase in particle size for plasmid/PEI complexes is reported upon lyophilization. In comparison, Brus et al. [10] found plasmid/LPEI polyplexes to increase in size from 100 nm to about 500 nm after lyophilization, however at low sucrose/DNA ratios. Hinrichs et al. [18] showed that the size of PEI polyplexes increased to 160% or 240% when using inulin or dextran as stabilizers at an oligosaccharide/DNA ratio of 1000. It is well-reported in literature that in addition to stresses during freezing, dehydration may influence complex function [22].

During the drying step the separation of the particles inside the glass matrix, that was formed during freezing, can potentially be maintained [23]. In addition to the entrapment in the glassy matrix the “water replacement hypothesis” [40] is discussed as a stabilizing mechanism during drying, as product vitrification was found to be not obligatory to maintain particle size [6,21]. According to this concept, the excipients directly interact with the surface of the particles, replace the surrounding water and mimic the “hydrated” condition, thus preserving particle size and transfection efficiency of non-viral vectors in the dried state [6,22].

The z-average diameter of the polyplexes in the selected isotonic formulations only marginally changed after lyophilization compared to the samples stressed by one time freeze-thawing, indicating that in the presence of stabilizers the increase in particle size usually occurs during the freezing step rather than during the drying step of the lyophilization process. Comparable results were reported for lipid/ DNA complexes [21,23,26]. However, for PDMAEMA complexes dehydration seemed to be a more destructive stress [28].

Particle size is not only an important criterion for quality control but can also influence transfection efficiency in vitro. In general, particle size may influence endosomal uptake, the transport in the cytoplasm and the migration through the nucleopores into the nucleus and the size dependency may differ in different cell types and applications [41]. The observed increase in particle size for the freeze-thawed and lyophilized polyplexes in the absence of stabilizers correlated with a pronounced decrease in transfection efficiency. This confirms the necessity of cryo- and lyoprotectants for maintaining polyplex function during lyophilization. Accordingly, Talsma et al. [7] reported an at least 3 log units drop in gene expression of freeze-dried pCMV/ transferrin-PEI complexes in the absence of sucrose. It is reported that in the case of large particle formation the reduction of transfection rates is presumably due to structural

alterations within the complexes or perturbed interaction between plasmid DNA and cationic polymer [6]. Transfection efficiency and metabolic activity of lyophilized polyplexes formulated with lactosucrose and HP- β -CD /sucrose was comparable to the freshly prepared formulations. When formulated with lactosucrose transfection efficiency was only slightly decreased when stored for 6 weeks at 40 °C. These findings are similar to the 25% decrease in transfection efficiency of freeze-dried PDMAEMA complexes when stored at 40 °C for 10 months; storage at 4 °C or 20 °C resulted in retained transfection efficiency [27]. Freshly prepared PVP/sucrose formulations were found to be cytotoxic in contrast to the lyophilized formulations. Although we did not further investigate this effect, we suggest that peroxide impurities [42] in the povidone might influence metabolic activity of murine neuroblastoma cells and that the peroxide impurities are removed by the use of lyophilization. Kumar and Kalonia [43] demonstrated that vacuum drying can be used to remove peroxides in polyethylene glycols resulting in an increased stability of biotech and pharmaceutical formulations, supporting our findings. However, when the PVP/sucrose formulations were stored at 40 °C a drastic four log unit decrease in transfection efficiency was observed. As metabolic activity and particle size were only marginally changed we presume a chemical change in the formulation due to the increased storage temperature, but this presumption was not further investigated. Numerous studies have demonstrated that structural modifications due to chemical changes in the formulation other than alterations in particle size can also influence gene delivery efficiency [26].

In order to investigate supplementary physical characteristics turbidity and number of subvisible particles were analyzed as well. Turbidity only refers to the presence of large aggregated particles, when it is clearly increased, as it was observed for the freeze-thawed polyplex sample without stabilizers. The samples with stabilizers showed an increased turbidity after lyophilization and

reconstitution. But the increased turbidity also manifested in the placebo formulations. This can be explained by the fact that small particles are formed by the excipient itself after lyophilization and reconstitution. This observation was also described by Anchordoquy et al. [15]. In addition, the fact that for the lyophilized HP- β -CD/sucrose samples additional peaks were detected in the DLS size distribution by intensity, regardless of whether polyplexes were present or not, might be related to the particle formation of the excipient itself. It is reported in literature, that cyclodextrins form self assembled aggregates or nanoparticles at increased concentrations (>1%) [44]. The particularly high turbidity in combination with a large number of subvisible particles in the very low micrometer range for samples containing lactosucrose may be presumably related to impurities that favour particle formation upon lyophilization as the raw material has only a purity of $\geq 90\%$. Interestingly, only the lactosucrose placebo formulations showed raised turbidities with increasing storage temperature but the formation of excipient particles was inhibited by the presence of polyplexes via an unknown and not further investigated mechanism. In general, all placebo and verum samples showed large numbers of subvisible particles $\geq 1 \mu\text{m}$. Thus, it can be stated that the excipients themselves and the manufacturing environment may lead to these high numbers of small particles. However, all samples meet the current standard limits for small volume parenterals specified in the Ph.Eur. [34] and USP [45]. Moreover, in accordance with literature [29], no correlations between turbidity or number of subvisible particles and transfection efficiency were observed, confirming our hypothesis that the variation in turbidity and number of subvisible particles is not evoked by the formation of polyplex aggregates.

All formulations showed substantially higher T_g' values compared for example to pure sucrose samples for which a T_g' of about -31°C is reported in literature [39]. According to the Fox-Flory theory [46], the T_g' increases with

increasing molecular weight. This is the reason for the increased T_g' found for the lactosucrose and HP- β -CD/sucrose or povidone/sucrose samples. For pure HP- β -CD and pure povidone T_g' values of about $-15.4\text{ }^\circ\text{C}$ and $-22.1\text{ }^\circ\text{C}$ are reported in literature [47]. The mixtures with sucrose result in a T_g' value which is in correspondence to the mixing ratio used. The T_g of the freeze-dried formulations showed the same trend of higher T_g values for the formulations containing excipients with higher molecular weights, when compared to the T_g value of pure sucrose of $72\text{ }^\circ\text{C}$ mentioned in literature [48]. The T_g of $113.6\text{ }^\circ\text{C}$ determined for the lactosucrose sample in our study is in accord with the T_g reported for spray-dried lactosucrose [49]. For pure PVP a T_g of $110\text{ }^\circ\text{C}$ and for β -CD a T_g of $108\text{ }^\circ\text{C}$ are reported [47,50]. However, when comparing T_g values residual moisture has to be considered, which was very low in our study. In general, residual moisture contents of less than 1% after lyophilization are considered to be optimal for storage stability [9]. The observed increase in residual moisture at elevated storage temperature could be explained by the fact that at higher temperatures the potential for water transfer out of the stopper to the dried cake is more pronounced [51]. In general, an increase in water content can be critical for storage stability as it is associated with a decrease in the glass transition temperature. As complexes have to be remained spatially separated in the dried cake to prevent aggregation, product vitrification may not be important for the particle stabilization during lyophilization but is essential for long-term stability [23]. After storage, all formulations exhibit still high glass transition temperatures compared e.g. to pure sucrose. Therefore, oligosaccharides and polymers are more auspicious lyoprotectants than disaccharides because they can be exposed to higher relative humidity during storage without passing the glass transition temperature and can therefore optimize storage stability [39].

In general all three selected formulations, 14% lactosucrose, 10% HP- β -CD with 6.5% sucrose or 10% PVP with 6.3% sucrose, are suitable to preserve polyplex particle size upon lyophilization and storage at isotonic concentrations. However, the knock-out criterion of the PVP/ sucrose formulation is its pronounced cytotoxicity and reduced transfection efficiency. For lactosucrose the increased turbidity and number of subvisible particles in the low micrometer range is a less critical constraint, as the current standard limits of small volume parenterals are met. The HP- β -CD /sucrose formulations exhibited an additional peak in the intensity versus size distribution of the DLS measurements after lyophilization and storage, indicating the formation of nano-meter ranged HP- β -CD aggregates. But this represents only an analytical limitation. As the lactosucrose and HP- β -CD sucrose formulations preserved the particle size and showed comparable transfection efficiencies and metabolic activities, we suggest these two formulations as very promising selections to conserve polyplexes and other non-viral vectors. However, the stability of the complexes against freezing and drying stresses has to be considered, which might depend on the actual composition e.g. DNA versus siRNA or non-pegylated versus pegylated, the size and surface charge of the complexes. We suggest to evaluate the complex stability in a freeze-thawing study at first. If the complexes require an even increased excipient to polyplex mass ratio, the HP- β -CD/sucrose formulation might be a promising alternative, as the mass of HP- β -CD at the expense of the mass of sucrose can be easily increased without exceeding isotonicity. In addition to the suitability of the lactosucrose and HP- β -CD/sucrose for the manufacturing of lyophilized non-viral vector formulations, we suggest that these formulations are beneficial in all cases in which a high excipient amount is required but isotonicity levels should not be exceeded e.g. for high concentrated protein formulations or other nanoparticulate systems. Furthermore, the high Tg' and Tg values are

promising. The increased T_g' will allow primary drying at elevated shelf temperatures resulting in shorter, less expensive freeze-drying cycles. The high T_g values will positively influence storage stability.

5 Conclusion

To summarize, by changing the initial HBG buffer to a more acidic L-histidine buffer system smaller, more homogeneous and more positively charged polyplexes with potentially higher stability due to increased repulsion are obtained. Prior to lyophilization, freeze-thawing studies were performed to select the most effective cryoprotectant. Using lactosucrose, HP- β -CD /sucrose and PVP/sucrose at isotonic concentrations, effective protection against freeze-thawing induced aggregation of the polyplexes was observed. By using these formulations the polyplex size can also be far better preserved upon lyophilization and storage compared to previous studies. All samples met the current standard limits for particulate contamination for small volume parenterals. However, turbidity and number of subvisible particles are influenced by the formation of excipient particles. The lyophilized and stored polyplexes formulated with lactosucrose or HP- β -CD /sucrose show comparable transfection efficiencies and metabolic activities in cell culture. However, transfection efficiency along with metabolic activity decreases when using PVP/sucrose as stabilizers. Lyophilized and stored samples showed low residual moistures and high glass transition temperatures and were found to be totally amorphous. The lactosucrose and HP- β -CD sucrose formulations are not only promising for the stabilization of non-viral gene delivery systems in general but also for their applications like highly concentrated protein formulations.

In conclusion, in this study we could show that lyophilization is an excellent method to achieve stable polyplex formulations with maintained particle size and transfection potential. Lyophilized formulations are not only ideal for shipping and storage they also reduce the risk of critical batch to batch variations in clinical studies if freshly prepared samples prior to administration are required. Moreover, lyophilization allows the concentration of non-viral gene

delivery formulations by reconstitution of the lyophilized samples with reduced quantities of water [19].

The possibility to reproducibly produce large standardized batches of well-defined, transfection efficient polyplexes with long-term stability by using a micro-mixer preparation method followed by lyophilization is an important step closer from a promising technology to application

6 References

- [1] A. Pathak, S. Patnaik, K.C. Gupta, Recent trends in non-viral vector-mediated gene delivery, *Biotechnol. J.* 4 (2009) 1559–1572.
- [2] T.J. Anchordoquy, G.S. Koe, Physical stability of nonviral plasmid-based therapeutics, *J. Pharm. Sci.* 89 (2000) 289–296.
- [3] T.J. Anchordoquy, S.D. Allison, M.d.C. Molina, L.G. Girouard, T.K. Carson, Physical stabilization of DNA-based therapeutics, *Drug Discov. Today* 6 (2001) 463–470.
- [4] D. Schaffert, E. Wagner, Gene therapy progress and prospects: synthetic polymerbased systems, *Gene Ther.* 15 (2008) 1131–1138.
- [5] J. Clement, K. Kiefer, A. Kimpfler, P. Garidel, R. Peschka-Süss, Large-scale production of lipoplexes with long shelf-life, *Eur. J. Pharm. Biopharm.* 59 (2005) 35–43.
- [6] S.D. Allison, T.J. Anchordoquy, Lyophilization of nonviral gene delivery systems, in: M.A. Findeis (Ed.), *Nonviral Vectors for Gene Therapy: Methods and Protocols*, Humana Press Inc., New York, 2001, pp. 225–252.
- [7] H. Talsma, J.-Y. Cherng, H. Lehrmann, M. Kurs, M. Ogris, W.E. Hennink, M. Cotten, E. Wagner, Stabilization of gene delivery systems by freeze-drying, *Int. J. Pharm.* 157 (1997) 233–238.
- [8] F. Franks, Freeze-drying of bioproducts: putting principles into practice, *Eur. J. Pharm. Biopharm.* 45 (1998) 221–229.
- [9] X. Tang, M. Pikal, Design of freeze-drying processes for pharmaceuticals: practical advice, *Pharm. Res.* 21 (2004) 191–200.
- [10] C. Brus, E. Kleemann, A. Aigner, F. Czubayko, T. Kissel, Stabilization of oligonucleotide–polyethylenimine complexes by freeze-drying: physicochemical and biological characterization, *J. Control. Release* 95 (2004) 119–131.
- [11] W. Abdelwahed, G. Degobert, S. Stainmesse, H. Fessi, Freeze-drying of nanoparticles: formulation, process and storage considerations, *Adv. Drug Delivery Rev.* 58 (2006) 1688–1713.
- [12] B.S. Chang, B.S. Kendrick, J.F. Carpenter, Surface-induced denaturation of proteins during freezing and its inhibition by surfactants, *J. Pharm. Sci.* 85 (1996) 1325–1330.
- [13] K.A. Pikal-Cleland, N. Rodríguez-Hornedo, G.L. Amidon, J.F. Carpenter, Protein denaturation during freezing and thawing in phosphate buffer systems: monomeric and tetrameric [beta]-galactosidase, *Arch. Biochem. Biophys.* 384 (2000) 398–406.
- [14] J.Y. Cherng, P.v.d. Wetering, H. Talsma, D.J.A. Crommelin, W.E. Hennink, Stabilization of polymer-based gene delivery systems, *Int. J. Pharm.* 183 (1999) 25–28.

- [15] T.J. Anchordoquy, J.F. Carpenter, D.J. Kroll, Maintenance of transfection rates and physical characterization of lipid/DNA complexes after freeze-drying and rehydration, *Arch. Biochem. Biophys.* 348 (1997) 199–206.
- [16] J.F. Carpenter, J.H. Crowe, The mechanism of cryoprotection of proteins by solutes, *Cryobiology* 25 (1988) 244–255.
- [17] G. Strauss, P. Schurtenberger, H. Hauser, The interaction of saccharides with lipid bilayer vesicles: stabilization during freeze-thawing and freeze-drying, *Biochim. Biophys. Acta* 858 (1986) 169–180.
- [18] W.L.J. Hinrichs, F.A. Manceñido, N.N. Sanders, K. Braeckmans, S.C. De Smedt, J. Demeester, H.W. Frijlink, The choice of a suitable oligosaccharide to prevent aggregation of PEGylated nanoparticles during freeze thawing and freeze drying, *Int. J. Pharm.* 311 (2006) 237–244.
- [19] T.J. Anchordoquy, T.K. Armstrong, M.d.C. Molina, Low molecular weight dextrans stabilize nonviral vectors during lyophilization at low osmolalities: concentrating suspensions by rehydration to reduced volumes, *J. Pharm. Sci.* 94 (2005) 1226–1236.
- [20] T.J. Anchordoquy, T.K. Armstrong, M.D.C. Molina, S.D. Allison, Y. Zhang, M.M. Patel, Y.K. Lentz, G.S. Koe, Formulation considerations for DNA-based therapeutics, in: D.R. Lu, S. Oeie (Eds.), *Cellular Drug Delivery*, Humana Press Inc., Totowa, 2004, pp. 237–263.
- [21] M.d.C. Molina, S.D. Allison, T.J. Anchordoquy, Maintenance of nonviral vector particle size during the freezing step of the lyophilization process is insufficient for preservation of activity: insight from other structural indicators, *J. Pharm. Sci.* 90 (2001) 1445–1455.
- [22] S.D. Allison, J.A. Thomas, Mechanisms of protection of cationic lipid–DNA complexes during lyophilization, *J. Pharm. Sci.* 89 (2000) 682–691.
- [23] S.D. Allison, M.d.C. Molina, T.J. Anchordoquy, Stabilization of lipid/DNA complexes during the freezing step of the lyophilization process: the particle isolation hypothesis, *Biochim. Biophys. Acta* 1468 (2000) 127–138.
- [24] B. Li, S. Li, Y. Tan, D.B. Stolz, S.C. Watkins, L.H. Block, L. Huang, Lyophilization of cationic lipid–protamine–DNA (LPD) complexes, *J. Pharm. Sci.* 89 (2000) 355–364.
- [25] O. Zelphati, C. Nguyen, M. Ferrari, J. Felgner, Y. Tsai, P.L. Felgner, Stable and monodisperse lipoplex formulations for gene delivery, *Gene Ther.* 5 (1998) 1272–1282.
- [26] T.J. Anchordoquy, L.G. Girouard, J.F. Carpenter, D.J. Kroll, Stability of lipid/DNA complexes during agitation and freeze-thawing, *J. Pharm. Sci.* 87 (1998) 1046–1051.
- [27] J.-Y. Cherng, H. Talsma, D. Crommelin, W. Hennink, Long term Stability of poly((2-dimethylamino)ethyl methacrylate)-based gene delivery systems, *Pharm. Res.* 16 (1999) 1417–1423.

- [28] J.-Y. Cherng, P. van de Wetering, H. Talsma, D.J.A. Crommelin, W.E. Hennink, Freeze-drying of poly((2-dimethylamino)ethyl methacrylate)-based gene delivery systems, *Pharm. Res.* 14 (1997) 1838–1841.
- [29] T.K. Armstrong, T.J. Anchordoquy, Immobilization of nonviral vectors during the freezing step of lyophilization, *J. Pharm. Sci.* 93 (2004) 2698–2709.
- [30] M. Kursa, G.F. Walker, V. Roessler, M. Ogris, W. Roedl, R. Kircheis, E. Wagner, Novel shielded transferrin–polyethylene glycol–polyethylenimine/DNA complexes for systemic tumor-targeted gene transfer, *Bioconjugate Chem.* 14 (2002) 222–231.
- [31] M. Lenter, P. Garidel, J. Pelisek, E. Wagner, M. Ogris, Stabilized Nonviral Formulation for the Delivery of MCP-1 Gene into Cells of the Vasculoendothelial System, *Pharm. Res.* 21 (2004) 683–691.
- [33] J.C. Kasper, D. Schaffert, M. Ogris, E. Wagner, W. Friess, The establishment of an up-scaled micro-mixer method allows the standardized and reproducible preparation of well-defined plasmid/LPEI polyplexes, *Eur. J. Pharm. Biopharm.* 77 (2011) 182–185.
- [32] D. Schaffert, M. Kiss, W. Rödl, A. Shir, A. Levitzki, M. Ogris, E. Wagner, Poly(I:C) mediated tumor growth suppression in EGF-receptor overexpressing tumors using EGF-polyethylene glycol-linear polyethylenimine as carrier, *Pharm. Res.*, 28 (2011) 731-741.
- [34] 2.9.19. Particulate contamination: sub-visible particles, *European Pharmacopoeia*, 2008, pp. 300–302.
- [35] T. Mosmann, Rapid colorimetric assay for cellular growth and survival: application to proliferation and cytotoxicity assays, *J. Immunol. Methods* 65 (1983) 55–63.
- [36] <http://www.accessdata.fda.gov/scripts/cder/iig/index.cfm>, Inactive Ingredients in Approved FDA Drugs, 2009.
- [37] M. Ogris, Gene delivery using polyethylenimine and copolymers, in: M.M. Amiji (Ed.), *Polymeric Gene Delivery*, CRC Press LLC, Boca Raton, Principles and Applications, 2005, pp. 97–106.
- [38] E. Lai, J.H. van Zanten, Monitoring DNA/poly-l-lysine polyplex formation with time-resolved multiangle laser light scattering, *Biophys. J.* 80 (2001) 864–873.
- [39] W.L.J. Hinrichs, N.N. Sanders, S.C. De Smedt, J. Demeester, H.W. Frijlink, Inulin is a promising cryo- and lyoprotectant for PEGylated lipoplexes, *J. Control. Release* 103 (2005) 465–479.
- [40] J.H. Crowe, L.M. Crowe, J.F. Carpenter, Preserving dry biomaterials: the water replacement hypothesis. Part 1, *BioPharm* 6 (1993) 28–298 32–33.
- [41] S.C. De Smedt, J. Demeester, W.E. Hennink, Cationic polymer based gene delivery systems, *Pharm. Res.* 17 (2000) 113–126.

- [42] K.J. Hartauer, G.N. Arbuthnot, S.W. Baertschi, R.A. Johnson, W.D. Luke, N.G. Pearson, E.C. Rickard, C.A. Tingle, P.K.S. Tsang, R.E. Wiens, Influence of peroxide impurities in povidone and crospovidone on the stability of raloxifene hydrochloride in tablets: identification and control of an oxidative degradation product, *Pharm. Dev. Technol.* 5 (2000) 303–310.
- [43] V. Kumar, D. Kalonia, Removal of peroxides in polyethylene glycols by vacuum drying: implications in the stability of biotech and pharmaceutical formulations, *AAPS PharmSciTech* 7 (2006) E47–E53.
- [44] M. Messner, S.V. Kurkov, P. Jansook, T. Loftsson, Self-assembled cyclodextrin aggregates and nanoparticles, *Int. J. Pharm.* 387 (2010) 199–208.
- [45] <788>, Particulate matter in injections, *USP (U.S. Pharmacopeia)* 34 (2011) 326–328.
- [46] T.G. Fox, P.J. Flory, Second-order transition temperatures and related properties of polystyrene. I. Influence of molecular weight, *J. Appl. Phys.* 21 (1950) 581–591.
- [47] W. Abdelwahed, G. Degobert, H. Fessi, Investigation of nanocapsules stabilization by amorphous excipients during freeze-drying and storage, *Eur. J. Pharm. Biopharm.* 63 (2006) 87–94.
- [48] M.d.C. Molina, T.K. Armstrong, Y. Mayank, Z.M. Patel, Y.K. Lentz, T.J. Anchordoquy, The stability of lyophilized lipid/DNA complexes during prolonged storage, *J. Pharm. Sci.* 93 (2004) 2259–2273.
- [49] R. Fuhrherr, Spray-dried antibody powders for pulmonary application, in: Ph.D. Thesis Ludwig-Maximilian University, Munich, 2005.
- [50] S.J. Prestrelski, K.A. Pikal, T. Arakawa, Optimization of lyophilization conditions for recombinant human interleukin-2 by dried-state conformational analysis using Fourier-transform infrared spectroscopy, *Pharm. Res.* 12 (1995) 1250–1259.
- [51] E.Y. Shalaev, G. Zografi, How does residual water affect the solid-state degradation of drugs in the amorphous state? *J. Pharm. Sci.* 85 (1996) 1137–1141.

Chapter 6

Investigation on polyplex stability during the freezing step of lyophilization using controlled ice nucleation

The following chapter is intended for publication:

Julia C. Kasper, Michael J. Pikal, Wolfgang Friess

Investigations on polyplex stability during the freezing step of lyophilization using controlled ice nucleation – The importance of residence time in the low viscous state;
in preparation.

Abstract

Lyophilization has proven to be an attractive way to achieve long-term stable nanoparticulate gene delivery formulations. However, freezing induced stresses are known to induce particle aggregation, unless particles are formulated at a sufficient stabilizer/DNA mass ratio.

The “preferential exclusion hypothesis”, the “vitrification hypothesis”, and the “particle isolation hypothesis” mechanisms have been discussed, but are not capable to fully explain the stabilization of gene delivery particles during freezing. Thus, this study was aimed to comprehensively investigate the influence of the freezing step on the stability of gene delivery particles.

Plasmid/LPEI were formulated at two DNA concentrations (10 µg/mL or 50 µg/mL) and at increasing sucrose/DNA ratio from 1200 to 14000. At first, particle size of polyplexes after freezing by the “standard” depressurization method in comparison to conventional shelf-ramp freezing was investigated. In a next, step the influence of ice nucleation temperature, residence time of the particles in an unstable frozen state, or proceeding freezing was investigated separately. Moreover, the increase in sucrose concentration and system viscosity during freeze-concentration and corresponding bimolecular reaction rates were theoretically modeled.

The “standard” depressurization method was more stressful to particles compared to shelf-ramp freezing, but comparable results were achieved when temperature equilibration after ice nucleation was omitted. The ice nucleation temperature only affected the stability at low DNA concentrations. But in general, particle stability during freezing was highly temperature- and time-dependent. Particle stability was markedly affected during the early part of freezing ($< -3^{\circ}\text{C}$). In this phase freeze-concentration is already far progressed leading to high particle concentration and an increase in bimolecular reaction rate which cannot be inhibited by the still very low system viscosity. Low shelf-

ramp rates negatively affect particle stability. In general, below a critical temperature ($\sim \leq -18^{\circ}\text{C}$) no further particle aggregation occurred due to the drastic increase in sample viscosity that strongly reduce the reaction rates. Moreover, an initially high sucrose/DNA ratio and sample viscosity is capable to fully inhibit an increase in bimolecular reaction rates during freezing.

Thus, it can be concluded that the initial sample viscosity rather than the unfrozen volume is the predominant factor in particle stabilization. In addition, the residence time of particles in the low viscous state is of importance. This extended understanding of the underlying stabilization mechanisms during freezing of nanoparticles will facilitate the development of improved formulations and optimized lyophilization processes.

Keywords

Non-viral gene delivery, lyophilization, freezing, stabilization, cryoprotection, viscosity

1 Introduction

Nucleic acid-based therapeutics are a promising new class of biopharmaceuticals [1]. The most common non-viral carriers for the nucleic acids are lipoplexes and polyplexes [1]. These nanoparticulate carriers are based on cationic lipids or cationic polymers which form condensed complexes with the negatively charged nucleic acids via electrostatic interaction [1]. One general limitation is the poor long-term stability of nanoparticles, specifically non-viral vectors tend to aggregate in aqueous solutions, which is known to correlate with a loss in transfection efficiency of nucleic acid based systems [2]. Consequently, lyophilization has proven to be an attractive way for the production of long-term stable, transfection efficient gene delivery formulations. Although lyophilization is a very gentle drying process it involves two potential stresses: freezing and drying [3]. These stresses typically cause damage of macromolecules and nanoparticles, unless appropriate stabilizers are added to the formulation [4].

In a previous study we found that the undesirable aggregation of plasmid/LPEI polyplexes occurs predominantly during the freezing and not during the drying step of the lyophilization process [5] (see Chapter 5). Similar observations were also reported for lipid/DNA complexes [6-8]. In general sugars, especially disaccharides like sucrose, are very efficient cryoprotectants [9-11]. But the choice of excipient is not the predominant factor in particle stabilization, unless crystallization or phase separation of the excipient occurs [5, 7]. Instead, it was observed that the mass ratio of stabilizer to gene delivery particle is critical in order to provide sufficient stabilization during the freezing step [5-7].

During freezing, the product temperature is lowered and samples experience supercooling until ice nucleation occurs [12-13]. As the freezing process continues, more and more water is converted into ice. This leads to cryoconcentration of the samples until a critical concentration is exceeded, and

vitrification of amorphous or eutectic crystallization of crystalline excipients occurs [12-13]. Thus, there are two main stress factors that could potentially impact the stability of gene delivery particles during freezing: ice formation and cryoconcentration [14]. Ice formation can threaten particle stability via their exposure to ice-liquid interfaces or due to mechanical damage by growing ice crystals [14]. Cryoconcentration leads to both solute and particle rich liquid phase and might facilitate particle aggregation due to an increase in ionic strength, pH shifts or simply particle crowding [4, 7, 14].

Several mechanisms how cryoprotectants may stabilize non-viral gene delivery particles during freezing have been discussed [2, 15]. The “preferential exclusion hypothesis”, which was established to explain protein stabilization, states that solutes are preferentially excluded from a protein surface leading to the formation of a stabilizing solvent layer [2, 15-16]. However, it is doubtful whether the “preferential exclusion hypothesis” can be adapted to non-viral vectors, as this hypothesis requires exclusion of the sugar, but for non-viral vectors direct interaction of sugar molecules with the particles is reported [15]. According to the “glass formation or vitrification hypothesis”, non-viral vectors are entrapped in the amorphous glassy matrix that is formed when the sample is cooled below the glass transition temperature of the maximally freeze-concentrated system (T_g') [2, 15]. The high viscosity of the glassy matrix immobilizes gene-delivery particles and, thus, prevents particle aggregation [2, 15]. However, the “vitrification hypothesis” is not capable to explain the requirement of a critical mass ratio of stabilizer to gene delivery particle, as glass formation during freezing is independent of the initial stabilizer concentration [15].

In a study on the freeze-thaw stability of lipid/DNA complexes, Allison et al. [7] demonstrated that glass formation is not obligatory as sugars like glucose are also capable to preserve particle size at temperatures above T_g' .

Consequently, the “particle isolation hypothesis” was proposed [7]. This hypothesis is based on the fact that crowding of particles facilitates particle aggregation and that the separation of individual particles in the unfrozen fraction prevents particle collision during freezing [7]. At higher stabilizer/particle mass ratios, the volume of the unfrozen fraction increases, leading to a more distinct dilution and more effective separation of the particles in the freeze-concentrate [7]. In a further study, Armstrong et al. [17] showed that particle aggregation can result from the formation of ice as well as from prolonged incubation in the frozen state above, but not below, a critical temperature well above T_g . Therefore, they concluded that below this critical temperature particles are already sufficiently immobilized in the freeze-concentrate preventing particle aggregation [17].

Until now, no detailed study on the influence of different freezing parameters, such as ice nucleation temperature or freezing rate, on the stability of non-viral gene delivery particles is available. These parameters highly affect the freezing behavior and the structure of the non-frozen fraction and thus, might also highly impact particle stability during freezing. Literature is focused on the influence of the freezing process on protein stability or performance of the lyophilization process [13]. With regard to the stability of non-viral gene delivery particles, it is only reported that fast freezing in a dry ice/alcohol bath, in liquid nitrogen, or in a $-70\text{ }^{\circ}\text{C}$ freezer resulted in a better preservation of lipoplexes compared to slow freezing in a $-20\text{ }^{\circ}\text{C}$ freezer or at $-2.5\text{ }^{\circ}\text{C}/\text{min}$ to $-40\text{ }^{\circ}\text{C}$ [6, 18].

But these difficult to control fast freezing methods are not practical on large scale. Instead shelf-ramp freezing, where the filled vials are placed on the shelves of the freeze-drier and the shelf temperature is decreased linearly (with $-0.1\text{ }^{\circ}\text{C}/\text{min}$ to $-5\text{ }^{\circ}\text{C}/\text{min}$, depending on the capacity of the freeze-drier) with time, is the most commonly used freezing method [13]. During shelf-ramp freezing, ice nucleation occurs stochastically, resulting in vial-to-vial or batch-to-

batch heterogeneity and up-scaling issues [13]. Therefore, different methods based on ultrasound, electro-freezing, vacuum-induced surface freezing, an ice fog or depressurization have been developed in order to control nucleation at the desired nucleation temperature [13]. Depressurization is a rather newly established method which has gained substantial attraction. Nucleation is induced by suddenly depressurizing the freeze-drier chamber that was pressurized with argon gas before [19-20]. Bursac et al. [19] reported larger pores, lower surface area and improved lactate dehydrogenase recovery for samples frozen by depressurization at $\sim -3^{\circ}\text{C}$ with an ~ 15 min hold step compared to samples produced by shelf-ramp freezing.

The objective of this study was to investigate the influence of different freezing procedures on the stability of plasmid/LPEI polyplexes, in order to get an extended understanding of critical freezing parameters and the underlying stabilization mechanisms during freezing of non-viral gene delivery particles. Plasmid/LPEI polyplexes were formulated at different plasmid DNA concentrations and at increasing sucrose/polyplex mass ratios. In a first step, the influence of the "standard" depressurization method in comparison to conventional shelf-ramp freezing on polyplex particle size was investigated. Secondly, the influence of the ice nucleation temperature and the residence time of the particles above T_g' during freezing were studied individually with the aid of the depressurization method. In a next step, the influence of the proceeding of freezing on polyplex particle size was investigated. Furthermore, the increase in sucrose concentration and sample viscosity during freezing was theoretically calculated and correlated with bimolecular reactions rates. These theoretical results were then compared to the obtained experimental data. The identification of critical parameters and a better understanding of the stabilization mechanisms involved during freezing should help to design less

stressful lyophilization processes and lyophilized products with improved quality.

2 Materials and methods

2.1 Materials

The plasmid (pCMVLuc) was produced by PlasmidFactory (Bielefeld, Germany). 22 kDa linear polyethylenimine (LPEI) was synthesized by acid-catalyzed hydrolyses from poly(2-ethyl-2-oxazoline) (Sigma Aldrich, Steinheim, Germany) as described in [21]. L-histidine was obtained from Merck (Darmstadt, Germany) and sucrose from Sigma Aldrich (St Louis, MO, USA). 3 mL glass vials (glass type: 8412-G) with their according LyoTec™ stoppers were used (West Pharmaceutical Services, Lionville, PA, USA).

2.2 Sample preparation

Plasmid/LPEI polyplexes were prepared at a N/P ratio (molar ratio of LPEI nitrogen (N) to DNA phosphate (P)) of 6:1 and at a DNA concentration of 100 µg/ml in 10 mM L-histidine buffer pH 6.0 with an established micro-mixer method [22] using a 5.0 mL syringe and a plunger speed of 1.0 cm/min. Polyplexes were incubated for 30 min at room temperature in order to ensure complete polyplex formation.

Table 6-1: Overview on polyplex formulations tested.

10 µg/mL DNA		50 µg/mL DNA	
sucrose/DNA mass ratio	sucrose conc. [% w/v]	sucrose/DNA mass ratio	sucrose conc. [% w/v]
2000	2	1200	6
4000	4	1600	8
6000	6	2000	10
8000	8	2400	12
10000	10	2800	14
12000	12	3200	16
14000	14	3600	18
		4000	20

Sucrose stock solutions at various concentrations [% w/v] were prepared in 10 mM L-histidine buffer pH 6.0. Polyplex formulations at DNA concentrations of 10 or 50 µg/mL and at various sucrose/DNA mass ratios (Table 6-1) were prepared by adequately mixing the polyplex stock solution with the sucrose stock solutions.

2.3 Freeze-thaw studies using different freezing protocols

Freeze-thawing studies were performed on a pilot scale freeze-drier (FTS LyoStar™ 3, SP Scientific, Stone Ridge, NY, USA) equipped with the ControlLyo™ technology (Praxair, Burr Ridge, IL, USA) for ice nucleation temperature control. 500 µL of each polyplex formulation in 3 mL vials were investigated in triplicates in each freeze-thawing experiment. Vials were placed on the middle of the shelf in a hexagonal array and all edge vials were surrounded by placebo vials containing 5% sucrose solution. All samples were equilibrated at 20 °C for 15 min prior to freezing. In all complete freeze-thaw experiments, samples were frozen to a final shelf temperature of –45 °C and held at this temperature over night for 10 h. Thawing was always performed by a shelf ramp rate to 20 °C at 2.5 °C/min with a 60 min hold at 20 °C. In order to monitor product temperature profiles during freezing, thin wire T-type thermocouples (Omega, Stamford, CT, USA) were dipped into thermal grease and fixed with tape on the outside of selected vials close to the vial bottom. Product temperature data and shelf inlet temperature data were collected every minute.

2.3.1 *Conventional shelf-ramp freezing*

Conventional shelf-ramp freezing was performed at a shelf ramp rate of –1 °C/min or –5 °C/min to –45 °C.

2.3.2 "Standard" depressurization method

The "standard" depressurization method for controlled ice nucleation was performed according to the method described by Konstantinidis et al. [20]. Samples were cooled at a shelf ramp rate of $-1\text{ }^{\circ}\text{C}/\text{min}$ to $5\text{ }^{\circ}\text{C}$ and equilibrated at that temperature for 15 min. Air from the product chamber was purged once by pressurizing at 10 psig (171 kPa) for 2 min with argon gas and depressurizing to a final pressure of 2 psig (115 kPa) within 20 s. The product chamber was pressurized with argon gas to approximately 28 psig (294 kPa). Subsequently, samples were cooled at $-1\text{ }^{\circ}\text{C}/\text{min}$ to $-4\text{ }^{\circ}\text{C}$ and equilibrated at that temperature for 30 min. In order to induce ice nucleation, the chamber pressure was quickly released to 2 psig (115 kPa). After ice nucleation, the shelf temperature was held for another 15 min at $-4\text{ }^{\circ}\text{C}$. Subsequently, samples were cooled at a shelf ramp rate of $-1\text{ }^{\circ}\text{C}/\text{min}$ to $-45\text{ }^{\circ}\text{C}$. The aforementioned parameters applied during purging, pressurization, and depressurization of the product chamber were used in all further freeze-thaw experiments.

2.3.3 Varying ice nucleation temperatures via controlled ice nucleation

In order to vary ice nucleation temperature during freezing, samples were cooled at $-1\text{ }^{\circ}\text{C}/\text{min}$ to $-4\text{ }^{\circ}\text{C}$, $-8\text{ }^{\circ}\text{C}$ or $-12\text{ }^{\circ}\text{C}$ after pressurization and equilibrated at that temperature for 30 min, before ice nucleation was induced. Subsequently, samples were directly cooled at $-5\text{ }^{\circ}\text{C}/\text{min}$ to $-45\text{ }^{\circ}\text{C}$ without any further equilibration step.

2.3.4 Varying shelf-ramp rates after controlled ice nucleation

After pressurization, samples were cooled at $-1\text{ }^{\circ}\text{C}/\text{min}$ to $-12\text{ }^{\circ}\text{C}$ and equilibrated at that temperature for 30 min before ice nucleation was induced. Subsequently, samples were directly cooled at varying shelf-ramp rates of $-0.1\text{ }^{\circ}\text{C}/\text{min}$, $-0.5\text{ }^{\circ}\text{C}/\text{min}$, $-1.0\text{ }^{\circ}\text{C}/\text{min}$ or $-5.0\text{ }^{\circ}\text{C}/\text{min}$ to $-45\text{ }^{\circ}\text{C}$ without any further equilibration step.

2.3.5 Interruption of the freezing process after controlled ice nucleation

Samples were cooled at $-1\text{ }^{\circ}\text{C}/\text{min}$ to $-12\text{ }^{\circ}\text{C}$ after pressurization and equilibrated at that temperature for 30 min before ice nucleation was induced. Then, samples were directly cooled at $-0.1\text{ }^{\circ}\text{C}/\text{min}$ to a shelf temperature of $-12.5\text{ }^{\circ}\text{C}$, $-14.0\text{ }^{\circ}\text{C}$, $-20.0\text{ }^{\circ}\text{C}$ and $-26.0\text{ }^{\circ}\text{C}$. Subsequently, thawing at $2.5\text{ }^{\circ}\text{C}/\text{min}$ was started.

2.4 Lyophilization

Lyophilization was performed on the same pilot scale freeze-drier as described in 2.3. 500 μL of selected polyplex formulations in 3 mL vials were frozen to $-45.0\text{ }^{\circ}\text{C}$ using different freezing protocols, and held at $-45.0\text{ }^{\circ}\text{C}$ for 60 min. For primary drying, the shelf temperature was increased at $0.2\text{ }^{\circ}\text{C}/\text{min}$ to $-30.0\text{ }^{\circ}\text{C}$ and the pressure was reduced to 65 mTorr (8.7 Pa). After ~ 18 h, the endpoint of primary drying was confirmed by manometric endpoint determination. Secondary drying was performed at $40\text{ }^{\circ}\text{C}$ (shelf ramp rate of $0.1\text{ }^{\circ}\text{C}/\text{min}$) and 65 mtorr (8.7 Pa) for 6 h. Samples were stoppered under vacuum.

2.5 Polyplex characterization

Size determination of siRNA polyplexes was performed by dynamic light scattering (DLS) using the Nanosizer ZS (Malvern Instruments, Westborough, MA, USA). The samples were diluted 1:20 with 10 mM L-histidine buffer pH 6.0 to a final volume of 1 mL. The diluted samples were analyzed in single-use polystyrene semi-micro PMMA cuvettes (Brand, Wertheim, Germany) with a path length of 10 mm. After an equilibration time of 1 min at $20\text{ }^{\circ}\text{C}$, each sample was recorded three times with 5 subruns of 10 s using the multimodal mode. The z-average diameter was calculated from the correlation function using the Zetasizer Software 6.20 (Malvern Instruments).

2.6 Specific surface area determination

The specific surface area (SSA) of selected lyophilisates was determined via BET surface area analysis using a Flowsorb II 2300 instrument (Micromeritics, Norcross, GA, USA). Prior to each measurement, the instrument was calibrated via injection of 1 mL of 100% krypton gas at known ambient temperature and pressure. Approximately 100 mg of the lyophilisates were transferred into the sample holder and sealed with sealing film in a dry bag, purged with nitrogen, and then, connected to the instrument. For out gassing samples were heated on a heating mantle at 40 °C for 2 hours in a gas flow of a helium and krypton mixture. No difference in SSA results was observed for out gassing for more than 2 hours. Subsequently, samples were exposed to a mixture of helium (inert carrier gas) and krypton (adsorbate) (0.1 mol % krypton in helium). The adsorption at 0.1 mol% krypton was determined in single point measurements and analyzed with the BET equation. For each formulation and freezing condition three samples from independent vials were analyzed at least twice. From these results the average SSA [m^2/g] along with the standard deviation was calculated. In order to include the effect of variable ice surface area in samples of variable sucrose levels, the absolute SSA [$m^2/100mL$] was calculated by [23]:

$$absoluteSSA \left[\frac{m^2}{100mL} \right] = SSA \left[\frac{m^2}{g} \right] \cdot \%solute \left[\frac{g}{100mL} \right] \quad (6-1)$$

2.7 Karl-Fischer titration

The residual moisture content of the lyophilisates was determined by coulometric Karl Fischer titration using a Metrohm 756 KF Coulometer (Metrohm, Herisau, Switzerland). About 500 μ L dried Methanol (HydranalTM-Methanol, Sigma-Aldrich, Germany) was injected into the sealed vial through the stopper and the lyophilized samples were dissolved by slightly shaking the vial. The water content was determined by injecting about 300 μ L of the

methanol samples into the titration solution (HydranalTM-Coulomat AG, Riedel-de Haen, Seelze, Germany) and was calculated in mass percentage water per mg lyophilized sample [% w/w]. HydranalTM Water Standard 0.10 (Sigma-Aldrich, Steinheim, Germany) was used as reference. For each selected formulation and freezing condition three vials were analyzed.

2.8 Theoretical modeling of the change in sucrose concentration or viscosity during freeze-concentration and correlation to reaction rates

The change in sucrose concentration and viscosity during freeze-concentration and corresponding relative reaction rates were theoretically modeled as previously published [24]. As in our study the weight ratio of L-histidine buffer to sucrose was very small, the effect of buffer was neglected. At first, the reduction of product temperature with each minute time increment was simulated via estimation of the heat transfer from the shelf to the product and subsequent evaluation of the amount of ice formed.

The heat transfer rate from the shelf to the product, Q_s [cal/s], is given by,

$$Q_s = A_v \cdot K_{v(P)} \cdot (T_s - T_p) \quad (6-2)$$

where A_v and K_v are the cross sectional area and heat transfer coefficient at a defined pressure (P) of the vial, respectively, and T_s and T_p are shelf temperature and product temperature [25]. A_v was $\sim 2.19 \text{ cm}^2$. The vial heat transfer coefficient K_v [cal/(m²Ks)] is composed of three terms: the contact, K_c , the radiation, K_r , and the gas conduction term, K_g . The following constants for typical tubing vials were used: $10^4 K_c \sim 1.0$, $10^4 K_r \sim 1.5$ and $10^4 K_g \sim 4.3$ (at atmospheric pressure, with a mean separation distance of 1 mm).

The ratio R of the heat transfer rate needed to remove heat created by the phase change (Q_{pc}) (i.e. forming of ΔX_w grams of water) to the heat transfer rate needed to cool both the solution and the ice formed (Q_{cool}) by the temperature change in the time interval Δt is calculated by:

$$R = \frac{Q_{pc} \cdot \Delta t}{Q_{cool} \cdot \Delta t} \quad (6-3)$$

The heat transfer rate needed to freeze ΔX_w grams of water is given by,

$$Q_{pc} \cdot \Delta t = \Delta X_w \cdot \Delta H_f \quad (6-4)$$

where ΔH_f is the heat fusion of ice (79.72 cal/g). The heat transfer rate for cooling both the solution and the ice formed is given by,

$$Q_{cool} \cdot \Delta t = (X_w \cdot C_{water} + (X_w^0 - X_w) \cdot C_{ice} + m_{vial} \cdot C_{glass}) \cdot \Delta T_{\Delta t} \quad (6-5)$$

where X_w^0 is the initial mass of water and X_w is the mass of water that is still present. C_{water} , C_{ice} and C_{glass} are the specific heats of water, ice and the glass vials with 0.99 cal/gK, 0.49 cal/gK and 0.20 cal/gK, respectively. The mass of the vials (m_{vial}) was ~5.15 g. $\Delta T_{\Delta t}$ is the change in temperature of the sample in the time interval Δt , and was calculated from the difference in the freezing point depression ΔT_f between each time interval. The freezing point depression ΔT_f is given by an empirical equation found to fit the data in [26]:

$$\Delta T_f = 2.54 \cdot \frac{m_{solute}}{X_w} * \exp(0.259 \cdot \frac{m_{solute}}{X_w}) \quad (6-6)$$

where m_{solute} is the mass of sucrose in g per vial.

Using the calculated factor R (equation 3), the heat provided from the shelf in order to form ice was determined. Thus, the amount of formed ice ΔX_w during each time interval could be calculated from equation 4, and the amount of unfrozen water X_w in the sample at each time point could be determined. For each sample composition the temperature of the solution could be calculated from equation 6. From that, the concentration of sucrose at each time point, until the maximum freeze-concentration of sucrose of ~80.9% [27] is reached, was calculated.

In a next step, a relationship between the variables, product temperature and sucrose concentration and the viscosity of the sucrose sample was developed. Therefore, viscosity data of sucrose solutions at various concentrations and temperatures given in [26] and quoted by C.A. Angell [28] were used. In order to

obtain an accurate viscosity estimation outside the available data range, the data was fitted with a Vogel-Tammann-Fulcher (VTF) type equation:

$$\ln(\eta) = \ln(A) + \frac{K}{T - T_0} \quad (6-7)$$

This equation relates viscosity ($\eta_{[\text{poise}]}$) to the absolute temperature (T) and the “zero mobility” temperature T_0 , where A is a constant, which should be $1 \cdot 10^{-4}$ [28]. T_0 depends on the composition of the system as T_0 is related to the glass transition temperature T_g . It was assumed that the relationship between T_0 and the systems composition in a binary system is similar to the relationship between T_g and the system composition. Thus, a variation of the Fox equation was used to represent the composition dependence of T_0 ,

$$\frac{1}{T_0} = \frac{1}{T_{00}} + b_1 \cdot c + b_2 \cdot c^2 \quad (6-8)$$

where T_{00} is the “zero mobility” temperature for pure water (i.e., when $c=0$). According to C.A. Angell $T_{00}=125$ K [28]. Moreover, b_1 and b_2 are pure constants to be determined by a fit to the data. For the constant K, which may also be dependent of the system composition, a simple linear relation to the concentration c was assumed:

$$K = K_0 + k_1 \cdot c \quad (6-9)$$

Thus, using the last three equations with the fit parameters $K_0=751$, $k_1=855$, $b_1=0.001551$ and $b_2=-0.00617$, viscosity over the entire range of concentrations and temperatures during freeze-concentration could be calculated.

In order to estimate the dependence between reaction rate and viscosity, a second-order reaction, with an Arrhenius temperature dependence and an activation energy of 20 kcal/mol, was assumed. Moreover, reaction rate was coupled inversely proportional to the relative increase in viscosity, as a diffusion-controlled reaction was assumed, with the diffusion constant being inversely proportional, as in the Stokes-Einstein equation. Polyplex concentration was calculated based on the assumption that one polyplex

contains five plasmid strands each consisting of 6233 base pairs. The relative reaction rate was related to the reaction rate at the point of ice nucleation at a DNA concentration of 50 $\mu\text{g/mL}$, which was defined as 1.

2.9 Statistical analysis

Differences between mean particle sizes were statistically challenged by performing a two-tailed student t test using the QuickCalcs, GraphPad Software (La Jolla, CA, USA). Mean values with a p value < 0.05 were judged as significantly different.

3 Results

3.1 Influence of the “standard” depressurization method in comparison to conventional shelf-ramp freezing on polyplex stability

As aforementioned, it is reported that a better protein recovery of lactate dehydrogenase was observed for samples frozen with the “standard” depressurization technique compared to stochastic shelf-ramp freezing [19]. Thus, in a first step, the influence of the “standard” controlled nucleation in comparison to conventional shelf-ramped freezing on polyplex stability was investigated. Therefore, polyplex samples formulated at 10 µg/mL and 50 µg/mL DNA, and at increasing sucrose/DNA mass ratio (Table 6-1) were frozen via depressurization at $-4\text{ }^{\circ}\text{C}$ with a 15 min equilibration step and at a subsequent shelf ramp rate of $-1\text{ }^{\circ}\text{C}/\text{min}$, or via conventional shelf-ramp freezing at a shelf ramp rate of $-1\text{ }^{\circ}\text{C}/\text{min}$ or $-5\text{ }^{\circ}\text{C}/\text{min}$. After thawing, plasmid/LPEI polyplex samples were analyzed for particle size.

The two most divergent product temperature profiles obtained during these three different freezing procedures, are displayed in Figure 6-1A. Using conventional shelf-ramp freezing, ice nucleation occurs very stochastically at random product temperatures ($-12.4 \pm 1.0\text{ }^{\circ}\text{C}$ or $-9.7 \pm 1.6\text{ }^{\circ}\text{C}$) and random points in time. In contrast, when ice nucleation is induced in a controlled manner, using the depressurization technique, ice nucleation occurs at almost the same product temperature ($-2.3 \pm 0.1\text{ }^{\circ}\text{C}$) and at the same point in time. Moreover, the different ramp rates or the application of a 15 min equilibration step after depressurization result in different residence times. Here, the residence time was defined as time period between ice nucleation and the point at which a product temperature of $-30\text{ }^{\circ}\text{C}$ is reached. The residence time was $7.8 \pm 0.5\text{ min}$ when samples were frozen at a shelf-ramp rate of $-5\text{ }^{\circ}\text{C}/\text{min}$ and

increased to 14.8 ± 3.6 min at a slower shelf-ramp rate of -1 °C/min. In contrast, a markedly prolonged residence time of 51.8 ± 0.8 min was observed when the samples were frozen via the “standard” depressurization method.

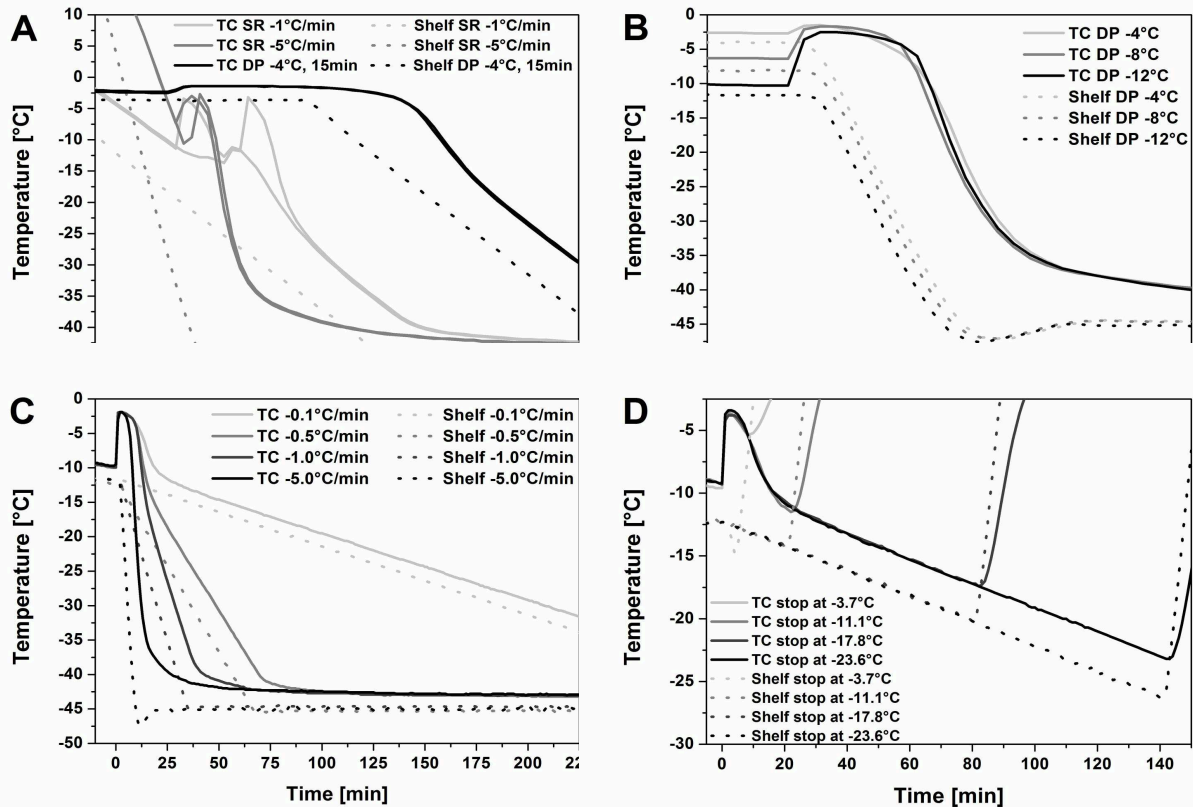


Figure 6-1: Product temperature profiles of 10% sucrose samples monitored with thermocouples (TC) and inlet temperatures of the shelf (shelf) during freezing using various freezing procedures. A) Conventional shelf ramping (SR) at -1 °C/min or -5 °C/min or via the “standard” depressurization method (DP) at -4 °C with a subsequent 15 min equilibration step and a shelf ramp rate of -1 °C/min. The displayed product temperature data represent the two most divergent profiles obtained during the varying freezing procedures. B) Nucleation induced by depressurization at a shelf temperature of -4 °C, -8 °C or -12 °C and a subsequent shelf ramp rate of -5 °C/min. C) Nucleation induced by depressurization at a shelf temperature of -12 °C and subsequent varying shelf ramp rates of -0.1 °C/min, -0.5 °C/min, -1.0 °C/min or -5.0 °C/min. D) Nucleation induced by depressurization at a shelf temperature of -12 °C and subsequent shelf ramp rate of -0.1 °C/min. The freezing procedure was stopped at a product temperature of -3.7 °C, -11.1 °C, -17.8 °C and -23.6 °C.

The z-average diameter of the plasmid/LPEI polyplexes after freeze-thawing using the three different freezing procedures is displayed in Figure 6-2.

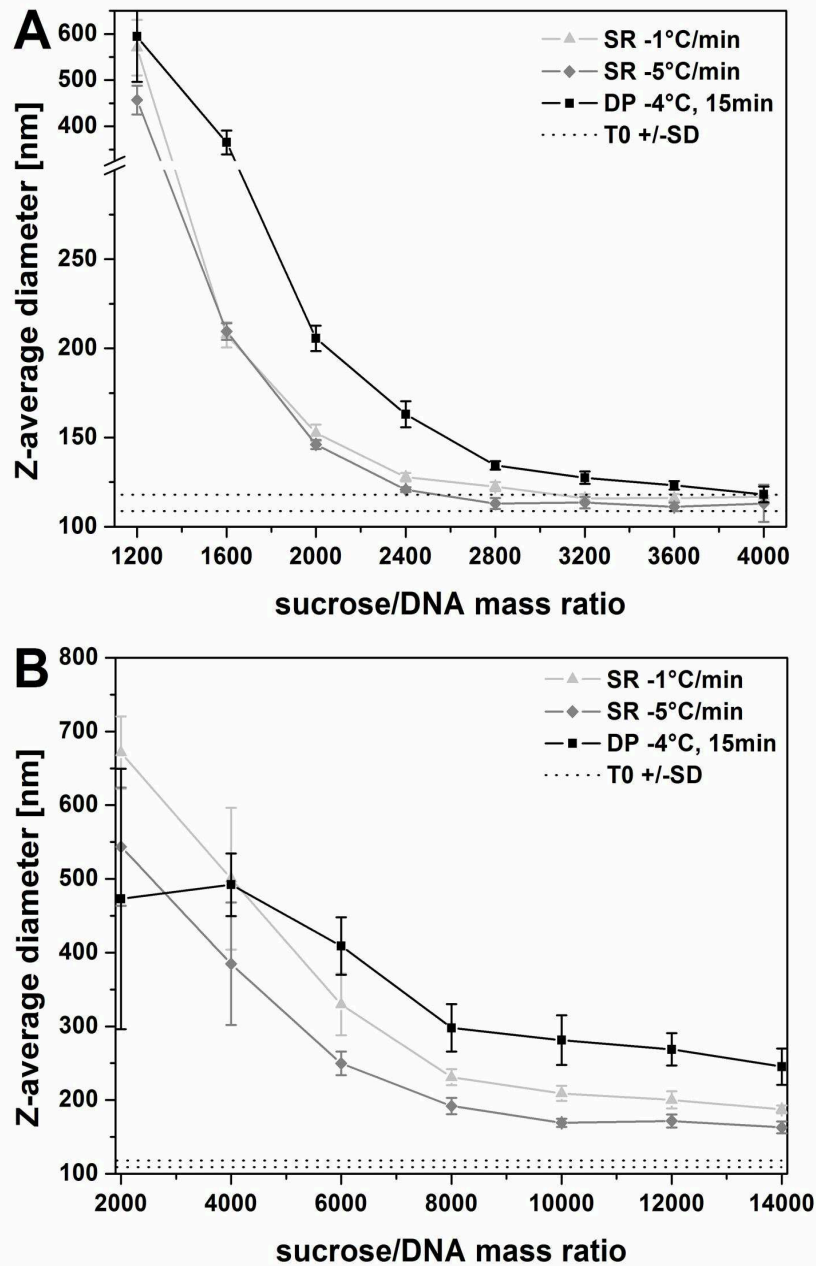


Figure 6-2: Z-average diameter of plasmid DNA/LPEI polyplexes after freeze-thawing when formulated at a DNA concentration of 50 µg/ml (A) or 10 µg/ml (B) and at increasing sucrose/DNA mass ratio. Samples were frozen via conventional shelf ramping (SR) at $-1\text{ }^{\circ}\text{C}/\text{min}$ or $-5\text{ }^{\circ}\text{C}/\text{min}$ or via the “standard” depressurization method (DP) at $-4\text{ }^{\circ}\text{C}$ with a 15 min equilibration step and a subsequent shelf ramp rate of $-1\text{ }^{\circ}\text{C}/\text{min}$. The dotted lines represent the mean + SD and mean – SD of the Z-average diameter of freshly prepared (T0) polyplexes. Each value represents the mean \pm SD of three measurements on triplicate samples.

In general, particle size becomes better preserved with increasing sucrose/DNA ratio. At a fixed sucrose/DNA ratio the “standard” depressurization method had a more negative impact on particle size compared to conventional shelf-ramp freezing. For instance, the size of plasmid/LPEI polyplexes at a concentration of 50 µg/mL and at a sucrose/DNA ratio of 2000 increased from ~113 nm to ~153 nm or ~146 nm when frozen at a shelf-ramp rate of -1 °C/min or -5 °C/min, respectively (Figure 6-2A). However, when frozen with the “standard” depressurization method, the increase in particle size to ~205 nm was significantly ($p < 0.05$) more pronounced. Moreover, the freezing procedure also impacts the critical sucrose/DNA ratio, at which full retention of the particle size is achieved. At a DNA concentration of 50 µg/ml, significant ($p > 0.05$) retention of particle size was observed at a sucrose/DNA ratio of 3200 or 2800, when frozen at a shelf-ramp rate of -1 °C/min or -5 °C/min, respectively. In comparison, a sucrose/DNA ratio of 4000 was required to significantly ($p > 0.05$) preserve particle size, when samples were frozen with the “standard” depressurization method. Analogous trends were observed for plasmid/LPEI polyplexes at a DNA concentration of 10 µg/mL. However, at this DNA concentration full retention of particle size could not be achieved in any formulation and freezing protocol. As described above, there are two important factors that can be used to discriminate between freezing procedures: nucleation temperature and residence time. Thus, the influence of these two factors on polyplex particle size was investigated separately in the following experiments.

3.2 Influence of ice nucleation temperature on polyplex stability

In order to investigate the influence of ice nucleation temperature on polyplex stability, the samples were equilibrated at various temperatures ($-4\text{ }^{\circ}\text{C}$, $-8\text{ }^{\circ}\text{C}$ or $-12\text{ }^{\circ}\text{C}$) prior to depressurization. This resulted in product temperatures of $-2.2 \pm 0.2\text{ }^{\circ}\text{C}$, $-6.3 \pm 0.3\text{ }^{\circ}\text{C}$ or $-10.4 \pm 0.2\text{ }^{\circ}\text{C}$ at the time of ice nucleation. Subsequently, samples were directly cooled at $-5\text{ }^{\circ}\text{C}/\text{min}$, in order to achieve residence times which do not significantly differ ($p > 0.05$) ($13.2 \pm 1.0\text{ min}$, $12.8 \pm 0.9\text{ min}$ and $12.3 \pm 0.6\text{ min}$ resp.). The difference in ice nucleation temperature and the consistency in residence time is reflected by the monitored temperature profiles (exemplarily shown for 10% sucrose samples in Figure 6-1B).

At a DNA concentration of $50\text{ }\mu\text{g}/\text{mL}$ (Figure 6-3A), no significance difference ($p > 0.05$) in particle size was observed at fixed sucrose/DNA ratios. For all ice nucleation temperatures a complete retention of particle size was achieved at a sucrose/DNA ratio of 3200. At the lower DNA concentration of $10\text{ }\mu\text{g}/\text{mL}$ (Figure 6-3B), the trend, that particle size was slightly better preserved when freezing was induced at lower ice nucleation temperatures, was observed. However, this trend was only significant ($p < 0.05$) for all three ice nucleation temperatures at sucrose/DNA ratios of 8000 and 10000. Again, at the lower DNA concentration no complete particle stabilization could be achieved.

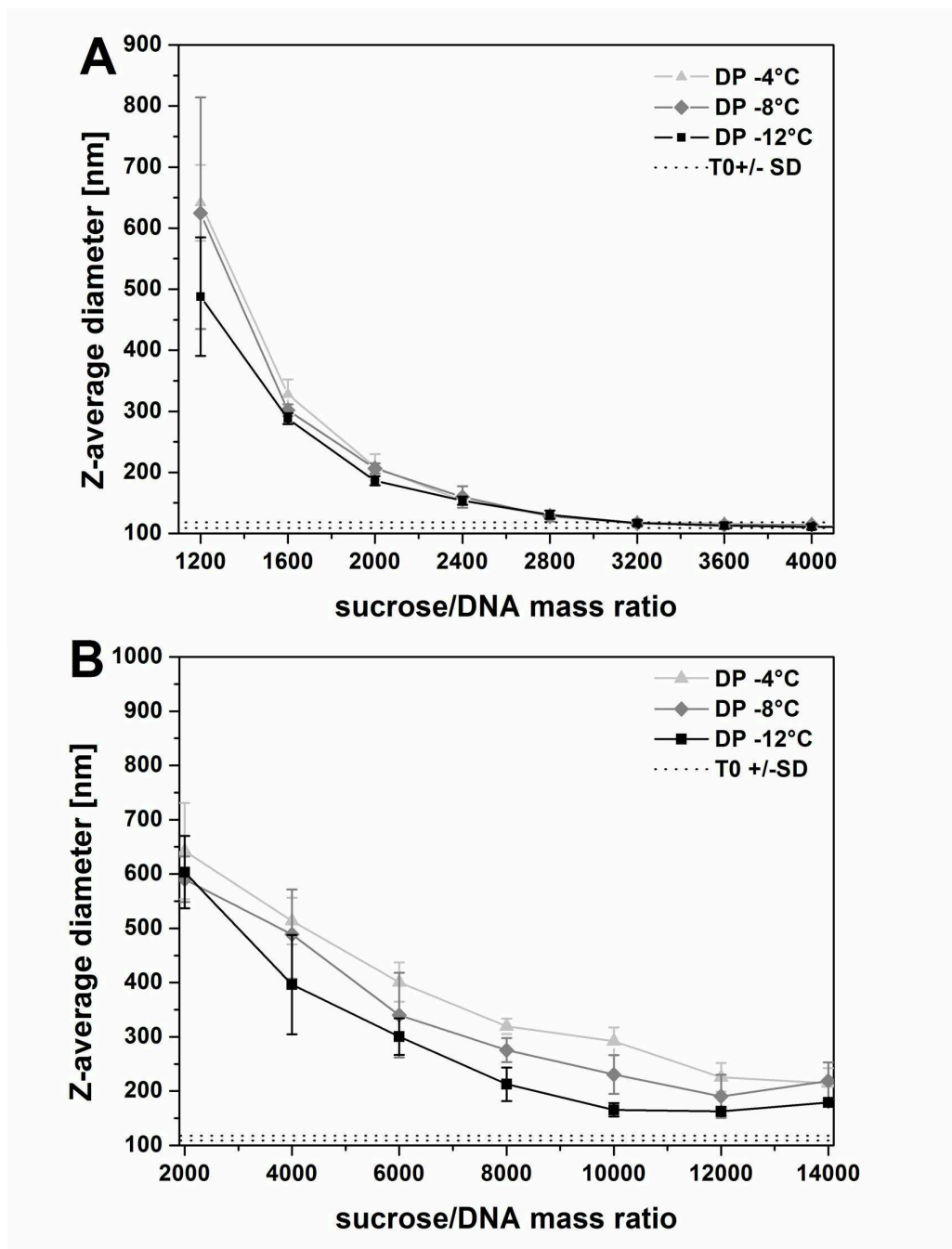


Figure 6-3: Z-average diameter of plasmid DNA/LPEI polyplexes after freeze-thawing when formulated at a DNA concentration of 50 µg/ml (A) or 10 µg/ml (B) and at increasing sucrose/DNA mass ratio. Samples were frozen at varying ice nucleation temperatures induced by depressurization (DP) at a shelf temperature of $-4\text{ }^{\circ}\text{C}$, $-8\text{ }^{\circ}\text{C}$ or $-12\text{ }^{\circ}\text{C}$ and a subsequent shelf ramp rate of $-5\text{ }^{\circ}\text{C}/\text{min}$. The dotted line represents the mean + SD and mean - SD of the Z-average diameter of freshly prepared (T0) polyplexes. Each value represents the mean \pm SD of three measurements on triplicate samples.

3.3 Influence of residence time on polyplex stability

In addition, the influence of residence time on polyplex stability was investigated. Therefore, ice nucleation of all polyplex samples was induced via depressurization after equilibration at a shelf temperature of $-12\text{ }^{\circ}\text{C}$. Subsequently, samples were frozen at varying shelf ramp rates of $-0.1\text{ }^{\circ}\text{C}/\text{min}$, $-0.5\text{ }^{\circ}\text{C}/\text{min}$, $-1.0\text{ }^{\circ}\text{C}/\text{min}$ or $-5.0\text{ }^{\circ}\text{C}/\text{min}$. The obtained temperature profiles are displayed in Figure 6-1C. The varying shelf ramp rates after controlled ice nucleation resulted in highly different residence times of $206.0 \pm 3.4\text{ min}$, $48.5 \pm 1.7\text{ min}$, $29.0 \pm 0.8\text{ min}$ or $12.8 \pm 0.5\text{ min}$, respectively.

At a DNA concentration of $50\text{ }\mu\text{g}/\text{mL}$ (Figure 6-4A) polyplex particle size did not significantly ($p > 0.05$) differ when frozen with shelf ramp rates of $-1\text{ }^{\circ}\text{C}/\text{min}$ or $-5\text{ }^{\circ}\text{C}/\text{min}$ after controlled ice nucleation. At fixed sucrose/DNA ratios, particle size increased with decreasing shelf ramp rate from $-1\text{ }^{\circ}\text{C}/\text{min}$ to $-0.5\text{ }^{\circ}\text{C}/\text{min}$ or $-0.1\text{ }^{\circ}\text{C}/\text{min}$. But the variations between all of these three different freezing rates were only significant ($p < 0.05$) for the samples formulated at sucrose/DNA ratios between 2000 and 3200. Significant preservation ($p > 0.05$) of particle size was achieved at a sucrose/DNA ratio of 3200, when frozen at $-1\text{ }^{\circ}\text{C}/\text{min}$ or $-5\text{ }^{\circ}\text{C}/\text{min}$. At the lower shelf ramp rate of $-0.5\text{ }^{\circ}\text{C}/\text{min}$ a sucrose/DNA ratio of 4000 was required for the significant ($p < 0.05$) stabilization of particle size. However, when samples were frozen at $-0.1\text{ }^{\circ}\text{C}/\text{min}$, particle size could not completely be maintained within the investigated range of sucrose/DNA ratios.

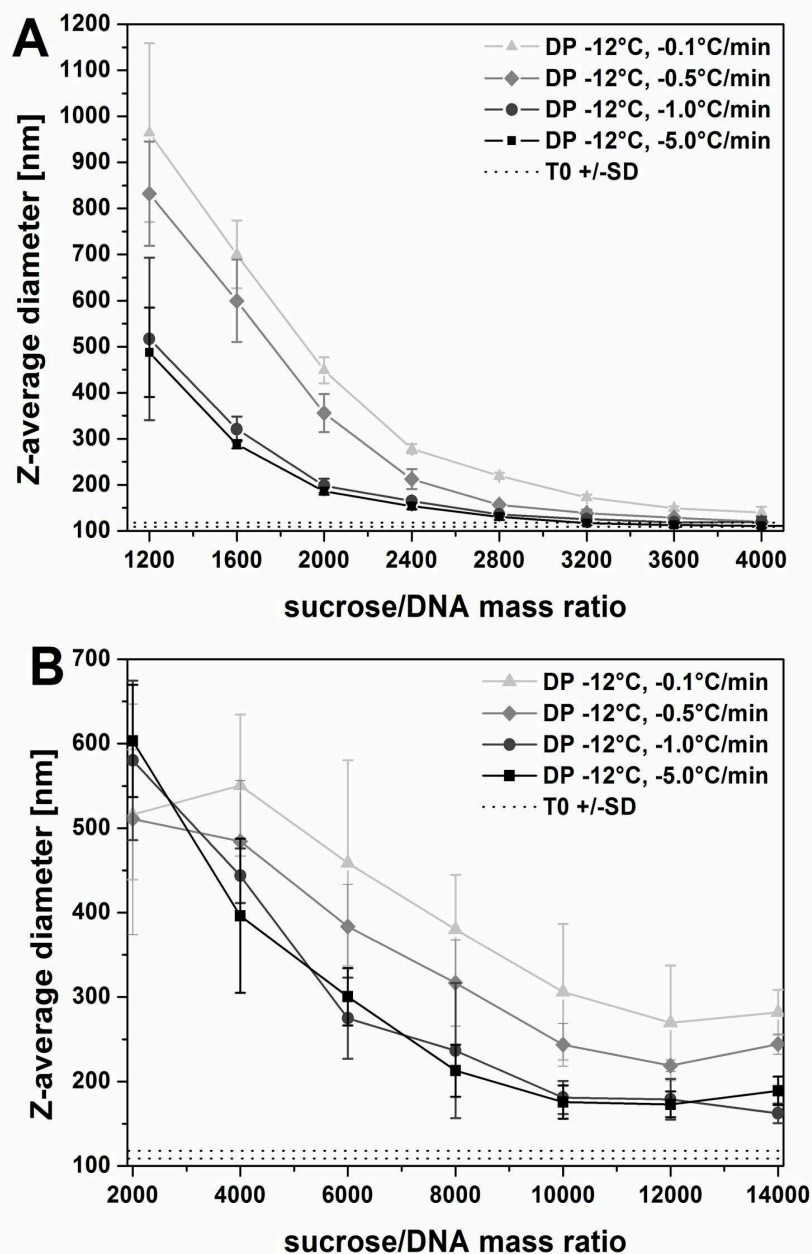


Figure 6-4: Z-average diameter of plasmid DNA/LPEI polyplexes after freeze-thawing when formulated at a DNA concentration of 50 µg/ml (A) or 10 µg/ml (B) and at increasing sucrose/DNA mass ratios. Samples were frozen with controlled ice nucleation via depressurization (DP) at -12°C and subsequent varying shelf ramp rates of $-0.1^{\circ}\text{C}/\text{min}$, $-0.5^{\circ}\text{C}/\text{min}$, $-1.0^{\circ}\text{C}/\text{min}$ or $-5.0^{\circ}\text{C}/\text{min}$. The dotted line represents the mean + SD and mean - SD of the Z-average diameter of freshly prepared (T0) polyplexes. Each value represents the mean \pm SD of three measurements on triplicate samples.

At a lower DNA concentration of 10 µg/mL particle size did also not significantly ($p > 0.05$) differ between samples prepared at shelf ramp rates of $-1^{\circ}\text{C}/\text{min}$ or

–5 °C/min (Figure 6-4B). Moreover, an analogous trend with an increase in particle size when shelf ramp rates are decreased was observed at the lower DNA concentration. This variation in particle size with differing shelf ramp rates was only significant between samples that were frozen at –1/–5 °C/min or –0.1 °C/min, when formulated at sucrose/DNA ratios ≥ 6000 . For instance, the decrease in the freezing rate from –1 °C/min to –0.1 °C/min resulted in an 120 nm increase in particle size after freeze-thawing from 162 ± 12 nm to 282 ± 27 nm, when formulated at a sucrose/DNA ratio of 14000. In general, for both DNA concentrations, the increase in polyplex particle size was comparable when samples were frozen with the depressurization technique in combination with a fast shelf ramp rate of –1 °C/min or –5 °C/min or by conventional shelf-ramp freezing at shelf ramp rates of –1 °C/min or –5 °C/min (see 3.1).

3.4 Influence of the proceeding of freezing on polyplex stability

In order to investigate the influence of the proceeding of freezing, samples were directly cooled at –0.1 °C/min after controlled ice nucleation at –12°C and the freezing process was stopped by subsequent thawing at shelf temperatures of –12.5 °C, –14.0 °C, –20.0 °C or –26.0 °C. This approach resulted in freezing of the samples down to a product temperature of –3.7 °C, –11.1 °C, –17.8 °C or –23.6 °C before thawing was started. The corresponding product temperature and shelf inlet temperature profiles are displayed in Figure 6-1D.

At a DNA concentration of 50 µg/mL, particle size did not significantly ($p > 0.05$) differ, except for a sucrose/DNA ratio of 2400, when samples were frozen at a shelf ramp rate of –0.1 °C/min to a product temperature of –3.7 °C or when samples were frozen at a shelf ramp rate of –5 °C/min to –45 °C (Figure 6-5A).

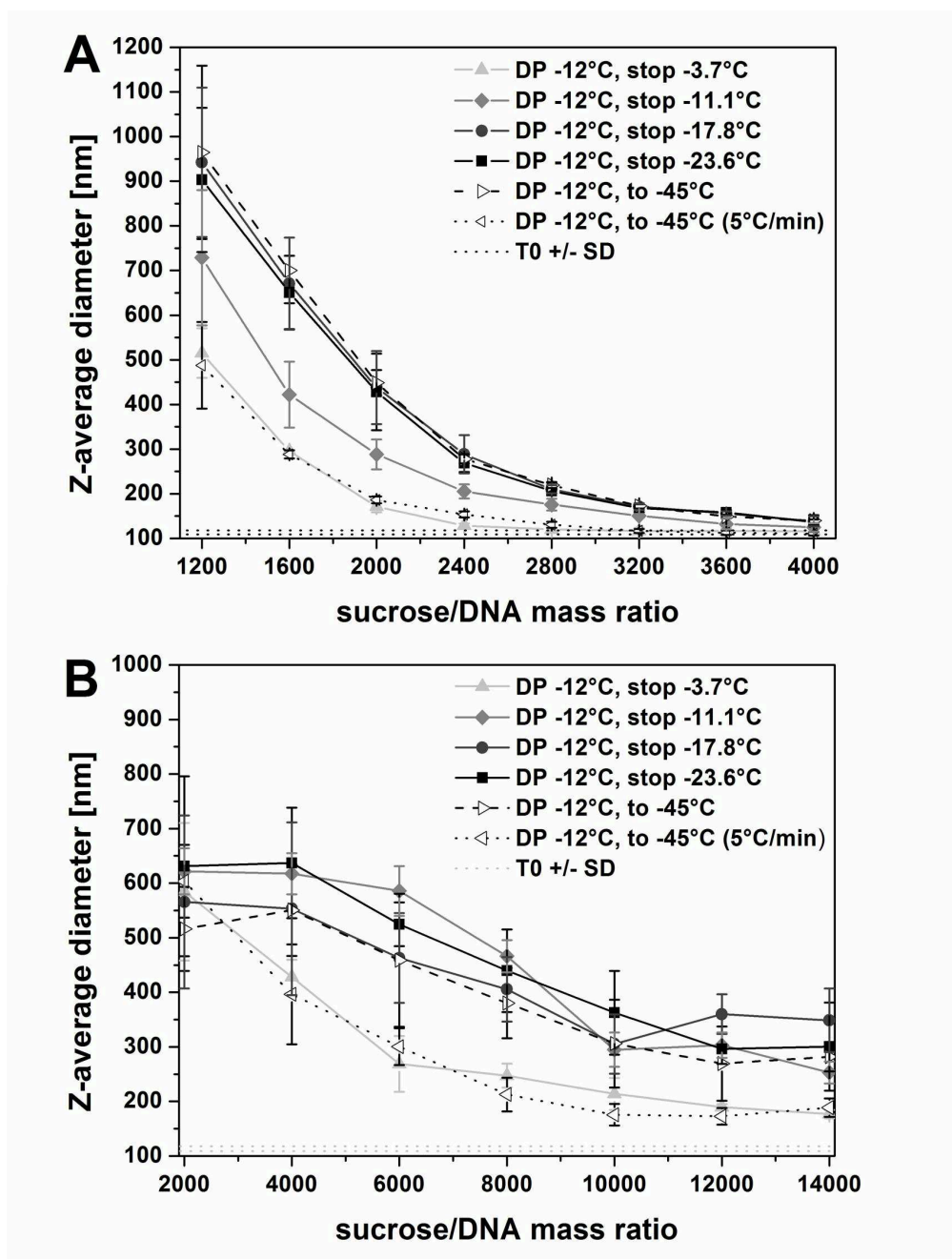


Figure 6-5: Z-average diameter of plasmid DNA/LPEI polyplexes after freeze-thawing when formulated at a DNA concentration of 50 $\mu\text{g/mL}$ (A) or 10 $\mu\text{g/mL}$ (B) and at increasing sucrose/DNA mass ratio. Samples were frozen with controlled ice nucleation via depressurization (DP) at -12°C and with a subsequent shelf ramp rate of -0.1°C/min . The freezing procedure was stopped at a product temperature of -3.7°C , -11.1°C , -17.8°C and -23.6°C . For comparison reasons, data obtained for samples frozen with controlled ice nucleation via depressurization (DP) at -12°C and subsequent shelf ramp rates of -0.1°C/min and -5.0°C/min are also displayed. The dotted line represents the mean + SD and mean - SD of the Z-average diameter of freshly prepared (T0) polyplexes. Each value represents the mean \pm SD of three measurements on triplicate samples.

In these two cases, complete preservation of particle size was achieved at a sucrose/DNA ratio of 3200. When the samples were further frozen at a shelf ramp rate of $-0.1\text{ }^{\circ}\text{C}/\text{min}$ to $-11.1\text{ }^{\circ}\text{C}$ particle size significantly further increased ($p < 0.05$) for all formulations at a sucrose/DNA ratios ≥ 1600 , and full recovery of particle size was observed at a sucrose/DNA ratio of 4000. The proceeding of freezing from $-11.1\text{ }^{\circ}\text{C}$ to a product temperature of $-17.8\text{ }^{\circ}\text{C}$ resulted in a further significant raise ($p < 0.05$) in particle size. However, when freezing further proceeded from $-17.8\text{ }^{\circ}\text{C}$ to product temperatures $\leq -23.6\text{ }^{\circ}\text{C}$ no significant ($p > 0.05$) further change in particle size was observed. For the latter two cases, no complete polyplex stabilization could be obtained within the investigated range of sucrose/DNA ratios. At the lower DNA concentration of $10\text{ }\mu\text{g}/\text{mL}$ this clear correlation could not be observed (Figure 6-5B). Again, freezing at a shelf ramp rate of $-0.1\text{ }^{\circ}\text{C}/\text{min}$ to a product temperature of $-3.7\text{ }^{\circ}\text{C}$ or freezing at a shelf ramp rate of $-5\text{ }^{\circ}\text{C}/\text{min}$ to $-45\text{ }^{\circ}\text{C}$ resulted in comparable particles sizes after freeze-thawing. For all other investigated freezing procedures an increase in particle sizes, but no significant correlation to the proceeding of freezing was found. But a clear trend to further destabilization with freezing was observed when comparing the particle size at a product temperature of $-3.7\text{ }^{\circ}\text{C}$ to all other lower product temperatures.

3.5 Surface area and residual moisture content of selected lyophilized samples

Moreover, selected samples (6%, 10%, 14% and 20% sucrose) were lyophilized using different freezing procedures, in order to establish a correlation between the freezing procedure and the resulting SSA or residual moisture content of the lyophilisates (Table 6-2).

Table 6-2: Specific surface area (SSA) [m²/g] or absolute SSA [m²/100 mL] and residual moisture contents (RM) [%w/w] of selected lyophilized formulations (6%, 10%, 14% and 20% sucrose). The samples were frozen via depressurization (DP) at –12 °C or –4 °C at a subsequent ramp rate of –5 °C/min or –0.1 °C/min or via depressurization at –4 °C with a 15 min equilibration step and a ramp rate of –1 °C/min.

		6% sucrose	10% sucrose	14% sucrose	20% sucrose
DP –12 °C, –5 °C/min	SSA [m ² /g]	0.82 ± 0.07	0.78 ± 0.04	0.58 ± 0.02	0.51 ± 0.03
	SSA [m ² /100ml]	4.92 ± 0.42	7.80 ± 0.40	8.12 ± 0.28	10.20 ± 0.60
	RM [%w/w]	0.19 ± 0.03	0.23 ± 0.04	0.35 ± 0.04	0.40 ± 0.04
DP –4 °C, –5 °C/min	SSA [m ² /g]	0.62 ± 0.03	0.44 ± 0.02	0.32 ± 0.01	0.30 ± 0.01
	SSA [m ² /100ml]	3.72 ± 0.18	4.40 ± 0.20	4.48 ± 0.28	6.00 ± 0.20
	RM [%w/w]	0.20 ± 0.04	0.28 ± 0.02	0.42 ± 0.05	0.55 ± 0.02
DP –12 °C, –0.1 °C/min	SSA [m ² /g]	0.73 ± 0.04	0.59 ± 0.04	0.43 ± 0.03	0.40 ± 0.02
	SSA [m ² /100ml]	4.38 ± 0.16	5.90 ± 0.40	6.02 ± 0.42	8.00 ± 0.40
	RM [%w/w]	0.38 ± 0.04	0.43 ± 0.09	0.44 ± 0.06	0.52 ± 0.05
DP –4 °C, 15 min, –1 °C/min	SSA [m ² /g]	0.51 ± 0.02	0.30 ± 0.01	0.23 ± 0.01	0.19 ± 0.01
	SSA [m ² /100ml]	3.06 ± 0.12	3.00 ± 0.10	3.22 ± 0.14	3.80 ± 0.20
	RM [%w/w]	0.46 ± 0.03	0.49 ± 0.06	0.75 ± 0.02	0.83 ± 0.10

For all formulations, the SSA [m²/g] decreased, the absolute SSA [m²/100 mL] increased and the residual moisture content increased with increasing sucrose concentration. In general, the freezing procedure highly influenced SSA and residual moisture. The increase in ice nucleation temperature by 8 °C (from –12 °C to –4 °C) at consistent subsequent shelf-ramp rates of –5 °C/min resulted in a significant ($p < 0.05$) decrease in both SSA [m²/g] and absolute SSA [m²/100 mL] and a slight, but not significant increase ($p > 0.05$, except for the 20% sucrose sample) in residual moisture for all formulations. The decrease in the shelf-ramp rate from –5 °C/min to –0.1 °C/min after controlled nucleation at –12 °C led to significantly ($p < 0.05$) lowered SSA [m²/g] and absolute SSA [m²/100 mL] as well as a significantly ($p < 0.05$) higher residual moisture content for all formulations. Freezing of the samples using the “standard” depressurization method rendered the lowest SSA [m²/g] and absolute SSA [m²/100 mL] and the highest residual moisture content for all formulations.

3.6 Theoretical modeling of the change in sucrose concentration or viscosity during freeze-concentration and correlation to reaction rates

In order to correlate the experimental observations with the increase in viscosity of the samples during freeze-concentration, theoretical product temperature profiles were modeled and used to calculate the change in sucrose concentration and sample viscosity over time. In addition relative reaction rates were estimated assuming a second-order reaction with an Arrhenius temperature dependence and relative reaction rates over time were estimated. The simulated temperature profiles and the calculated sucrose concentrations and viscosities of a 10% sucrose sample, that was nucleated at -12°C and subsequently frozen at a shelf ramp rate of $-5^{\circ}\text{C}/\text{min}$ or $-0.1^{\circ}\text{C}/\text{min}$, are displayed in Figure 6-6. In general, the theoretically modeled temperature profiles showed rather good agreement to real product temperature data. When the initial ice nucleation occurs product temperature rises rapidly to the equilibrium freezing point. Further ice crystal growth is then controlled by the latent heat release due to ice formation and the cooling rate of the shelf which the sample is exposed to. At first, heat release and cooling are at equilibrium, leading to a temperature plateau. Later, when cooling of the shelf dominates, product temperature drops and further decreases depending on the shelf ramp rate used. During the first part of the freezing step, when ice formation and heat release is still in equilibrium, most ice is formed. In this temperature region the sucrose concentration of the sample sharply increases followed by a further slower increase until the maximum freeze-concentration is reached at T_g . For instance, a more than 5 fold increase in the sucrose concentration from 10% to $\sim 55\%$ is already reached when the product temperature falls below -4°C after ice nucleation. When freezing proceeds to product temperatures of $\sim -12^{\circ}\text{C}$, sucrose concentration further increases to $\sim 72\%$. At the product temperature of

~ -18 °C, at which no further increase in particle size is observed during slow freezing, sucrose concentration accounted for $\sim 76\%$. Analogously, viscosity also tremendously increases during the first part of freezing. Due to the temperature dependence of the viscosity, a further pronounced increase is seen also at temperatures well below T_g . For instance, viscosity values increase to ~ 0.14 Pa*s, 20.2 Pa*s, 741.0 Pa*s, $53.3 \cdot 10^6$ Pa*s or $1.5 \cdot 10^{12}$ Pa*s when a product temperature of ~ -4 °C, -12 °C, -18 °C, -32 °C or -45 °C is reached, respectively. Obviously, a faster increase in sucrose concentration and samples viscosity is observed, when samples are frozen at a shelf ramp rate of -5 °C/min compared to freezing at a shelf ramp rate of -0.1 °C/min.

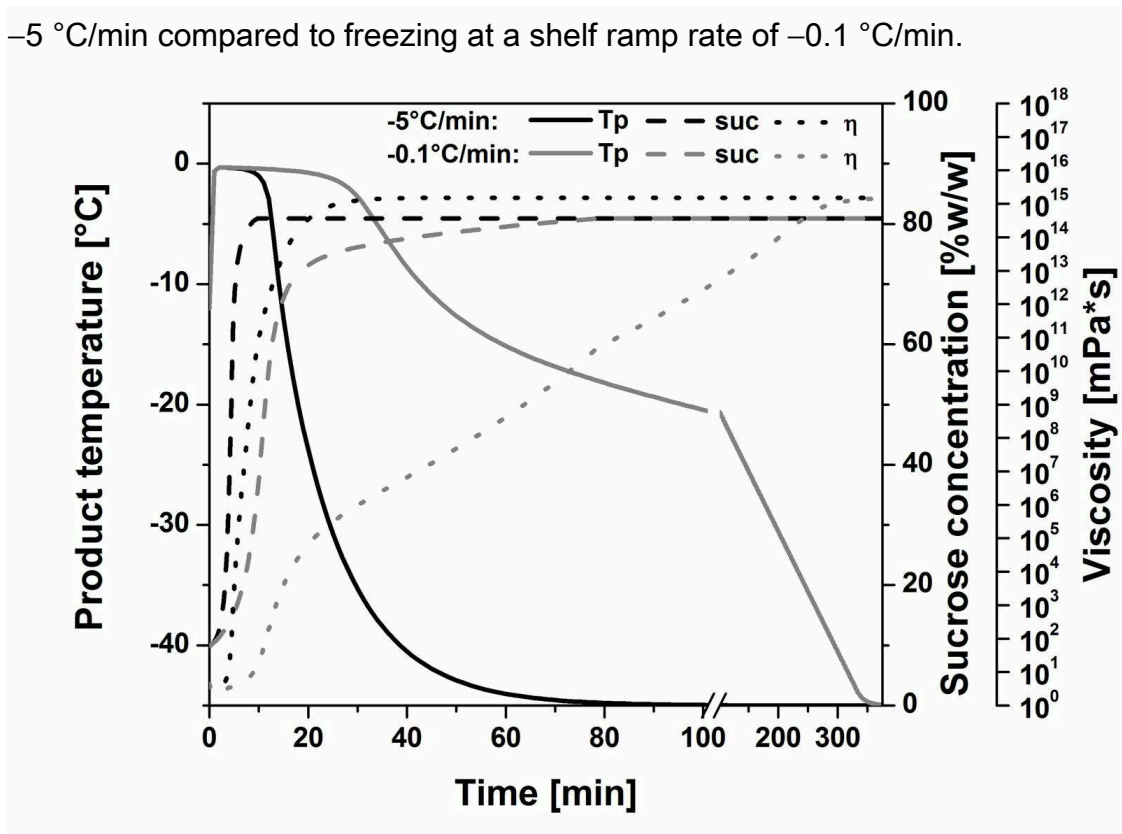


Figure 6-6: Theoretical simulation of product temperature (T_p), sucrose concentration (suc) and viscosity (η) of $500 \mu\text{L}$ 10% sucrose solution in a 3 mL vial during shelf-ramp freezing at a shelf ramp rate of $-5^\circ\text{C}/\text{min}$ or -0.1 °C/min.

Figure 7 displays the estimated relative reaction rate over time and the corresponding viscosity at different shelf ramp rates or different initial sucrose concentrations.

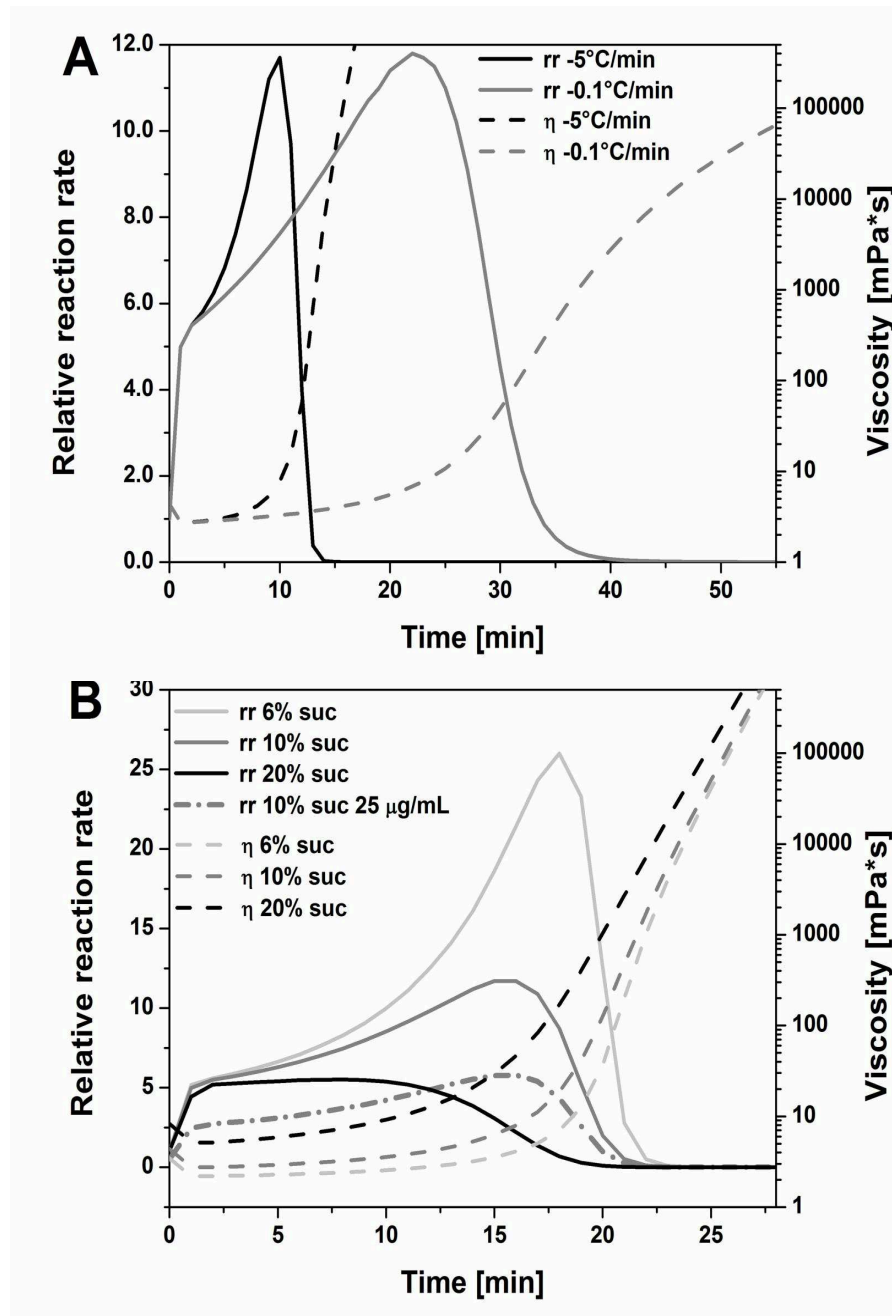


Figure 6-7: Theoretical relative bimolecular reaction rate (rr) of a second order reaction of polyplexes during shelf-ramp freezing at a sample volume of 500 μL in a 3 mL vial. Corresponding simulated viscosity values (η) are also displayed. Reaction rates were calculated with Arrhenius temperature dependence and inversely proportional correlated to modeled viscosity values. A) Freezing of a 10% sucrose formulation at a DNA concentration of 50 $\mu\text{g/mL}$ at a shelf ramp rate of $-5\text{ }^{\circ}\text{C/min}$ or $-0.1\text{ }^{\circ}\text{C/min}$. B) Freezing of a 6%, 10% or 20% sucrose formulation at a DNA concentration of 50 $\mu\text{g/mL}$ or of a “half concentrated” 10% sucrose formulation at a DNA concentration of 25 $\mu\text{g/mL}$ at a shelf ramp rate of $-1\text{ }^{\circ}\text{C/min}$.

During freezing of a 10% sucrose formulation (Figure 6-7A) the reaction rate already increases five fold at the point of ice nucleation and increases more

than ten fold during further freezing. The maximum relative reaction rate is reached when the sample viscosity is ~ 7 mPa*s at a product temperature of ~ -1 °C. When a sample viscosity of ~ 50 mPa*s is reached at a product temperature of ~ -3 °C the relative reaction rate falls below the initial reaction rate in the liquid formulation at the point of ice nucleation. Subsequently, the relative reactions rate converges against zero (< 0.01) at a viscosity of ~ 16500 mPa*s at a product temperature of ~ -12 °C. When samples are frozen at a shelf ramp rate of -5 °C/min, the initial reaction rate level is regained already after ~ 12 min, whereas it takes ~ 30 min to reach this point when samples are frozen at -0.1 °C/min.

When 50 $\mu\text{g/mL}$ DNA samples with different initial sucrose concentration are frozen at -1 °C/min (Figure 6-7B), the reaction rate also increases ~ 5 fold during initial ice nucleation for all formulations. During further freezing the reaction rate increased drastically in presence of 6% and 10% to a maximum of relative reaction rate of 26.0 and 11.7 respectively. In contrast, the reaction rate did not further increase when samples contained 20% sucrose. This might be related to the already ~ 2.4 fold higher viscosity of 20% sucrose formulations compared to the 6% samples at the point of ice nucleation. When polyplexes were formulated at higher sucrose concentrations relative reaction rates returned to 1 much earlier during freezing. But for all formulations reaction rates close to zero (< 0.01) were found at almost the same time point ~ 24 min after ice nucleation. Additionally, the reaction rate for a polyplex formulation at half of the original DNA concentration containing 10% sucrose was modeled. In this case, the initial reaction rate was lower due to the reduced polyplex concentration. The maximum in reaction rate was reached at the same point in time, as observed for the original 10% sucrose formulation. But the level of the maximum reaction rate was comparable to the 20% sucrose formulation which has the same initial sucrose/DNA ratio.

4 Discussion

Several studies have demonstrated that stable transfection rates of non-viral gene delivery particles are closely correlated with the maintenance of particle size [6, 29]. Even in the absence of reduced *in-vitro* transfection rates with a change in particle size, the parameter particle size is a critical quality attribute for *in-vivo* application and overall for a pharmaceutical product [30]. Therefore, this study focused solely on particle size as an indicator of aggregation reflecting physicochemical instability which can be affected by freeze-thawing and lyophilization. In general, aggregation of gene delivery particles originates from colloidal mechanisms, involving electrostatic and/or van-der-Waals interactions [2, 31].

In accordance with previous studies [5-7, 10], it was observed that the particle size of plasmid/LPEI polyplexes is drastically affected by freeze-thawing and that, particle size became better preserved as the ratio of sucrose to plasmid DNA was increased. It is well known from literature, that maintenance of particle size requires a critical stabilizer/DNA ratio, which is highly dependent on the type of non-viral gene delivery particle. For instance, the maintenance of particle size of LPEI [5], PEI [8], transferrin-PEI [9], or DMAEMA [29] polyplexes could be achieved at sucrose/DNA ratios of 4000, 7500, 10000, or 1250, respectively. In contrast, it is well known, that lipid-based complexes require much lower excipient/DNA ratios for size protection compared to polymer-based complexes [8]. For example, DOTAP-DOPE [8], DOTAP-Chol [8], or DMRIE-C [7] lipoplexes could be stabilized at sucrose/DNA ratios of 1250, 900, or 500, respectively. This existence of a critical stabilizer/DNA ratio led to the development of the “particle isolation hypothesis” by Allison et al. [7]. These authors concluded that the volume of the unfrozen fraction, in which particles are suspended during freezing, must be only high enough to isolate the

complexes in order to prevent particle collision. There is no doubt that particle crowding promotes aggregation during freezing, and that particles have to be separated in order to inhibit particle aggregation. However, there are two observations in our study that indicate that the “particle isolation hypothesis”, based on the availability of a large enough volume of the unfrozen fraction, is not suitable to solely explain the stabilization of non-viral gene delivery particles during freezing.

At first, it was observed that the stability of non-viral vectors upon freeze-thawing is not only dependent on the type of vector, but also on the initial DNA or particle concentration of the sample. Moreover, it was found that the increase in particle size of plasmid/LPEI polyplexes was more pronounced in more dilute samples (10 µg DNA/ mL) compared to more concentrated samples (50 µg DNA/ mL) at the same sucrose/DNA ratio. In contrast to the more concentrated samples, for which complete particle stabilization could be achieved at a sucrose/DNA ratio of more than 2800, the complete preservation of particle size of more diluted plasmid/LPEI polyplexes was even not possible at very high sucrose/DNA ratios of 14000. Similarly, Allison et al. [7] reported that the freezing of more dilute samples of lipoplexes (8 µg DNA/mL) resulted in significantly larger particle sizes than freezing of more concentrated samples (160 µg DNA/mL), when formulated at the same sucrose/DNA ratio [7]. However, in this case, the doubling of the sucrose/DNA ratio to 1000 was sufficient to stabilize the more diluted lipoplex samples [7].

As in our study the size of an individual gene delivery particle was always consistent in the initial solution, independent of the DNA concentration, a lower DNA concentration can be equated with a lower particle concentration. As an estimate one would assume that a five fold decrease in the number of gene delivery particles per sample volume would result in a five fold lower absolute

amount of stabilizer necessary to achieve an identical volume per particle in the freeze-concentrate. Thus, the stabilizer/DNA ratio required for particle stabilization is expected to stay constant in accordance to the “particle isolation hypothesis”, independently of the initial particle concentration. However, this was not the case for plasmid/LPEI polyplexes, in our study, nor for plasmid/DMRIE-C lipoplexes, as reported by Allison et al. [7]. Other hypotheses, that might explain the observed lowered particle stability in more diluted samples and the inability to completely stabilize low-concentrated plasmid/LPEI polyplexes, will be discussed below.

Secondly, besides the dependence of particle stability on the type of gene delivery particle or on the initial DNA concentration, it was observed that the freezing procedure highly influences the freeze-thaw stability of plasmid/LPEI polyplexes. For instance, we found that freezing of plasmid/LPEI polyplexes by conventional shelf-ramp freezing resulted in a less pronounced increase in particle size compared to freezing by the “standard” depressurization method. Moreover, the critical sucrose/DNA ratio, at which complete preservation of particle size can be achieved, was significantly lower when high-concentrated samples were frozen by conventional shelf-ramp freezing in comparison to the “standard” depressurization method. However, the volume of the unfrozen fraction is independent of the freezing procedure and only controlled by the initial excipient concentration prior to freezing and the concentration of the maximum freeze-concentrate, which is reported to be ~81% for sucrose [27]. Thus, particle stabilization during freezing cannot only be explained by the available volume of the unfrozen fraction, but other parameters during freezing might be involved in the stabilization mechanism.

When comparing the conventional shelf-ramp freezing with the “standard” depressurization method, two freezing parameters were identified, that could

explain the observed differences in particle stability: ice nucleation temperature and residence time of the particles in the freeze-concentrate until glass formation occurs. These two parameters were investigated separately by the aid of the “depressurization method” which enables to dictate ice nucleation temperature. Moreover, various shelf-ramp rates after controlled ice nucleation were used in order to achieve different residence times. In general, the depressurization method is a very elegant, easy to apply method that can be used to guarantee homogeneous ice formation at a defined ice nucleation temperature, in comparison to conventional shelf-ramp freezing, during which ice nucleation occurs stochastically. This was also approved by the temperature profiles that were collected during the different freezing procedures. In addition, in this study, the depressurization method was highly useful in order to discriminate between the effect of ice nucleation temperature and subsequent freezing rates on the stability of an active pharmaceutical ingredient. Previously, only a few, but more intricate and unhandy methods were available to study the effect of ice nucleation temperature on protein activity, such as seeding with ice crystals [23], ultrasound-controlled ice nucleation [32], or the ice fog technique [33].

When different ice nucleation temperatures at constant residence times were applied during freezing, no effect on particle stability in high-concentrated plasmid/LPEI polyplex formulations was observed. In contrast, for the low-concentrated plasmid/LPEI polyplex formulations the trend that particle size was slightly better maintained, when freezing was induced at lower ice nucleation temperatures, was noticed. In general, as the ice nucleation temperature decreases, the number of formed ice crystals increases, thereby resulting in the formation of an increased ice-water interfacial area [13]. For example, in our study, SSA measurements showed that the decrease of ice nucleation

temperature from $-4\text{ }^{\circ}\text{C}$ to $-12\text{ }^{\circ}\text{C}$ results in an increase of the absolute ice surface per vial between 32% and 81%, depending on the initial sucrose concentration. This is in accordance with literature, in which an increase in the ice surface area by nearly 50% is reported, when the ice nucleation temperature was decreased from $-1\text{ }^{\circ}\text{C}$ to $-11\text{ }^{\circ}\text{C}$ [34]. Moreover, the observed increase of the SSA per sample vial with increasing solid content, agrees also well with literature [23]. For proteins, it is well known, that surface-induced denaturation can be damaging [35] and that the difference in ice nucleation temperature can highly influence protein stability [23, 36]. Here, it is assumed that proteins adsorb on the ice crystals and thus, suffer a loss of conformational stability [24]. But still, there is a lack of understanding of the source of surface-induced denaturation. It is speculated that the mechanism involves very strong electric fields [24]. These electric fields might be generated during ice crystallization in dilute electrolyte solutions due to preferential incorporation of one ionic species into the ice, while the other ionic species remain in the freeze-concentrate [24, 37]. The strength of the electric field depends on the freezing rate, the type of solvent, and the type and concentration of ionic species present in solution [24, 38-39]. As in our study an improved particle preservation was observed at lower ice nucleation temperatures, which induces the formation of large ice-water interfaces, the sole presence of a certain amount of additional interfaces can not explain the observed trend in particle destabilization. Rather, it is assumed that the aforementioned process dependent generation of electric fields on the ice surface might contribute to the destabilization of the plasmid/LPEI particles, as these particles are only based on electrostatic interactions of the negatively charged nucleic acid and the positively charged polymer. However, it is arguable why the generation of electrically charged ice surfaces should only predominantly influence non-viral gene delivery particles in diluted formulations when formulated at the same absolute amount of stabilizer

(e.g. 14% sucrose). Speculatively, it might be assumed that only a certain amount of gene delivery particles interacts with the ice-water surface during freezing, and that thus, this interaction plays a relatively larger role in more dilute samples in comparison to more concentrated samples.

Consequently, one can conclude that for dilute samples ice formation is one destabilizing factor for gene delivery particles during freezing. In this case, it is not unexpected, that non-surface active excipients, like sucrose, are not capable to fully stabilize against this surface-induced stress, even at very high sucrose/DNA ratios. Analogously, Allison et al. [7] stated that the reduced stability of lipoplexes in more dilute samples could be explained in general by an increased interaction with the ice crystal surface area. In contrast to our study, Allison et al. [7] could achieve a complete preservation of particle size for more dilute lipoplex samples. Presumably, as polyplexes are only based on electrostatic interactions, whereas lipoplexes are additionally stabilized by hydrophobic interactions, polyplex stability might be more disturbed during the formation of charged ice interfaces as compared to the integrity of lipoplexes. Furthermore, our results give experimental evidence, that, in the case of more concentrated formulations, other factors than ice formation are responsible for the destabilization of gene delivery particles during freezing.

In order to investigate the time-dependence of particle stability during freezing, plasmid/LPEI polyplexes were frozen at different shelf ramp rates after ice nucleation at a constant temperature. In general, particle size of the polyplexes strongly increased with increasing residence times. Moreover, the critical sugar/DNA ratio, that is required for full particle size protection, is highly elevated for prolonged residence times. Both observations hold true for high- and low-concentrated polyplex formulations. Thus, not only the volume of the unfrozen fraction but also the time span during which a particle is exposed to

freezing induced stresses is of high importance for particle stability during freezing. Moreover, these results give experimental evidence that particle stability is not only time-dependent during incubation in the frozen state as reported by Armstrong et al. [17], but is highly time-dependent already during the freezing process, as well. This negative effect of prolonged residence times in the critical temperature region during freezing also explains why the “standard depressurization technique”, which involves a temperature equilibration step after ice nucleation as described in [20], led to a more pronounced increase in particle size compared to conventional shelf-ramp freezing at fast freezing rates. However, the combination of the depressurization technique with subsequent fast freezing rates resulted in comparable particles size after freezing as shelf-ramp freezing.

It was found that the decrease in the shelf ramp rate after controlled nucleation resulted in a decrease in the SSA, although ice nucleation temperature was kept constantly. Theoretically, the number of ice crystals that is initially formed during nucleation is defined by the ice nucleation temperature and thus, determines the resulting ice surface area. But our results show that, besides ice nucleation temperature, also the freezing rate influences the dimension of the resulting surface area. It can be speculated that the slow freezing rate leads to a situation that is comparable to a short annealing phase, during which larger crystals grow at the expense of smaller ones [40], leading to a reduced specific surface area of the product [41].

At first, we defined the residence time as the period of time between ice nucleation and the point at which a product temperature of $-30\text{ }^{\circ}\text{C}$ is reached. The latter temperature is around the T_g of the glassy sucrose matrix [42], below which particle mobility should be highly limited. However, further experiments showed that freezing at very slow shelf ramp rates is only critical with regard to particle stability until a product temperature of $\sim -18\text{ }^{\circ}\text{C}$ is

reached. Thus, besides the aforementioned time-dependence, stabilization of non-viral gene delivery particles during freezing seems also to be highly temperature dependent. Similarly, Armstrong et al. [17] showed that particle aggregation does not occur during prolonged incubation in the frozen state at temperatures ≤ -22 °C. Moreover, these results suggest that glass formation or vitrification of the sample is not required for gene delivery particle stabilization during freezing, which is in accordance with literature [7]. However, although vitrification is not necessary for particle stabilization in the frozen state, the maintenance of the glassy state might be essential for the long-term storage stability of lyophilized formulations [2, 43].

Furthermore, it was, interestingly, observed that the initial proceeding of slow freezing to a product temperature of ~ -3 °C was as stressful as fast freezing to -45 °C. This indicates that particle aggregation essentially occurs during initial ice formation and that the further proceeding of freezing is negligible as long as a fast enough freezing rate is used.

This observed time-dependence of particle destabilization during freezing indicates that destabilization of non-viral particles during freezing is to a marked degree kinetically controlled. As particle aggregation originates from colloidal interaction, particle mobility is a prerequisite for this bimolecular reaction. Particle mobility during freezing is strongly coupled with system viscosity and thus, particle stabilization can be achieved by a viscosity-driven decrease in the reaction rate constants [14]. In general, according to Arrhenius kinetics, a decrease in temperature would decrease the bimolecular reaction rates [14]. However, when ice formation occurs during freezing, solutes and particles present in the starting solution will experience a high increase in concentration. By the aid of our theoretical modeling, it could be illustrated that sucrose concentration and consequently viscosity strongly increases especially in the

initial part of freezing during which the product temperature almost remains constant. This increase in the concentration of the solutes and particles in the freeze-concentrate causes an increase in the rate of bimolecular reactions [14] and, thus, competes with the Arrhenius dependent decrease in reaction rate. In order to estimate the course of the bimolecular reaction rate of gene delivery particles during freezing, a second order reaction with Arrhenius temperature dependence was assumed. Moreover, the reaction rate was coupled to viscosity assuming a diffusion-controlled reaction with the diffusion constant being inversely proportional, as in the Stokes-Einstein equation [24]. It is undisputable that hereby calculated reaction rates are only rough estimations. But nevertheless this model might help to illustrate the interrelation between bimolecular reaction rate and system viscosity, which is dependent on the freezing protocol and on initial solute concentration. During ice nucleation a ~5 fold increase in the relative reaction rate was observed for all samples. However, here, one has to keep in mind that all reaction rates are presented as relative reaction rates, which are related to the reaction rate at the point of ice nucleation at a DNA concentration of 50 µg/mL. At this point, the liquid, ice-free sample has reached the lowest temperature during cooling before ice formation starts. Thus, the reaction rate that was used as reference is low compared for example to the reaction rate in the liquid state at room temperature. The reaction rate in a liquid sample at 20 °C was determined to be ~5 fold higher compared to the reaction rate at -12 °C.

When 50 µg/mL polyplexes were formulated at 10% sucrose, which is below the critical sucrose/DNA ratio, reaction rates increased during proceeding of freezing. However, in all cases, the maximum rate was reached already at a rather high product temperature of ~ -1 °C and a very low system viscosity of ~7 mPa*s. Thus, when polyplexes are formulated at a too low initial sucrose concentration, bimolecular reactions will be accelerated during the very early

part of freezing as the particle concentration increases and the viscosity increase cannot compensate for this. However, as the product temperature further decreases viscosity increases substantially limiting particle diffusion and collision. At a certain point during freezing this latter effect becomes dominant resulting in decreased bimolecular reaction rates. In our model, the initial reaction rate was reached at a product temperature of $\sim -3^\circ\text{C}$ and viscosity of $\sim 50\text{ mPa}\cdot\text{s}$, indicating that the period before is the most critical temperature region during freezing. This is in very good agreement with our experimental observations. Moreover, our model indicates that the bimolecular reaction rates converge against zero at a temperature of -12°C and a viscosity of $\sim 16500\text{ mPa}\cdot\text{s}$. This is also in good accordance to our experimental results as no further particle aggregation, even at very slow shelf ramp rates, was found when the product temperature fell below a critical temperature between -11°C and -18°C . This highlights, that in this temperature region the system viscosity is already high enough in order to almost completely inhibit particle mobility and that glass formation is not required. Armstrong et al. [17] reported that a viscosity of the freeze-concentrate of $2.10 \cdot 10^4\text{ Pa}\cdot\text{s}$ was required to prevent particle interaction when samples were incubated at -22°C for 24h. But this study was performed at a quite low sucrose/DNA ratio of 200 that was not capable to completely inhibit particle aggregation during initial freezing. By the aid of our model, we could show that the point, beyond which no further aggregation occurs, is reached much earlier when freezing is performed at accelerated shelf ramp rates, as was expected. Furthermore, we could show that the initial stabilizer concentration strongly impacts the maximum reaction rates during freezing. When a sufficiently high initial excipient concentration is chosen, the increase in the bimolecular reaction rate during freezing after initial ice formation may be suppressed completely. This indicates that the initial

system viscosity, which is directly related to the initial excipient concentration, is decisive for the course of the reaction rate during freezing.

Allison et al. [7] also mentioned that the high viscosity of the unfrozen fraction may serve to immobilize complexes and prevent aggregation. However, they reported that viscosity is not capable to explain the observed critical sugar/DNA ratio, as the solute concentration in the freeze-concentrate is only dependent on the sample temperature but not on the initial solute concentration. Thus, finally, they concluded that the distance between complexes in the unfrozen fraction, which is defined by the initial solute concentration, determines whether particles can physically interact or not [7]. Besides the aforementioned results that do not fit to this theory, this hypothesis can be reinvestigated by the aid of our modeled data. For instance, the sucrose concentration in the unfrozen fraction of a 6% and a 20% sucrose formulation is doubled to 12% and 40% at product temperatures of $-0.4\text{ }^{\circ}\text{C}$ and $-2.2\text{ }^{\circ}\text{C}$, respectively. This small difference in product temperature leads to a substantial difference in the viscosity of this unfrozen fraction (3.2 mPa*s versus 29.4 mPa*s) and in the reaction rate (~ 16 versus ~ 3). Thus, although the same volume of the unfrozen fraction is given, particle stability considerably differs mainly due to the clear difference in sample viscosity at a minute difference in product temperature.

In conclusion, these results confirm, that the initial excipient concentration and, accordingly, the excipient/DNA ratio are of high importance for particle stability. To some degree this is due to the volume of the unfrozen fraction provided by the stabilizer. But the positive effect of higher stabilizer concentrations is to a great extent related to the fact that a high initial stabilizer concentration provides a higher viscosity in the initial phase of freezing. This increase in viscosity compensates the increase in particle concentration which drives the reaction rate up. Thus, the choice of the excipient is of minor importance as long as comparable viscosity is achieved and no phase separation or crystallization

occurs, which is the case for sucrose or glucose, but not for mannitol or hydroxyethyl starch [2, 7, 44].

In contrast to our observations on the stability of polyplexes, a better stability of lactate dehydrogenase was reported when samples were frozen with the “standard” depressurization method in comparison to shelf-ramp freezing [19]. However, Bhatnagar et al. [23] could show that ice formation and not freeze-concentration is the critical destabilizing factor during freezing of lactate dehydrogenase. Thus, this comparison shows that an optimized freezing procedure cannot just simply be transferred to another pharmaceutical active ingredient. Rather, an extended understanding of the involved destabilization mechanism has to be accomplished in order to design an optimal freezing process during lyophilization, varying from case to case.

5 Summary and conclusion

The aim of the study was to provide an extended understanding of the critical freezing parameters and the mechanisms by which non-viral gene delivery particles are stabilized during the freezing step of lyophilization. In general, it was observed that the particle size of plasmid/LPEI polyplexes is better preserved with an increase in sucrose/DNA ratio, but that the critical ratio above which particle aggregation is completely suppressed is highly dependent on the freezing process used, e.g. the “standard” depressurization method was more stressful to plasmid/LPEI polyplexes in comparison to conventional shelf-ramp freezing. In order to explain this discrepancy, the influence of ice nucleation temperature and residence time was investigated separately by the aid of the depressurization method. Only the stability of particles at low concentration correlated negatively with an increase in ice nucleation temperature corresponding to a decrease in SSA. This observation can potentially be related to the generation of electric fields at the ice interface. For both DNA concentrations, a more distinct increase in particle size was detected when samples were frozen at decreased shelf-ramp rates after controlled ice nucleation. Depressurization in combination with fast subsequent ramp-rates resulted in comparable particle sizes as conventional shelf-ramp freezing, indicating that an equilibration step after ice nucleation is critical with regard to particle stability. Destabilization of particles during freezing occurs predominantly during the initial temperature decrease down to ~ -3 °C after ice nucleation. In this phase, cryoconcentration has already advanced but sample viscosity is still too low in order to fully inhibit particle mobility. This experimental observation matched well with our theoretical model. Here, a maximum of the reaction rates was found at a product temperature of ~ -1 °C and reaction rates reached their initial levels at product temperatures of ~ -3 °C. No further particle aggregation was observed at temperatures below $\sim \leq -18$ °C indicating that,

despite of the absence of glassy state, particle mobility is sufficiently inhibited with reaction rates close to zero due to the high sample viscosity. Furthermore, our modeled data showed that the level of the maximum reaction rate is determined by the initial sucrose/DNA ratio. This fully explains the need of a critical sucrose/DNA for complete particle stabilization.

In conclusion our results show that the time span that a particle spends in the low viscous state after ice nucleation is decisive for the stability of non-viral gene delivery particles during freezing. This phase of low viscosity but increased particle concentration is strongly affected by the initial sample viscosity, which is directly related to the initial excipient concentration, but also by the applied freezing rate. This extended understanding of the involved stabilization mechanisms during freezing will facilitate the development of optimized formulations and less stressful lyophilization processes, always to be performed hand in hand.

6 References

- [1] A. Pathak, S. Patnaik, K.C. Gupta, Recent trends in non-viral vector-mediated gene delivery, *Biotechnol. J.*, 4 (2009) 1559-1572.
- [2] S.D. Allison, T.J. Anchordoquy, Lyophilization of Nonviral Gene Delivery Systems, in: M.A. Findeis (Ed.) *Nonviral Vectors for Gene Therapy: Methods and Protocols*, Humana Press Inc., New York, 2001, pp. 225-252.
- [3] T.J. Anchordoquy, G.S. Koe, Physical stability of nonviral plasmid-based therapeutics, *J. Pharm. Sci.*, 89 (2000) 289-296.
- [4] W. Abdelwahed, G. Degobert, S. Stainmesse, H. Fessi, Freeze-drying of nanoparticles: Formulation, process and storage considerations, *Adv. Drug Deliv. Rev.*, 58 (2006) 1688-1713.
- [5] J.C. Kasper, D. Schaffert, M. Ogris, E. Wagner, W. Friess, Development of a lyophilized plasmid/LPEI polyplex formulation with long-term stability--A step closer from promising technology to application, *J. Controlled Release*, 151 (2011) 246-255.
- [6] T.J. Anchordoquy, L.G. Girouard, J.F. Carpenter, D.J. Kroll, Stability of lipid/DNA complexes during agitation and freeze-thawing, *J. Pharm. Sci.*, 87 (1998) 1046-1051.
- [7] S.D. Allison, M.d.C. Molina, T.J. Anchordoquy, Stabilization of lipid/DNA complexes during the freezing step of the lyophilization process: the particle isolation hypothesis, *Biochim. Biophys. Acta (BBA) - Biomembranes*, 1468 (2000) 127-138.
- [8] M.d.C. Molina, S.D. Allison, T.J. Anchordoquy, Maintenance of nonviral vector particle size during the freezing step of the lyophilization process is insufficient for preservation of activity: Insight from other structural indicators, *J. Pharm. Sci.*, 90 (2001) 1445-1455.
- [9] H. Talsma, J.-Y. Cherng, H. Lehrmann, M. Kursa, M. Ogris, W.E. Hennink, M. Cotten, E. Wagner, Stabilization of gene delivery systems by freeze-drying, *Int. J. Pharm.*, 157 (1997) 233-238.
- [10] J.Y. Cherng, P.v.d. Wetering, H. Talsma, D.J.A. Crommelin, W.E. Hennink, Stabilization of polymer-based gene delivery systems, *Int. J. Pharm.*, 183 (1999) 25-28.
- [11] T.J. Anchordoquy, J.F. Carpenter, D.J. Kroll, Maintenance of Transfection Rates and Physical Characterization of Lipid/DNA Complexes after Freeze-Drying and Rehydration, *Arch. Biochem. Biophys.*, 348 (1997) 199-206.
- [12] J. Liu, Physical Characterization of Pharmaceutical Formulations in Frozen and Freeze-Dried Solid States: Techniques and Applications in Freeze-Drying Development, *Pharm. Dev. Technol.*, 11 (2006) 3-28.
- [13] J.C. Kasper, W. Friess, The freezing step in lyophilization: Physico-chemical fundamentals, freezing methods and consequences on process performance and quality attributes of biopharmaceuticals, *Eur. J Pharm. Biopharm.*, 78 (2011) 248-263.

- [14] B.S. Bhatnagar, R.H. Bogner, M.J. Pikal, Protein Stability During Freezing: Separation of Stresses and Mechanisms of Protein Stabilization, *Pharm. Dev. Technol.*, 12 (2007) 505-523.
- [15] T.J. Anchordoquy, T.K. Armstrong, M.d.C. Molina, S.D. Allison, Y. Zhang, M.M. Patel, Y.K. Lentz, G.S. Koe, Physical Stabilization of Plasmid DNA-based Therapeutics During Freezing and Drying, in: H.R. Costantino, P. M.J. (Eds.) *Lyophilization of Biopharmaceuticals*, AAPS Press, Arlington, VA, 2004, pp. 605-641.
- [16] J.F. Carpenter, J.H. Crowe, The mechanism of cryoprotection of proteins by solutes, *Cryobiology*, 25 (1988) 244-255.
- [17] T.K. Armstrong, T.J. Anchordoquy, Immobilization of nonviral vectors during the freezing step of lyophilization, *J. Pharm. Sci.*, 93 (2004) 2698-2709.
- [18] O. Zelphati, C. Nguyen, M. Ferrari, J. Felgner, Y. Tsai, P.L. Felgner, Stable and monodisperse lipoplex formulations for gene delivery, *Gene Ther.*, 5 (1998) 1272-1282.
- [19] R. Bursac, R. Sever, B. Hunek, A Practical Method for Resolving the Nucleation Problem in Lyophilization, *BioProcessInternational*, (2009) 66-72.
- [20] A.K. Konstantinidis, W. Kuu, L. Otten, S.L. Nail, R.R. Sever, Controlled nucleation in freeze-drying: Effects on pore size in the dried product layer, mass transfer resistance, and primary drying rate, *J. Pharm. Sci.*, 100 (2011) 3453-3470.
- [21] D. Schaffert, M. Kiss, W. Rödl, A. Shir, A. Levitzki, M. Ogris, E. Wagner, Poly(I:C)-Mediated Tumor Growth Suppression in EGF-Receptor Overexpressing Tumors Using EGF-Polyethylene Glycol-Linear Polyethylenimine as Carrier, *Pharm. Res.*, 28 (2011) 731-741.
- [22] J.C. Kasper, D. Schaffert, M. Ogris, E. Wagner, W. Friess, The establishment of an up-scaled micro-mixer method allows the standardized and reproducible preparation of well-defined plasmid/LPEI polyplexes, *Eur. J. Pharm. Biopharm.*, 77 (2011) 182-185.
- [23] B.S. Bhatnagar, M.J. Pikal, R.H. Bogner, Study of the individual contributions of ice formation and freeze-concentration on isothermal stability of lactate dehydrogenase during freezing, *J. Pharm. Sci.*, 97 (2008) 798-814.
- [24] M.J. Pikal, Mechanisms of protein stabilization during freeze-drying and storage: The relative importance of thermodynamic stabilization and glassy state relaxation dynamics., in: L. Rey, J.C. May (Eds.) *Freeze-Drying/Lyophilization of Pharmaceutical and Biological Products*, Marcel Dekker, Inc., New York, 2004.
- [25] M.J. Pikal, M.L. Roy, S. Shah, Mass and heat transfer in vial freeze-drying of pharmaceuticals: Role of the vial, *J. Pharm. Sci.*, 73 (1984) 1224-1237.
- [26] CRC, *Handbook of chemistry and physics*, 84th ed., CRC Press, Baco Raton, FL, USA, 2003.

- [27] J. Liesebach, T. Rades, M. Lim, A new method for the determination of the unfrozen matrix concentration and the maximal freeze-concentration, *Thermochimica Acta*, 401 (2003) 159-168.
- [28] C.A. Angell, R.D. Bressel, J.L. Green, H. Kanno, M. Oguni, E.J. Sare, Liquid fragility and the glass transition in water and aqueous solutions, *J. Food Eng.*, 22 (1994) 115-142.
- [29] J.-Y. Cherng, P. van de Wetering, H. Talsma, D.J.A. Crommelin, W.E. Hennink, Freeze-Drying of Poly((2-dimethylamino)ethyl Methacrylate)-Based Gene Delivery Systems, *Pharm. Res.*, 14 (1997) 1838-1841.
- [30] D.W. Pack, A.S. Hoffman, S. Pun, P.S. Stayton, Design and development of polymers for gene delivery, *Nat. Rev. Drug Discov.*, 4 (2005) 581-593.
- [31] M.X. Tang, F.C. Szoka, The influence of polymer structure on the interactions of cationic polymers with DNA and morphology of the resulting complexes, *Gene Ther.*, 4 (1997) 823-832.
- [32] S. Passot, I.C. Trelea, M. Marin, M. Galan, G.J. Morris, F. Fonseca, Effect of Controlled Ice Nucleation on Primary Drying Stage and Protein Recovery in Vials Cooled in a Modified Freeze-Dryer, *J. Biomech. Eng.*, 131 (2009) 074511-074515.
- [33] S. Patel, C. Bhugra, M. Pikal, Reduced Pressure Ice Fog Technique for Controlled Ice Nucleation during Freeze-Drying, *AAPS PharmSciTech*, 10 (2009) 1406-1411.
- [34] S. Rambhatla, R. Ramot, C. Bhugra, M. Pikal, Heat and mass transfer scale-up issues during freeze drying: II. Control and characterization of the degree of supercooling, *AAPS PharmSciTech*, 5 (2004) 54-62.
- [35] B.S. Chang, B.S. Kendrick, J.F. Carpenter, Surface-induced denaturation of proteins during freezing and its inhibition by surfactants, *J. Pharm. Sci.*, 85 (1996) 1325-1330.
- [36] T. Cochran, S.L. Nail, Ice nucleation temperature influences recovery of activity of a model protein after freeze drying, *J. Pharm. Sci.*, 98 (2009) 3495-3498.
- [37] E.J. Workman, S.E. Reynolds, Electrical Phenomena Occurring during the Freezing of Dilute Aqueous Solutions and Their Possible Relationship to Thunderstorm Electricity, *Phys. Rev.*, 78 (1950) 254-259.
- [38] A.W. Cobb, G.W. Gross, Interfacial Electrical Effects Observed during the Freezing of Dilute Electrolytes in Water, *J. Electrochem. Soc.*, 116 (1969) 796-804.
- [39] G. Gross, Solute interference effects in freezing potentials of dilute electrolytes, in: H. Jellinek (Ed.) *Water structure at the water-polymer interface*. edition, Plenum Press, New York, 1972, pp. 106-125.
- [40] J.A. Searles, Freezing and annealing phenomena in lyophilization, in: L. Rey, J.C. May (Eds.) *Freeze-Drying/Lyophilization of Pharmaceutical and Biological Products*, Marcel Dekker, Inc., New York, 2004.

- [41] X. Tang, M. Pikal, Design of Freeze-Drying Processes for Pharmaceuticals: Practical Advice, *Pharm. Res.*, 21 (2004) 191-200.
- [42] X. Tang, M.J. Pikal, Measurement of the Kinetics of Protein Unfolding in Viscous Systems and Implications for Protein Stability in Freeze-Drying, *Pharm. Res.*, 22 (2005) 1176-1185.
- [43] J.-Y. Cherng, H. Talsma, D. Crommelin, W. Hennink, Long Term Stability of Poly((2-dimethylamino)ethyl Methacrylate)-Based Gene Delivery Systems, *Pharm. Res.*, 16 (1999) 1417-1423.
- [44] S.d. Allison, T.J. Anchordoquy, Mechanisms of protection of cationic lipid-DNA complexes during lyophilization, *J. Pharm. Sci.*, 89 (2000) 682-691.

Chapter 7

Formulation development of lyophilized, long-term stable siRNA/oligoaminoamide polyplexes

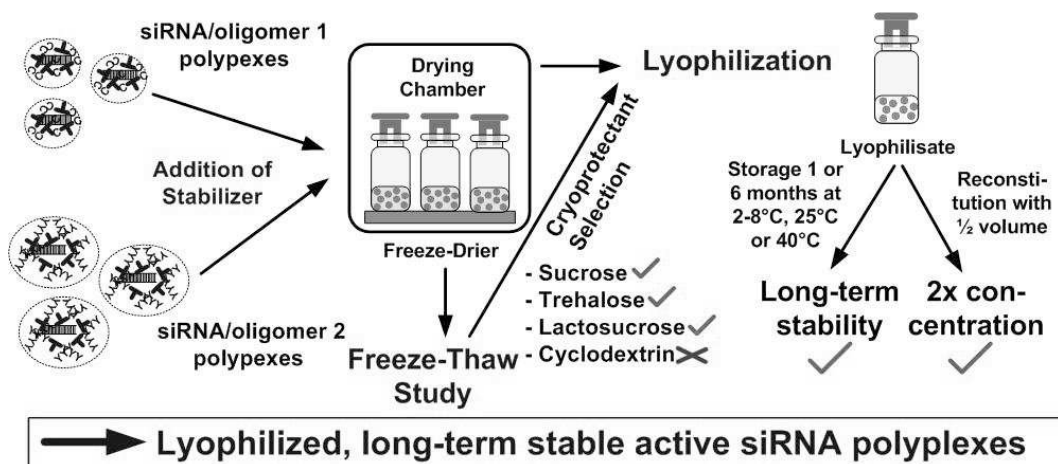
The following chapter is intended for publication:

Julia Christina Kasper, Christina Troiber*, Sarah Küchler, Ernst Wagner, Wolfgang Friess

Formulation development of lyophilized, long-term stable siRNA/oligoaminoamide polyplexes; *submitted*.

*Polymer synthesis and cell culture experiments were performed by C. Troiber.

Graphical Abstract



Abstract

Polyplexes based on precise oligoaminoamides exhibited promising results in non-viral siRNA delivery. However, one serious limitation is insufficient stability of polyplexes in liquid, raising the demand for lyophilized, long-term stable formulations.

Two different siRNA/oligoaminoamide polyplexes were prepared. Freeze-thaw experiments were performed, in order to test various formulations containing sucrose, trehalose, lactosucrose and hydroxypropyl- β -cyclodextrin for their cryoprotective potential, and to investigate the influence of the oligomer structure on particle stability. Selected formulations were lyophilized and tested for storage stability up to 6 months. Moreover, reconstitution of the lyophilisates in reduced volume was studied. Samples were analyzed for particle size, gene silencing, cytotoxicity, turbidity, sub-visible particles, osmolarity, residual moisture content, glass transition temperature and morphology.

Depending on the oligomer, siRNA polyplexes maintained particle size and gene silencing efficiency in the absence or presence of low amounts (7%) of stabilizers after freeze-thawing, lyophilization and reconstitution. The difference in formulation stability was not related to covalent disulfide bridges internally stabilizing the polyplexes. Hydroxypropyl- β -cyclodextrin did not provide sufficient stability. For lyophilized 5%/10% sucrose and 7% lactosucrose formulations, long-term stability was demonstrated even at 40°C with constant turbidity values, low numbers of subvisible particles at low residual moisture levels and sufficiently high glass transition temperatures.

Keywords

Freeze-drying, lyophilization, non-viral RNA delivery, polyplexes, siRNA delivery, stability testing

1 Introduction

Gene therapy offers significant promise to cure, treat or prevent diseases, such as cancer, cardiovascular or inherited monogenic diseases, by altering or manipulating genes [1-2]. In traditional gene therapy, gene substitutes (DNA) are introduced into cells in order to replace defective genes [1]. Within the last few years, RNA interference by which harmful genes can be “silenced” [3], has provided promising therapeutic opportunities [4]. In this case, small interfering RNA (siRNA) with a length of only 21-23 base pairs [5] induces specific posttranscriptional gene silencing upon delivery into the cytoplasm [6].

Under *in vivo* conditions, “naked” nucleic acid is rapidly degraded by serum nucleases [4] and is only inefficiently taken up by target cells, because of its negative charge and large size [6]. Thus, *in vivo* gene therapy necessitates gene delivery vectors that ideally protect nucleic acids in the extracellular environment and mediate their delivery to the target site [7]. Currently, viral vectors are still the most efficient delivery systems, but possess several drawbacks, such as immunogenic and toxic reactions or the potential for viral recombination [7-8]. Due to these concerns, non-viral vectors are attractive alternatives [7-8]. Most non-viral vectors are composed of cationic lipids or cationic polymers, which form electrostatic nano-sized complexes (lipo-/polyplexes) with the negatively charged nucleic acids [1]. Among many polycations, polyethylenimine (PEI) is considered as the “gold standard”, because of its high transfection efficiency [9-10]. PEI exhibits polydispersity, significant toxicity, limited degradability [9], and in the case of siRNA transfer only modest delivery efficiency [11-12]. Therefore, modified polymers, which allow to establish structure activity relationships, are required for efficient and safe clinical siRNA delivery [13-14]. Currently, a library of more than 300 sequence-defined, monodisperse, precisely tailored oligomers has been

generated by solid-phase assisted synthesis, including a number of oligomers that were highly efficient in siRNA transfer [15].

A major drawback that holds true for most non-viral vectors is their poor long-term stability in aqueous systems, including the tendency to form aggregates, which is often correlated with a loss in transfection efficiency [16-18]. However, the mandatorily repeated fresh preparation of the non-viral complexes, prior to administration in clinical application, possess the risk of batch to batch variations and is highly afflicted with safety concerns [19-20]. Thus, for successful therapeutic use, one major requirement is the development of formulations, which can be reproducibly manufactured and stored for an extended period of time with full retention of particle integrity and biological activity.

Previously, it was shown that lyophilization of non-viral vectors is an attractive way in order to achieve long-term stable gene delivery formulations [17], with most of the literature describing systems based on plasmid DNA or oligonucleotides [19-27]. Although lyophilization is a rather gentle drying process, it involves two main stress factors, freezing and water removal, which can result in nanoparticle damage unless appropriate stabilizers are added [28]. Suitable stabilizers were for example monosaccharides (glucose), disaccharides (sucrose, trehalose), oligosaccharides (inulin, lactosucrose), or polysaccharides/polymers (cyclodextrins, dextrans, povidone).

Unfortunately, only limited information is available with regard to lyophilization of non-viral siRNA delivery systems. Wu et al. [29] showed that siRNA-loaded lipid particles could be prepared by hydration of a stable freeze-dried matrix, containing siRNA and lipids. However, they only compared this preparation method to an established direct preparation procedure and did not investigate the influence of the lyophilization process itself on particle size and biological activity. Kundu et al. [30] determined particle size and gene silencing efficiency

of a lyophilized lipid-based siRNA nanosome formulation upon storage, but also did not investigate the influence of the lyophilization process. Moreover, Andersen et al. [31] described lyophilized chitosan or lipid siRNA formulations that are coated on cell culture plates as high-throughput screening tool and showed that 10% sucrose was required to adequately retain particle size and gene silencing activity. Additionally, Yadava et al. [32] reported that siRNA lipoplexes could only be lyophilized without loss of transfection efficacy and with only a slight increase in particle size in the presence of lyoprotectants, such as glucose or sucrose. Similar results were published by Werth et al. [33], who required 5% glucose to preserve the transfection efficacy of low molecular weight polyethylenimine based siRNA polyplexes, but atomic force microscopy demonstrated a broadening of the polyplex particle size.

In most studies, the main focus was on the preservation of the transfection efficiency of non-viral complexes after lyophilization. However, other crucial quality control parameters have been ignored. For example, retention of particle size, number of subvisible particles in a formulation, or relevant characteristics of the lyophilisates, such as physical state, glass transition temperature or water content, which can highly influence storage stability. In a previous work [25], we focused on the improvement of a lyophilized plasmid/LPEI polyplex formulation. The aim of the present study was to transfer this approach to the formulation development of lyophilized, long-term stable siRNA polyplexes based on novel oligoaminoamides. Due to the smaller size and the limited number of negative charges of siRNA, siRNA forms more rigid and less electrostatically stabilized complexes [4, 13]. Thus, siRNA complexes were assumed to be more susceptible to freezing and drying induced stresses, compared to plasmid DNA complexes. The availability of long-term stable, lyophilized siRNA polyplex formulations would highly facilitate the application of siRNA technology in clinical trials.

In a first step, a micro-mixer method [34] was transferred to up-scale the preparation of siRNA/oligoaminoamide polyplexes. Secondly, freeze-thaw studies were performed to select the most effective cryoprotectants in particle stabilization. In order to provide a better understanding of the correlation between the chemical structure of the used oligomers and the freeze-thaw stability of the corresponding siRNA polyplexes, oligomer analogs were synthesized and tested in a further freeze-thaw experiment. Selected formulations were lyophilized and the possibility to achieve higher concentrated siRNA polyplex formulations by reconstitution to reduced volumes was investigated. Moreover, stability of selected lyophilized formulations was tested up to 6 months. The siRNA/oligoaminoamide polyplexes were analyzed with respect to their particle size using dynamic light scattering (DLS), as well as their metabolic activity and gene silencing efficiency in cell culture. Furthermore, liquid formulations were characterized for their osmotic pressure, turbidity and number of subvisible particles. Lyophilisates were examined by Karl Fischer titration, differential scanning calorimetry (DSC) and X-ray powder diffraction (XRD).

2 Materials and methods

2.1 Materials

Oligoaminoamides **49** and **460** were synthesized analogously as described in [15] and [35], respectively. The oligotyrosine containing T-shape oligoaminoamides **332** and **454** were also obtained by solid-phase assisted synthesis (unpublished results; C. Troiber and E. Wagner, manuscript in preparation). When indicated, free terminal cysteines of oligomer **49** were blocked by incubation with a 10-fold molar excess of N-ethylmaleimide (NEM) (Sigma-Aldrich, Steinheim, Germany) overnight, followed by a saturation of the excessive NEM with a 10-fold molar surplus of acetylcysteine (Sigma-Aldrich, Steinheim, Germany). The chemical sequences of the used oligoaminoamides are listed in Table 7-1.

Table 7-1: Chemical sequences of the used polymers 49, 332, 454 and 460. S: succinic anhydride, tp: tetraethylenpentamine, OleA: oleic acid, C: cysteine, Y: tyrosine, A: alanine, JK: lysine with branching at α,ϵ -amino groups.

Oligomer	Sequence
49	C-Stp ₂ -(OleA) ₂ KJK-Stp ₂ -C
332	Y ₃ -Stp ₂ -(OleA) ₂ KJK-Stp ₂ -Y ₃
454	C-Y ₃ -Stp ₂ -(OleA) ₂ KJK-Stp ₂ -Y ₃ -C
460	A-Stp ₂ -(OleA) ₂ KJK-Stp ₂ -A

GFP-siRNA (sense: 5'-AuAucAuGGccGAcAAGcAdTsdT-3'; antisense: 5'-UGCUUGUCGGCcAUGAuAUdTsdT-3'; small letters: 2'methoxy-RNA; s: phosphorothioate) and control-siRNA siCtrl (sense: 5'-AuGuAuuGGccuGuAuuAGdTsdT-3'; antisense: 5'-CuAAuAcAGGCcAAuAcAUdTsdT-3') were kindly provided by Axolabs GmbH (Kulmbach, Germany; formerly Roche Kulmbach GmbH).

Purified water (ELGA LabWater, Celle, Germany) served as solvent for all solutions. siRNA and oligomer stock solutions were diluted in 20 mM 4-(2-hydroxyethyl)-1-piperazineethanesulfonic acid (HEPES) (Merck, Darmstadt, Germany) buffer pH 7.4, so that mixing equal volumes of the two solutions resulted in a N/P ratio of 12:1 (molar ratio of protonable oligomer nitrogen (N) to siRNA phosphor (P)) and a siRNA concentration of 200 µg/mL, which is referred to the siRNA concentration of the sample.

Stabilizer stock solutions at various concentrations [% w/v] of sucrose (Südzucker, Mannheim, Germany), trehalose 100 (Hayashibara, Okayama, Japan), hydroxypropylbetadex (HP-β-CD) (Cavasol™ W7 HP, Wacker Chemie, Munich, Germany), lactosucrose (Nyuka-Oliga™ LS-90P, Hayashibara, Okayama, Japan) and polysorbate 20 (Tween 20™, Merck, Darmstadt, Germany) were prepared in 20 mM HEPES buffer pH 7.4 without any further purification. Stabilizer stock solutions were filtered with a 0.2 µm cellulose acetate membrane syringe filters (VWR International, Ismaning, Germany) and mixed 1:1 with the formed siRNA polyplexes. For cell culture experiments all samples were prepared under aseptic conditions.

2R glass vials (Fiolax® clear, Schott AG, Müllheim, Germany) with their according rubber stoppers (West Pharmaceutical Services, Eschweiler, Germany) with a filling volume of 150 µL or 500 µL were used.

2.2 Preparation of siRNA polyplexes

The siRNA polyplexes were prepared by a micro mixer method that was originally established for plasmid/LPEI polyplexes [34]. 5.0 mL syringes with luer lock tip (Terumo, Leuven, Belgium) and a plunger speed of 1.0 cm/min were used for this mixing process. After mixing, the polyplexes were incubated for 30 min at room temperature. In order to ensure the suitability of the micro mixer method for the preparation of siRNA polyplexes, polyplexes were also

prepared via admixing 75 μL siRNA stock solution into the same volume of oligomer stock solution in 1.5 mL Eppendorf tubes in comparison.

2.3 Freeze-thawing studies

For the freeze-thawing studies, 75 μL siRNA polyplex solution at a concentration of 200 $\mu\text{g}/\text{mL}$ was mixed with 75 μL stabilizer solution at various concentrations in 2R vials resulting in a polyplex concentration of 100 $\mu\text{g}/\text{ml}$ and various stabilizer concentrations (5%, 10% and 20% sucrose, 10% sucrose/ 0.01% polysorbate 80, 5% and 10% trehalose, 7% and 14% lactosucrose, 10% HP- β -CD/ 6.3% sucrose). Freeze-thawing experiments were performed on a pilot-scale freeze-drier (Lyostar II, FTS Systems, SP Industries, Stone Ridge, USA). The samples were equilibrated at 20 $^{\circ}\text{C}$ for 10 min, frozen at $-1^{\circ}\text{C}/\text{min}$ to -45°C with a 30 min hold at -45°C . Thawing was performed at $1^{\circ}\text{C}/\text{min}$ to 20 $^{\circ}\text{C}$ with a 30 min hold at 20 $^{\circ}\text{C}$. This procedure was performed three times.

2.4 Lyophilization of siRNA polyplexes

500 μL of the selected samples (5% and 10% sucrose, 5% and 10% trehalose, 7% and 14% lactosucrose) were lyophilized in 2R vials. Samples were prepared by mixing 250 μL siRNA polyplex solution with 250 μL stabilizer solution at various concentrations. Lyophilization was performed on a pilot scale freeze-drier (Lyostar II). Samples were frozen at $-1^{\circ}\text{C}/\text{min}$ to -45°C and held for 120 min. Primary drying was performed at -20°C and 34 mTorr with manometric endpoint determination. Secondary drying was performed at reduced pressure of 8 mTorr at 20 $^{\circ}\text{C}$. Samples were stoppered under slight vacuum at 600 Torr nitrogen and vials were crimped with aluminum seals.

2.5 Long-term stability testing of lyophilized samples

For long-term stability testing, selected lyophilisates (5% and 10% sucrose, 7% lactosucrose) were stored at 2-8 $^{\circ}\text{C}$, 25 $^{\circ}\text{C}$ and 40 $^{\circ}\text{C}$ over a period of 1 month and 6 months.

2.6 Reconstitution of lyophilized samples

Lyophilized samples were reconstituted with 250 μL (5% sucrose, 5% trehalose and 7% lactosucrose samples) or 500 μL (10% sucrose, 10% trehalose and 14% lactosucrose samples) purified water. This resulted in samples with siRNA concentrations of 200 $\mu\text{g}/\text{ml}$ or 100 $\mu\text{g}/\text{mL}$, respectively.

2.7 siRNA polyplex characterization

Size determination of siRNA polyplexes was performed by DLS using the Nanosizer ZS (Malvern, Herrenberg, Germany). The samples were diluted 1:20 with 20 mM HEPES buffer pH 7.4 to a final volume of 1 mL. The diluted samples were measured in single-use polystyrene semi-micro PMMA cuvettes (Brand, Wertheim, Germany) with a path length of 10 mm after an equilibration time of 1 min at 20 °C. Each sample was recorded three times with 3 subruns of 10 s using the multimodal mode. The z-average diameter (Zave) or the number mean diameter, and the polydispersity index (pdi) were calculated from the correlation function using the Zetasizer Software 6.20 (Malvern).

Freshly prepared siRNA polyplexes were analyzed for their zeta-potential with laser Doppler anemometry using the Zetasizer Nano ZS (Malvern). Each sample was analyzed in a DTS 1060c cell (Malvern) with 10 up to 100 subruns of 10 s at 20 °C (n=3). The zeta-potential was calculated by the Smoluchowski equation.

2.8 Cell culture: metabolic activity and gene silencing

Freshly prepared, freeze-thaw stressed, lyophilized, and lyophilized and stored GFP-siRNA polyplex formulations were diluted to 25 $\mu\text{g}/\text{mL}$ with HBG (5% glucose, 20 mM HEPES pH 7.4) for cell culture experiments. Control-siRNA polyplexes were freshly prepared and treated in exactly the same manner.

Mouse neuroblastoma cells (Neuro2A/EGFP_{Luc} cells), stably transfected with the EGFP_{Luc} gene, were grown in Dulbecco's modified Eagle's medium

(DMEM), supplemented with 10% FCS, 4 mM glutamine, 100 U/mL penicillin, and 100 µg/mL streptomycin and incubated at 37 °C and 5% CO₂. In order to determine the metabolic activity or the knock down efficiency of the siRNA polyplexes, Neuro2A/EGFPLuc cells were seeded into 96-well plates at a density of 5000 cells/well 24 h prior to transfection. Subsequently, cell culture medium was replaced with 80 µL fresh medium containing 10% FCS. 20 µL of the diluted transfection complexes in HBG were added to each well and incubated for 48 hours at 37 °C and 5% CO₂. 20 µL HBG buffer was used as negative control. All experiments were performed in triplicates, respectively.

Subsequently, metabolic activity was evaluated. Therefore, 10 µL MTT (5 mg/ml) were added to each well, reaching a final concentration of 0.5 mg MTT/mL. After an incubation time of 2 h, unreacted dye and medium were removed and the plates were frozen at -80 °C for at least 1 h. The purple formazan product was dissolved in 80 µL/well dimethyl sulfoxide and quantified by a UV plate reader (Tecan, Groedig, Austria) at 590 nm with background correction at 630 nm. The metabolic activity (%) was calculated relative to HBG controls.

To determine gene knock down efficiency, the transfected cells were treated with 100 µL lysis buffer (0.5x) 48 h post transfection. Subsequently, luciferase activity in the cell lysate was determined with a Centro 960 plate reader luminometer (Berthold Technologies, Bad Wildbad, Germany). The relative light units (RLU) were presented as percentage of the luciferase gene expression obtained with only HBG treated control cells.

2.9 Osmometry

The osmotic pressure of 150 µL of each lyophilized and reconstituted sample was determined in triplicates with an automatic semi-micro osmometer (Knauer, Berlin, Germany). The instrument was checked with aqueous NaCl solutions of 75, 150 and 300 mM.

2.10 Turbidimetry

Turbidity of the samples in formazine nephelometric units (FNU) was determined by using a NEPHLA turbidimeter (Dr. Lange, Düsseldorf, Germany). Samples were analyzed in triplicates in LUMIstox™ glass cuvettes (Dr. Lange, Düsseldorf, Germany). Prior to the measurement, the instrument was checked by measuring the turbidity of purified water.

2.11 Light obscuration

Light obscuration tests were carried out according to Ph.Eur. 2.9.19. The particle counting of subvisible particles in a size range between 1 and 200 μm was conducted using a SVSS-C instrument and associated analysis software (PAMAS GmbH, Rutesheim, Germany). For each sample (n=3) four measurements of a volume of 0.3 mL with a pre-run volume of 0.3 mL at fixed fill rate, emptying rate and rinse rate of 5 mL/min were performed. Prior to each measurement the system was rinsed with 0.2 μm filtered purified water until particle counts of less than 100 particles/mL $\geq 1 \mu\text{m}$ and less than 10 particles/mL $\geq 10 \mu\text{m}$ were determined. The obtained results represented the mean value of the particle counts of three measurements, referred to a sample volume of 1.0 mL.

2.12 Karl Fischer titration

The residual moisture of the lyophilisates directly after lyophilization and after storage was determined in triplicates by coulometric Karl Fischer titration using a Metrohm 756 KF Coulometer (Metrohm, Herisau, Switzerland). The lyophilisates were dissolved in 0.5 mL dried Methanol (Hydranal™-Methanol Dry, Sigma-Aldrich, Steinheim, Germany). The water content of the samples was determined by injecting 0.3 mL of the methanol samples into the titration solution (Hydranal™-Coulomat AG, Sigma-Aldrich) and the water content was calculated as % w/w. Empty vials were treated identically throughout

preparation and storage to obtain comparable blank values. Hydranal™ Water Standard 0.10 (Sigma-Aldrich) was used as reference.

2.13 Differential scanning calorimetry (DSC)

DSC experiments were performed in 40 μL aluminum crucibles using a Mettler Toledo DSC 821e (Mettler-Toledo GmbH, Giessen, D). In order to determine the glass transition temperature of the maximally freeze-concentrated solution (T_g), 30 μL of the liquid samples were cooled at $-5\text{ }^\circ\text{C}/\text{min}$ from $20\text{ }^\circ\text{C}$ to $-40\text{ }^\circ\text{C}$, and subsequently, at $-2\text{ }^\circ\text{C}/\text{min}$ from $-40\text{ }^\circ\text{C}$ to $-50\text{ }^\circ\text{C}$, held at $-50\text{ }^\circ\text{C}$ for 10 min and reheated at $10\text{ }^\circ\text{C}/\text{min}$ to $20\text{ }^\circ\text{C}$. For the determination of the glass transition temperature of the lyophilisates (T_g), approximately 10 mg were weighed into the aluminum crucibles in a glove box purged with dry air. Samples were equilibrated at $25\text{ }^\circ\text{C}$ for 5 min and heated at $10\text{ }^\circ\text{C}/\text{min}$ to $110\text{ }^\circ\text{C}$. T_g and T_g' were defined as the midpoint of the glass transition in the heat heating scan of the DSC experiment. All analyses were performed in triplicates.

2.14 X-ray powder diffraction (XRD)

The morphology of the lyophilisates directly after lyophilization and after storage was analyzed by XRD on an X-ray diffractometer XRD 3000 TT (Seifert, Ahrensburg, Germany). Samples were fixed on a copper sample holder with 1 mm fill depth, exposed to CuK α radiation ($U = 40\text{ kV}$, $I = 30\text{ mA}$, $\lambda = 154.17\text{ pm}$), and scanned from 5 to 45° $2-\Theta$ with steps of 0.1° $2-\Theta$ and a duration of 1 s per step.

2.15. Statistical analysis

Results were determined to be statistically different by performing a two-tailed student t test using the QuickCalcs, GraphPad Software (La Jolla, CA, USA). Mean values with a p value < 0.05 are considered as significantly different.

3 Results

3.1 Up-scaled preparation and characterization of the siRNA polyplexes

In order to guarantee a standardized and reproducible preparation of siRNA/oligoaminoamide polyplexes at a larger scale, a micro-mixer method established for the preparation of plasmid/LPEI polyplexes [34] was transferred to the siRNA polyplexes. Therefore, siRNA/oligomer **332** and siRNA/oligomer **49** polyplexes were prepared by classical pipetting and by the micro mixer method. In a preliminary study (Troiber et al., unpublished results, manuscript in preparation), polyplex size obtained by DLS, fluorescence correlation spectroscopy, AFM and nanoparticle tracking analysis were compared. For siRNA/oligomer **332** polyplexes the Zave and for siRNA/oligomer **49** polyplexes the volume or number mean diameter in DLS provided the most realistic and representative size results. Consequently, these parameters were employed for size characterization of polyplexes prepared by the different methods.

For siRNA/oligomer **332** polyplexes, Zave and pdi were not significantly ($p > 0.05$) influenced by the preparation method (pipetting Zave: 131.0 ± 7.1 nm, pdi: 0.17 ± 0.02 ; micro-mixer Zave 122.0 ± 1.4 nm, pdi: 0.17 ± 0.02). Similarly, for siRNA/oligomer **49** polyplexes, no significant difference in the mean number diameter (18.4 ± 2.0 nm vs. 18.0 ± 1.2 nm), or the mean volume diameter (23.5 ± 4.2 nm vs. 24.9 ± 4.5 nm) was observed. The polydispersity of the siRNA/oligomer **49** polyplexes was slightly improved, when prepared with the micro-mixer method (0.37 ± 0.13), compared to classical pipetting (0.58 ± 0.24). Additionally, silencing efficiency of siRNA/oligomer **332** polyplexes in mouse neuroblastoma cells was significantly independent from the preparation method, at comparable metabolic activities. The luciferase activity was $4.0 \pm 0.5\%$ after pipetting and $3.8 \pm 0.5\%$ using the micro-mixer method. The

siRNA/oligomer **49** polyplexes prepared by the micro-mixer method showed a significantly better gene silencing efficiency (luciferase activity of $34.8 \pm 3.8\%$), compared to polyplexes prepared via classical pipetting (luciferase activity of $47.8 \pm 4.0\%$). Moreover, in 20 mM HEPES buffer pH 7.4, the zeta-potential of siRNA/oligomer **332** or siRNA/oligomer **49** polyplexes was 38.1 ± 0.8 mV or 20.8 ± 0.6 mV, respectively. For all further formulation studies, polyplexes were prepared with the micro-mixer method.

3.2 Freeze-thawing studies

Prior to lyophilization, freeze-thawing studies were performed, in order to select the most effective cryoprotectant at its required concentration. The siRNA/oligoaminoamide polyplexes were freeze-thawed three times in 20 mM HEPES buffer pH 7.4 without or with the addition of 5%, 10% and 20% sucrose, 10% sucrose/ 0.01% polysorbate 80, 5% and 10% trehalose, 7% and 14% lactosucrose, or 10% HP- β -CD/ 6.3% sucrose. As aforementioned, siRNA/oligomer **332** polyplexes were characterized by the Zave and siRNA/oligomer **49** polyplexes were characterized by the number mean diameter, as the volume mean diameter results were for technical reasons highly influenced by the presence of stabilizer molecules.

After freeze-thawing in absence of stabilizers, Zave and pdi of siRNA/oligomer **332** polyplexes drastically increased up to 1068 ± 170 nm and 0.9 ± 0.1 , respectively (Figure 7-1A). This drastic particle formation and precipitation was easily observable by visual inspection. The presence of low amounts of disaccharides, such as 5% sucrose or 5% trehalose, was capable to limit this high increase in particle size. Nevertheless, the particle size after freeze-thawing was significantly increased for these formulations, when compared to freshly prepared particles. Higher amounts of sucrose (10% and 20%) with or without polysorbate, trehalose (10%), or lactosucrose (7% and 14%) completely preserved the particle size upon freeze-thawing.

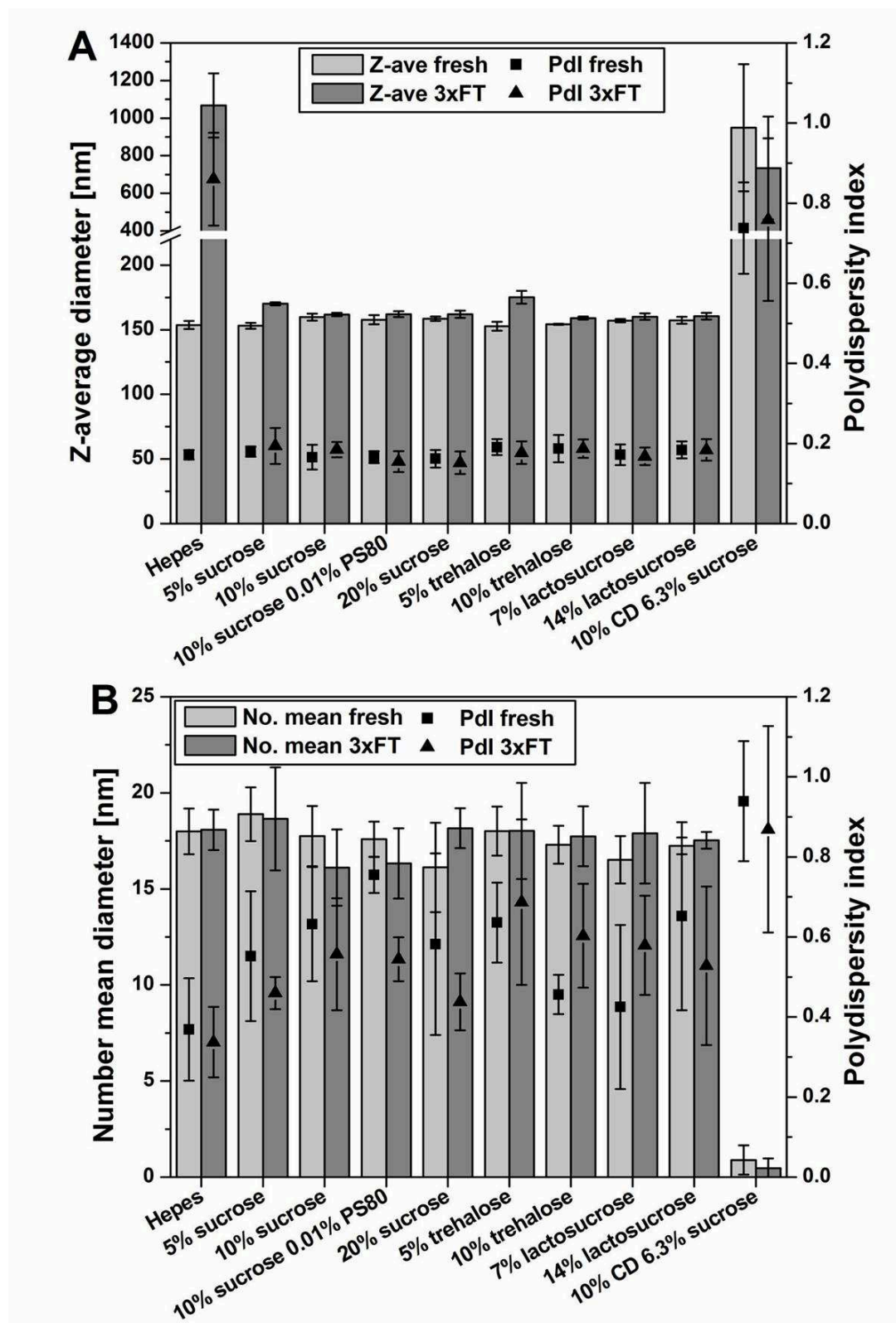


Figure 7-1: A) Z-average diameter (oligomer 332) or B) number mean diameter (oligomer 49) and polydispersity index of freshly prepared or three times freeze-thaw stressed (3xFT) siRNA polyplexes. Polyplexes were formulated in 20 mM HEPES buffer pH 7.4 without (HEPES) or with the addition of stabilizers (5%, 10% and 20% sucrose, 10% sucrose/0.01% polysorbate 80, 5% and 10% trehalose, 7% and 14% lactosucrose, 10% HP- β -CD/ 6.3% sucrose).

However, the presence of HP- β -CD led to a pronounced increase in particle size and polydispersity already in freshly prepared formulations. After freeze-thawing, these high values further persisted. In contrast, the addition of stabilizers was not necessary for the maintenance of particle size after freeze-thawing for siRNA/oligomer **49** polyplexes (Figure 7-1B). All formulations, except for the HP- β -CD/sucrose formulation, showed no significance difference in particle size after freeze-thawing compared to freshly prepared formulations. In the case of siRNA/oligomer **49** polyplexes the HP- β -CD/sucrose samples, both freshly prepared and freeze-thawed, did not show particle aggregation, but dissociation of the particles with a mean number diameter of around 1 nm.

Cell culture experiments in mouse neuroblastoma cells (data not shown) did not show an influence of the different formulations on metabolic activity (~80%). Gene silencing activity of siRNA/oligomer **332** polyplexes was slightly decreased after freeze-thawing, when formulated in HEPES buffer without the addition of stabilizers. In this case, the luciferase activity was only reduced by ~80%. In contrast, the luciferase activity was decreased by ~92% for all other effective formulations. For HP- β -CD/sucrose formulations gene silencing activity of the siRNA/oligomer **332** polyplexes was strongly reduced with a reduction in luciferase activity of only ~40%. In contrast, siRNA/oligomer **49** polyplexes formulated in HEPES buffer and with stabilizers showed comparable gene silencing activity after freeze-thawing with a decrease in luciferase activity of ~75%. Only the HP- β -CD/sucrose formulations showed a distinctive reduction in biological activity with a reduced luciferase expression by only ~15%.

All freshly prepared or freeze-thawed placebo formulations (without polyplexes) displayed low turbidity values of ~0.6 FNU, close to the turbidity of purified water. A high turbidity of ~10 FNU was observed in the case of freshly prepared siRNA/oligomer **332** polyplexes in buffer. This high turbidity was also detected for almost all freshly prepared and freeze-thawed formulations. A decreased

turbidity to ~1 FNU was observed for the freeze-thawed buffer formulation and both fresh and freeze-thawed HP- β -CD/sucrose formulations. In these cases, huge aggregates were formed, which led to particle precipitation. All siRNA/oligomer **49** polyplex formulations showed very low turbidity values in the range of 0.6 to 0.8 FNU, except for the HP- β -CD/sucrose formulations, which exhibited a turbidity of ~3.5 FNU after preparation, but which completely vanished after freeze-thawing as complexes precipitated.

Similar trends were observed for the number of subvisible particles of the various samples. An increased number of particles $\geq 1 \mu\text{m}$ was detected for freshly prepared siRNA/oligomer **332** polyplexes, compared to the corresponding placebo samples. All siRNA/oligomer **332** polyplex formulations showed a slight increase in the number of particles $\geq 1 \mu\text{m}$ after freeze-thawing from ~250 to ~2000 particles/mL, except the HP- β -CD/sucrose formulation, which showed a decrease in the number of particles $\geq 1 \mu\text{m}$ from 1700 to 1000 particles/mL as polyplexes precipitated. All siRNA/oligomer **332** polyplex formulations exhibited low numbers of subvisible particles $\geq 10 \mu\text{m}$ (≤ 5 particles/mL) and $\geq 25 \mu\text{m}$ (≤ 3 particles/mL). In comparison, only the siRNA/oligomer **49** polyplexes, formulated in HP- β -CD/sucrose, showed increased numbers of particles (~2000 particles/mL $\geq 1 \mu\text{m}$; ~600 particles $\geq 10 \mu\text{m}$, ~80 particles $\geq 25 \mu\text{m}$). All other siRNA/oligomer **49** polyplex formulations exhibited only a small gain in the number of particles $\geq 1 \mu\text{m}$ after freeze-thawing (from ~100 to ~500 particles/mL) and showed low numbers of subvisible particles $\geq 10 \mu\text{m}$ (≤ 8 particles/mL) and $\geq 25 \mu\text{m}$ (≤ 2 particles/mL).

Thus interestingly, siRNA/oligomer **49** polyplexes were resistant against freezing and thawing without addition of stabilizer. In contrast, siRNA/oligomer **332** polyplexes required at least small amounts of stabilizers. It was assumed that the unexpectedly high freeze-thaw stability of

siRNA/oligomer **49** polyplexes might be associated with the terminal cysteine groups of oligomer **49**, which are known to form internal cross-linking disulfide bonds after siRNA complexation that may stabilize the polyplexes. In order to test this hypothesis, oligomer **454** and oligomer **460** were synthesized. In comparison to oligomer **332**, oligomer **454** had additional terminal cysteines, whereas in oligomer **460** the terminal cysteines of oligomer **49** were substituted with alanine residues. Additionally, the terminal cysteines of oligomer **49** were blocked with N-ethylmaleimide (NEM) prior to polyplex formation. Polyplexes using these variants were prepared in 20 mM HEPES buffer pH 7.4 via pipetting and exposed to freeze-thaw stress without addition of stabilizers.

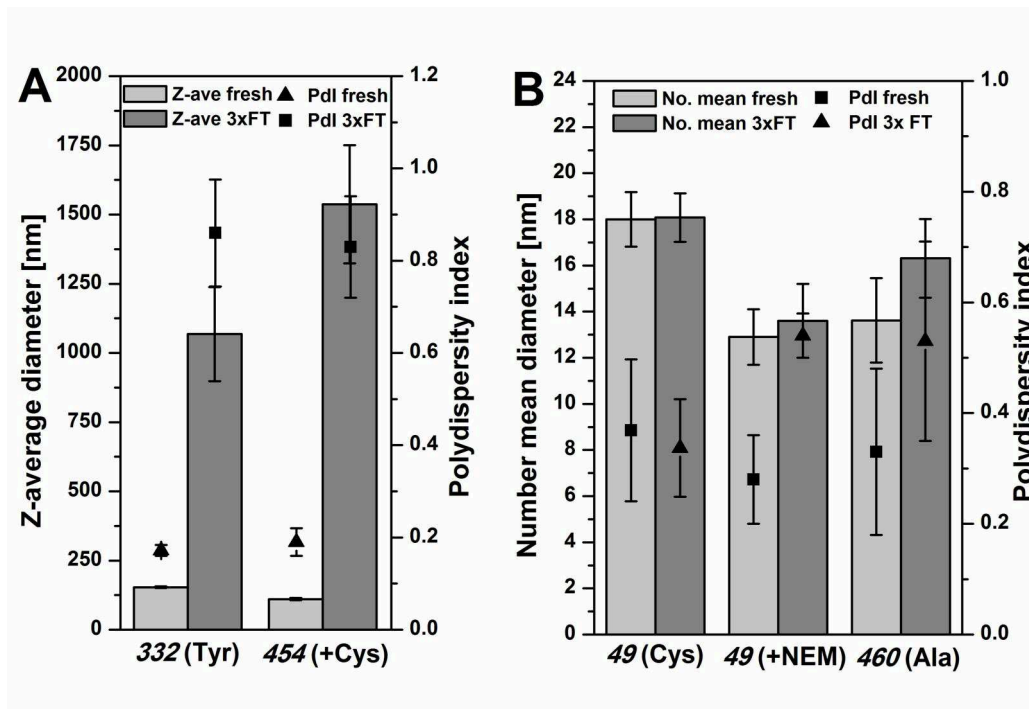


Figure 7-2: A) Z-average diameter (oligomer **332** and oligomer **454**) and B) number mean diameter (oligomer **49**, oligomer **49**NEM and oligomer **460**) of freshly prepared or three times freeze-thaw stressed (3xFT) siRNA polyplexes formulated in 20 mM HEPES buffer pH 7.4.

Despite of the additional cysteines, siRNA/oligomer **454** polyplexes showed the same distinctive increase in Zave and pdi as the siRNA/oligomer **332** polyplexes (Figure 7-2A). In contrast, neither the blockage of the free cysteine groups of oligomer **49** by NEM, nor the substitution of the free cysteines of

oligomer **49** by alanines (oligomer **460**) influenced the mean number diameter of the polyplexes significantly ($p > 0.05$) (Figure 7-2B).

3.3 Lyophilization of siRNA/oligoaminoamide polyplexes

Selected formulations of the siRNA/oligoaminoamide polyplexes in pure buffer, 5% or 10% sucrose, 5% or 10% trehalose, or 7% or 14% lactosucrose were lyophilized using a conservative lyophilization process. The product temperature was maintained below the T_g of the samples (Table 7-2) at least in the first two-thirds of the primary drying step. All lyophilisates, except the samples without stabilizers, exhibited good cake appearance.

Table 7-2: Glass transition temperature of the maximally freeze concentrate (T_g) prior to lyophilization (prior to lyo) and glass transition temperature (T_g) and residual moisture content (RM) of solid lyophilized formulations directly after lyophilization (after lyo) and after storage for 1 month (1 m) or 6 months (6 m) at 2-8 °C, 25 °C, and 40 °C (n=3).

	5% sucrose		10% sucrose		7% lactosucrose	
	T_g/T_g [°C]	RM [%w/w]	T_g/T_g [°C]	RM [%w/w]	T_g/T_g [°C]	RM [%w/w]
Prior to lyo	-33.4 ± 0.1		-31.7 ± 0.5		-25.9 ± 0.1	
After lyo	58.4 ± 0.5	0.21 ± 0.01	56.2 ± 2.7	0.56 ± 0.02	97.8 ± 2.0	0.14 ± 0.03
1m 2-8°C	57.3 ± 1.5	0.31 ± 0.03	56.3 ± 1.5	0.56 ± 0.04	92.0 ± 2.3	0.17 ± 0.01
1m 25°C	57.0 ± 0.2	0.37 ± 0.02	50.8 ± 1.0	0.73 ± 0.05	91.0 ± 1.0	0.21 ± 0.01
1m 40°C	55.0 ± 1.8	0.54 ± 0.02	49.8 ± 1.9	0.75 ± 0.03	89.7 ± 2.7	0.36 ± 0.03
6m 2-8°C	55.7 ± 0.9	0.53 ± 0.04	52.4 ± 0.7	0.60 ± 0.06	91.1 ± 0.8	0.16 ± 0.01
6m 25°C	55.3 ± 1.3	0.68 ± 0.06	49.4 ± 0.7	0.75 ± 0.03	89.4 ± 0.7	0.22 ± 0.01
6m 40°C	52.4 ± 0.8	0.70 ± 0.07	47.9 ± 0.4	0.80 ± 0.06	86.5 ± 0.7	0.41 ± 0.03

The possibility to concentrate siRNA polyplex formulations, by reconstitution to reduced volumes after lyophilization, was investigated. Therefore, the 10% sucrose, 10% trehalose and 14% lactosucrose formulations were reconstituted in the original volume, whereas the 5% sucrose, 5% trehalose and 7%

lactosucrose were reconstituted in only half of the original volume. All lyophilisates, except the siRNA/oligomer **332** polyplex samples without stabilizers, instantly (< 5 s) dissolved upon reconstitution. After reconstitution, few large, visible particles were observed for the non-stabilized siRNA/oligomer **332** polyplexes. All other reconstituted lyophilisates showed no particle formation or turbidity that was visible by the naked eye. After reconstitution, the osmolarity of the sucrose, trehalose or lactosucrose samples was 318 ± 7 , 313 ± 8 or 308 ± 5 mOsm/kg, if reconstituted in the original volume, and 347 ± 11 , 341 ± 8 or 321 ± 13 mOsm/kg, if reconstituted in half of the original volume, respectively.

After lyophilization and reconstitution, Zave and pdi of siRNA/oligomer **332** polyplexes was substantially increased in the absence of any stabilizer (Figure 7-3A). All other siRNA/oligomer **332** polyplex formulations showed only a marginal change in particle size after lyophilization and reconstitution (Figure 7-3A). This change in particle size of less than 6% between freshly prepared and lyophilized samples was significant ($p \leq 0.05$), for all formulations, except for the 7% lactosucrose formulations. Unexpectedly, for siRNA/oligomer **49** polyplexes (Figure 7-3B) no significant change in particle size was caused by lyophilization in the absence of any stabilizers or in the presence of sucrose. For the siRNA/oligomer **49** polyplexes formulated with trehalose or lactosucrose a slight difference was observed. Furthermore, samples that were reconstituted in the original volume and samples that were reconstituted in only half of the original volume did not significantly differ in size for both, siRNA/oligomer **332** polyplexes and siRNA/oligomer **49** polyplexes.

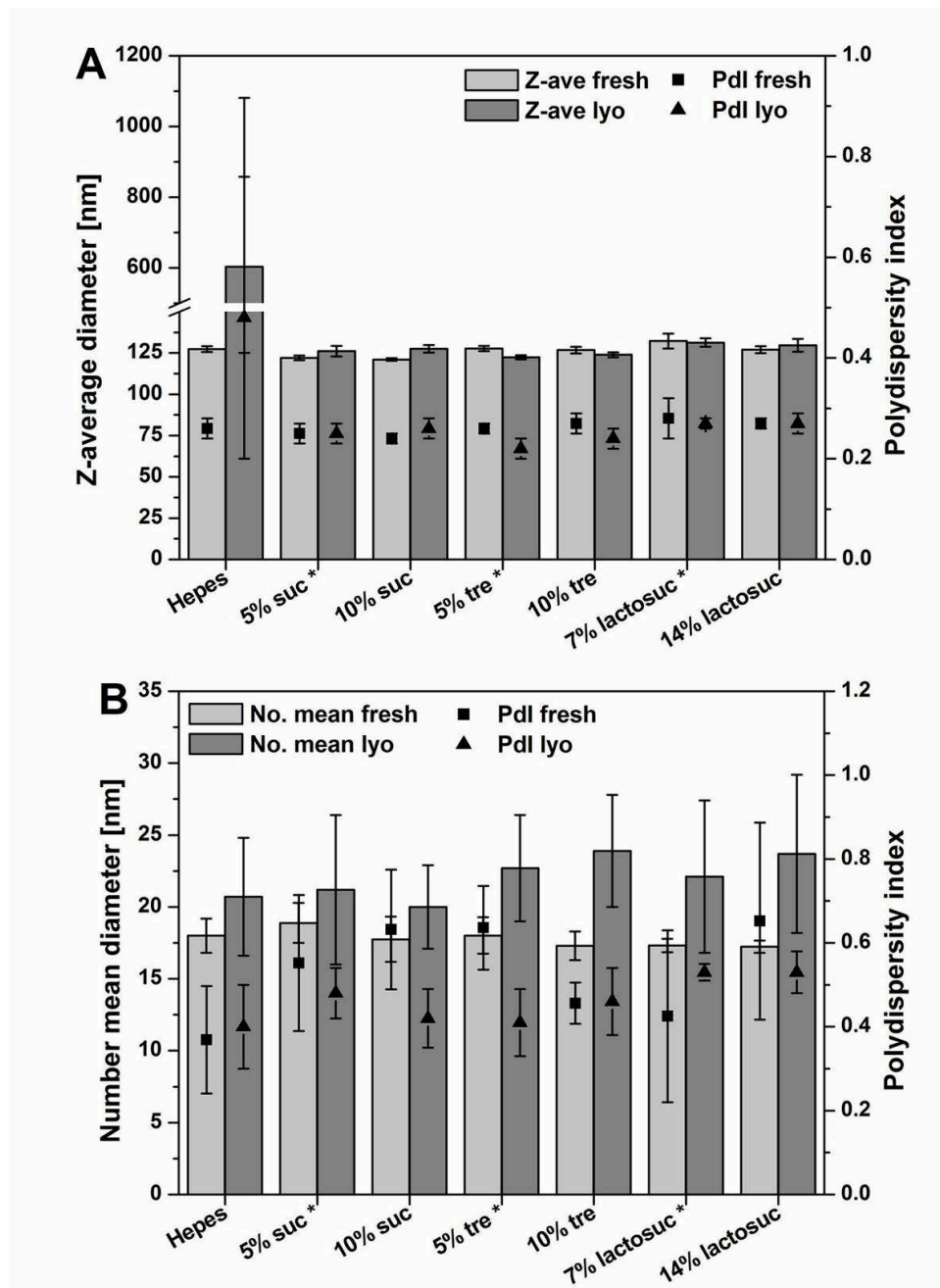


Figure 7-3: A) Z-average diameter (oligomer 332) and B) number mean diameter (oligomer 49) of siRNA polyplexes formulated in 20 mM HEPES buffer pH 7.4 with 5% or 10% sucrose or 7% lactosucrose. Samples were freshly prepared (fresh) and lyophilized (lyo). The 5% sucrose, 5% trehalose and 7% sucrose formulations were reconstituted in half of the original volume after lyophilization (*).

In cell culture experiments, siRNA/oligomer 332 polyplexes lyophilized in pure HEPES showed a decreased gene silencing activity with a limited reduction of the luciferase activity by ~75% (data not shown). All other lyophilized and reconstituted formulations for both siRNA polyplexes, siRNA/oligomer 332 and

siRNA/oligomer **49**, retained their initial gene silencing activity at comparable metabolic activity.

Similar to placebo formulation, turbidity of all siRNA/oligomer **332** polyplex formulations (data partly shown in Figure 7-6) was not increased after lyophilization and reconstitution in the original volume. A nearly doubled turbidity was detected for the samples that were reconstituted with only half of the original volume. All siRNA/oligomer **49** formulations showed a slight increase in turbidity after lyophilization and reconstitution from ~0.6 FNU to maximally 1.0 FNU.

For both, siRNA/oligomer **332** and siRNA/oligomer **49**, polyplex formulations, a distinctive increase in the number of subvisible particles $\geq 1 \mu\text{m}$ from < 500 particles/mL to up to 9000 particles/mL was monitored (data partly shown in Figure 7-7A). However, an increase in the number of subvisible particles $\geq 1 \mu\text{m}$ up to 3500 particles/mL was also observed for the placebo formulations. In general, for all lyophilized and reconstituted siRNA formulations, very low numbers of subvisible particles $\geq 10 \mu\text{m}$ (≤ 30 particles/mL) and $\geq 25 \mu\text{m}$ (≤ 5 particles/mL) were found (data partly shown in Figure 7-7B and Figure 7-7C).

3.4 Long-term stability of lyophilized siRNA/oligoaminoamide polyplexes

Consequently, formulations containing 5% sucrose, 10% sucrose, or 7% lactosucrose, were investigated for long-term stability over 6 months at 2-8 °C, 25 °C, or 40 °C. After reconstitution of the 5% sucrose and 7% lactosucrose formulations with half of the original volume and of the 10% sucrose formulation with the original volume, samples were characterized for particle size, biological and metabolic activity, turbidity and number of subvisible particles. In addition, lyophilisates were analyzed for residual moisture content, Tg and amorphous state.

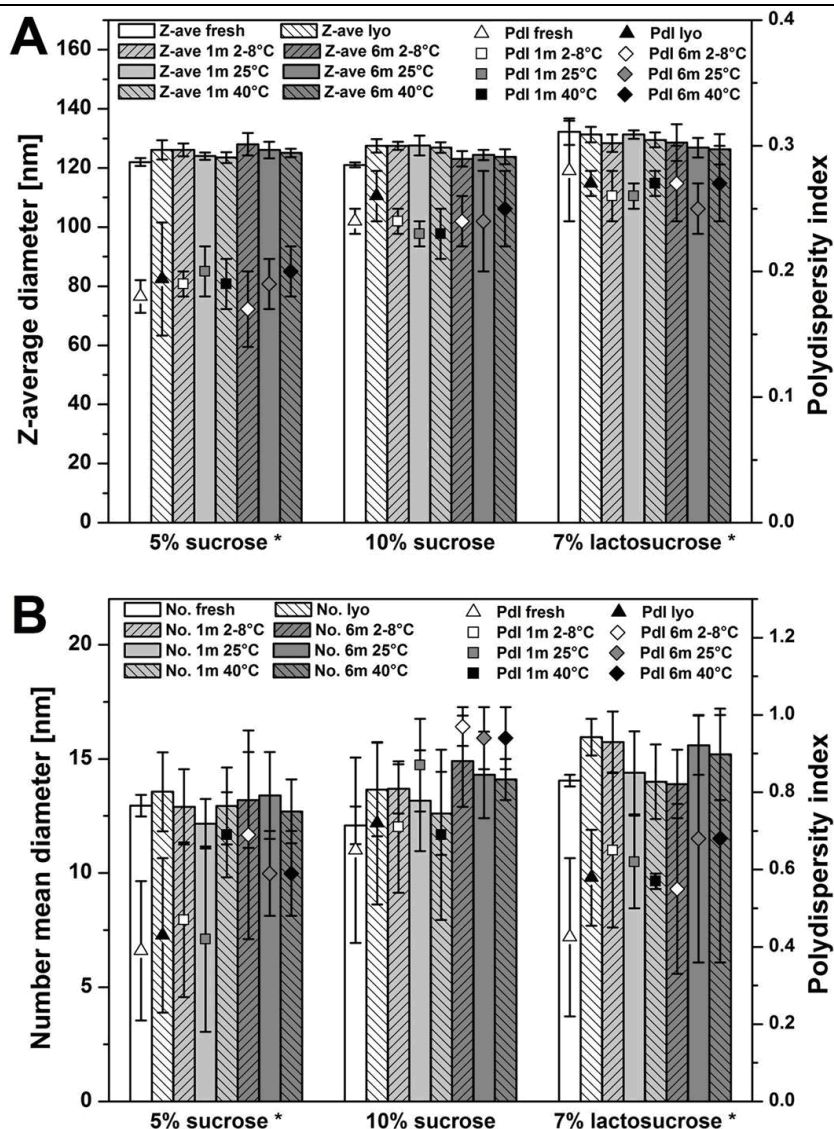


Figure 7-4: A) Z-average diameter (oligomer 332) and B) number mean diameter (oligomer 49) of siRNA polyplexes formulated in 20 mM HEPES buffer pH 7.4 with 5% or 10% sucrose or 7% lactosucrose. Samples were freshly prepared (fresh), lyophilized (lyo) or lyophilized and stored at 2-8 °C, 25 °C or 40 °C for 1 month (1 m) or 6 months (6 m). The 5% sucrose and 7% sucrose were reconstituted only in half of the original volume after lyophilization (*).

Zave and pdi of siRNA/oligomer 332 polyplexes did not significantly change over time compared to the samples that were directly analyzed after lyophilization, independent of the formulation or storage temperature (Figure 7-4A). Comparable results were observed for siRNA/oligomer 49 polyplexes, as no significant change in the mean number diameter was found over storage; only for the 5% sucrose formulation stored for 1 month at 40 °C and the 10% sucrose formulations stored for 6 months at 2-8 °C or 25 °C a slight increase in pdi was observed (Figure 7-4B).

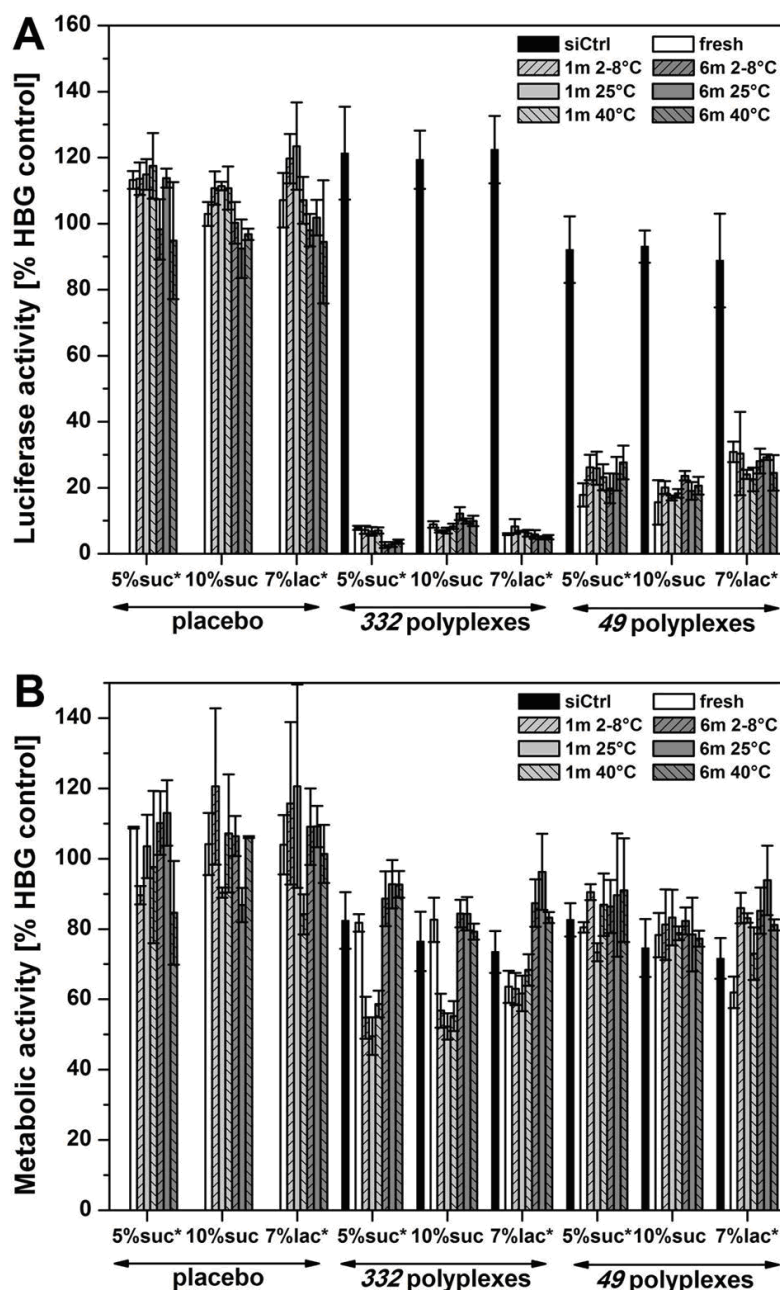


Figure 7-5: Influence of the formulation of siRNA/oligomer 332 and siRNA/oligomer 49 polyplexes and corresponding placebo samples on (A) the luciferase activity of Neuro-2A cells and (B) the metabolic activity in Neuro-2A cells (n=3). Samples were formulated in 20 mM HEPES buffer pH 7.4 with the addition 5% sucrose, 10% sucrose or 7% lactosucrose. Samples were freshly prepared (fresh), lyophilized (lyo) or lyophilized and stored at 2-8 °C, 25 °C or 40 °C for 1 month (1 m) or 6 months (6 m). The 5% sucrose and 7% sucrose were reconstituted in half of the original volume after lyophilization (*). Freshly prepared siCtrl polyplexes in HEPES buffer were used as controls.

Cell culture experiments in Neuro2A/EGFPLuc cells (Figure 7-5A and 7-5B) showed similar results for luciferase activity and metabolic activity for all

placebo samples, independently from the storage conditions. Control experiments with fresh siCtrl/oligomer **332** or siCtrl/oligomer **49** polyplexes, which were tested along with fresh or 6 months stored polyplexes, revealed luciferase activities of ~120% for the siCtrl/oligomer **332** polyplexes and ~95% for the siCtrl/oligomer **49** polyplexes at comparable metabolic activities of ~75%. Slight differences in the knock down efficiency were found for the siRNA/oligomer **332** polyplexes, which varied between 97.4% and 87.9%, and for siRNA/oligomer **49** polyplexes, which varied between 15.6% and 30.8%. However, no correlation with storage time or storage temperature were identified. The same holds true for metabolic activities which ranged between 55% and 93%.

Turbidity values of all formulations including placebo did not change significantly ($p > 0.05$) over 6 months (Figure 7-6).

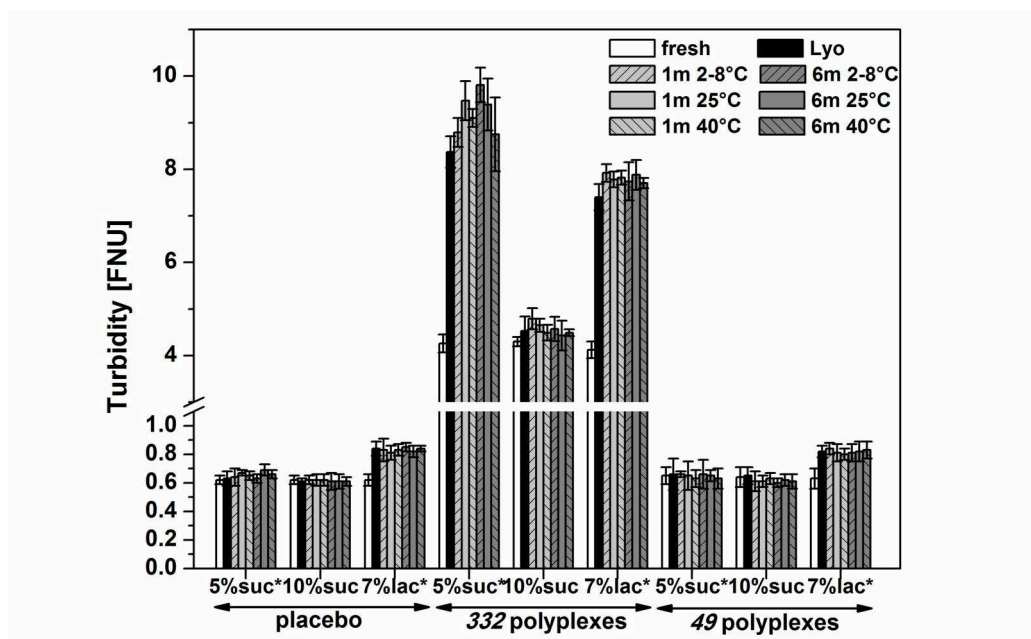


Figure 7-6: Turbidity in formazine nephelometric units (FNU) of siRNA/oligomer **332** polyplexes, siRNA/oligomer **49** polyplexes and corresponding placebo samples formulated in 20 mM HEPES buffer pH 7.4 with the addition 5% sucrose, 10% sucrose or 7% lactosucrose. Samples were freshly prepared (fresh), lyophilized (lyo) or lyophilized and stored at 2-8 °C, 25 °C or 40 °C for 1 month (1 m) or 6 months (6 m). The 5% sucrose and 7% sucrose were reconstituted in half of the original volume after lyophilization (*).

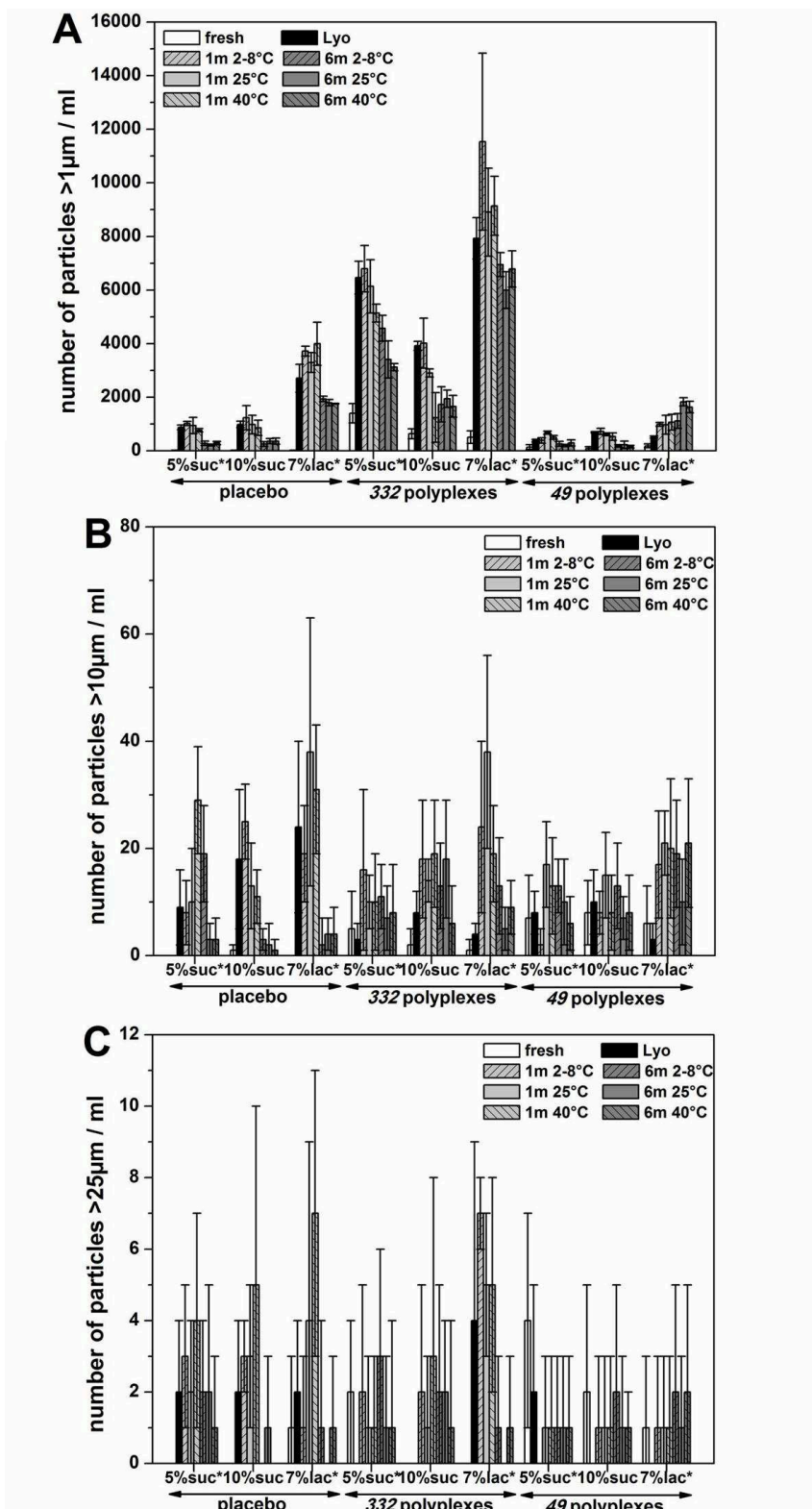


Figure 7-7: Number of sub-visible particles/mL with a particle diameter $\geq 1\ \mu\text{m}$ (A), $\geq 10\ \mu\text{m}$ (B) or $\geq 25\ \mu\text{m}$ (C) of /oligomer 332 and siRNA/oligomer 49 polyplexes and corresponding placebo samples formulated in 20 mM HEPES buffer pH 7.4 with the addition 5% sucrose, 10% sucrose or 7% lactosucrose. Samples were freshly prepared (fresh), lyophilized (lyo) or lyophilized and stored at 2-8 °C, 25 °C or 40 °C for 1 month (1 m) or 6 months (6 m). The 5% sucrose and 7% sucrose were reconstituted in half of the original volume after lyophilization (*).

In general, no trend in the number of particles $\geq 1 \mu\text{m}$ was observed in the long-term stability study (Figure 7-7A). In general, the formulations containing lactosucrose showed higher particle numbers. The number of subvisible particles $\geq 10 \mu\text{m}$ (≤ 40 particles/mL) and $\geq 25 \mu\text{m}$ (≤ 8 particles/mL) was very low for all samples and again no trend could be assessed with storage time or storage temperature (Figure 7-7B and 7-7C).

The residual moisture levels of all lyophilisates increased with proceeding storage time and increasing storage temperature (Table 7-2). The lowest residual moisture was observed for lactosucrose formulations, which increased from 0.14% directly after lyophilization to 0.41% when stored for 6 months at 40 °C. In general, 10% sucrose formulations showed higher water content (0.56% to 0.8%) compared to 5% sucrose formulations (0.21% to 0.70%). Correspondingly, the T_g values decreased with proceeding storage time and increasing storage temperature (Table 7-2). Lactosucrose formulations yielded the highest T_g values between 97.8 °C and 86.5 °C. In accordance with the observed water content, 5% sucrose formulations showed slightly higher T_g (58.4 °C to 52.4 °C), compared to 10% sucrose formulations (56.2 °C to 47.9 °C). All lyophilisates were completely amorphous after storage over 6 month as no signs of crystallinity were observed by X-ray powder diffraction (data not shown).

4 Discussion

The standard method to prepare siRNA polyplexes is to mix siRNA and polymer solutions via pipetting at small volumes. The quality of the particles obtained via this poorly controlled and standardized process highly depends on the preparation conditions, like the way of admixing, or pipette handling inconsistencies among different operators [16, 34, 36-37]. Therefore, a controlled and easily up-scalable micro-mixer method that had recently been established for the preparation of plasmid/LPEI polyplexes [34], was successfully transferred to the preparation of siRNA polyplexes. Both siRNA/oligomer **332** and siRNA/oligomer **49** polyplexes, prepared with the micro-mixer method at large volume (5 mL), showed similar particle size, slightly improved polydispersity and similar gene silencing efficiency, as compared to systems prepared via pipetting at common small volumes (150 μ L). It is known from our previous study [34] that at larger volumes, the heterogeneity of polymer-based gene delivery particles is even more pronounced, when prepared via pipetting. But larger sample volumes of polyplexes with a defined quality are necessary for adequate formulation development, preclinical and clinical studies. Moreover, our results showed that the micro-mixer method is well suited for the standardized and reproducible preparation of plasmid DNA, siRNA and thus, presumably, also oligonucleotide polyplexes. Analogous methods have also been successfully introduced for the preparation of cationic lipopolyplexes [20, 36].

It is known that particle stability can be negatively influenced during freezing [28, 38]. This results from cryoconcentration as ice separates, rendering a complex and solute rich liquid phase with increased risk of particle association at reduced interparticle distance [28, 39-40]. Moreover, interaction of the particles with the formed ice-liquid interfaces [41], selective crystallization of

buffer components, leading to a pH shift [42], or mechanical damage of the particles by the growing ice or excipient crystals [40], can affect particle stability. Freeze-thawing experiments demonstrated a drastic increase in particle size and polydispersity of siRNA/oligomer **332** polyplexes in the absence of stabilizers. A similar effect is also reported for DNA-based DOTAP/DOPE [43] or PEGylated lipoplexes [24], and PDMAEMA [23, 44] or LPEI [25] polyplexes, if formulated without stabilizer. In contrast, in the absence of stabilizers siRNA/oligomer **49** polyplexes were completely stable against freezing induced stresses. The preservation of particle size upon freeze-thawing is also reported for siRNA-based DOTAP/DOPE lipoplexes [32] and in addition for DNA- and siRNA- low molecular weight PEI complexes [45]. Thus, the question arises on what causes this substantial difference in particle stability upon freezing.

In order to approve or disapprove the hypothesis that the polyplex-stabilizing intermolecular disulfide bridges between the cysteines of oligomer **49** might be responsible for the unexpectedly high colloidal stability, oligomer analogs were investigated. It is well-established that the presence of cysteine groups in the systems is essential for efficient DNA and siRNA delivery [15, 35]. In this case, intra-particulate disulfide bridge formation increases the polyplex stability and inhibits particle dissociation during cellular uptake. However, neither blockage nor substitution of the cysteines in oligomer **49** reduced the high colloidal stability of the particles. Thus the presence of disulfide bridges was not essential for the polyplex formulation stability. Moreover, the addition of cysteines to oligomer **332** did not improve colloidal particle stability upon freeze-thawing. This indicates that different mechanisms are involved regarding the stabilization of an individual polyplex particle and the inter-particulate colloidal stability of polyplex particles.

Besides the general discrepancy in the chemical structure of the two oligomers, the particle size of the corresponding polyplexes significantly differs, with

~150 nm for siRNA/oligomer **332** polyplexes and ~20nm for siRNA/oligomer **49** polyplexes. This might be one important factor governing particle stability upon freeze-thawing. This hypothesis is supported by the afore cited literature, where an increase in particle size upon freeze-thawing was observed for all particles with sizes of ~ 125 to 250 nm [23-25, 43-44], whereas particle size was maintained for all complexes with ~ 30 to 60 nm [32, 45]. During freezing, the formation and the further growth of ice crystals results in cryoconcentration of the sample within the interstitial region. Depending on the initial solute concentration of the sample and the presence or absence of microcollapse the thickness of the interstitial region roughly varies between ~100 nm and ~1 μ m [46]. Although the absolute number of particles with an increase in diameter is reduced at a fixed ratio of polymer to siRNA, the general probability of particle collision in these narrow channels might be increased for larger particles. Moreover, it could be possible that larger particles could get stuck at very narrow parts of the interstitial region, which might promote particle agglomeration.

Another possible explanation for the different aggregation behavior of the two siRNA polyplexes might be their potential to stabilize interactions among individual particles. In the case of the oligotyrosine containing oligomer **332**, the interaction between individual particles and the stabilization of these inter-particulate interactions might be favored due to the strong pi interactions among the aromatic amino acid residues, known as pi-pi stacking [47-48]. siRNA oligomer **49** polyplexes might also get into contact with each other during cryoconcentration, but in this case, the stabilization of the inter-particulate interactions to “stable” agglomerates might not be favored and the agglomerates might dissociate again to the original particles size upon thawing.

In order to stabilize siRNA/oligomer **332** polyplexes against freezing induced stresses, only low amounts of sucrose, trehalose and lactosucrose were necessary and these stabilizers showed similar potential. In contrast, HP- β -CD significantly affected the polyplexes, which is discussed below. Thus, in accordance with literature [21, 28], the mass ratio of polyplex to amorphous matrix material is more critical than the choice of stabilizer, apart from cyclodextrins. For the stabilization of siRNA/oligomer **332** polyplexes, 7% [m/V] of stabilizer was required to fully maintain particle size, corresponding to a stabilizer/siRNA ratio of 700. In comparison, a stabilizer/DNA mass ratio of 4000 was necessary to stabilize plasmid/LPEI polyplexes [25]. Even higher stabilizer/DNA ratios of 7500 [49] or 10000 [19] were reported for the adequate protection of DNA/PEI polyplexes. However, a comparable stabilizer/DNA ratio of 1250 was sufficient for the preservation of DMAEMA polyplexes [23]. However, until now, no detailed studies on stabilizer to siRNA ratios in order to retain the particle size of siRNA based gene delivery complexes were available. Various mechanisms, such as preferential exclusion [50], vitrification [50] and particle isolation [51], are discussed in order to explain how cryoprotectants can preserve non-viral gene delivery particles during freezing. It is still not clear, whether the preferential exclusion hypothesis [52], according to which proteins are stabilized by a solvent layer that is formed around the macromolecules, can be transferred to the stabilization of non-viral gene delivery particles [50]. According to the vitrification hypothesis, non-viral gene delivery particles are immobilized in the highly viscous glassy matrix, when samples are cooled below T_g [17, 53-54]. Additionally the particles may be stabilized by isolation as crowding of particles favors their aggregation and a critical stabilizer/particle ratio that leads to a certain degree of spatial separation of the particles is necessary for full particle protection [51].

The high stabilizer/particle ratios that are required for certain gene delivery particles initiated the introduction of higher molecular weight excipients [22, 24-25, 55], in order to ensure low osmolarity, when applying formulation containing higher masses of stabilizer. For example, stabilization of plasmid/LPEI polyplexes in isotonic formulations could only be achieved by using oligosaccharides, such as lactosucrose or a combination of HP- β -CD with sucrose [25]. siRNA/oligomer **332** polyplexes were also well protected against freeze-thawing stress using lactosucrose. However, comparable particle stabilization could also be achieved with the commonly used disaccharides sucrose and trehalose, without markedly exceeding the isotonicity level.

The presence of HP- β -CD strongly influenced particle size and polydispersity of both, fresh and freeze-thawed, siRNA polyplexes. For siRNA/oligomer **332** polyplexes a pronounced increase in particle size was induced, whereas siRNA/oligomer **49** polyplexes dissociated. Both formulations displayed an increase in polydispersity. The effect might be caused by the insertion of the lipophilic oleic acid moiety of the oligomer into the lipophilic cavities of the cyclodextrin molecules. In the case of siRNA/oligomer **332** polyplexes, the remaining tyrosines supporting strong and attractive pi-pi interactions [47-48] outside the cavity, may lead to the formation of large aggregates. In the case of siRNA/oligomer **49** polyplexes, the formation of cyclodextrin inclusion of the oleic acid chains induces the disruption of the polyplexes into small fragments. Thus, interactions based on the poorly water soluble lipophilic moiety appear to be essential for particle formation and stability. In this freeze-thaw study the cyclodextrin stock solution was added to the siRNA/oligomer **49** polyplexes after incubation for 30 min, when still about 75% of the free thiol groups were present [15] and the formed disulfide bonds do not provide sufficient stabilization of the polyplexes.

T_g values for the selected sucrose and lactosucrose samples were in good accordance with literature [34, 56]. The higher T_g for lactosucrose formulations, compared to sucrose formulations, can be explained by the Fox-Flory theory [57], according to which the T_g increases with increasing molecular weight of the excipient. This increased T_g would allow primary drying at elevated temperatures, reducing time and cost of lyophilization processes.

Lyophilization experiments confirmed the need of small amounts of stabilizers, in order to maintain the particle size of siRNA/oligomer **332** polyplexes. It is well established that stabilizers act not only in the course of freezing, but stabilize particles in the dry state via entrapment of the particles in a glassy matrix, which allows particle separation and inhibits particle collision, known as “vitrification hypothesis” [50]. Additionally, the “water replacement hypothesis” is discussed for protection against dehydration induced stresses, according to which the stabilizer molecules replace the escaping water by direct interaction with the particle surface [50]. Again, siRNA/oligomer **49** polyplexes showed unexpectedly high stability and even in the case of gross collapse due to absence of any stabilizer, the polyplexes did not show any tendency to aggregate. However, all samples lyophilized without stabilizers did not form a proper cake, which is required for pharmaceutically acceptable lyophilized products, and exhibited longer reconstitution times.

For all formulations, the polyplex particle size was not significantly changed after lyophilization, compared to samples analyzed after freeze-thawing. This indicates that the predominant stress factor for siRNA polyplexes during lyophilization is the freezing step, and not the drying phase. This is in accordance with literature on DNA lipoplexes [51] and DNA/LPEI polyplexes [25]. In contrast, Yadava et al. [32] reported a dramatic increase in size for siRNA lipoplexes after lyophilization in the absence of stabilizers and a slight

increase in presence of sucrose or glucose, whereas in none of the formulations the particle size was affected by freeze-thawing.

In comparison, Yadava et al. [32] could limit the size increase only to 43% or 320% for their lyophilized lipoplex formulations, when formulated with 5% glucose or 9.5% sucrose, respectively. Andersen et al. [31] showed that 10% sucrose was required for sufficient stabilization of siRNA/chitosan particles during lyophilization. Werth et al. [33] reported that siRNA polyplexes, based a low molecular weight PEI, can be lyophilized in the presence of 5% glucose, but a slight broadening of particle size distribution was observed based on AFM measurements. Thus, in our study, it is the first time that non-viral siRNA gene delivery particles could be successfully lyophilized without any limitation.

Lyophilization of formulations at initial “half-isotonic” concentrations, in combination with reconstitution in only half of the initial volume, allowed doubling of the siRNA polyplex concentration for in-vivo and clinical studies, where high concentrations are required, without affecting particle size and gene silencing activity. It is well known that particle size and polydispersity of gene delivery particles increase, when the particles are prepared at higher concentrations [34, 58]. Similarly, the possibility to concentrate plasmid/PEI polyplexes, formulated with low molecular weight dextrans by a factor of four, was described by Anchordoquy et al. [22]. Zillies et al. [27] proved that oligonucleotide-loaded gelatin nanoparticles, which required only a rather low stabilizer to particle ratio, could be concentrated even 30-fold without an increase in particle size.

In general, particle size is not only an important quality criterion, but can also affect gene silencing efficiency *in vitro* and *in vivo*. In our study, the size of siRNA/oligomer **332** polyplexes drastically increased after freeze-thawing and lyophilization in the absence of any stabilizer. This correlated with a 2.5 fold

decrease in gene silencing activity. In literature, it is reported that the uptake of larger particles in cell culture experiments might be even increased, due to sedimentation of the larger particles onto the cells [59]. However, in order to achieve successful gene transfer *in vivo*, preservation of particle size is crucial, as large aggregated particles are in general ineffective *in vivo* and can even be toxic due to embolism in the lung [10].

All tested polyplex formulations in the presence of stabilizers were able to maintain gene silencing efficiency after freeze-thawing and lyophilization. This demonstrates that the addition of stabilizers to siRNA/oligomer **332** polyplexes is required not only to maintain particle size, but also to retain gene silencing efficiency. Similar results are reported in literature for siRNA/chitosan particles [31], siRNA/low molecular weight PEI complexes [33] and siRNA lipoplexes [32]. SiRNA/oligomer **49** polyplexes could be lyophilized with preserved gene silencing efficiency in the absence of stabilizers. This can be directly correlated to the maintenance of particle size after lyophilization. Andersen et al. [31] reported that siRNA/*TransIT*-TKO lipoplexes could also effectively induce knockdown after lyophilization in the absence of stabilizer, but did not report the particle size.

For all HP- β -CD/sucrose formulations the changes in particle size for both particle types led to a highly pronounced decrease in gene silencing activity. This effect may not only be ascribed to the change in particle size, but also to the structural alterations within the particles or the perturbed interactions between siRNA and the oligomer [17].

In our storage stability study, variations in gene silencing efficiency and metabolic activity were observed, which did not correlate with storage time or temperature, but instead reflected the common differences between independent cell culture experiments, as the samples were analyzed separately after lyophilization, after 1 month and after 6 months of storage.

The results indicate that the initial sizes and gene silencing efficiencies of both siRNA/oligoaminoamide polyplex formulations could be maintained during storage for 6 months at up to 40 °C, when samples were lyophilized in the presence of appropriate stabilizers. Only Andersen et al. [31] investigated storage stability of lyophilized siRNA gene delivery particles with gene silencing efficiency, but without particle size as quality criterion. The knockdown efficiency of siRNA/*TransIT*-TKA lipoplexes completely vanished and the knockdown efficiency of siRNA/chitosan particles decreased from 67% to 32%, when stored for 2 month at 25 °C.

Moreover, turbidity and number of subvisible particles were investigated to provide a more comprehensive characterization of the formulations. Due to the larger size of the siRNA/oligomer **332** polyplexes, high turbidity values were already observed for fresh preparations, as turbidity scales as the radii to the sixth power [22]. A low turbidity of siRNA/oligomer **332** polyplex samples was only observed after freeze-thawing and lyophilization in the absence of any stabilizer, as in this case polyplexes precipitated. When siRNA/oligomer **332** polyplex lyophilisates were reconstituted in reduced volume, turbidity values approximately doubled. Turbidity values of siRNA/oligomer **49** polyplex formulations were markedly lower at the start and slightly increased after lyophilization. This slight increase in turbidity was also observed for corresponding placebo samples, suggesting that it is caused by a marginal particle formation of the excipients themselves, or due to a particle contamination during the non-aseptic lyophilization process as previously reported [21, 25]. The changes in particle size observed for the HP- β -CD polyplex formulations inversely correlated with the observed turbidity values, with a drastic increase in particle size and decrease in the turbidity for siRNA/oligomer **332** polyplexes due to particle precipitation and a decrease in

particle size and increase in the turbidity of siRNA/oligomer **49** polyplexes due to particle dissociation. In general, the increase in turbidity correlated with an increase in the number of subvisible particles $\geq 1 \mu\text{m}$. All samples met the current standard limits for small volume parenterals specified in the Ph.Eur. [60] or USP [61].

The storage stability of lyophilized formulations strongly correlates with other relevant characteristics of the lyophilisates, such as T_g , water content, or amorphous state. The T_g values of lactosucrose formulations were significantly higher as compared to sucrose formulations, and for both sucrose and lactosucrose, T_g values compared well to literature [25, 62]. The T_g was slightly lower for samples with higher water content as water acts as plasticizer [63]. The increase in water content with increasing storage time and temperature is in accordance with literature [64]. In general, all water contents were very low ($< 1\%$) after storage. Moreover, the investigated storage temperatures did not exceed the T_g of the samples or influence the amorphous state of all samples. This is important, as product vitrification guarantees particle separation and low mobility in the glassy matrix, which is essential for long-term stability [51]. Consequently, lactosucrose might be a beneficial lyoprotectant compared to sucrose, as it can withstand higher residual moisture contents during storing, without the T_g falling below the storage temperature.

5 Conclusion

To summarize, a currently established micro-mixer method was successfully applied to the standardized and reproducible preparation of siRNA/oligoaminoamide polyplexes. This guarantees a constant and defined quality of the particles, especially when prepared at large volumes. Freeze-thawing and freeze-drying studies showed that siRNA/oligotyrosine-oligomer **332** polyplexes required only low amounts of stabilizers (mass ratio of ~700). The type of stabilizer was of minor importance, as sucrose, trehalose and lactosucrose formulations showed similarly good particle preservation. In contrast, siRNA/oligomer **49** polyplexes were stable against freezing and drying induced stresses, even in the absence of any stabilizer. These results showed that siRNA polyplexes are less prone to lyophilization related stresses compared to DNA polyplexes. Further freeze-thawing experiments, using polyplexes based on oligomer analogs, showed that the presence of cysteines which internally stabilize polyplexes by disulfide forming are not responsible for the different colloidal stability of the two siRNA/oligoaminoamide polyplexes. Cyclodextrin was not suitable as stabilizer; destabilization of particles was induced by the formation of inclusion complexes between the lipophilic moieties of oligomers and cyclodextrin cavities. Selected lyophilized formulations maintained particle size and gene silencing efficiency, also when reconstituted with reduced volumes. Furthermore, long-term stability of both siRNA polyplexes, formulated with 5% sucrose, and 10% sucrose, or 7% lactosucrose, was demonstrated, when stored over 6 months up to 40 °C. All freeze-thawed, lyophilized and stored formulations exhibited only slightly altered turbidity values, met the standard limits for particulate contamination for small volume parenterals, and did not markedly exceed isotonicity level. In addition, all lyophilisates were amorphous with low residual moisture contents and sufficiently high glass transition temperature. The well established

lyoprotectants sucrose and trehalose were appropriate for successful lyophilization of siRNA polyplexes. However, the use of oligosaccharides might be advantageous with respect to the achievable concentration level of the samples, the potential of time-, and thus cost-reduction in the lyophilization process, and the potentially better storage stability at higher temperature and moisture levels. In conclusion, lyophilization is a promising approach to achieve long-term stable siRNA polyplexes with maintenance of particle size and gene silencing efficiency at pharmaceutically defined high quality.

6 References

- [1] A. Pathak, S. Patnaik, K.C. Gupta, Recent trends in non-viral vector-mediated gene delivery, *Biotechnol. J.*, 4 (2009) 1559-1572.
- [2] M.L. Edelstein, M.R. Abedi, J. Wixon, Gene therapy clinical trials worldwide to 2007- an update, *J. Gene Med.*, 9 (2007) 833-842.
- [3] R. Almeida, R.C. Allshire, RNA silencing and genome regulation, *Trends Cell Biol.*, 15 (2005) 251-258.
- [4] D.J. Gary, N. Puri, Y.-Y. Won, Polymer-based siRNA delivery: Perspectives on the fundamental and phenomenological distinctions from polymer-based DNA delivery, *J. Controlled Release*, (2007) 64-73.
- [5] P.D. Zamore, T. Tuschl, P.A. Sharp, D.P. Bartel, RNAi: Double-Stranded RNA Directs the ATP-Dependent Cleavage of mRNA at 21 to 23 Nucleotide Intervals, *Cell*, 101 (2000) 25-33.
- [6] L. Aagaard, J.J. Rossi, RNAi therapeutics: Principles, prospects and challenges, *Adv. Drug Deliv. Rev.*, 59 (2007) 75-86.
- [7] J. Wang, Z. Lu, M. Wientjes, J. Au, Delivery of siRNA Therapeutics: Barriers and Carriers, *The AAPS Journal*, 12 (2010) 492-503.
- [8] W. Kim, S. Kim, Efficient siRNA Delivery with Non-viral Polymeric Vehicles, *Pharm. Res.*, 26 (2009) 657-666.
- [9] D. Schaffert, E. Wagner, Gene therapy progress and prospects: synthetic polymer-based systems, *Gene Ther*, 15 (2008) 1131-1138.
- [10] D.W. Pack, A.S. Hoffman, S. Pun, P.S. Stayton, Design and development of polymers for gene delivery, *Nat. Rev. Drug Discov.*, 4 (2005) 581-593.
- [11] M. Meyer, E. Wagner, Recent Developments in the Application of Plasmid DNA-Based Vectors and Small Interfering RNA Therapeutics for Cancer, *Hum. Gene Ther.*, 17 (2006) 1062-1076.
- [12] A. Kwok, S.L. Hart, Comparative structural and functional studies of nanoparticle formulations for DNA and siRNA delivery, *Nanomed. Nanotechnol. Biol. Med.*, 7 (2011) 210-219.
- [13] E. Wagner, Polymers for siRNA Delivery: Inspired by Viruses to be Targeted, Dynamic, and Precise, *Acc. Chem. Res.*, doi: 10.1021/ar2002232 (2012).
- [14] C. Troiber, E. Wagner, Nucleic Acid Carriers Based on Precise Polymer Conjugates, *Bioconjugate Chem.*, 22 (2011) 1737-1752.
- [15] D. Schaffert, C. Troiber, E.E. Salcher, T. Fröhlich, I. Martin, N. Badgujar, C. Dohmen, D. Edinger, R. Kläger, G. Maiwald, K. Farkasova, S. Seeber, K. Jahn-Hofmann,

- P. Hadwiger, E. Wagner, Solid-Phase Synthesis of Sequence-Defined T-, i-, and U-Shape Polymers for pDNA and siRNA Delivery, *Angew. Chem. Int. Ed.*, 50 (2011) 8986-8989.
- [16] T.J. Anchordoquy, G.S. Koe, Physical stability of nonviral plasmid-based therapeutics, *J. Pharm. Sci.*, 89 (2000) 289-296.
- [17] S.D. Allison, T.J. Anchordoquy, Lyophilization of Nonviral Gene Delivery Systems, in: M.A. Findeis (Ed.) *Nonviral Vectors for Gene Therapy: Methods and Protocols*, Humana Press Inc., New York, 2001, pp. 225-252.
- [18] M. Ogris, P. Steinlein, M. Kursa, K. Mechtler, R. Kircheis, E. Wagner, The size of DNA/transferrin-PEI complexes is an important factor for gene expression in cultured cells, *Gene Ther.*, 5 (1998) 1425-1433.
- [19] H. Talsma, J.-Y. Cherng, H. Lehrmann, M. Kursa, M. Ogris, W.E. Hennink, M. Cotten, E. Wagner, Stabilization of gene delivery systems by freeze-drying, *Int. J. Pharm.*, 157 (1997) 233-238.
- [20] J. Clement, K. Kiefer, A. Kimpfler, P. Garidel, R. Peschka-Süss, Large-scale production of lipoplexes with long shelf-life, *Eur. J. Pharm. Biopharm.*, 59 (2005) 35-43.
- [21] T.J. Anchordoquy, J.F. Carpenter, D.J. Kroll, Maintenance of Transfection Rates and Physical Characterization of Lipid/DNA Complexes after Freeze-Drying and Rehydration, *Arch. Biochem. Biophys.*, 348 (1997) 199-206.
- [22] T.J. Anchordoquy, T.K. Armstrong, M.d.C. Molina, Low molecular weight dextrans stabilize nonviral vectors during lyophilization at low osmolalities: concentrating suspensions by rehydration to reduced volumes, *J. Pharm. Sci.*, 94 (2005) 1226-1236.
- [23] J.-Y. Cherng, P. van de Wetering, H. Talsma, D.J.A. Crommelin, W.E. Hennink, Freeze-Drying of Poly((2-dimethylamino)ethyl Methacrylate)-Based Gene Delivery Systems, *Pharm. Res.*, 14 (1997) 1838-1841.
- [24] W.L.J. Hinrichs, F.A. Manceñido, N.N. Sanders, K. Braeckmans, S.C. De Smedt, J. Demeester, H.W. Frijlink, The choice of a suitable oligosaccharide to prevent aggregation of PEGylated nanoparticles during freeze thawing and freeze drying, *Int. J. Pharm.*, 311 (2006) 237-244.
- [25] J.C. Kasper, D. Schaffert, M. Ogris, E. Wagner, W. Friess, Development of a lyophilized plasmid/LPEI polyplex formulation with long-term stability- A step closer from promising technology to application, *J. Controlled Release*, 151 (2011) 246-255.
- [26] C. Brus, E. Kleemann, A. Aigner, F. Czubayko, T. Kissel, Stabilization of oligonucleotide-polyethylenimine complexes by freeze-drying: physicochemical and biological characterization, *J. Controlled Release*, 95 (2004) 119-131.
- [27] J.C. Zillies, K. Zwioerek, F. Hoffmann, A. Vollmar, T.J. Anchordoquy, G. Winter, C. Coester, Formulation development of freeze-dried oligonucleotide-loaded gelatin nanoparticles, *Eur. J. Pharm. Biopharm.*, 70 (2008) 514-521.

- [28] W. Abdelwahed, G. Degobert, S. Stainmesse, H. Fessi, Freeze-drying of nanoparticles: Formulation, process and storage considerations, *Adv. Drug Delivery Rev.*, 58 (2006) 1688-1713.
- [29] S. Wu, L. Putral, M. Liang, H.-I. Chang, N. Davies, N. McMillan, Development of a Novel Method for Formulating Stable siRNA-Loaded Lipid Particles for in-vivo use, *Pharm. Res.*, 26 (2009) 512-522.
- [30] A.K. Kundu, P.K. Chandra, S. Hazari, G. Ledet, Y.V. Pramar, S. Dash, T.K. Mandal, Stability of lyophilized siRNA nanosome formulations, *Int. J. Pharm.*, 423 (2012) 525-534.
- [31] M.Ø. Andersen, K.A. Howard, S.R. Paludan, F. Besenbacher, J. Kjems, Delivery of siRNA from lyophilized polymeric surfaces, *Biomaterials*, 29 (2008) 506-512.
- [32] P. Yadava, M. Gibbs, C. Castro, J. Hughes, Effect of Lyophilization and Freeze-thawing on the Stability of siRNA-liposome Complexes, *AAPS PharmSciTech*, 9 (2008) 335-341.
- [33] S. Werth, B. Urban-Klein, L. Dai, S. Höbel, M. Grzelinski, U. Bakowsky, F. Czubyko, A. Aigner, A low molecular weight fraction of polyethylenimine (PEI) displays increased transfection efficiency of DNA and siRNA in fresh or lyophilized complexes, *J. Controlled Release*, 112 (2006) 257-270.
- [34] J.C. Kasper, D. Schaffert, M. Ogris, E. Wagner, W. Friess, The establishment of an up-scaled micro-mixer method allows the standardized and reproducible preparation of well-defined plasmid/LPEI polyplexes, *Eur. J. Pharm. Biopharm.*, 77 (2011) 182-185.
- [35] T. Fröhlich, D. Edinger, R. Kläger, C. Troiber, E. Salcher, N. Badgajar, I. Martin, D. Schaffert, A. Cengizerogly, P. Hadwiger, H.-P. Vornlocher, E. Wagner, Structure-activity relationships of siRNA carriers based on sequence-defined oligo (ethane amino) amides, (manuscript in revision).
- [36] O. Zelphati, C. Nguyen, M. Ferrari, J. Felgner, Y. Tsai, P.L. Felgner, Stable and monodisperse lipoplex formulations for gene delivery, *Gene Ther*, 5 (1998) 1272-1282.
- [37] M.T. Kennedy, E.V. Pozharski, V.A. Rakhmanova, R.C. MacDonald, Factors governing the assembly of cationic phospholipid-DNA complexes, *Biophys. J.*, 78 (2000) 1620-1633.
- [38] T.J. Anchordoquy, S.D. Allison, M.d.C. Molina, L.G. Girouard, T.K. Carson, Physical stabilization of DNA-based therapeutics, *Drug Discov. Today*, 6 (2001) 463-470.
- [39] F. Franks, Freeze-drying of bioproducts: putting principles into practice, *Eur. J. Pharm. Biopharm.*, 45 (1998) 221-229.
- [40] X. Tang, M. Pikal, Design of Freeze-Drying Processes for Pharmaceuticals: Practical Advice, *Pharm. Res.*, 21 (2004) 191-200.
- [41] C. Körber, G. Rau, M.D. Cosman, E.G. Cravalho, Interaction of particles and a moving ice-liquid interface, *J. Crystl. Growth*, 72 (1985) 649-662.

- [42] K.A. Pikal-Cleland, Rodri , amp, x, N. guez-Hornedo, G.L. Amidon, J.F. Carpenter, Protein Denaturation during Freezing and Thawing in Phosphate Buffer Systems: Monomeric and Tetrameric β -Galactosidase, *Arch. Biochem. Biophys.*, 384 (2000) 398-406.
- [43] T.J. Anchordoquy, L.G. Girouard, J.F. Carpenter, D.J. Kroll, Stability of lipid/DNA complexes during agitation and freeze-thawing, *J. Pharm. Sci.*, 87 (1998) 1046-1051.
- [44] J.Y. Cherng, P.v.d. Wetering, H. Talsma, D.J.A. Crommelin, W.E. Hennink, Stabilization of polymer-based gene delivery systems, *Int. J. Pharm.*, 183 (1999) 25-28.
- [45] S. Höbel, R. Prinz, A. Malek, B. Urban-Klein, J. Sitterberg, U. Bakowsky, F. Czubayko, A. Aigner, Polyethylenimine PEI F25-LMW allows the long-term storage of frozen complexes as fully active reagents in siRNA-mediated gene targeting and DNA delivery, *Eur. J. Pharm. Biopharm.*, 70 (2008) 29-41.
- [46] J. Liu, Physical Characterization of Pharmaceutical Formulations in Frozen and Freeze-Dried Solid States: Techniques and Applications in Freeze-Drying Development, *Pharm. Dev. Technol.*, 11 (2006) 3-28.
- [47] C.A. Hunter, J.K.M. Sanders, The nature of pi-pi interactions, *J. Am. Chem. Soc.*, 112 (1990) 5525-5534.
- [48] R. Chelli, F.L. Gervasio, P. Procacci, V. Schettino, Stacking and T-shape Competition in Aromatic- Aromatic Amino Acid Interactions, *J. Am. Chem. Soc.*, 124 (2002) 6133-6143.
- [49] M.d.C. Molina, S.D. Allison, T.J. Anchordoquy, Maintenance of nonviral vector particle size during the freezing step of the lyophilization process is insufficient for preservation of activity: Insight from other structural indicators, *J. Pharm. Sci.*, 90 (2001) 1445-1455.
- [50] S.D. Allison, J.A. Thomas, Mechanisms of protection of cationic lipid-DNA complexes during lyophilization, *J. Pharm. Sci.*, 89 (2000) 682-691.
- [51] S.D. Allison, M.d.C. Molina, T.J. Anchordoquy, Stabilization of lipid/DNA complexes during the freezing step of the lyophilization process: the particle isolation hypothesis, *Biochim. Biophys. Acta, Biomembr.*, 1468 (2000) 127-138.
- [52] J.F. Carpenter, J.H. Crowe, The mechanism of cryoprotection of proteins by solutes, *Cryobiology*, 25 (1988) 244-255.
- [53] T.J. Anchordoquy, T.K. Armstrong, M.D.C. Molina, S.D. Allison, Y. Zhang, M.M. Patel, Y.K. Lentz, G.S. Koe, Formulation considerations for DNA-based therapeutics, in: D.R. Lu, S. Oeie (Eds.) *Cellular Drug Delivery*, Humana Press Inc. , Totowa, 2004, pp. 237-263.
- [54] T.K. Armstrong, T.J. Anchordoquy, Immobilization of nonviral vectors during the freezing step of lyophilization, *J. Pharm. Sci.*, 93 (2004) 2698-2709.
- [55] W.L.J. Hinrichs, N.N. Sanders, S.C. De Smedt, J. Demeester, H.W. Frijlink, Inulin is a promising cryo- and lyoprotectant for PEGylated lipoplexes, *J. Controlled Release*, 103 (2005) 465-479.

- [56] S.P. Duddu, P.R. Dal Monte, Effect of Glass Transition Temperature on the Stability of Lyophilized Formulations Containing a Chimeric Therapeutic Monoclonal Antibody, *Pharm. Res.*, 14 (1997) 591-595.
- [57] T.G. Fox, P.J. Flory, Second-Order Transition Temperatures and Related Properties of Polystyrene. I. Influence of Molecular Weight, *J. Appl. Phys.*, 21 (1950) 581-591.
- [58] J.G. Duguid, C. Li, M. Shi, M.J. Logan, H. Alila, A. Rolland, E. Tomlinson, J.T. Sparrow, L.C. Smith, A Physicochemical Approach for Predicting the Effectiveness of Peptide-Based Gene Delivery Systems for Use in Plasmid-Based Gene Therapy, *Biophys. J.*, 74 (1998) 2802-2814.
- [59] E.C. Cho, Q. Zhang, Y. Xia, The effect of sedimentation and diffusion on cellular uptake of gold nanoparticles, *Nat. Nano*, 6 (2011) 385-391.
- [60] 2.9.19. Particulate contamination: sub-visible particles, in: *European Pharmacopoeia* 2008, pp. 300-302.
- [61] <788>, Particulate matter in injections, in: *United States Pharmacopeia*, 2010.
- [62] M.d.C. Molina, T.K. Armstrong, Y. Mayank, Z.M. Patel, Y.K. Lentz, T.J. Anchordoquy, The Stability of lyophilized lipid/DNA complexes during prolonged storage, *J. Pharm. Sci.*, 93 (2004) 2259-2273.
- [63] B.C. Hancock, G. Zografi, The Relationship Between the Glass Transition Temperature and the Water Content of Amorphous Pharmaceutical Solids, *Pharm. Res.*, 11 (1994) 471-477.
- [64] J. Yu, T.J. Anchordoquy, Effects of moisture content on the storage stability of dried lipoplex formulations, *J. Pharm. Sci.*, 98 (2009) 3278-3289.

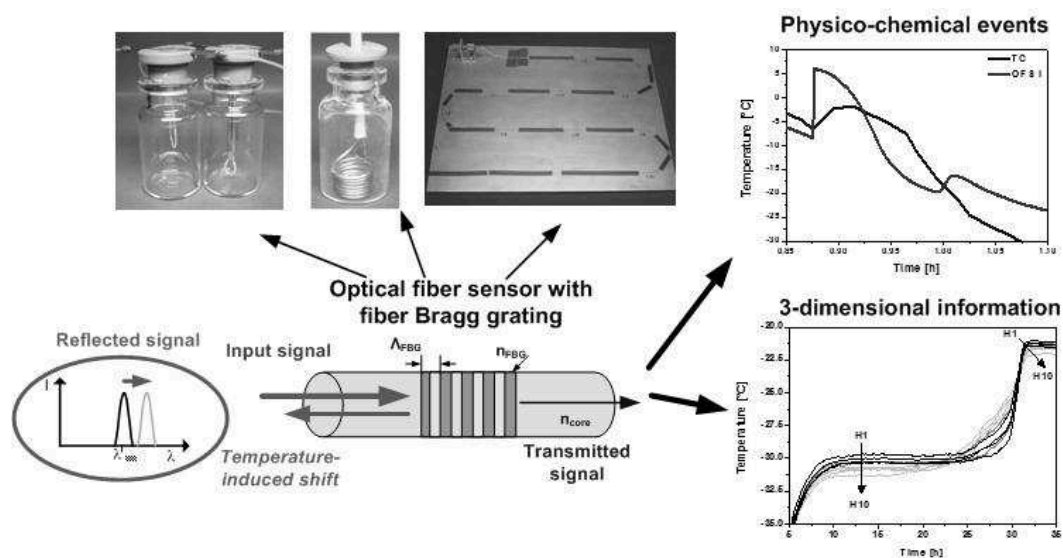
Chapter 8

Implementation and evaluation of an optical fiber system as novel process monitoring tool during lyophilization

The following chapter is intended for publication:

Julia Christina Kasper, Michael Wiggenghorn, Manfred Resch, Wolfgang Friess
Implementation and evaluation of an optical fiber system as novel process monitoring tool during lyophilization; *submitted*.

Graphical Abstract



Abstract

Lyophilization is an important and well-established pharmaceutical drying process. Product temperature is the most critical process parameter during lyophilization as it impacts both product quality and process efficiency. Traditionally, thermocouples (TC) or resistance temperature detectors (RTD) and recently, manometric temperatures measurements (MTM) have been used to monitor the product temperature. But all of these techniques have several drawbacks. The objective of this study was the implementation and evaluation of an optical fiber system as novel process monitoring tool during lyophilization. Therefore, temperature profiles of mannitol, sucrose or trehalose were recorded with various prototypes of the optical fiber sensors (OFS) and compared to data obtained with conventional TCs or Pirani/capacitance manometry with respect to the endpoint of primary drying. The OFS allowed easy handling and easy center bottom positioning. Data obtained with the OFS in contact with product were in good agreement with data obtained via TCs or Pirani/capacitance manometry. The OFSs showed significantly higher sensitivity, faster response and better resolution compared to TCs. This allowed for the detection of additional excipient crystallization events. It was found that force effects on unshielded sensors enabled to detect glass transitions. Three-dimensional temperature profiles were obtained with an OFS helix configuration. The possible integration of a glass fiber with several OFSs in series into the shelf surface enables non-invasive, automatic loading compatible monitoring of the drying process. In conclusion, these advantages turn the novel optical fiber systems into a highly attractive process monitoring tool during lyophilization.

Keywords

Freeze-drying, lyophilization, PAT, process monitoring, optical fiber sensors

1 Introduction

Freeze-drying also known as lyophilization is a common, well-established drying process to improve the long-term stability of labile pharmaceuticals, such as proteins or nucleic acids [1-3]. The concept of freeze-drying is based on the sublimation of ice from a frozen product at low temperature and reduced pressure [4]. A traditional lyophilization process consists of three major steps: freezing, primary and secondary drying [5-6]. During freezing, most of the water will form ice crystals and the solutes are concentrated until they crystallize or transform into a solid amorphous state [5-6]. In the course of primary drying, pressure in the product chamber is reduced and shelf temperature is increased to provide sufficient energy that is needed for sublimation of the formed ice [1]. Primary drying is complete when all frozen water is removed [1]. However, at this stage non-frozen water is still absorbed in the interstitial region and has to be desorbed in a secondary drying step at elevated shelf temperature and low chamber pressure, to finally achieve the desired low residual moisture content [5].

Lyophilization is an extremely time- and thus cost-intensive drying process [4]. For that reason, process development efforts aim to design well-understood and more efficient lyophilization processes. In a Food and Drug Administration's (FDA) guidance for industry [7] the concept of "Process Analytical Technology" (PAT) was established. Its main objective is to enhance scientific understanding and control of the manufacturing process through timely measurements of critical quality and process attributes, with the goal to consistently ensure a predefined final product quality (Quality by Design) [7-8]. In order to fulfill this objective the implementation of PAT tools, such as process analyzers or process control tools, is required [7, 9].

Therefore, various PAT-tools have been implemented to monitor and control the lyophilization process. Batch methods comprise spectroscopy based

measurements such as tunable diode laser absorption spectroscopy (TDLAS), mass spectrometry or other residual gas analyzers, manometric temperature measurement (MTM), and Pirani/capacitance manometry [9-11]. Single vial methods comprise near infrared (NIR) or Raman spectroscopy, temperature, conductivity or moisture sensors, microbalance technique, and offline analytics after sampling [9-11].

As product temperature is undisputable the main critical parameter during lyophilization, product temperature monitoring is the most important and most often applied technique [11]. In general, product temperature, which depends on the shelf temperature, the chamber pressure, the container system and other formulation properties, cannot be directly controlled [12]. In order to prevent product collapse product temperature is maintained below the critical temperature of the formulation. This is the glass transition temperature (T_g) or the collapse temperature (T_c) for amorphous systems, and the eutectic temperature (T_{eu}) for crystalline systems [1, 3]. Product collapse may negatively influence product properties such as residual moisture content, reconstitution time or stability of the active pharmaceutical ingredient (API) but will also lead to product rejections because of unaesthetic appearance [2, 13].

Traditionally, 100-ohm platinum resistance temperature detectors (RTDs) or type T copper-constantan thermocouples (TCs) have been used to measure product temperature in a few selected vials [11, 14]. RTDs, that are preferred in manufacturing because of their chemical inertness and mechanical robustness, disadvantageously require an electrical current for measurement of the temperature dependent electrical resistance, which might cause elevated heat transfer to the product. Moreover, the large mass of the sensing tip results in an average temperature across the length of the tip rather than at a precise location, which might be troublesome with small product container or low fill volumes [14-15]. TCs, which are more frequently used in laboratory scale

freeze-dryers, have the advantage that they allow temperature measurements at the precise location of the junction of the two dissimilar metal wires, where a temperature related voltage is generated. However, TCs pose the risk of chemical erosion leading to sterility concerns [14].

One main disadvantage for product temperature measurements with RTDs or TCs is the fact that these sensors are not compatible with automatic loading systems during manufacturing scale freeze-drying [8]. Therefore, wireless temperature sensors have been developed [15-18]. "Active sensors" require batteries and data is only available after the run [17], or they are connected to a power module inside the product chamber [16]. "Passive transponders" allow to circumvent these problems but the number of available sensors is limited and their distance from the receiver can become critical in large freeze-driers [15, 18]. Another main disadvantage that holds true for any invasive thermo-sensor is its influence on ice nucleation and heat transfer, thereby causing bias in both freezing and drying behavior relative to vials not containing sensors. Thus vials bearing sensors may not be representative for the entire batch [8, 11].

Manometric temperature measurement (MTM) is capable of non-invasive prediction of the product temperature at the sublimation interface of a vial reflecting the batch average. With this technique, the valve connecting the chamber and the condenser is closed momentarily (~25s) and the pressure rise in the chamber is recorded over time [11]. By fitting a MTM equation to the pressure data [19], an average temperature of the entire batch can be obtained. But MTM delivers data that is often biased towards colder running vials [20] and only representative in the first 2/3 of primary drying [21]. Furthermore, MTM is not reliable when processing high concentration amorphous samples [22], is currently only available on production scale [22], and cannot be used for monitoring of heterogeneities in a batch like "edge vial effects" [23].

Besides the assurance that the critical product temperature will not be exceeded during drying, product temperature measurements are also used to detect the endpoint of drying [11]. The endpoint is commonly defined by the time point when product temperature is equivalent to the shelf temperature or (in case of elevated radiative heat transfer to the product) when the temperature reading is higher than the shelf temperature and constant over time [15].

More recently, researchers more and more stress the importance of the freezing step in lyophilization [24-29]. The freezing step does not only influence process performance during primary and secondary drying, but also sample morphology, stability of the API as well as physical state of the product [25]. Product temperature measurement is one of the few direct, in-line analytical tools in order to get a deeper insight into the freezing behavior.

In conclusion, product temperature measurements during lyophilization are of high importance. However, all available techniques exhibit certain disadvantages such as invasive sample placement, lack of sensitivity, risk of corrosion, sterility concerns, incompatibility with automatic loading systems, or measurement inaccuracies. Consequently, there is an urgent need for new temperature measurement technologies that overcome at least one or some of the disadvantages of the aforementioned temperature monitoring devices.

The objective of this study was the implementation of an optical fiber system [30], that is based on fiber Bragg gratings (FBGs), as a novel process monitoring tool during lyophilization. Several different design variations of the optical fiber sensors (OFSs) were created and evaluated for their potential use in product temperature monitoring during lyophilization and freezing experiments in comparison to conventional T-type thermocouples. At first, the general suitability of the OFSs for product temperature measurements and end point detection during lyophilization was investigated. Moreover, the sensitivity of the OFS to detect physico-chemical events during freezing such as ice

nucleation, crystallization of crystalline or glass formation of amorphous excipients was examined. In addition, the influence of the shielding or unshielding of the OFS on temperature profiles was studied. An OFS helix was tested for the detection of three-dimensional temperature profiles. Furthermore, two additional design variations of the OFS were evaluated for their use as non-invasive temperature measurement devices.

2 Materials and methods

2.1 Materials

5, 10 or 20 % [m/V] solutions of the common lyophilization excipients D(-)-mannitol (Riedel-de Haën, Seelze, Germany), trehalose (Hayashibara, Okayama, Japan) or sucrose (Südzucker, Mannheim, Germany), were used as model formulations. Purified water (ELGA LabWater, Celle, Germany) served as solvent for all solutions. All model formulations were filtered with 0.2 μm cellulose acetate membrane syringe filters (VWR International GmbH, Ismaning, Germany). 2R or 6R glass vials (Fiolax™ clear, Schott, Müllheim, Germany) with corresponding rubber stoppers (West, Eschweiler, Germany) at 1, 2 or 4 mL filling volume were used.

2.2 The optical fiber system

The optical fiber system [30] consists of a FBG suitable optical fiber that is guided via a connection fiber through one of the flanges on the top of the freeze-drier into the product chamber. Outside the freeze-drier, the fiber is connected to an interrogation unit, which acts as laser light source and detector at the same time. The interrogator is coupled to a computer with special software for in process data evaluation.

2.2.1 Optical fiber sensor (OFS) structure and characteristics

The heart of the novel system is the optical fiber itself. The optical fiber is a hair-thin cylindrical filament made of glass that is able to guide light by its assembly of three different regions with different refractive indices (Figure 8-1A). In the central position is the fiber core (6 μm in diameter) made of highly transparent germanium-doped silicate. A region having a lower refractive index, the cladding (125 μm in diameter), surrounds the fiber core. Due to this lower refractive index of the cladding light is entrapped inside the fiber core and is

guided along the fiber via total internal reflection. A coating made of Ormocer™, an inorganic polymer material that is obtained by controlled hydrolysis and condensation of organically modified silicium alkoxides, surrounds the cladding (195 μm in diameter), resulting in high tensile strength of the fiber [31].

The key element of the OFS is the FBG, which represents a wavelength-dependent reflector generated by adding a periodic variation to the refractive index within the fiber core (Figure 8-1B).

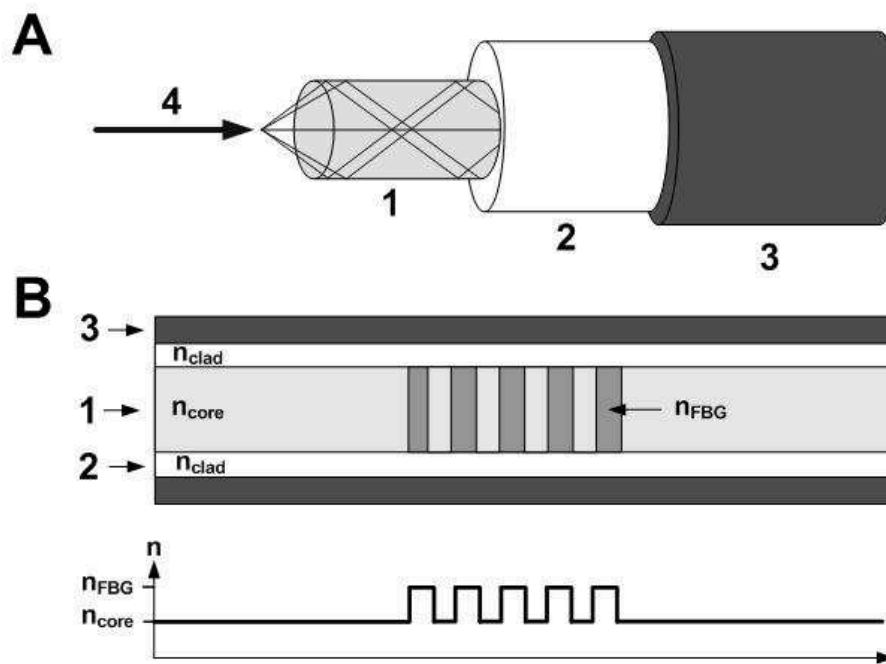


Figure 8-1: Schematic representation of the structure and characteristics of the optical fiber sensor: A) The optical fiber consists of the fiber core (1), the cladding (2) and the coating (3). The laser light (4) is guided by total internal reflection inside the fiber core. B) A Fiber Bragg Grating (FBG) is achieved by adding a periodic variation to the refractive index of the fiber core. This figure was modified from [31].

This is usually achieved by irradiation with spatially-varying pattern of intensive UV-light. The high content of germanium increases the photosensitivity of the material and thus allows the creation of gratings with one excimer laser pulse only. With this single writing technique FBGs can be manufactured directly during the fiber drawing process with excellent reflectivity values (draw tower grating (DTG)) [32]. The total length and number of grating periods in a FBG

depends on the strength or amplitude of the grating. DTGs typically have a sensor length of 5 to 10 mm and a grating period spacing of about 2 mm, which ensures a reflectivity of typically more than 15% using a wavelength in the range about 1550 nm [33].

2.2.2 Operation principle

The operation principle of an OFS is depicted in Figure 8-2.

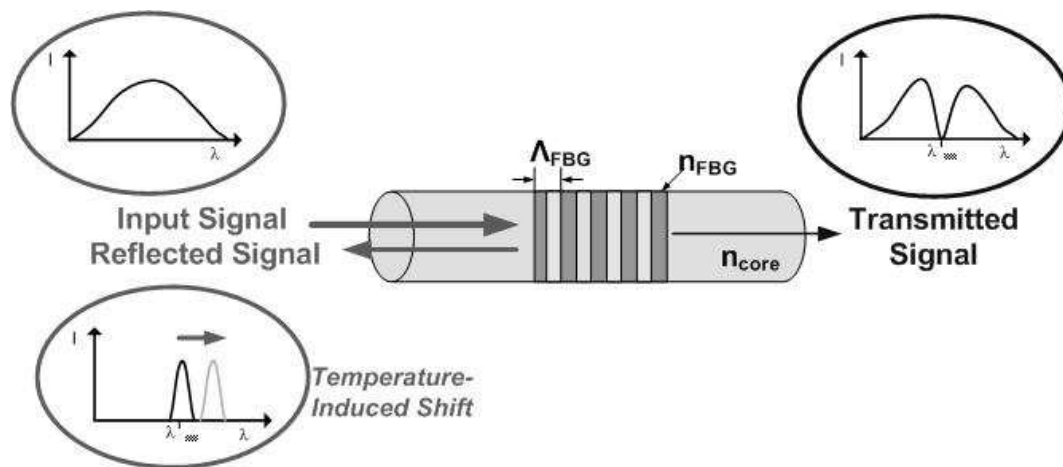


Figure 8-2: Schematic representation of the operation principle of the optical fiber sensor: most of the broad spectrum laser light is transmitted and only a narrow part is reflected at a FBG specific, temperature dependent wavelength (λ_{FBG}). This figure was modified from [31].

The fundamental operation principle is based on Fresnel reflection, where light traveling between media of different refractive indices may both reflect and refract at the interface. Thus, when a broad spectrum laser light beam reaches the FBG most of the light will be transmitted. Only a small portion will be reflected, centered at the Bragg wavelength according to Bragg's law [34]:

$$\lambda_{FBG} = 2 \cdot n \cdot \Lambda \quad (8-1)$$

where λ_{FBG} is the reflected Bragg wavelength, n is the refractive index of the grating in the fiber core and Λ is the grating periodic spacing. Any change in the refractive index of the grating or in the grating periodic spacing (Λ) that is caused by temperature or strain will result in a shift of the Bragg wavelength. In

general, the temperature sensitivity of a FBG is primarily based on the temperature dependence of the refractive index, and to a lesser extent on the thermal expansion of the fiber, changing the grating period spacing. The shift $\Delta\lambda$ in the reflected Bragg wavelength at a certain temperature shift (ΔT) can be specified as

$$\frac{\Delta\lambda}{\lambda_{FBG}} = \left(\frac{\delta\Lambda}{\delta T} + \frac{\delta n}{\delta T} \right) \cdot \Delta T \quad (8-2)$$

where $\frac{\delta\Lambda}{\delta T}$ is the thermal expansion in the material, which is usually $\sim 5 \cdot 10^{-7} \text{ } ^\circ\text{C}^{-1}$, and $\frac{\delta n}{\delta T}$ is the thermo-optic coefficient of the material, which is usually $\sim 8 \cdot 10^{-6} \text{ } ^\circ\text{C}^{-1}$. In this case, formula (2) can be simplified to

$$\frac{\Delta\lambda}{\Delta T} \approx 10 \frac{pm}{^\circ C} \quad (8-3)$$

indicating that the shift in the Bragg wavelength is in the order of 10 pm per 1 $^\circ\text{C}$ [31]. Thus, after a temperature calibration the detected shift in the Bragg wavelength can be directly converted into temperature values.

As each FBG is written at a unique wavelength the use of several FBGs in wavelength division multiplexing techniques (WDM) is possible [34]. In this case, each FBG in series is encoded at a certain section of the input broadband spectrum and the specific Bragg wavelength shift of each FBG can be interrogated individually. Most WDM interrogators use high power sweeping lasers as light source instead of broadband light. The benefits are a longer range due to the high power source, a broader wavelength window for a higher sensor capacity and the possibility to simultaneously interrogate several fibers with several sensors [31].

2.2.3 System and design variations

In this study, a sm130 interrogation unit (Micron Optics, Atlanta, GA, USA) with a high power sweeping laser in the wavelength range from 1510 to 1590 nm, four optical channels, and a scan frequency up to 1kHz (frequency utilized for

measurements was 5 Hz) was used. Data management was performed using the ENLIGHT^{Pro} Sensing Analysis Software (Micron Optics, Atlanta, GA, USA). All raw fibers with DTG achieved FBGs were obtained from FBGS Technologies GmbH (Jena, Germany) and are able to operate in a temperature range from -180 to 200 °C. A single-ended, metal-embedded OFS was obtained from Micron Optics. This OFS has been calibrated (temperature range: -200 to 300 °C, accuracy: ± 0.05 °C, repeatability: ± 0.013 °C) against a NIST traceable platinum resistance thermometer.

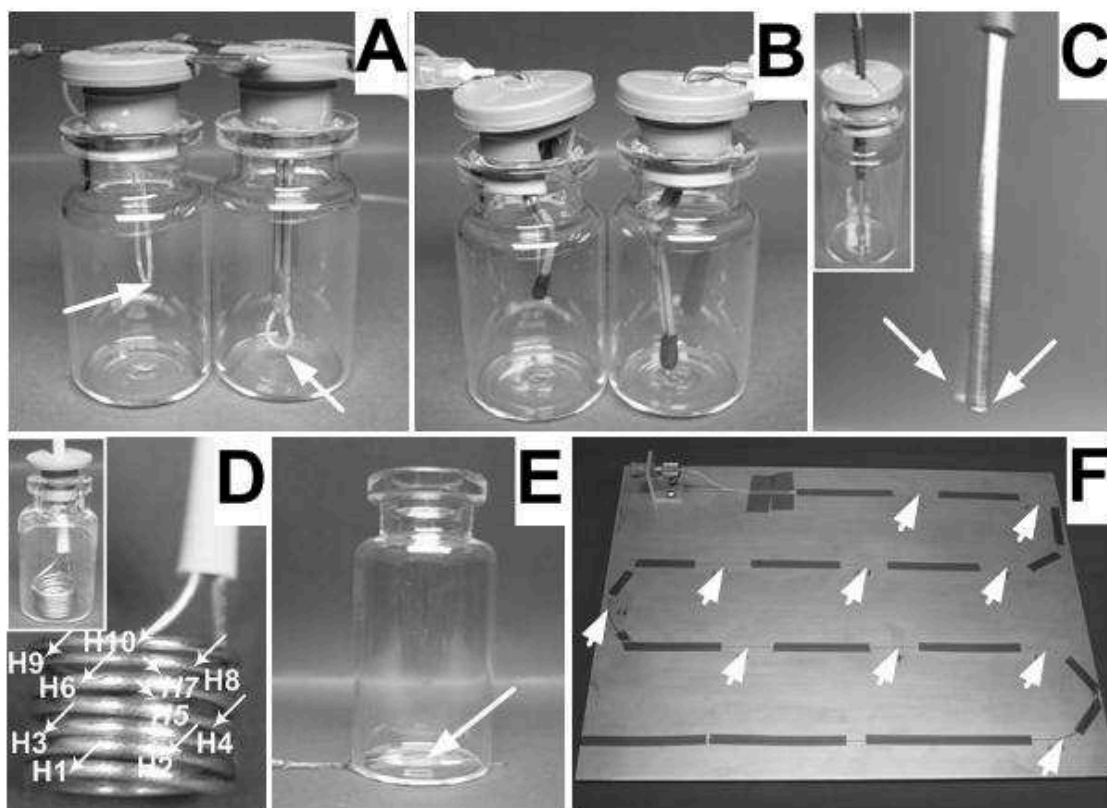


Figure 8-3: Design variations of the optical fiber sensors (OFSs): A) prototype I (OFS I): glass fiber is coated with PTFE and the FBG is fixed in center bottom position (right) or above position (left), B) comparative placement of conventional thermocouples (TCs) in center bottom position (right) and above position (left), C) prototype II (Fix/Flex): the fixed OFS is embedded into a metal tube and a sconded OFS is non-coated and thus very flexible, D) prototype III (Helix): glass fiber with ten FBGs in series is formed to the shape of a helix inside a metal tube, D) prototype IV (OFS IV): glass fiber is fused into the bottom of a 6R vial with the FBG in center bottom position, E) prototype V (Plate): glass fiber with ten FBGs in series is embedded into the surface of a metal plate.

The different design variations of the OFSs used in our study are displayed in Figure 8-3. For prototype I (Figure 8-3A), the glass fiber is covered with a tubular holder made of PTFE and the FBG is fixed at the lower tip of the loop in center bottom position or above position at the lyophilization stopper through metal tubes. In this setup five OFSs (4x center bottom position, 1x above position) were used in series. The comparative placement of conventional T-type thermocouples (PVC insulated, epoxy coated tip, 24 AWG, 36" length) (SP Scientific, Stone Ridge, NY, USA) is displayed in Figure 8-3B. For prototype II (Figure 8-3C), the aforementioned single-ended, metal-embedded OFS was combined with a non-coated, highly flexible OFS in order to investigate the effect of the flexibility of the sensors on temperature readouts. For prototype III (Figure 8-3D), the glass fiber with ten FBGs in series was formed to the shape of a helix inside a metal tube in order to allow the measurement of "three-dimensional" temperature profiles. For prototype IV (Figure 8-3E), the glass fiber was fused into the bottom of a 6R vial with the FBG in center bottom position in order to allow non-invasive temperature measurements from beneath the glass surface of the vial in center bottom position. For prototype V (Figure 8-3F), a glass fiber with ten FBGs in series was embedded into a metal plate in order to allow non-invasive temperature measurements below the vials "at the shelf".

2.3 Temperature calibration

Prototypes I to IV were calibrated in the temperature range from $-50\text{ }^{\circ}\text{C}$ to $+30\text{ }^{\circ}\text{C}$ at $10\text{ }^{\circ}\text{C}$ steps by immersion into an ethanol bath. Therefore, ethanol was pre-cooled in a $-80\text{ }^{\circ}\text{C}$ freezer and transferred into a Dewar vessel. The temperature of the stirred ethanol bath was adjusted by adding pre-heated ethanol. The wavelength of the reflected signal of each FBG was recorded after temperature equilibration for at least 30 min. The NIST calibrated OFS was used as temperature reference.

Prototype V was calibrated by placing the OFS plate onto the shelf of the freeze-drier. In this case, conventional TCs were used as temperature reference. The preset temperature calibration of the conventional T-type thermocouples was verified at -20°C, 0°C and 20°C using the aforementioned ethanol bath. The TCs were in close contact to the FBGs of the glass fiber using heat transfer paste. Subsequently, the shelf temperature was varied from -60 °C to 40 °C and after temperature equilibration for at least 30 min the wavelength of the reflected signal of each FBG was recorded.

For all OFSs the recorded wavelengths were plotted against the reference temperature and a temperature calibration function was obtained by a second order polynomial fit (OriginLab 8.0, Northampton, MA, USA). R^2 of the polynomial fit was always higher than 0.9980.

2.4 Measurement of product temperature profiles during lyophilization and freezing experiments

Several lyophilization cycles (Table 8-1) were performed on a laboratory scale freeze-drier (Lyostar II, FTS Systems, Stone Ridge, NY, USA).

Table 8-1: Lyophilization cycles used for the lyophilization experiments with the various OFS design variations. FV: filling volume, ST 1°: shelf temperature during primary drying, CP 1°: chamber pressure during primary drying, ST 2°: shelf temperature during secondary drying, CP 2°: chamber pressure during secondary drying.

Sample	OFS	FV [ml]	ST 1° [°C]	CP 1° [mtorr]	ST 2° [°C]	CP 2° [mtorr]
10% sucrose	I	1	-15	34	20	8
10% trehalose	III	2	-20	100	30	100
10% trehalose	IV	4	-20	100	30	100
5% mannitol	V	4	-15	34	20	8

The endpoint of primary drying was determined via manometric endpoint determination using a capacitance manometer (MKS Baratron™ Type, MKS Instruments, Wilmington, MA, USA) in combination with a Pirani gauge (Mini-Convectron™ vacuum gauge, Helix Technology Corp., Mansfield MA, USA). In all experiments secondary drying was performed for 8 to 10 hours. In addition to the lyophilization experiments several freezing experiments were performed (Table 8-2).

Table 8-2: Freezing and thawing rates used for the freezing experiments with the various OFS design variations. FV: filling volume.

Sample	OFS	FV [ml]	freezing rate [°C/min]	thawing rate [°C/min]
10% sucrose	I	1	-2.5	
5% mannitol	I	1	-2.5	
20% trehalose	I	4	-2.5	2.5
5% mannitol	II	4	-1	1

In all lyophilization and freezing experiments, samples were placed in a hexagonal packing on the shelf. Each sample was surrounded by empty vials in order to eliminate influence from the surrounding vials on product temperature profiles, especially during the freezing experiments. In the experiments using prototype V, samples were directly placed on the ten FBGs of the OFS plate surrounded by six empty vials which were fixed with tape on the plate in order to ensure exact sample positioning.

2.5 Differential scanning calorimetry

Differential scanning calorimetry (DSC) was used to confirm thermal events. 30 µl samples were analyzed in 40 µl aluminum crucibles using a Mettler Toledo DSC821 (Mettler Toledo GmbH, Giessen, Germany). Samples were cooled from 20 °C to -50 °C at -1 °C/min, held at -50 °C for 10 min and reheated at 10 °C/min to 20 °C

3 Results and discussion

3.1 Product temperature measurements and end point detection

In order to evaluate the general suitability of the OFSs for product temperature measurements and end point detection, temperature profiles of prototype I sensors and conventional T-type TCs obtained in center bottom position during lyophilization of 1 mL 10% sucrose samples were compared (Figure 8-4). Pirani/capacitance manometry was used to additionally determine the endpoint of drying.

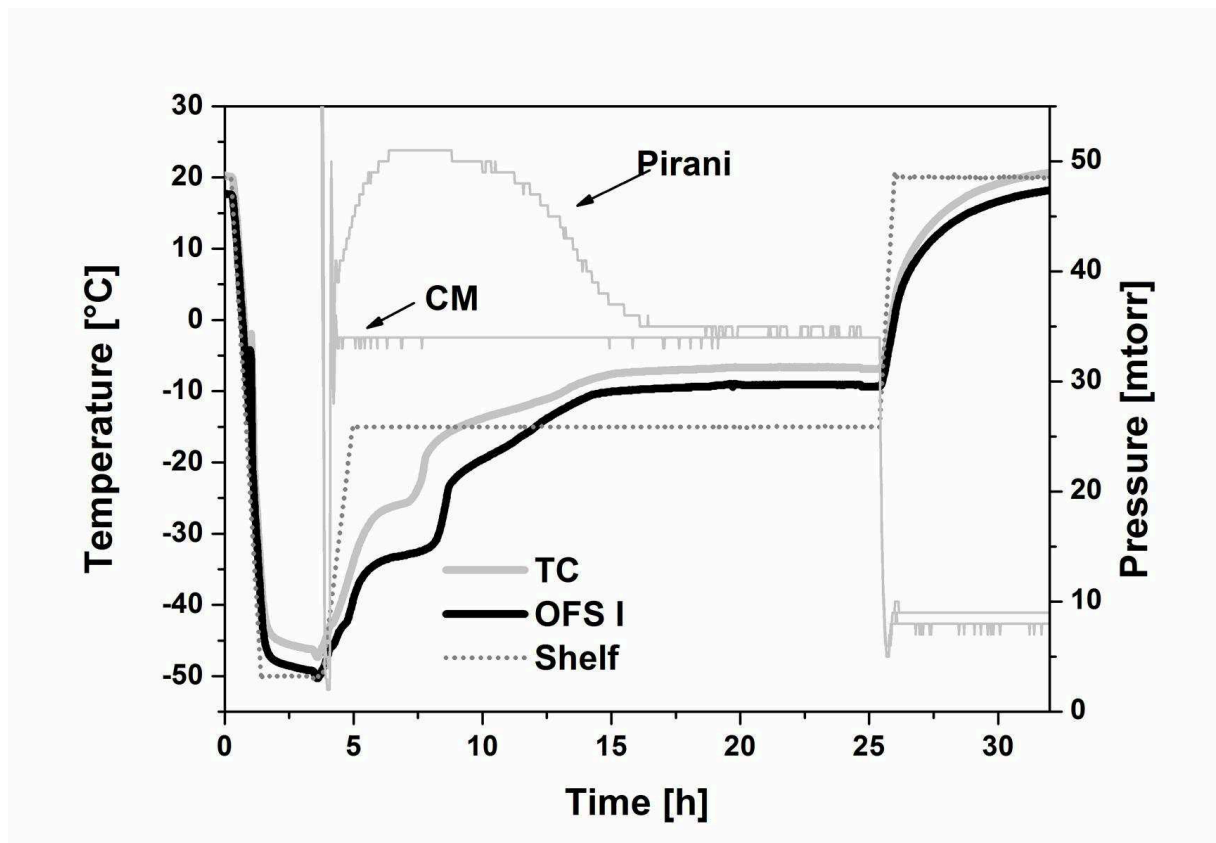


Figure 8-4: Temperature profiles of 1 mL 10% [m/V] sucrose samples in 2R vials obtained with a conventional thermocouple (TC) or the prototype I of the optical fiber sensors (OFS I) during a complete freeze-drying cycle with comparative Pirani/capacitance (CM) manometry.

The temperature profiles observed with the prototype I OFSs and the TCs were in very good agreement. It should be noted that the positioning of the prototype I OFSs in the center bottom position could be ensured without any

problems as the glass fiber is fixed within a tubular holder made of PTFE at the lyophilization stopper. In contrast, the positioning of the TCs in center bottom position is rather difficult. Despite the fixation of the TC at a bent cannula, the center bottom position could not completely be ensured due to the very rigid wires necessary for each individual TC. As in general ice sublimation proceeds from the top to the bottom and to a lesser extent, from the side to the center of the sample [35], slightly distinctive sensor positioning could in general result in varying temperature profiles.

As aforementioned, the endpoint of primary drying is indicated when product temperature is in parallel to the shelf temperature. The product temperature profiles observed with the prototype I OFS and the TC indicated the same endpoint of primary drying. In addition, manometric endpoint determination was performed. Here, the endpoint of primary drying is reached when the reading of the Pirani gauge converges with the reading of the capacitance manometer [1]. The endpoint determined with manometric endpoint detection was in very good agreement with the endpoint determined with the OFS. It is well known from literature, that a shorter primary drying time might be observed for vials containing invasive temperature probes and that thus a safety margin of primary drying time of at least 10% of the primary drying time of the vials containing the invasive probe is suggested [1].

3.2 Sensitivity to physico-chemical events during freezing

In a next step, the sensitivity of the OFSs to detect physico-chemical events such as ice nucleation, crystallization or glass formation of excipients during freezing was investigated.

3.2.1 Supercooling and ice nucleation

When a solution is cooled during the freezing process, it supercools to temperatures well below the equilibrium freezing point before ice starts to

nucleate and crystallize [36]. When ice nucleation occurs, the product temperature rises rapidly to near the equilibrium freezing point. Subsequently the temperature decreases at first slowly until most of the water has crystallized and then sharply when the product is cooled to the shelf temperature [25, 37]. Figure 8-5 displays the temperature profiles that were obtained with TCs or the prototype I of the OFSs in center bottom and above position during freezing of 10% sucrose samples. Both sensor types showed comparable onsets of ice nucleation / supercooling of $-8.6\text{ }^{\circ}\text{C}$ for the OFS and $-7.8\text{ }^{\circ}\text{C}$ for the TC. The OFSs showed a significantly higher sensitivity and faster response in center bottom position and in above position in comparison to the TCs.

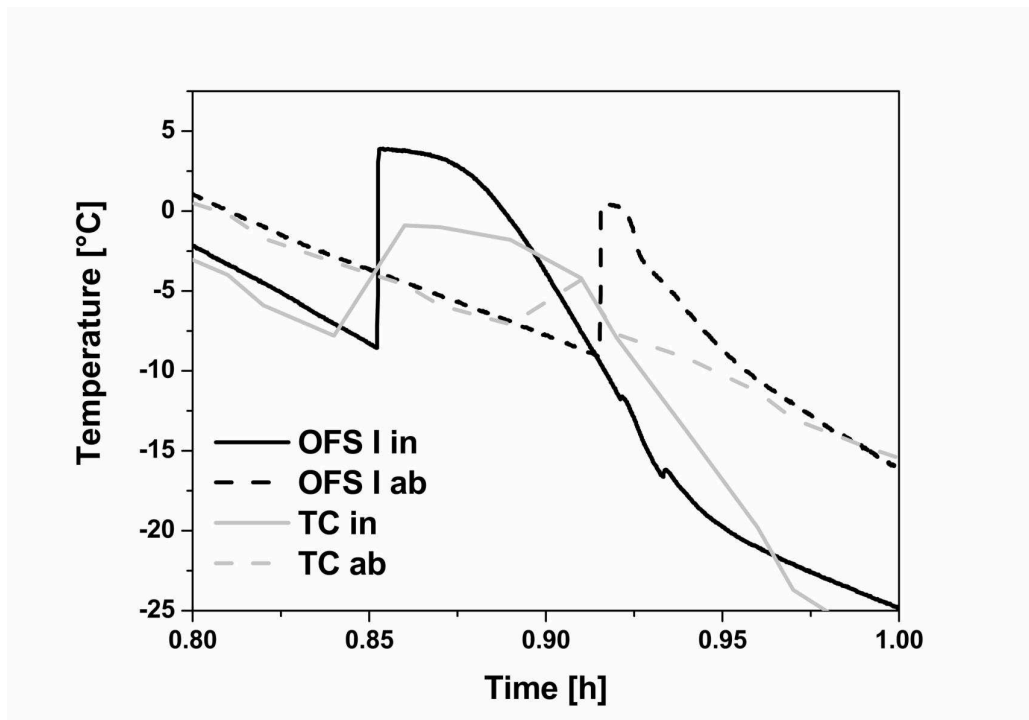


Figure 8-5: Temperature profiles during ice nucleation of 1 mL 10% [m/V] sucrose samples in 2R vials obtained with a conventional thermocouple (TC) or the prototype I of the optical fiber sensors (OFS I) in center bottom (in) and above (ab) position when cooled at a shelf temperature ramp rate of $-2.5\text{ }^{\circ}\text{C}/\text{min}$.

In general, ice nucleation is a random and stochastic event [24]. It is well known that ice nucleation can be catalyzed by external factors such as the insertion of invasive temperature probes [6]. Therefore, vials holding invasive probes show

less supercooling and thus can form larger ice crystals which finally results in lower product resistance, faster sublimation and shorter drying time compared to the rest of the batch [1]. In the semi-clean environment of the laboratory, this freezing bias is negligible, but can become relevant in a particulate free, sterile manufacturing environment [11]. It is assumed that the minute size and thus small effective surface area of the OFSs (diameter of the glass fiber: 195 μ m) compared to conventional TCs (diameter of the TC tip: 2 mm) which is in contact with the sample will decrease the probability of heterogeneous nucleation in well controlled manufacturing environment.

The higher sensitivity and faster response of the OFSs can be explained by the high sampling frequency (5 Hz) of the optical system that allows the detection of very rapid temperature changes with higher resolution. In addition, the low mass of the OFS compared to TCs or even RTDs contributes to the higher response rate and sensitivity of the optical system. It was observed that the temperature measured with the OFS during ice nucleation exceeds the equilibrium freezing point by about 4.5 °C. It is assumed that this “overshoot”, which also contributes to the high response rate of the OFSs, is caused by additional effects of strain on the FBG during ice crystal formation. Further investigations and discussion on this assumption can be found below. However, the general higher sensitivity and response rate is additionally confirmed by the non-invasive measurements in above position, in which strain effects can be excluded. Here, a much faster and better resolved response to ice nucleation was observed with the OFSs compared to the TCs, as well.

3.2.2 Crystallization of excipients

During freezing, cryoconcentration of the solute constituents of the sample occurs in the interstitial region between the growing ice crystals [6]. Some of the solutes will crystallize when a certain solute concentration is reached at the eutectic melting temperature. For example, mannitol, glycine, and sodium

chloride are known to crystallize upon freezing, if present as the major component [38]. Mannitol is widely used as bulking agent in freeze-dried formulations as it shows good cake-supporting properties [39].

The temperature versus time profile of 5% mannitol samples obtained with conventional TCs and the prototype I of the OFSs during freezing is shown in Figure 8-6. The conventional TC is only able to detect one broad exothermal peak when ice nucleation starts. In contrast, the OFS at first detects one sharp ice nucleation peak. But subsequently an additional, less distinctive peak is detected, that is not observed for pure water samples. Therefore, this peak was ascribed to the crystallization of mannitol. This observation again highlights the high sensitivity and resolution of the novel optical fiber system.

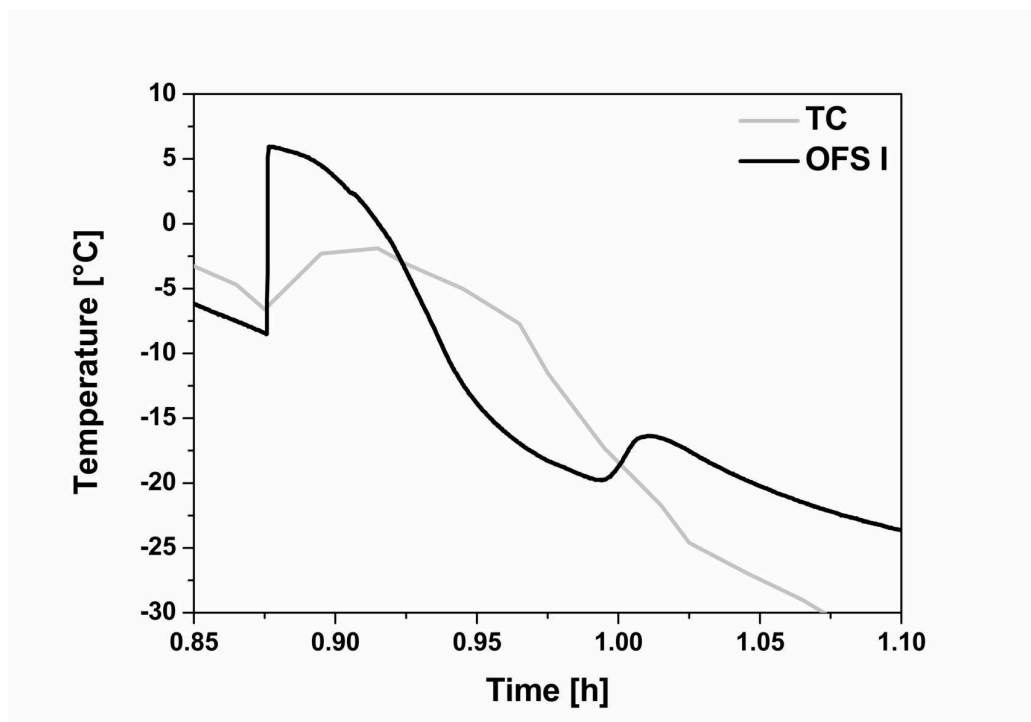


Figure 8-6: Temperature profiles of 1 mL 5% [m/V] mannitol samples obtained with a conventional thermocouple (TC) or the prototype I of the optical fiber sensors (OFS I) in a 2R vial when cooled at a shelf temperature ramp rate of $-2.5\text{ }^{\circ}\text{C}/\text{min}$.

Up to now, mannitol crystallization in such a case could only be detected by off-line analytics such as X-ray powder diffraction [39] or expensive spectroscopic on-line monitoring tools such as Raman or NIR spectroscopy [40]. When

dealing with lyophilized formulations incomplete mannitol crystallization or semi-crystalline mannitol is very critical as the recrystallization of mannitol during drying can lead to vial breakage [41] or the crystallization of mannitol during storage can influence the long-term storage stability of the product [42]. Thus, the general ability to monitor the crystallization behavior of samples during freezing is highly desirable.

3.2.3 Glass formation of excipients

In the case that solutes do not crystallize during freezing, the solute concentration increases until at the glass transition temperature (T_g) a glass forms [6, 25]. This freezing behavior is observed for polyhydroxy compounds such as sucrose or trehalose, which are often used in freeze-dried formulations due to their high potential to stabilize proteins [2].

The temperature versus time profile of 4 mL 20% trehalose samples measured with conventional TCs and the prototype I of the OFSs during freezing and thawing is shown in Figure 8-7. In contrast to the conventional TCs, during freezing the OFS after the ice nucleation peak showed an additional small exothermal signal in the temperature region of $-30\text{ }^{\circ}\text{C}$ (Figure 8-7A). This event was noticeably more pronounced during thawing (Figure 8-7B). At lower solid contents (10%) and slower freezing and thawing rates only non-significant traces of this event, which was attributed to the glass transition or the collapse temperature of the sample, could be detected. Using DSC, the onset of the glass transition temperature was determined to be at $-31.4\text{ }^{\circ}\text{C}$ and the midpoint of the glass transition temperature was determined to be at $-30.2\text{ }^{\circ}\text{C}$, which is in very good agreement with our observation.

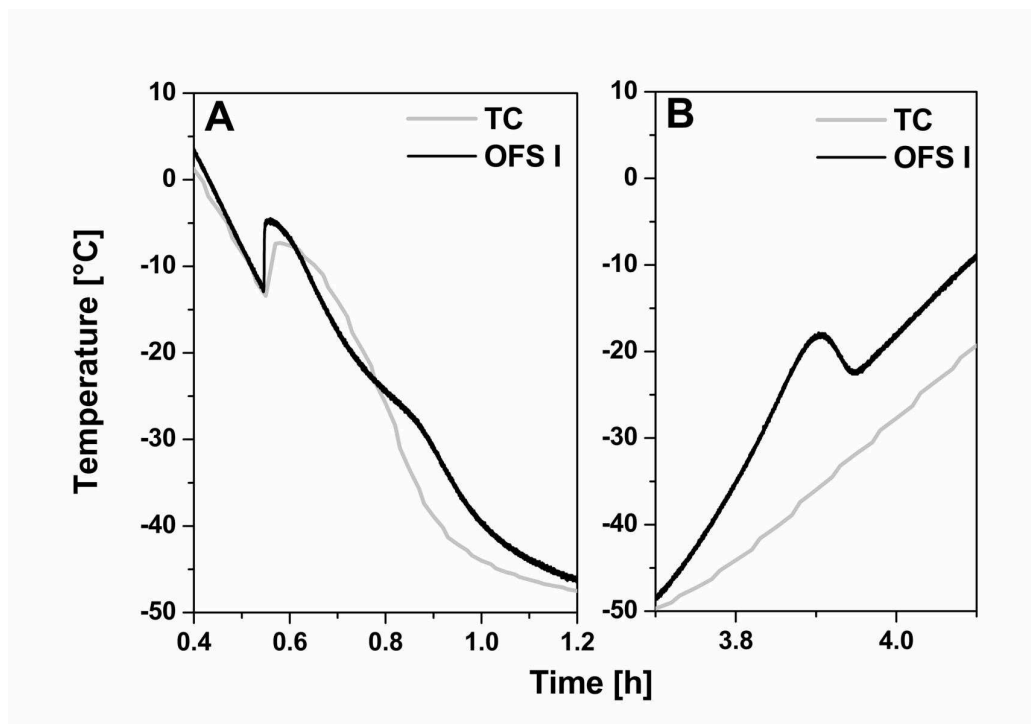


Figure 8-7: Temperature profiles of 4 mL 20% [m/V] trehalose samples in 6R vials obtained with a conventional thermocouple (TC) or the prototype I of the optical fiber sensors (OFS I) when cooled (A) or thawed (B) at a shelf temperature ramp rate of ± 2.5 °C/min.

The glass transition temperature T_g' is defined as the temperature at which a time or frequency dependent reversible change in the physical state of a material from an rigid, amorphous solid to a rubber-like, viscous liquid [43]. In the region of the glass transition, which represents a temperature range of a few degrees, the viscosity of the freeze-concentrate changes about four orders of magnitude up to 10^{14} Pa s [36, 44]. This transition is related with a temperature dependent change in the enthalpy or heat capacity of the sample [43]. This property, and not an endo- or exo-thermal event as it is e.g. observed for the (re-)/crystallization of mannitol, is used in DSC to determine the T_g' of a sample. Thus, the peaks observed in the temperature profile detected with the OFSs cannot be attributed to a change in the product temperature but to viscosity related strain effects on the unshielded OFSs. The influence of the unshielding of the OFSs on temperature readouts will be discussed below. The OFS was only sensitive enough to detect the glass transition at high solid contents of the

sample. It is also reported for DSC experiments that a higher solute concentration of a sample leads to a higher sensitivity of the measurement as the ratio of freeze-concentrate phase to ice is then increased [45]. Similarly, a larger portion of the freeze-concentrate is assumed to lead to more pronounced force effects which are responsible for the response of the OFSs. In addition, the observed response of the sensors at only high freezing and thawing rates can be correlated to well-known observations in DSC experiments. In the latter, high heating rates are used to enhance the sensitivity by increasing the magnitude of the shift in the baseline due to the heat capacity change that accompanies the glass transition [45]. In accordance, only a fast change in temperature and therefore in sample viscosity leads forces which are high enough to be detected by the OFS. Moreover, comparable to DSC measurements, in which the heating scan is always used for the determination of glass transition temperatures, a higher glass transition sensor readout was observed during thawing in our vial experiments. As the detection of this event with the OFS is presumably related to a fast change in the viscosity of the sample, the OFS may also indicate the collapse temperature (T_c) of a sample. In literature [46-47] a T_c of trehalose, determined via freeze-drying microscopy, of around $-34\text{ }^{\circ}\text{C}$ to $-28.5\text{ }^{\circ}\text{C}$ is reported with is close tot the T_g ` of trehalose and would fit to the transition detected with the OFS in the sample.

In general, the possibility to detect the glass transition of a sample directly in the lyophilization vial inside the freeze-drier during freezing would be an enormous advantage as the other typical off-line analytical methods like DSC or freeze-drying microscopy can never simulate the exact same conditions e.g. temperature ramp rate and sample volume, as used in the freeze-drier.

3.3 Influence of the shielding or unshielding of the OFSs on temperature profiles

As aforementioned, due to non-realistic, shifted temperature readouts during ice crystal formation and due to the detectability of non-temperature related events such as glass transition, it is assumed that the OFSs do not only respond to temperature but also to strain effects. In order to investigate the influence of the shielding or unshielding of the OFSs on the detected temperature profiles, the temperature profile of a 5% mannitol sample during freezing and annealing was measured with a fixed, metal-embedded OFS in combination with a very flexible, completely unshielded OFS in comparison to a conventional TC (Figure 8-8).

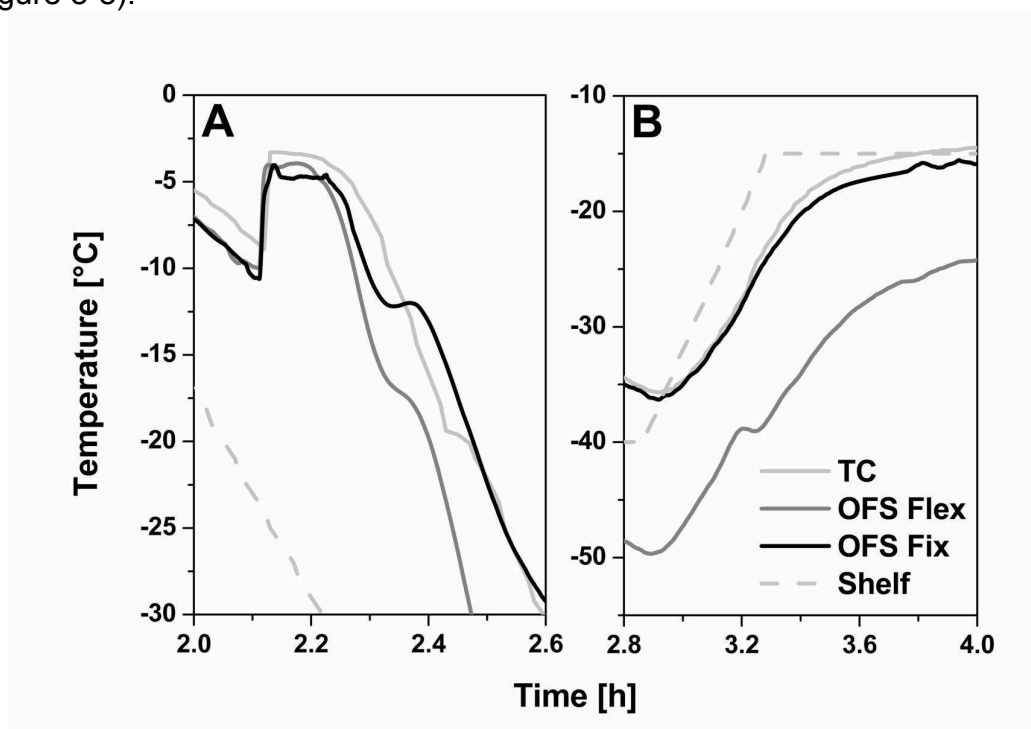


Figure 8-8: Temperature profiles of 4 mL 5% [m/V] mannitol samples in 6R vials obtained with a conventional thermocouple (TC) or the prototype II consisting of a fixed (Fix) and a flexible (Flex) optical fiber sensor during cooling (A) or during the heating phase of the annealing step (B) at a shelf temperature ramp rate of ± 1 °C/min.

Annealing, where by the product temperature is increased to a temperature between the T_g of the amorphous phase and the T_m of the crystalline phase,

is performed to allow efficient crystallization of the crystalline bulking agents, such as mannitol, in order to minimize inter-vial heterogeneity or to optimize drying performance [48].

The temperature readouts of the shielded OFS were in good agreement with the TC data. In contrast, especially after ice crystal formation, the unshielded sensor showed a drift towards lower temperatures (Figure 8-8A). This indicates that shielding of the OFSs is necessary to guarantee correct temperature readouts. The crystallization peak for mannitol during freezing could be detected with both, the shielded and the unshielded OFSs but not with the conventional TC. Thus, the general sensitivity of the OFS towards fast temperature changes is high enough and a sensitivity to strain by unshielding of the OFS is not required for the detection of exothermic events. However, the additional event during heating to the annealing temperature, could only be detected with the completely unshielded OFS (Figure 8-8B). This event might be related to the glass transition of the meta-stable amorphous mannitol phase, which is reported to occur at temperatures between -32°C and -27°C depending on the heating rate [45]. Thus, for correct temperature readouts shielded OFS are required, which additionally allow for the detection of temperature related events such as ice formation or mannitol crystallization. However, in order to allow for the detection of force and not temperature related changes of the sample unshielded sensors are necessary.

3.4 Three-dimensional information on temperature profiles in a vial

In order to obtain three-dimensional information on the temperature profiles of a sample during lyophilization, an optical fiber system helix with ten OFSs in series (H1 to H10) was used to measure the product temperature at different positions in a 10% trehalose sample (Figure 8-9).

During cooling (Figure 8-9A) a temperature gradient in the sample was observed, with the lowest temperature at the OFS closest to the vial bottom and

the shelf (H1), and the highest temperature at the OFS closest to the sample surface (H10). When ice nucleation started, the temperature increased at the same time point for all OFS (H1 to H10). This observation can be explained by the fact that a critical mass of ice nuclei is required to initiate ice crystal formation [44, 49-50], which then occurs very rapid and simultaneously in the entire system, resulting in a temperature increase close to the equilibrium freezing point [44, 49-50]. Once stable ice crystals are formed in the entire system, ice crystal growth proceeds by the addition of water molecules to the interface [49]. However, only a small fraction of the freezable water solidifies immediately, as the supercooled water can only absorb a small fraction of the heat that is given off by the exothermic ice formation [49]. Therefore, after the initial ice network has formed, additional heat has to be removed from the solution by further cooling in order to promote further ice crystal growth and thus complete solidification of the sample. As released heat in the sample due to ice crystal formation is faster removed by the colder shelf in positions close to the shelf, ice formation finishes quite early close to the vial bottom. This could be seen by the lacking of a temperature plateau and by the early decrease of the product temperature for the OFS close to the vial bottom (H1). However, for the OFS close to the sample surface (H10) a temperature plateau was observed before product temperature decreased. This indicates that at higher positions within the sample solidification requires more time to fully complete.

During further cooling the temperature gradient in the sample persists as observed prior to ice nucleation, with lower temperatures on the bottom and higher temperatures on the top. The general findings, that ice nucleation occurs at the same time throughout the entire system and that complete solidification proceeds from the bottom to the top of the sample, are in good accordance with the freezing behavior observed by visual recording of the samples in the lyophilizer during freezing via shelf-ramping [51]. Moreover, the product

temperature data obtained with the OFSs during freezing are in excellent agreement with the temperature profiles that were obtained for eight different vial positions via mathematical simulations by Nakagawa et al. [52]. However, this is now the first time that such freezing profiles could be experimentally approved with a high number of measurements points.

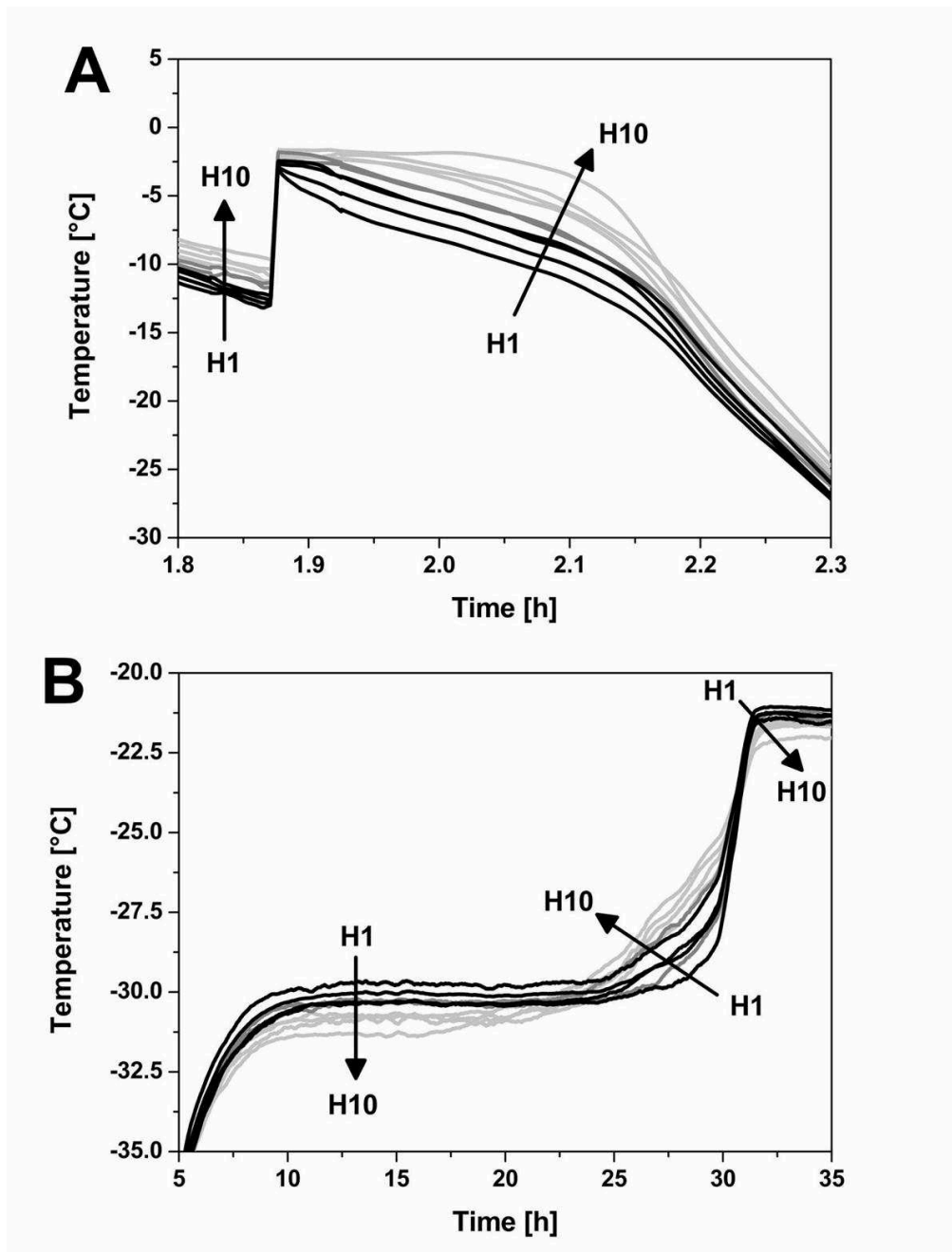


Figure 8-9: Three-dimensional temperature profile of 2ml 10% trehalose solution in a 2R vial obtained with the OFS helix (prototype III) during the freezing step (A) when cooled at a shelf temperature ramp rate of $-1\text{ }^{\circ}\text{C}/\text{min}$ and during the primary drying step (B).

During primary drying (Figure 8-9B) the observed temperature gradient was opposite to the one during freezing. Now, product temperature is higher close to the bottom of the sample and lower close to the top of the sample, as during primary drying the shelf, in this case set to -20°C , does not provide cooling of the samples but instead heat for ice sublimation. In general, when primary drying comes to its end, the product temperature increases first at the top and later at the bottom of the sample. This indicates that ice sublimation processes in general from the top to the bottom of the sample, which is also described in literature [53]. For the OFS closest to the sample surface (H10) the increase in product temperature during primary drying already starts after 16 hours with a moderate slope. In comparison, the OFS close to the vial bottom (H1) product temperature starts to increase quite sharply after 25 hours. But in both cases, the plateau at the endpoint of primary drying is reached at the same time (after ~ 31 hours). Traditionally, the endpoint of primary drying is defined by the time point when product temperature is equivalent or in parallel to the shelf temperature and constant over time [15]. However, from our experiment, it is obvious that primary drying in the upper parts of the sample is completed earlier compared to lower parts of the sample and that thus the traditional definition of the endpoint of primary drying holds only true for the section of the sample where drying is completed the latest. The time point at which the final plateau in product temperature is reached is the same for all sensor points. This effect is due to the fact that the energy provided by the shelf is needed for the sublimation of the still frozen part of the sample. The energy consequently does not reach the upper part of the sample, but the energy loss at the sublimation front is high enough to cool the already dry, upper part of the sample. In more detail, it was observed that the OFS closest to the sample surface (H10) indicated the first increase in product temperature at the end of primary drying. However, it was not the OFS closest to the vial bottom (H1) but the OFS almost

in the middle of the helix (H4) that showed the latest increase in product temperature. These results experimentally support the theory that the ice-vapor interface does not follow an “ideal” planar geometry, where drying is finished at the vial bottom, but that the ice-vapor interface follows an “actual” curved geometry, where drying is finished somewhere in the center of the vial [35]. According to Jennings [35], sublimation occurs first from a planar surface. As the sublimation process commences, sublimation occurs preferentially with respect to the walls of the vial, and the ice is mound-like shaped. The formation of the mound is an indication that the rate of sublimation in this region is lower than near the vial walls because this region obtained less energy for the sublimation process [35]. Near completion of the sublimation process, a small mound is formed and located in the center of the vial [35]. This change in the configuration of the ice during drying was also supported by Pikal and Shah [54]. They suggested that drying is faster along the vial walls than in the core region, resulting in a highly curved ice–vapor interface. They proposed that the reason for this observation might be a low resistance pathway for vapor escape along the vial wall as a result of product shrinkage close to the wall during drying.

When the endpoint of primary drying is reached, the same temperature gradient as in the beginning of primary drying is observed, with higher temperatures closer to the bottom and lower temperatures closer to the top, because of sample heating via the shelf. This small temperature gradient subsequently further persisted during secondary drying (data not shown).

3.5 Non-invasive temperature profiling during lyophilization

As aforementioned, invasive temperature measurements come with the disadvantageous that the obtained data are not fully representative for samples that do not contain any temperature probe. Therefore, non-invasive temperature measurements were performed using two additional OFS prototypes in order to

test whether due to the high sensitivity the OFS could provide adequate information on sample temperature or endpoint of primary and secondary drying.

At first, a non-invasive temperature profile during lyophilization of a 10% trehalose sample was measured with the prototype IV of the OFSs, for which the glass fiber was fused into the bottom of a 6R vial with the FBG in center bottom position (Figure 8-10).

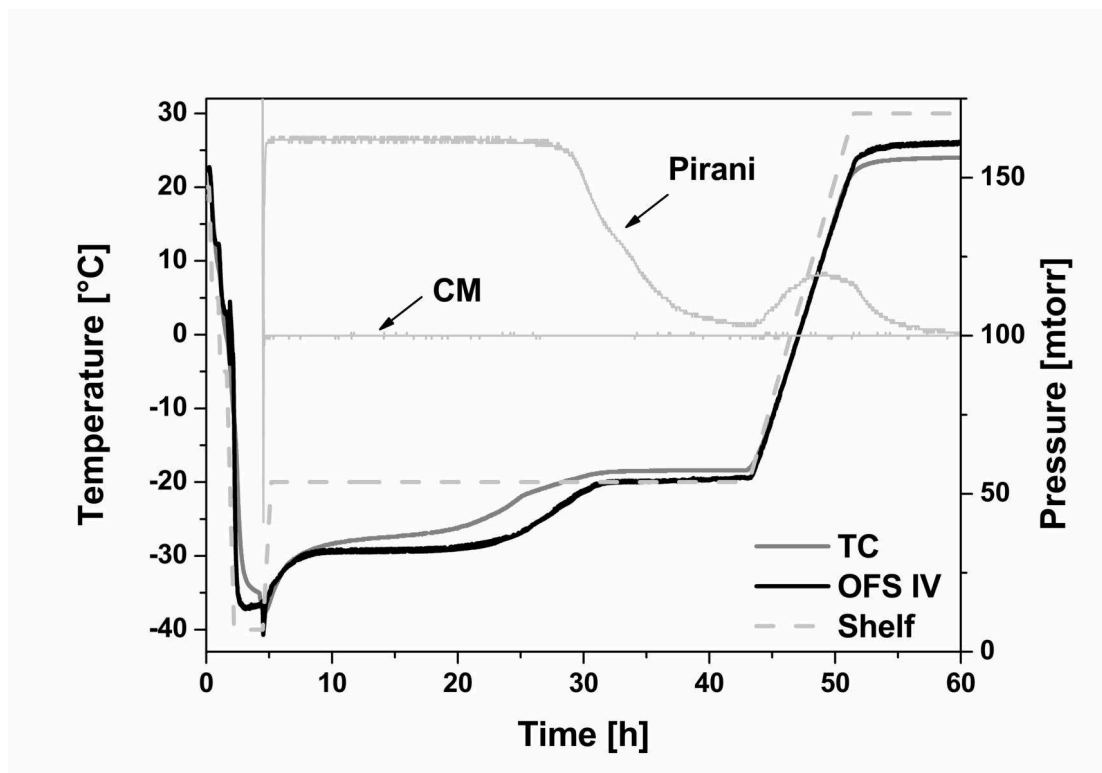


Figure 8-10: Temperature profiles of 4 mL 10% [m/V] trehalose samples in 6R vials obtained with a conventional thermocouple (TC) or the prototype IV of the optical fiber sensors (OFS IV) during a complete freeze-drying cycle with comparative Pirani/capacitance (CM) manometry.

During the freezing and secondary drying step product temperature behavior of the OFS was in very good agreement with TC data. Here, only a small temperature gradient was observed between the TC and the OFS temperatures. During primary drying the OFS showed a delayed increase in product temperature compared to the TC. This is due to the difference in sensor positioning, with the TC inside the sample in center bottom position and the

OFS fused into the vial bottom. However, the endpoint of primary drying (constant product temperature) with the OFS and the TC was observed at the same time (~32h) and was additionally in very good agreement with manometric endpoint determination. Consequently, this setup does not detect real product temperature, as always a temperature gradient between sample and vial bottom will be observed. However, Barresi et al. [55-56] showed that the measured external temperature at the bottom of the vial is suitable in order to calculate parameters such as the sublimating interface temperature, product temperature profile, heat and mass transfer coefficients using a mathematical model. But the data show that the aforementioned drawbacks that are related to invasive temperature probes can be overcome.

As the setup with the glass fiber on the bottom of the vial does not allow for automatic loading, a second non-invasive prototype (V) was designed and tested. Here, a glass fiber with ten OFSs in series was embedded into the surface of a metal plate. The metal plate was placed underneath the samples during lyophilization. Exemplarily, the temperature profile of a 5% mannitol sample obtained with this OFS plate in comparison to the profile obtained with a TC is displayed in Figure 8-11.

This optical fiber system prototype rendered temperature profiles which were highly adapted to the temperature of the shelf. But still this setup allowed for an endpoint detection of primary drying that was in very good agreement with the one obtained with the TC or with Pirani/capacitance manometry, and also to detect the endpoint of secondary drying reaching the plateau simultaneously with the TC.

In general, such a setup with more than 100 sensor points could be easily integrated directly in the surface of each shelf in a freeze-drier, even without the prerequisite of a plate between the samples and the shelf.

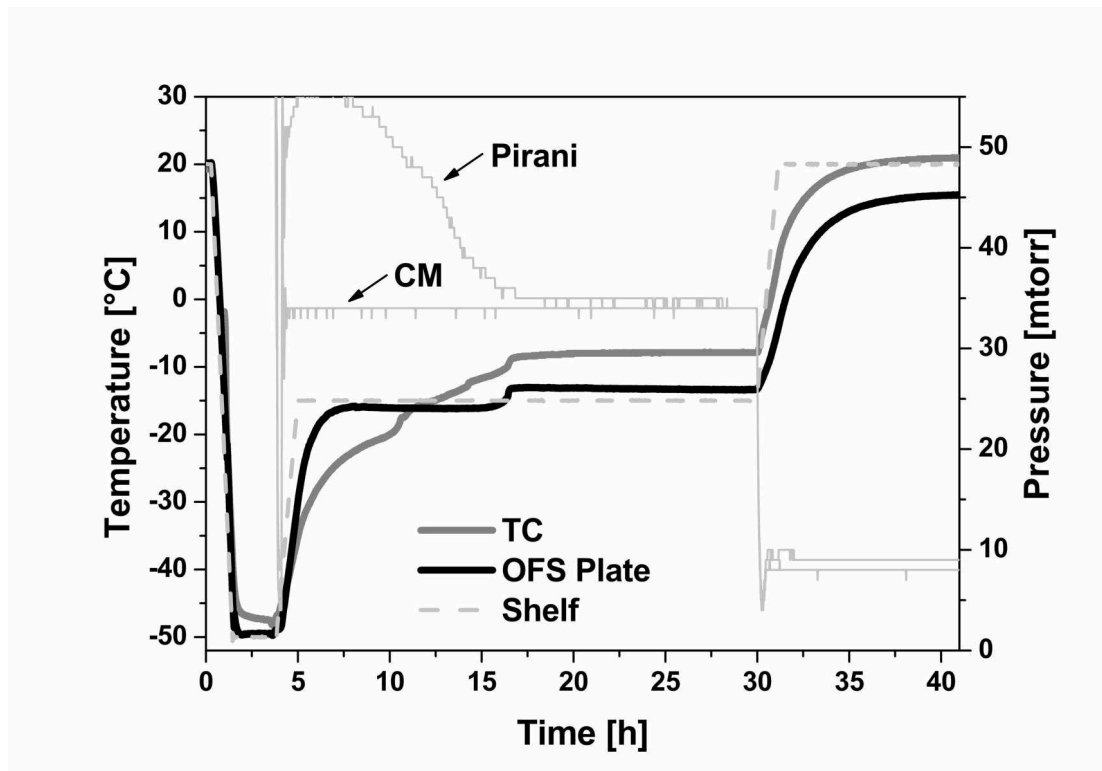


Figure 8-11: Exemplary temperature profiles of one 4 mL 5% [m/V] mannitol samples in 6R vials obtained with a conventional thermocouple (TC) or the prototype V of the optical fiber sensors (OFS Plate) during a complete freeze-drying cycle with comparative Pirani/capacitance (CM) manometry.

Thus, drying performance and drying heterogeneities of edge vials or other outliers with a large number of sample points in a batch could be easily monitored without the necessity of any sensor placement. In combination with a suitable mathematical model in order to calculate the “real” product temperature or other process parameters from the obtained “external” temperature data in analogy to Barresi et al. [55-56], this setup could be a highly advantageous PAT tool. Moreover, this setup could be easily applied in any laboratory and manufacturing scale freeze-drier and therefore used in order to facilitate a transfer from laboratory to production scale. In addition, the setup would also allow for monitoring of the shelf-temperature (“shelf-mapping”) with and without load during lyophilization cycles.

4 Conclusion

In this study, it was the first time that OFSs based on FBGs were used for temperature measurements during lyophilization. We could show that data obtained with the optical fiber systems were in good comparison to data obtained by conventional TCs or Pirani/capacitance manometry.

The chemically inert and sterilizable OFSs are simple and easy in handling due to less cable and the fixation of the sensors in center bottom position. The OFSs showed significantly higher sensitivity, faster response and better resolution compared to conventional TCs. This allowed for the monitoring of further physico-chemical events such as crystallization. It was found that force effects were responsible for temperature shifts of the unshielded OFSs. However with metal shielding this effect could be eliminated. On the other hand the force effects on unshielded sensors enable to detect non-temperature but viscosity related events like glass transition, which is not possible with conventional TCs.

By using an OFS helix three-dimensional temperature profiles at ten sensor points could be experimentally obtained. This helix setup allowed for the first time for the experimental detection of the three-dimensional freezing behavior of a sample. Moreover, temperature data obtained with the OFS helix during primary drying supported the theory that the ice-vapor interface follows a curved geometry, where drying is finished somewhere in the center of the vial.

Non-invasive temperature measurements showed similar temperature characteristics (with a small temperature gradient) to TC data and could be used for reasonable endpoint detection without the necessity of any sensor placement inside the sample. The integration of a OFS glass fiber with multiple sensor points on the surface of a plate or the shelf itself enables automatic loading, allows for non-invasive product temperatures of many vials at the same time, enables automatic loading and could also be used for “shelf-mapping”.

In conclusion, the novel optical fiber systems exhibit several substantial advantages compared to other process monitoring tools and thus could be developed into highly attractive new PAT tools.

5 References

- [1] X. Tang, M. Pikal, Design of Freeze-Drying Processes for Pharmaceuticals: Practical Advice, *Pharm. Res.*, 21 (2004) 191-200.
- [2] J.F. Carpenter, M.J. Pikal, B.S. Chang, T.W. Randolph, Rational Design of Stable Lyophilized Protein Formulations: Some Practical Advice, *Pharm. Res.*, 14 (1997) 969-975.
- [3] W. Wang, Lyophilization and development of solid protein pharmaceuticals, *Int. J. Pharm.*, 203 (2000) 1-60.
- [4] G.-W. Oetjen, P. Haseley, *Freeze-Drying*, Wiley-VHC Verlag, Weinheim, 2004.
- [5] P. Cameron, *Good Pharmaceutical Freeze-Drying Practice*, Interpharm Press, Inc., Buffalo Grove, USA, 1997.
- [6] F. Franks, T. Auffret, *Freeze-Drying of Pharmaceuticals and Biopharmaceuticals*, RSC Publishing, Cambridge, UK, 2007.
- [7] Guidance for Industry, PAT - A Framework for Innovative Pharmaceutical Development, Manufacturing and Quality Assurance, in: <http://www.fda.gov/Cder/OPS/PAT.htm>, 2004.
- [8] M. Galan, Monitoring and Control of Industrial Freeze-Drying Operations: The Challenge of Implementing Quality-by-Design (QbD), in: L. Rey, J.C. May (Eds.) *Freeze-Drying/Lyophilization of Pharmaceutical and Biological Products*, Marcel Dekker, Inc. USA, New York, 2010.
- [9] A.A. Barresi, D. Fissore, D.L. Marchisio, Process Analytical Technology in Industrial Freeze-Drying, in: L. Rey, J.C. May (Eds.) *Freeze-Drying/Lyophilization of Pharmaceutical and Biological Products*, Marcel Dekker, Inc. USA, New York, 2010.
- [10] M. Wiggendorff, I. Presser, G. Winter, The Current State of PAT in freeze drying, *Eur. Pharm. Review*, 10 (2005) 87-92.
- [11] S.M. Patel, M. Pikal, Process Analytical Technologies (PAT) in freeze-drying of parenteral products, *Pharm. Dev. Technol.*, 14 (2009) 567-587.
- [12] F. Franks, Freeze-drying of bioproducts: putting principles into practice, *Eur. J. Pharm. Biopharm.*, 45 (1998) 221-229.
- [13] M.J. Pikal, S. Shah, The collapse temperature in freeze drying: Dependence on measurement methodology and rate of water removal from the glassy phase, *Int. J. Pharm.*, 62 (1990) 165-186.
- [14] E. Trappler, Lyophilization Equipment, in: H.R. Constantino, M.J. Pikal (Eds.) *Lyophilization of Biopharmaceuticals*, AAPS Press, Arlington, VA, USA, 2004, pp. 3-41.

- [15] S. Schneid, H. Gieseler, Evaluation of a New Wireless Temperature Remote Interrogation System (TEMPRIS) to Measure Product Temperature During Freeze Drying, *AAPS PharmSciTech*, 9 (2008) 729-739.
- [16] S. Corbellini, M. Parvis, A. Vallan, A Plug & Play Architecture for Low-Power Measurement Systems, in: *Instrumentation and Measurement Technology Conference, Proceedings of the IEEE*, 2005, pp. 565-569.
- [17] M. Dwivedi, H.S. Ramaswamy, Comparative study of wireless versus standard thermocouples for data gathering and analyses in rotary cookers *J. Food Process. Preserv.*, 34 (2010) 557-574.
- [18] S. Corbellini, M. Parvis, A. Vallan, A low-invasive system for local temperature mapping in large freeze dryers, in: *Instrumentation and Measurement Technology Conference, Proceedings of the IEEE*, 2009, pp. 80-85.
- [19] N. Milton, M.J. Pikal, M.L. Roy, S.L. Nail, Evaluation of Manometric Temperature Measurement as a Method of Monitoring Product Temperature During Lyophilization, *PDA J. Pharm. Sci. Technol.*, 51 (1997) 7-16.
- [20] X. Tang, S. Nail, M. Pikal, Evaluation of manometric temperature measurement, a process analytical technology tool for freeze-drying: Part I, product temperature measurement, *AAPS PharmSciTech*, 7 (2006) E95-E103.
- [21] X. Tang, S.L. Nail, M.J. Pikal, Freeze-Drying Process Design by Manometric Temperature : Design of a Smart Freeze-Dryer, *Pharm. Res.*, 22 (2005) 685-700.
- [22] H. Gieseler, T. Kramer, M.J. Pikal, Use of manometric temperature measurement (MTM) and SMART™ freeze dryer technology for development of an optimized freeze-drying cycle, *J. Pharm. Sci.*, 96 (2007) 3402-3418.
- [23] S. Rambhatla, M. Pikal, Heat and mass transfer scale-up issues during freeze-drying, I: Atypical radiation and the edge vial effect, *AAPS PharmSciTech*, 4 (2003) 22-31.
- [24] M.J. Pikal, S. Rambhatla, R. Ramot, The Impact of the Freezing Stage in Lyophilization: Effects of the Ice Nucleation Temperature on Process Design and Product Quality, *American Pharm. Review*, 5 (2002) 48-53.
- [25] J.C. Kasper, W. Friess, The freezing step in lyophilization: Physico-chemical fundamentals, freezing methods and consequences on process performance and quality attributes of biopharmaceuticals, *Eur. J. Pharm. Biopharm.*, 78 (2011) 248-263.
- [26] A. Hottot, S. Vessot, J. Andrieu, Freeze drying of pharmaceuticals in vials: Influence of freezing protocol and sample configuration on ice morphology and freeze-dried cake texture, *Chem. Eng. Process.*, 46 (2007) 666-674.
- [27] J.A. Searles, J.F. Carpenter, T.W. Randolph, The ice nucleation temperature determines the primary drying rate of lyophilization for samples frozen on a temperature-controlled shelf, *J. Pharm. Sci.*, 90 (2001) 860-871.

- [28] T.W. Randolph, J.A. Searles, Freezing and Annealing Phenomena in Lyophilization: Effects Upon Primary Drying Rate, Morphology, and Heterogeneity, *American Pharm. Review*, 5 (2002) 40-47.
- [29] S. Passot, I.C. Trelea, M. Marin, M. Galan, G.J. Morris, F. Fonseca, Effect of Controlled Ice Nucleation on Primary Drying Stage and Protein Recovery in Vials Cooled in a Modified Freeze-Dryer, *J. Biomech. Eng.*, 131 (2009) 074511-074515.
- [30] W. Friess, M. Resch, M. Wiggendorfer, Monitoring device for a dryer, in, 2010.
- [31] MicronOptics, Micron Optics Optical Sensing Guide, available on http://micronoptics.com/sensing_doc_library.php, (2005).
- [32] C. Chojetzki, M. Rothhardt, J. Ommer, S. Unger, K. Schuster, H.-R. Mueller, High-reflectivity draw-tower fiber Bragg gratings - arrays and single gratings of type II, *journal article*, 44 (2005) 060503.
- [33] A. Othonos, Fiber Bragg gratings, *Rev. Sci. Instrum.*, 68 (1997) 4309-4341.
- [34] K.T.V. Grattan, T. Sun, Fiber optic sensor technology: an overview, *Sensors and Actuators A: Physical*, 82 (2000) 40-61.
- [35] T. Jennings, The Primary Drying Process, in: *Lyophilization, Introduction and Basic Principles*, Interpharm Press, Englewood, USA, 1999.
- [36] S.L. Nail, S. Jiang, S. Chongprasert, S.A. Knopp, Fundamentals of Freeze-Drying, in: S.L. Nail, M.J. Akers (Eds.) *Development and Manufacture of Protein Pharmaceuticals*, Kluwer Academic/ Plenum Publisher, New York, 2002.
- [37] M.J. Pikal, Mechanisms of Protein Stabilization During Freeze-Drying Storage: The Relative Importance of Thermodynamic Stabilization and Glassy State Relaxation Dynamics, in: L. Rey, J.C. May (Eds.) *Freeze-Drying/Lyophilization of Pharmaceutical and Biological Products*, Marcel Dekker, Inc. USA, New York, 2010.
- [38] J.A. Searles, Freezing and Annealing Phenomena in Lyophilization, in: L. Rey, J.C. May (Eds.) *Freeze-Drying/Lyophilization of Pharmaceutical and Biological Products*, Marcel Dekker, Inc. USA, New York, 2010.
- [39] R.K. Cavatur, N.M. Vemuri, A. Pyne, Z. Chrzan, D. Toledo-Velasquez, R. Suryanarayanan, Crystallization Behavior of Mannitol in Frozen Aqueous Solutions, *Pharm. Res.*, 19 (2002) 894-900.
- [40] T. De Beer, P. Vercruyssen, A. Burggraef, T. Quinten, J. Ouyang, X. Zhang, C. Vervaet, J. Remon, W. Baeyens, In-line and real-time process monitoring of a freeze drying process using Raman and NIR spectroscopy as complementary process analytical technology (PAT) tools, *J. Pharm. Sci.*, 98 (2009) 3430-3446.
- [41] N.A. Williams, Y. Lee, G.P. Poll, T.A. Jennings, The Effects of Cooling Rate on Solid Phase Transitions and Associated Vial Breakage Occurring in Frozen Mannitol Solutions, *PDA J. Pharm. Sci. Technol.*, 40 (1986) 135-141.

- [42] T.W. Randolph, Phase separation of excipients during lyophilization: Effects on protein stability, *J. Pharm. Sci.*, 86 (1997) 1198-1203.
- [43] D. Lechuga-Ballesteros, D.P. Miller, S.P. Duddu, Thermal Analysis of Lyophilized Pharmaceutical Peptide and Protein Formulations, in: H.R. Constantino, M.J. Pikal (Eds.) *Lyophilization of Biopharmaceuticals*, AAPS Press, Arlington, VA, USA, 2004, pp. 3-41.
- [44] M. Akyurt, G. Zaki, B. Habeebullah, Freezing phenomena in ice-water systems, *Energy Convers. Manage.*, 43 (2002) 1773-1789.
- [45] L.-M. Her, S.L. Nail, Measurement of Glass Transition Temperatures of Freeze-Concentrated Solutes by Differential Scanning Calorimetry, *Pharm. Res.*, 11 (1994) 54-59.
- [46] D.E. Overcashier, T.W. Patapoff, C.C. Hsu, Lyophilization of protein formulations in vials: Investigation of the relationship between resistance to vapor flow during primary drying and small-scale product collapse, *J. Pharm. Sci.*, 88 (2000) 688-695.
- [47] G.D.J. Adams, J.R. Ramsay, Optimizing the lyophilization cycle and the consequences of collapse on the pharmaceutical acceptability of erwinia L-Asparaginase, *J. Pharm. Sci.*, 85 (1996) 1301-1305.
- [48] J.A. Searles, J.F. Carpenter, T.W. Randolph, Annealing to optimize the primary drying rate, reduce freezing-induced drying rate heterogeneity, and determine T_g' in pharmaceutical lyophilization, *J. Pharm. Sci.*, 90 (2001) 872-887.
- [49] M. Matsumoto, S. Saito, I. Ohmine, Molecular dynamics simulation of the ice nucleation and growth process leading to water freezing, *Nature*, 416 (2002) 409-413.
- [50] G. Petzold, J. Aguilera, Ice Morphology: Fundamentals and Technological Applications in Foods, *Food Biophys.*, 4 (2009) 378-396.
- [51] <http://www.fastprecisecold.com/>, ControlLyo Technology Demo Video.
- [52] K. Nakagawa, A. Hottot, S. Vessot, J. Andrieu, Modeling of freezing step during freeze-drying of drugs in vials, *AIChE J.*, 53 (2007) 1362-1372.
- [53] M.J. Pikal, S. Shah, D. Senior, J.E. Lang, Physical chemistry of freeze-drying: Measurement of sublimation rates for frozen aqueous solutions by a microbalance technique, *J. Pharm. Sci.*, 72 (1983) 635-650.
- [54] M.J. Pikal, S. Shah, Intravial Distribution of Moisture During the Secondary Drying Stage of Freeze Drying, *PDA J. Pharm. Sci. Technol.*, 51 (1997) 17-24.
- [55] A.A. Barresi, S.A. Velardi, R. Pisano, V. Rasetto, A. Vallan, M. Galan, In-line control of the lyophilization process. A gentle PAT approach using software sensors, *Int. J. Refrig.*, 32 (2009) 1003-1014.
- [56] A.A. Barresi, R. Pisano, D. Fissore, V. Rasetto, S.A. Velardi, A. Vallan, M. Parvis, M. Galan, Monitoring of the primary drying of a lyophilization process in vials, *Chemical Engineering and Processing: Process Intensification*, 48 (2009) 408-423.

Chapter 9

Summary of the thesis

The general goal of the thesis was the lyophilization of cationic polymer-based nucleic acid nanoparticles. Here, the main focus was set on the development of lyophilized, long-term stable pDNA or siRNA polyplex formulations. Moreover, the underlying stabilization mechanism of polyplexes during freezing was investigated and a novel optical fiber system for advanced monitoring of the lyophilization process was evaluated.

In the general introduction the major steps of the lyophilization process and the essential components as well as their function in a freeze-drier were summarized in brief. Moreover, recent advances and further challenges in lyophilization were discussed. Special attention was drawn to the lyophilization of nucleic acid based pharmaceuticals. At first, a brief overview on the basic concepts of pDNA and siRNA delivery in gene therapy was given. The clinical practicability of nucleic acid nanoparticles is limited due to their instability in aqueous suspension raising the demand for lyophilized, long-term stable formulations. However, at that time, neither pDNA nor siRNA polyplexes have been successfully lyophilized without limitations.

In a first step, a micro-mixer method had to be established for the preparation of pDNA/LPEI polyplexes in order to guarantee their defined quality. Here, the

plasmid and LPEI solutions were mixed at the junction of a T-connector using two syringe drivers and the mixing speed was controlled by plunger speed and/or syringe size. It was found that the z-average diameter and polydispersity index of the polyplexes could be controlled via the mixing speed and were influenced by the pDNA concentration. This micro-mixer method could also be successfully transferred to up-scale the preparation of defined siRNA/oligo-aminoamide polyplexes. Hence, the micro-mixer method is a highly valuable method for the reproducible preparation of large, standardized batches of homogeneous, well-defined, and transfection-competent polyplexes.

For the development of a lyophilized, long-term stable pDNA/LPEI polyplex formulation, the initial HBG buffer was changed to the more acidic L-histidine buffer in order to improve homogeneity and stability of the polyplexes. In a first freeze-thaw study, high concentrations of the commonly used disaccharides, sucrose or trehalose, were required to maintain particle size, greatly exceeding isotonicity levels and indicating the prerequisite of a critical ratio of stabilizer to polyplex (~4000). Here, higher molecular weight excipients, such as lactosucrose, hydroxypropylbetadex (HP- β -CD), or povidone (PVP), were beneficial for sufficient particle stabilization at low osmotic pressure during freezing and drying. Using isotonic formulations with 14% lactosucrose, 10% HP- β -CD/6.5% sucrose, or 10% PVP/6.3% sucrose polyplex size was far better preserved (< 170 nm) upon lyophilization and storage over 6 weeks up to 40 °C compared to previous studies. Only PVP/sucrose samples showed decreased transfection efficiency and metabolic activity. Thus, by using lactosucrose or CD/sucrose formulations, pDNA/LPEI polyplexes could be the first time lyophilized with only a marginal increase in size and preserved biological activity at high pharmaceutical quality.

Plasmid/LPEI polyplexes are highly sensitive to freezing induced stresses unless formulated at a sufficient stabilizer/DNA mass ratio, but underlying stabilization mechanisms were still not fully understood. Thus, the effect of freezing on the stability of plasmid/LPEI polyplexes was thoroughly investigated by the aid of a controlled ice nucleation method. It was found that particle stability is not only dependent on the stabilizer/DNA ratio of the formulation but also on the freezing process. Ice nucleation temperature only affected particle stability at low DNA concentrations. For both, low and high DNA concentrations, particle size drastically increased when frozen at decreased shelf-ramp rates. Particle stability was markedly affected during the initial part of freezing down to temperatures of ~ -3 °C. In this temperature range the maximum in bimolecular reaction rates was observed as freeze-concentration is highly advanced at still low sample viscosities. Below a critical temperature ($\sim \leq -18$ °C) no further particle aggregation occurred as particle mobility is completely inhibited due to high sample viscosities even in the absence of vitrification. The initial sucrose/DNA ratio defined the maximum level of bimolecular reaction rates. In summary, the time span that the particles spend in the low viscous state after ice nucleation, determined by initial sample viscosity and applied freezing rate, is the predominant factor in the stabilization of nucleic acid nanoparticles during freezing.

In a next step, lyophilized, long-term stable formulations for siRNA/oligoaminoamide polyplexes based on two different oligomers had to be developed. In contrast to pDNA/LPEI polyplexes, siRNA polyplexes maintained particle size and gene silencing efficiency in absence or the presence of only low amounts (mass ratio of ~ 700) of stabilizers after freeze-thawing or lyophilization, depending on the polymer. Sucrose, trehalose, or lactosucrose exhibited similar good stabilizing potential. Only cyclodextrin had a destabilizing effect on siRNA

polyplexes. Freeze-thawing experiments using polyplexes based on oligomer analogs showed that the presence of cysteines, which internally stabilize polyplexes by disulfide formation, was not responsible for the difference in colloidal stability of the two siRNA polyplexes. The concentration of the siRNA polyplexes could be easily increased by reconstitution of the lyophilisates with reduced volume without affecting particle size or gene silencing efficiency. Long-term stability of both siRNA polyplexes over 6 months up to 40 °C was demonstrated when formulated with 5% or 10% sucrose or 7% lactosucrose. Thus, in this thesis, it was the first time that lyophilized stable siRNA polyplex formulations were achieved which showed excellent physicochemical and transfection stability.

Finally, a further objective of the thesis was the implementation and evaluation of an optical fiber system (OFSs) as novel process monitoring tool during lyophilization. The OFSs, which allowed easy sensor handling, showed significantly higher sensitivity, faster response, and better resolution in comparison to conventional thermocouples. This allowed for the monitoring of additional physico-chemical events such as crystallization or viscosity related glass transition. The detection of the latter event could be ascribed to force effects on unshielded sensors. By using an OFS helix, information on three-dimensional freezing and drying behavior could be gained. Non-invasive temperature measurements showed slightly shifted temperature characteristics, still appropriate for reasonable endpoint detection. The integration of a glass fiber with several OFSs into the surface of a plate or the shelf allows for non-invasive temperature measurements allowing for automatic loading. These advantages turn the novel optical fiber systems into a highly attractive monitoring tool during lyophilization.

In conclusion, in this thesis it was shown that an up-scaled preparation method in combination with subsequent lyophilization is a promising approach to reproducibly achieve long-term stable pDNA or siRNA polyplexes maintaining particle size and biological activity at pharmaceutically defined high quality. The results demonstrated that formulation development, highly dependent on the used type of polymer or nucleic acid, and process development in combination with appropriate process monitoring needs always to be performed hand in hand. All in all, this thesis makes an essential contribution in order to move closer from a promising biotechnological approach towards clinic-friendly drugs.

Appendix

Publications included in this thesis:

Research articles

J.C. Kasper, D. Schaffert, M. Ogris, E. Wagner, W. Friess; The Establishment of an Up-scaled Micro-Mixer Method Allows the Standardized and Reproducible Preparation of Well-Defined Plasmid/LPEI Polyplexes; *Eur. J. Pharm. Biopharm.* 77 (2011) 182-185.

J.C. Kasper, D. Schaffert, M. Ogris, E. Wagner, W. Friess: Development of a lyophilized plasmid/LPEI polyplex formulation with long-term stability- A step closer from promising technology to application; *J. Controlled Release* 151 (2011) 246-255.

This work was **highlighted** in the July 2011 issue of “Staying current; Formulation of Biopharmaceuticals”.

J.C. Kasper, M.J. Pikal, W. Friess; Investigations on polyplex stability during the freezing step of lyophilization using controlled ice nucleation – The importance of residence time in the low viscous state; *in preparation*.

This work was supported with a **graduate student scholarship** by the German Academic Exchange Service (**DAAD**).

J.C. Kasper, C. Troiber, S. Kuchler, E. Wagner, W. Friess; Formulation development of lyophilized, long-term stable siRNA/polyamidoamine polyplexes; *submitted*.

J.C. Kasper, M. Wiggenghorn, M. Resch, W. Friess; Implementation and evaluation of an optical fiber system as novel process monitoring tool during lyophilization; *submitted*.

Review articles

J. C. Kasper, W. Friess; The freezing step in lyophilization: physico-Chemical fundamentals, freezing methods and consequences on process performance and product quality; *Eur. J. Pharm. Biopharm.* 78 (2011) 248-263.

This work was **highlighted** in the 7/2011 issue of “Staying current, Formulation of Biopharmaceuticals”.

J.C. Kasper, W. Friess; Recent advances and further challenges in lyophilization; *in preparation*.

Further publications associated with this thesis:

Research articles

T.R.M. De Beer, M. Wiggenghorn, A. Hawe, **J.C. Kasper**, A. Almeida, T. Quinten, W. Friess, G. Winter, C. Vervaet, J.P. Remon; Optimization of a pharmaceutical freeze-dried product and its process using an experimental design approach and innovative process analyzers; *Talanta* 83 (2011) 1623-1633.

S. Pieters, T. De Beer, **J.C. Kasper**, D. Boulpaep, O. Waszkiewicz, M. Goodarzi, Christophe Tistaert, W. Friess, J.-P. Remon, C. Vervaet, Y. Vander Heyden; Near-infrared spectroscopy for in-line monitoring unfolding and interactions with lyoprotectants during the freeze-drying of proteins; *Anal. Chem.*, 2012, 84 (2) 947 – 955.

T.R.M. De Beer, **J.C. Kasper**, W. Friess, C. Vervaet, J.-P. Vervaet; Batch statistical process control of the freeze-drying process of a pharmaceutical formulation using spectroscopic monitoring tools; *in preparation*.

C. Troiber, **J.C. Kasper**, S. Milani, M. Scheible, F. Schaubhut, I. Marin, S. Küchler, J. Rädler, F.C. Simmel, W. Friess, E. Wagner; Analytical methods for the physico-chemical characterization of siRNA polyplexes: size and stability; *in preparation*.

Review articles

J.C. Kasper, S. Claus, W. Friess; Analytical methods to directly or indirectly characterize and monitor the freezing step in lyophilization, *in preparation*.

Book chapters

J.C. Kasper, S. Küchler, W. Friess; Lyophilization of synthetic gene carriers; In: Methods in Molecular Biology: Nanotechnology for Nucleic Acid Delivery, Eds.: D. Oupicky, M. Ogris, Springer Protocols, Humana Press, *in press*.

Presentations associated with this thesis:

Oral presentations

M. Wiggendorf, **J.C. Kasper**, W. Friess; Monitoring Lyophilization with Optical Fiber Sensors; Conference of Freeze-Drying of Pharmaceuticals and Biologicals, Garmisch-Partenkirchen, Germany, 28 September – 01 October, 2010.

J.C. Kasper, M. Wiggenghorn, M. Resch, W. Friess; Implementation and Evaluation of an Optical Fiber System as Novel Process Monitoring Tool During Freeze-Drying; Fourth pan-European PAT Science Conference, Kuopio, Finland, 5-6 May, 2010.

Poster presentations

J.C. Kasper, D. Schaffert, C. Troiber, M. Ogris, E. Wagner, W. Friess; Improving the quality and long-term stability of polymer-based gene-delivery systems – The benefit of “higher” molecular weight excipients in lyophilization; AAPS Annual Meeting & Exposition, Washington DC, USA, 23-27 October 2011.

This work was honored with the **IPEC Foundation Graduate Student Award**.

J.C. Kasper, C. Troiber, M. Scheible, S. Milani, F. Schaubhut, S. Kuchler, J. Rädler, F.C. Simmel, E. Wagner, W. Friess; Critical evaluation of analytical methods for the physico-chemical characterization of siRNA polyplexes; AAPS Annual Meeting & Exposition, Washington DC, USA, 23-27 October 2011.

C. Troiber, **J.C. Kasper**, S. Milani, M. Scheible, F. Schaubhut, S. Kuchler, J. Rädler, F.C. Simmel, W. Friess, E. Wagner; Analytical methods for the physico-chemical characterization of siRNA polyplexes; CeNS Workshop 2011; Nanosciences: From Molecular Systems to Functional Materials; Venice International University (VIU), San Servolo, Italy, September 19-23 2011.

J.C. Kasper, C.V. Duerr, W. Friess; Lyophilization of a highly concentrated monoclonal antibody formulation in the presence of tertiary butyl alcohol; Bioproduction Forum 2011, Ulm, Germany, 8-10 June, 2011.

J.C. Kasper, D. Schaffert, M. Ogris, E. Wagner, W. Friess: Up-scaled Preparation and Development of a Lyophilized Formulation with Long-Term Stability for Polyplexes; FIP Pharmaceutical Sciences 2010 World Congress in Association with the AAPS Annual Meeting and Exposition, New Orleans, USA, 14-18 November, 2010.

This work was honored with a **travel award** by the European Federation for Pharmaceutical Sciences (EUFEPS).

J.C. Kasper, D. Schaffert, M. Ogris, E. Wagner, W. Friess: Up-scaled Preparation and Development of a Lyophilized Formulation with Long-Term Stability for Polyplexes; PSWC 2010 Congress for Students and Postdoctoral Fellows, New Orleans, USA, November 13-14, 2010.

J.C. Kasper, David Schaffert, Manfred Ogris, Ernst Wagner, Wolfgang Friess: Development of a Stable Lyophilized Formulation for LPEI Polyplexes; 7th Annual Meeting of the German Society for Gene Therapy, Munich, Germany, October 7 -9, 2010. Abstract published in: Human Gene Therapy, September 2010, 21(9): 1169-1220.

J.C. Kasper, D. Schaffert, M. Ogris, E. Wagner, W. Friess; Development of a Lyophilized Formulation with Long-term Stability for Polyplexes; Conference of Freeze-Drying of Pharmaceuticals and Biologicals, Garmisch-Partenkirchen, Germany, 28 September - 01 October, 2010.

J.C. Kasper, D. Schaffert, M. Ogris, E. Wagner, W. Friess; Up-scaled Preparation and Formulation Development of Polyplexes; 7th World Meeting on Pharmaceutics, Biopharmaceutics and Pharmaceutical Technology, Valetta, Malta, 08-11 March, 2010.

J.C. Kasper, M. Wiggenghorn, M. Resch, W. Friess; Using an optical fiber system for temperature measurement during freeze-drying – a novel tool for process monitoring; Annual Conference of the German Pharmaceutical Society (DPhG), Jena, Germany, 28 September – 01 October, 2009.

Curriculum vitae

Julia Christina Kasper

Personal data

Date of birth: April 25, 1985
 Place of birth: Günzburg, Germany
 Nationality: German

Education

03/2009 – 04/2012 PhD studies, Department of Pharmacy, Pharmaceutical Technology and Biopharmaceutics, LMU, Munich
 Supervisor: Prof. Dr. W. Friess

08/2007 – 02/2009 Master studies in Pharmaceutical Sciences, LMU, Munich, final degree: M.Sc.

08/2007 – 02/2009 Parallel studies in Pharmacy State Examination, LMU, Munich

07/2008 1st State Examination Pharmacy, LMU, Munich

10/2004 – 08/2007 Bachelor studies in Pharmaceutical Sciences, LMU, Munich, final degree: B.Sc.

09/1995 – 06/2004 High School, St. Thomas Gymnasium Wettenhausen, Kammeltal, graduation with `Abitur`

Professional experience and academic training

03/2009 – 02/2012 Academic assistant, Department of Pharmacy, Pharmaceutical Technology and Biopharmaceutics, LMU, Munich

07/2011 – 10/2011 Visiting scientist, School of Pharmacy, group Prof. Dr. M.J. Pikal, University of Connecticut, USA

01/2010 – 02/2012 Voluntary note writer for APV News

08/2009 – 12/2011 Freelancer

09/2008 – 02/2009 Research intern, Leiden/Amsterdam Center for Drug Research, group Prof. Dr. W. Jiskoot, the Netherlands

01/2008 – 04/2008 Research intern, Department of Pharmacy, Pharmaceutical Technology and Biopharmaceutics, group Prof. Dr. W. Friess, LMU, Munich

08/2007 – 09/2007 Research intern, Scil Technology GmbH, Martinsried

03/2007 – 05/2007 Research intern, Scil Technology GmbH, Martinsried